# Utilization of halophytes as a potential source of pharmaceutical candidates

アハメド モハメド オスマン カミス

KYUSHU UNIVERSITY

# Utilization of halophytes as a potential source of pharmaceutical candidates

## Ahmed Mohamed Othman Khamis

A Thesis submitted in partial fulfillment of the requirements for the degree of Doctor of Philosophy in the field of Natural Products Chemistry and Pharmacognosy

Graduate School of Bioresource and Bioenvironmental Sciences

Kyushu University

2023

This is to certify that this Ph.D. thesis entitled "Utilization of halophytes as a potential source of pharmaceutical candidates" prepared by Mr. Ahmed Mohamed Othman Khamis in partial fulfillment of the requirements for the degree of "Doctor of Philosophy" is an official copy of the original thesis that has been examined and approved by the following Examination Committee:
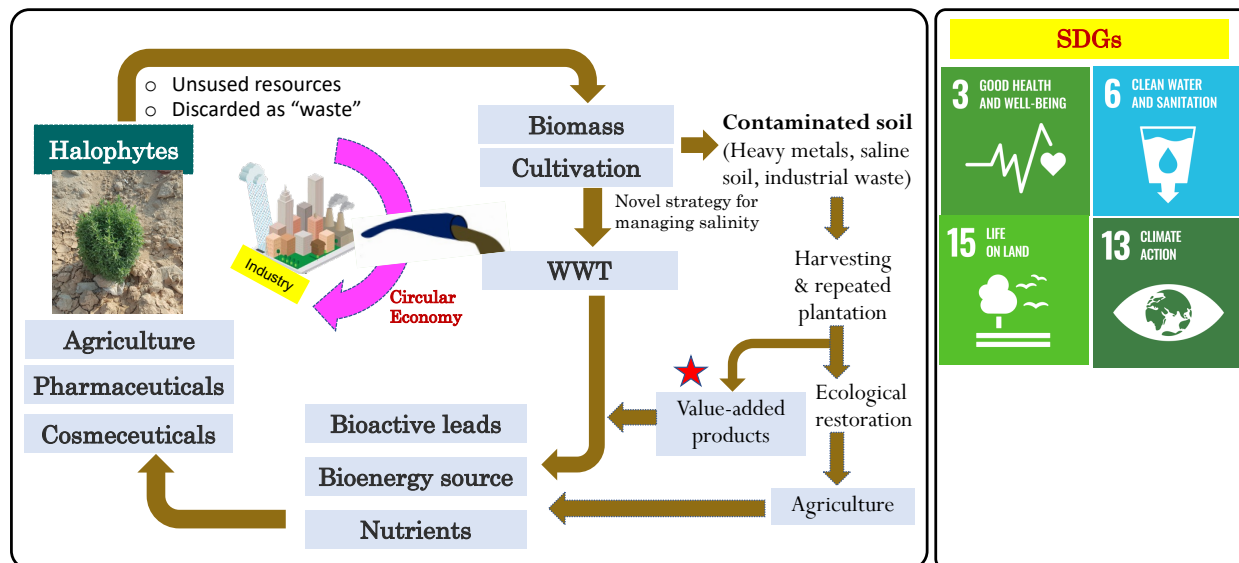
Fukuoka, February 2023


_____

Assoc. Prof. Kuniyoshi SHIMIZU, Chairman of the Examining Committee


_____

Prof. Atsushi KUME


_____

Prof. Yuji TSUTSUMI

# FRONTISPIECE



The area of research on exploitation of halophytes is still emerging. Their utilization is an important concept for the industry to produce values from the unused resources (Circular Economy). The current study aims to manage and convert the waste of halophytes into value-added products instead of their disposal.

# DECLARATION AND COPYRIGHT

I, Ahmed Othman, declare that this thesis is my own original work and that it has not been presented and will not be presented to any other university for a similar or any other degree award.

Signature: _____Date: _____

"Indeed, my prayer, my rites of sacrifice, my living and my dying are for Allah, Lord of the worlds. No partner has He. And this I have been commanded, and I am the first [among you] of the Muslims" (The Qur'an Explained in Detail: 6:162–163)

"And Allah has brought you forth from the wombs of your mothers– you did not know anything– and He gave you hearing and sight and hearts that you may give thanks" (The Qur'an Explained in Detail: 16:78)

"And His signs are the creation of heavens and earth and the diversity of your tongues and colors. Surely, there are signs in this for all the worlds" (The Qur'an Explained in Detail: 30:22)

# DEDICATION

I would like to dedicate my thesis work to the memory of my late father-in-law, **Mostafa Ahmed Hassan** (May ALLAH bless his soul and grant him the highest place in the Heavens), best father and best friend, who never saw the end of this adventure. I am deeply sad and sorry that I wasn't by his side in his last days. I miss him every day and his memory will remain forever. I ask the Almighty ALLAH to have mercy and forgiveness for him and to gather in a seat of truth (i.e. Paradise), near the Omnipotent King (ALLAH, the Owner of Majesty and Honor).

# ACKNOWLEDGMENTS

# ABSTRACT

 Recently, the scientific interest and particularly the economic significance of halophytes have been highly demanding due to the medicinal and nutraceutical potential of its bioactive compounds. The xero-halophyte herbs, *Bassia indica* and *Agathophora alopecuroides*, are deemed to be among the promising sources of natural compounds that need chemical and biological investigation.

Non-communicable diseases (NCDs) greatly burden societies and national governments owing to their high mortality rates. NCDs cover a wide range of health issues, such as neurological disorders, cancer, and dermatological conditions. The objectives of this study were; (i) to perform chemical studies on *B. indica* and *A. alopecuroides*, followed by structural characterization of the metabolites; (ii) to investigate the potential of metabolites for the treatment of Alzheimer's disease (AD), cancer, and skin diseases. A total of thirty-six compounds were isolated and several among them had promising therapeutic activity.

The first part of this study (Chapters 2-4) was conducted to address the potential application of halophytes-derived chemicals, especially amide alkaloids, for the treatment of AD. The chemical investigation of *B. indica* led to the isolation of twenty-five compounds. Their structures have been determined by 1D, 2D NMR, and HR-MS analysis. Among the isolates, a novel acylated flavonol tetraglycoside and an amide alkaloid, together with a new *seco*-glycosidic oleanane saponin, were identified for the first time. Moreover, the study reports on the isolation and identification of seven amide alkaloids from the aerial parts of *B. indica* and *A. alopecuroides*.

6,7-Dihydroxycoumarin, which has been isolated from *B. indica*, showed a pronounced anti-acetylcholinesterase activity. Besides, *N-trans*-feruloyl-3-methoxytyramine, *N-trans*-feruloyltyramine, *N-trans*-caffeoyltyramine, and 3-(4-hydroxy-3-methoxyphenyl)-*N*-[2-(4-hydroxyphenyl)methoxyethyl]acrylamide showed multi-targeting inhibition activity against monoamine oxidase B (MAO-B), β-secretase (BACE1), and anti-aggregation of Aβ-peptides.

The second part of thesis (Chapter 5) was aimed to assess the anti-tumor and anti-inflammatory activity of isolated compounds from *B. indica*. The methanol extract and the isolated triterpene oleanane saponins displayed promising anti-inflammatory activity. Additionally, *N-trans*-feruloyltyramine exhibited significant cytotoxicity against OVK-18 with $IC_{50}$ = 1.74 µg/mL, while 6,7-dihydroxycoumarin exhibited a potent inhibition against MCF-7 cells with $IC_{50}$ = 1.47 µg/mL. Moreover, two compounds exhibited remarkable cytotoxicity against HCT116 with $IC_{50}$ < 0.1 µg/m and six compounds exerted potent cytotoxicity against HepG2.

The third part of thesis (Chapter 6) was conducted to gain a detailed view of the protective effect of the halophyte herb *A. alopecuroides* in aged and diseased skin. This part reports on the isolation and structure elucidation of three previously undescribed compounds (glucosylceramide, flavonol triglycoside, and triterpene oleanane saponin), along with eight known ones from the methanol extract of *A. alopecuroides*. In addition, as ceramide synthase-3 (CerS3) plays a crucial role in epidermal hydration and restoration of the skin barrier function, the influence of *A. alopecuroides* extract and its isolated compounds on the mRNA expression levels of CerS3 in human keratinocyte cells (HaCaT) were evaluated. Importantly, the methanol extract significantly increased the mRNA expression levels of CerS3 by 1.2-fold. Among the isolates, isorhamnetin-3-*O*-glucoside significantly enhanced the expression levels of CerS3 by 4.3-fold. In addition, β-sitosterol, β-sitosterol-3-*O*-glucoside, and solysaponin A, significantly upregulated the mRNA expression levels of CerS3 by 1.9-, 4.2-, and 3.2-fold, respectively.

In conclusion, the potential of biomass resources, *B. indica* and *A. alopecuroides*, for the treatment of NCDs were evaluated. Herein, seven novel compounds were encountered and characterized for the first time. The study results reveal a new scaffold of amide alkaloids for AD treatment, as well as the future development of AD therapies. Furthermore, we provided scientific validation for the anti-tumor activities of *B. indica*. On the other hand, β-sitosterol, β-sitosterol-3-*O*-glucoside, isorhamnetin-3-*O*-glucoside, and solysaponin A from *A. alopecuroides* have the capacity to stimulate epidermal ceramide synthesis and recover aged dry skin in atopic dermatitis and psoriasis. Finally, the

chemical and biological properties reported here will be an important first step toward the future drug discovery and cosmetic field.

# TABLE OF CONTENTS

# LIST OF TABLES

# LIST OF FIGURES

# LIST OF APPENDICES

# LIST OF ABBREVIATIONS

| | |
|---|---|
| 1D | One dimension |
| 2D | Two dimensions |
| A549 | Lung cancer cell line |
| Ach | Acetylcholine |
| AChE | Acetylcholinesterase |
| AD | Alzheimer's disease |
| ADME | Absorption, distribution, metabolism, and excretion |
| Aβ | Amyloid beta peptide (Aβ) |
| APT | Attached Proton Test |
| BACE1 | β-secretase or β-site amyloid precursor protein cleaving enzyme 1 |
| br | Broad |
| BChE | Butyrylcholinesterase |
| BSA | Bovine serum albumin |
| °C | Celsius (degree centigrade) |
| $^{13}$C NMR | Carbon Nuclear Magnetic Resonance |
| CC | Column Chromatography |
| $CCl_4$ | Carbon tetrachloride |
| CerS3 | Ceramide synthase-3 |
| $CH_2Cl_2$ | Methylene Chloride |
| $CH_3OD$ | Deuterated methanol |

| | |
|---|---|
| cm | Centimeter |
| COSY | Correlation Spectroscopy |
| δ | Chemical shift in parts per million downfield from a standard |
| d | Doublet |
| DCM | Dichloromethane |
| dd | Doublet of doublet |
| DMSO-$d_6$ | Deuterated dimethyl sulfoxide |
| $D_2O$ | Deuterated water |
| e.g., | exempli gratia (for example) |
| et al. | et alii/alia (and others) |
| etc. | et cetera (and so on) |
| EtOAc | Ethyl acetate |
| Fr. | Fraction |
| Glc | Glucose or Glucopyranosyl |
| Gal | Galactose or Galactopyranosyl |
| GlcA | Glucuronic acid or Glucuronopyranosyl |
| g or gm | Gram |
| HL-60 | promyelocytic leukemia cell line |
| ^{1}H-NMR | Proton Nuclear Magnetic Resonance |
| $H_2O$ | Water |
| HCT-116 | Human colon carcinoma cell line. |

| | |
|---|---|
| HepG-2 | Human hepatocellular carcinoma cell line |
| HMBC | Heteronuclear Multiple Bond Connectivity |
| HPLC | High-performance liquid chromatography |
| HR-ESI-MS | High Resolution Electrospray Ionization Mass Spectroscopy |
| h | Hour |
| HSQC | Heteronuclear Single Quantum Coherence |
| Hz | Hertz |
| $IC_{50}$ | The half maximal inhibitory concentration |
| *J* | Coupling constant |
| kg | Kilogram |
| L | Liter |
| MAO-B | Monoamine oxidase enzyme-B |
| $MgCl_2$ | Magnesium chloride |
| *m* | Meta |
| m | Multiplet |
| M | Molar |
| MCF-7 | Human breast adenocarcinoma cell line |
| Me | Methyl |
| MeOH | Methanol |
| mg | Milligram |
| MHz | Megahertz |

| | |
|---|---|
| min | Minute |
| mL | Milliliter |
| mm | Millimeter |
| mM | Millimolar |
| MPLC | Medium Pressure Liquid Chromatography |
| MS | Mass Spectroscopy |
| MTT | 3-(4,5-Dimethylthiazol-2-yl)-2,5-diphenyltetrazolium bromide |
| *m*/*z* | Mass-to-Charge ratio |
| μ | Micro |
| μL | Microliter |
| μm | Micrometer |
| μg | Microgram |
| *n* | Normal |
| ng | Nanogram |
| nm | Nanometer |
| NMR | Nuclear Magnetic Resonance |
| NP | Normal phase |
| NP-TLC | Normal Preparative Thin Layer Chromatography |
| NF-κB | Nuclear factor kappa B |
| *O* | Ortho |
| OVK-18 | Ovarian cancer cell line |

| | |
|---|---|
| % | Percent |
| *P* | Para |
| ppm | Part Per Million |
| prep | Preparative |
| Rha | Rhamnose or Rhamnopyranosyl |
| ROESY | Rotating-frame Overhauser Effect Spectroscopy |
| RP-C18 | Reversed Phase C-18 |
| s | Singlet |
| Si | Silica |
| SIRT1 | Sirtuin (silent mating type information regulation 2 homolog) 1 |
| t | Triplet |
| TLC | Thin-Layer Chromatography |
| TMS | Tetra Methyl Silane |
| T2DM | Type 2 diabetes mellitus |
| UV | Ultra-Violet |
| WWT | Wastewater Treatment |
| WHO | World Health Organization |
| Xyl | Xylose or Xylopyranosyl |

# Chapter 1: Introduction and Background

## 1.1. Natural products as drug leads

Natural products (NPs) are well-known for their importance in drug discovery, as they frequently provide scaffolds and pharmacophores as valuable starting points for lead discovery [1]. Plant-derived compounds have played significant role in preventing human ailments for centuries [2]. Bioactive compounds obtained from natural sources as plants, animals, microorganisms, and marine organisms are of potential medicinal significance [3]. Natural products contain complex metabolites with diverse chemical structures; subsequently, they have a greater tendency to interact with different biological targets. Such characteristics make them valuable as structure leads for drug discovery programs [4]. For centuries, seeking for the treatment of diseases and improving the quality of life are urgent needs for humankind. As early as 1806, a German Pharmacist, Friedrich Wilhelm, reported the isolation of morphine and since then, NPs have remained the precious treasure for discovery of new candidates with therapeutic importance [2,4,5]. Approximately a quarter of all approved medications by the Food and Drug Administration (FDA) and/or the European Medical Agency (EMA) are plant-based products. Paclitaxel and Morphine are types of known drugs have been isolated from plants [6]. Additionally, over half of currently available drugs are or relate to natural compounds [7]. About 68% of anti-infectives (antibacterial, antifungal, antiparasitic, and antiviral compounds) are classified as naturally derived compounds. Moreover, many anti-tumor drugs are derived from natural sources have been identified and approved for cancer treatment during the last 60 years [4]. Examples of natural-based medicines include the synthesis of the anti-inflammatory agent acetylsalicylic acid derived from the natural molecule salicin which was isolated from the bark of *Salix alba*. Additionally, cardiotonic glycosides digoxin and digitoxin that can improve the cardiac contractility were isolated from *Digitalis purpurea*. In addition, L-histidine-derived alkaloid, pilocarpine, which has been used in the treatment of chronic glaucoma was found in *Pilocarpus jaborandi* [8]. Also, the most widely used anti-tumor drug for breast cancer is paclitaxel (Taxol®) which has been isolated from the bark of *Taxus brevifolia*. A drug licensed to treat symptoms of dementia in AD is galantamine which is produced from *Galanthus woronowii* and *Leucojum aestivum* [9].

Medicinal plants have been used as source of remedies in Egypt since ancient times. The Egyptian ecosystem is rich with wild plants that have been used in folk medicine and Vivi Laurent-Täckholm was one of the first scientists reported the flora of Egypt [10]. Nowadays, there is a growing movement toward the use of herbal medicine in treatment of diseases. Interestingly, one of the fast-growing industries in Egypt is the production of herbal drugs and herbal drug-based medicaments [11]. Considering the increasing interest in how natural remedies play an important role in the modern health care and in providing new leads in drug discovery programs, the search for unexplored plant species follows. Therefore, the search for new therapeutic entities derived from medicinal plants will be continued for their role in the prevention of diseases, such as cancer, diabetes, hypertension, and Alzheimer.

## 1.2. Halophytes as a potential source of lead compounds

Halophytes are plants able to grow in extreme conditions, such as high-salinity. They are common in the Mediterranean coastal regions, salt marshes, and desert areas [12]. The Mediterranean basin region is prosperous with halophytic plants that have been used for food and medicinal purposes for centuries [13,14]. Some halophytes are edible and utilized as sources of food products in food industry technology due to their high nutritional and commercial values [13]. Halophytes can be classified into two main types based on their habitat. One kind is hydro-halophytes which are plants can grow in aquatic soil or in wet environment such as mangroves and salt marsh species along coastal regions. The other kind of halophytes is xero-halophytes which can grow in dry and saline environment and many of them are succulents[15]. Halophytes have been traditionally consumed as folk remedies for pathological conditions including infectious diseases, diabetes, and various skin conditions [16,17]. Also, they have been recognized as leafy greens (vegetables) and basic ingredients of traditional dishes and local recipes in Mediterranean diet [18]. As seen in Table 1, some edible halophytes distributed in the Mediterranean region and their health benefits are discussed to highlight the importance of such halophytes as potential sources of natural bioactive compounds. Importantly, halophytes have attracted the scientific research attention in recent decades owing to their health-promoting effects as they can produce various primary and secondary metabolites as natural response to

oxidative stress [13,18,19]. Hence, they are suggested as part of plant-based nutraceuticals because of their role as natural antioxidants and phenolic content [20].

The utilization of halophytes for treatment of chronic diseases affecting modern societies, such as Alzheimer, diabetes, cancer, and heart diseases, are attributed for their medicinal properties [21]. Moreover, halophytes possess interesting biological activities as antidiabetic, antibacterial, anti-obesity, and anti-tumor, and cholesterol-reducing properties [17,22–26].

Biologically active compounds, such as polyunsaturated fatty acids, vitamins, sterols, carotenoids, terpenes, polysaccharides, glycosides, and phenolic compounds have been discovered in halophytes [21]. Notably, these bioactive compounds exhibit powerful antioxidant, antimicrobial, anti-inflammatory, neuroprotective, antidiabetic and anti-tumor activities and therefore considered as key lead compounds for the prevention and treatment of diseases, such as diabetes, cancer, inflammation, atherosclerosis, AD, and cardiovascular disorders [27]. Despite the increasing interest in the utilization of halophytes as food and for nutritional purposes, the studies regarding the chemical or biological investigation still barely limited, and more efforts are still needed for their valorization. Thus, the search will continue aiming to utilize halophytes as new sources of functional foods, nutraceuticals, and bioactive compounds.

**Table 1**: Edible halophytes with beneficial health effects

| Species | Health effects | Reported biological activity |
|---|---|---|
| *Beta vulgaris* | Leaves and stems are used as antidiabetic and for digestive disorders, burns, anemia, throat ailments, and for liver and kidney diseases. Also, it has been utilized as source of vitamin E [28,29] | Anticholinesterase, antidiabetic, antioxidant, anti-inflammatory, anti-tyrosinase, and anti-tumor [23,29] |
| *Kochia scoparia* | Fruits of *K. scoparia* have been used for inflammation, allergy, dysuria, skin ailments, breast masses and chest pain [30] | Cytotoxicity activity against breast cancer cell lines [30] |
| *Suaeda fruticosa* | The aqueous extract showed hypoglycemic and hypolipidemic activities [31] | Anti-inflammatory, anticancer against human lung carcinoma and colon carcinoma cell lines [31] |
| *Bassia eriohora* | *B. eriophora* infusion has been traditionally reported for the treatment of Alzheimer's and hair loss [32] | Ethanolic extract exerted a significant analgesic effect, anti-inflammatory and cytotoxic effect against MCF-7, HepG-2 and HCT-116 cell lines [33] |
| *Chenoodium album* | The plant has many medicinal properties reported in Ayurveda like anthelmintic, cardiotonic, carminative, digestive, diuretic, and laxative [34]. Decoction of aerial parts has been applied for arthritis and rheumatism [35] | Antimicrobial, antipruritic, antinociceptive, and anti-tumor activity against A549 cell lines [36] |

| | | |
|---|---|---|
| *Atriplex inflata* (*Atriplex lindleyi*) | Used for treatment of inflammation and against *Herpes simplex* virus [17] | Antidiabetic and hepatorenal protection activity, in addition to antiplasmodial and antimicrobial activity [37] |
| *Salicornia herbacea* | Used as neuroprotective, anti-inflammatory, hepatoprotective, skin whitening, antihyperlipidemic, antibacterial effects [38] In Korea, the plant has been reported for treatment of obesity, high blood glucose, and gastric disorders [39] | The seed extract exhibit cytotoxic activities against HCT 116 and HT-29 colon cancer cells [13]. Moreover, some compounds have been isolated from *S. herbacea* showed antiproliferative activities, an inhibitory activity against A549 and HepG2 cancer cells, and stimulating glucose uptake activity [40] |
| *Suaeda monoica* | The plant parts have been traditionally reported as antiviral, wound healing activities, and antiplasmodial effect against *Plasmodium falciparum* [41] | A compound isolated from *Suaeda monoica* has shown usefulness as a promising cell proliferating agent [41] |

## 1.2.1. Biological activities reported in halophytes

Halophytes produce wide range of bioactive secondary metabolites, and they are used as an important source of natural vitamins, fatty acids, amino acids, flavonoids, phenolic acids, alkaloids, terpenes, and isoflavonoids [13]. Alkaloids, flavonoids, and glycosides isolated from halophytes are responsible for wide variety of pharmacological activities. Various bioactive functions as antioxidant, antimicrobial, immunomodulatory, lipid-lowering activity, and cytotoxicity have been widely reported for halophytes owing to their nutraceutical potential and their content of novel compounds [42]. A phenolic compound, 3-caffeoyl-4-dihydro-caffeoyl quinic acid, and a flavonoid, isorhamnetin 3-$O$-$\beta$-D-glucopyranoside, isolated from *Salicornia herbacea* displayed promising inhibition activity against COX-2 and can be considered for therapeutic development [43]. The methanol extract of *Suaeda fruticosa* contains phenolic and flavonoid derivatives showed inhibition potential against AChE and BChE [44]. Luteolin obtained from *Bassia eriphora* exhibited strong anti-tumor effect against cancer cell lines including MCF-7, HepG2 and HCT-116, while diosmin and kaempferol-3-$O$-rutinoside displayed strong antiproliferative effect against MCF-7 [45]. Additional biological activities which have been reported from halophytes are summarized in Table 2.

**Table 2**. Some biological activities reported in halophytes

| Biological activity | Outcomes |
| --- | --- |
| **Antibacterial activity** | Methanol extract of *Kochia prostrata* showed antibacterial activity against number of pathogens including *Bacillus subtilis*, *Staphylococcus aureus*, *Escherichia coli*, *Pseudomonas aeruginosa*, and *Salmonella typhi* [46]. *n*-BuOH extract of *Atriplex inflata* showed antibacterial activity against *Pseudomonas aeruginosa*, *Escherichia coli* and *Staphylococcus aureus* [47] |
| **Antifungal activity** | Non-polar extract of *Atriplex inflata* fruits, in addition to methanol and acetone extracts of *Atriplex semibacata* showed antifungal activity [48] |
| | The *n*-BuOH extract of *Bassia indica* showed antifungal activity against *Macrophomina phaseolina* [26] |
| | Triterpenoidal saponins isolated from *Chenopodium quinoa* seeds have been reported to have antifungal activity against *Candida albicans* [49] |
| **Anticholinesterase activity** | *N*-acetyl tryptophan isolated from ethanol extract of *Salsola grandis* showed an inhibition activity against AchE [50] |
| **Anti-tyrosinase activity** | The extract of *Atriplex gmelinii* showed promising tyrosinase inhibitory activity and high elastase inhibitory effect [51] |
| **Anticancer activity** | The methanol extract of *Kochia scoparia* fruits inhibit the proliferation and induces apoptosis of breast cancer cells [30]. Moreover, lignanamides isolated from *Atriplex semibaccata* weakly inhibited the proliferation of leukemia CCRF-CEM cells with $IC_{50}$ values of 78.5, 46.3, and 71.2 µg/ml, respectively [52] |

| | |
|---|---|
| **Hepatoprotective activity** | Phenolic compounds isolated from *Suaeda glauca* showed hepatoprotective activity against tacrine-induced cytotoxicity in human liver-derived Hep G2 cells [53] |
| | The ethanolic extract of sugar beet roots exhibited significant dose-dependent hepatoprotective activity against carbon tetrachloride ($CCl_4$)-induced hepatotoxicity in rats [54] |

## 1.3. Adaptation mechanisms of halophytes to salt stress and their relations to the chemical content

Halophytes are group of plants capable of completing their life cycle in saline conditions of 200 mM NaCl or even higher [55]. They can employ several mechanisms including morphological, physiological, and biochemical modifications to adapt salinity and salt stress. These mechanism include development of succulence, selective uptake and transport of ions, osmotic adjustments by osmolytes, biosynthesis of antioxidant enzymes and molecules [56].

Osmolyte molecules are low molecular weight and highly soluble organic compounds that are non-toxic even at higher concentrations. Among osmolyte molecules, shikimic acid which is highly accumulated in halophytic plants and might be attributed to their content of complex secondary metabolites [57]. Shikimic acid is a precursor for the production of aromatic amino acids such as phenylalanine, tyrosine, and tryptophan, cinnamic acid derivatives, in addition to lignans, phenylpropenes, and coumarins following further modifications as shown in Figure 1. Also,  it is an important source of key compounds which are converted to a wide variety of natural products. The shikimate pathway and the acetate pathway are responsible for the biosynthesis of flavonoids, stilbenes, and flavonolignans [58].

Halophytes contain considerable amounts of phenylpropanoids thar are specialized metabolites correlated with  several aspects of plant growth and development and in the responses of plants to stress environmental conditions. The biosynthetic pathway of phenylpropanoids can provide important building blocks for generation of lignin and tannins that play a pivotal role in structural support and mechanical strength [59]. Further, the production of anthocyanins and flavonoids, essential for UV protection and plant-pathogen interactions, are biosynthesized through this pathway. In addition, phenylpropanoids are important nutraceutical components with neuroprotective antioxidant, and anti-inflammatory activities. Recently, numerous phenylpropanoids are considered high-value biochemicals can be employed in the production of pharmaceuticals and biopolymers [60]. Some representative chemical compounds reported in halophytes are summarized in Table 3. Importantly, phenylpropanoids and

their complex derivatives contained in halophytes are essential for the growth, stress responses, and they can impart potential health benefits for humans. Thus, utilization methods are needed to extract the components of halophytes to enhance the understanding related to the molecular mechanisms underlying medicinal and nutraceutical potential of these biomolecules. This study might contribute to these goals, covering various aspects related to the extraction of components, chemical studies and functionality evaluation of halophytes *Bassia indica* and *Agathophora alopecuroides*. Also, novel insights and different approaches related to utilization of halophytes and their complex molecules are expected to be elucidated in the future.
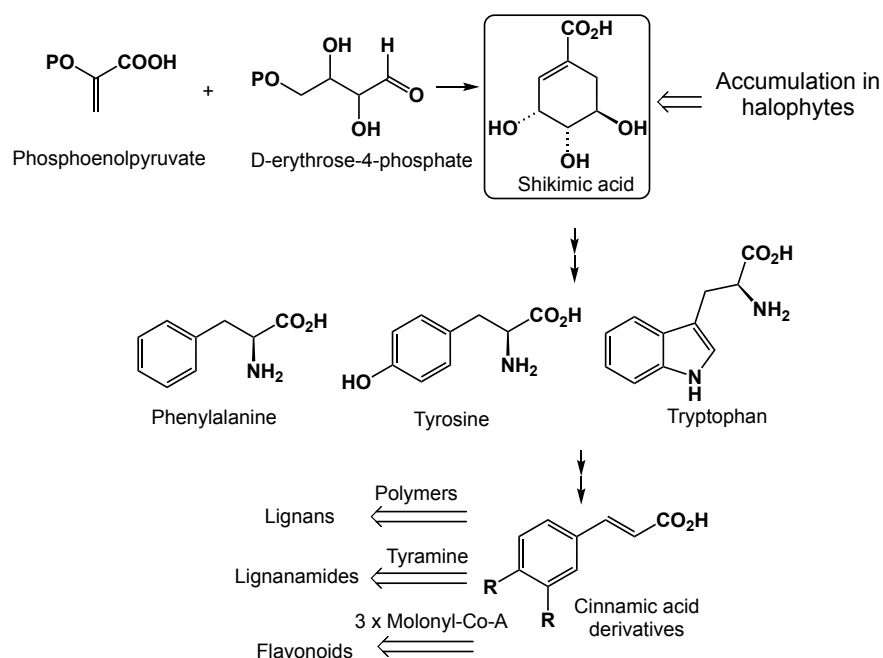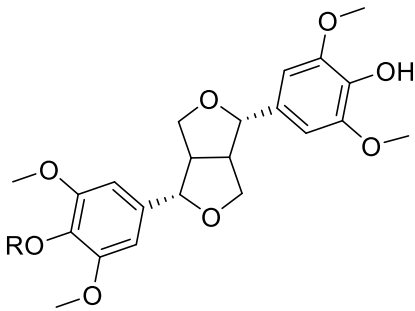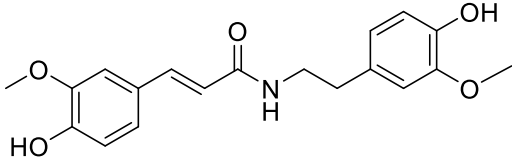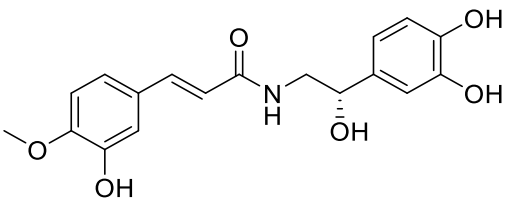


Figure 1: Possible biosynthetic pathway of complex scaffolds in halophytes

**Table 3**. Representative phytochemical compounds reported in halophytes

| Name | Class | Structure and reported biological activity |
|------|-------|---------------------------------------------|
| Syringaresinol Syringaresinol-4-*O*-*β*-D-glucoside | Lignan | <br><br>R = H<br><br>R= *β*-D-glucose<br><br>▪ Isolated from *Suaeda salsa* [61]<br><br>▪ Showed cytotoxic activity against four cell lines, HL-60, MCF-7, HepG2 and A549 [61] |
| *N-trans*-feruloyl-3-*O*-methyldopamine | Amide alkaloid | <br><br>▪ Isolated from *Beta vulgaris* [62]<br><br>▪ Showed anti-inflammatory activity [62] |
| *N*-[2-(3,4-dihydroxyphenyl)-2-hydroxyethyl] -3-(4-methoxyphenyl) prop-2-enamide | Amide alkaloid | <br><br>▪ Isolated from *Salsola foetida* [63]<br><br>▪ Showed tyrosinase inhibitory activity [63] |

| 24-Epi-makisterone A | Ecdysteroid |
| --- | --- |
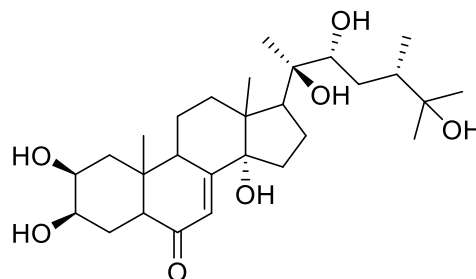


- Isolated from *Chenopodium quinoa* [49]
- Anabolic activity [49]
- Reduce high cholesterol levels

| Chikusetsusaponin V | Oleanane saponin |
| --- | --- |
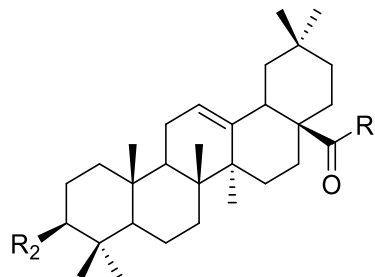


$R_1 = \beta$-D-Glu, $R_2 = \beta$-D-Glc-2-$\beta$-D-Glu

- Isolated from *Kochia indica* [64]
- Inhibits LPS-activated inflammatory responses via SIRT1/NF-κB signaling pathway [65]
- Similar compounds showed promising hypoglycemic activity [66,67]

| | | |
|---|---|---|
| 3-*O*-[5'''-*O*-feruloyl-*β*-D-apiofuranosyl (1'''→2'')-*β*-D-glucopyranoside] | Flavonoid glycoside |  |
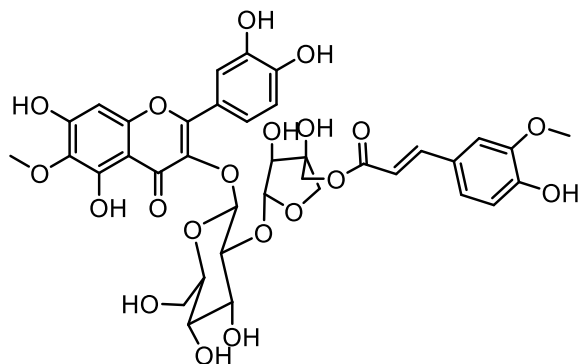
- Isolated from *Atriplex littoralis* [68]
- No reported biological activity in the literature [68]

| | | |
|---|---|---|
| Salsoline | Alkaloid |  |
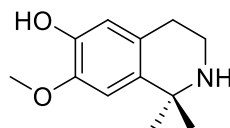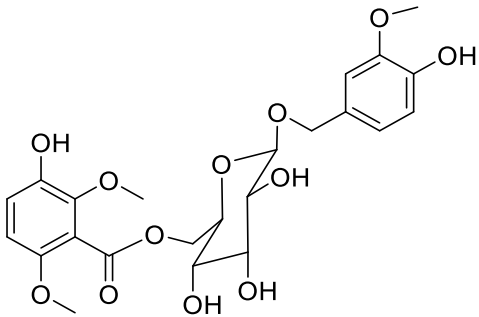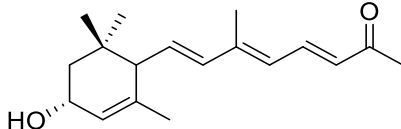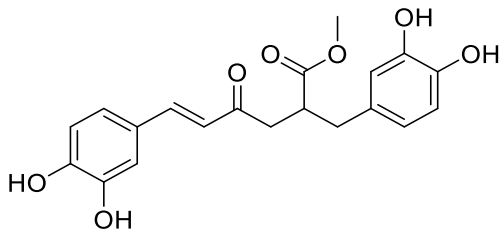
- Identified in *Salsola soda* and other Salsola species [69]
- Exhibited anticholinesterase activity [69]

| | | |
|---|---|---|
| Suaeglaucin A | Coumarono-chromone |  |
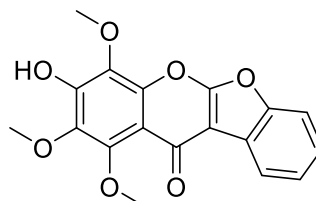
- Isolated from *Suaeda glauca* [70]
- No reported biological activity in the literature [70]

| | | |
|---|---|---|
| Chenoalbuside | Phenolic glycoside |  |

■ Isolated from *Chenopodium album* [71]

■ Has significant antioxidant activity [71]

| | | |
|---|---|---|
| (6S,7E,9*E*,11*E*)-3-oxo-13-apo-*R*-caroten-13-one | Carotenoids |  |

Isolated from Chenopodium album [72]

| | | |
|---|---|---|
| Methyl rosmarinate | Phenolic acid derivative |  |

■ Isolated from *Corispermum mongolicum*

■ Inhibit the production of NO, TNF-α, and IL-6 [73]

## 1.4. The potential utilization of halophytes

Generally, halophytes can be utilized to achieve two major goals. First, halophytes can be cultivated for the purpose of desalinization of degraded soils [74]. Second, they can be used for the recovery of value-added products with multiple applications [56].

Soil salinization and degraded lands are prominent limitations to plant growth and productivity. Thus, exploitation of halophytes can overcome such limitations and support sustainable agriculture [56]. Utilization of halophytes can be applied to recover the dry lands and remove contaminants from contaminated soils and make them suitable for cultivation of crops. Halophytes can synthesize complex biochemical substances to maintain growth, normal metabolism, and activity of enzymes even under very stressful conditions and in harsh environments [75].

To adapt saline environments, halophytes can produce a huge variety of secondary metabolites that have complex molecular mechanisms and are suggested to have wide array of bioactivities [56]. Consequently, they are regarded as a biofactory for key industrially significant chemicals. Importantly, this study deals with utilization of some halophytes for the production of value-added molecules as shown in Figure 2.

The xero-halophytes *Bassia indica* and *Agathophora alopecuroides* (Figures 3-4) are halophytes widely distributed in the Egyptian ecosystem [10]. These halophyte species are discarded as "waste" that led to environmental problems. Therefore, these halophyte species need effective approaches to minimize their environmental hazards induced by their disposal. Approaches that are environmentally friendly should be conducted in order to incorporate halophytes into production cycle to create values from such unused resources.

One of these approaches is the recovery of components from *B. indica* and *A. alopecuroides* by applying several chromatographic techniques to obtain bioactive molecules with beneficial biological properties. The possible management and utilization of such halophytes are summarized in Figure 2. Additionally, providing scientific evidence related the discovery of chemical content in halophytes (*B. indica* and *A. alopecuroides*) and evaluation of their possible therapeutic effects might be needed for their exploitation as promising candidates for medicinal and cosmetic applications.
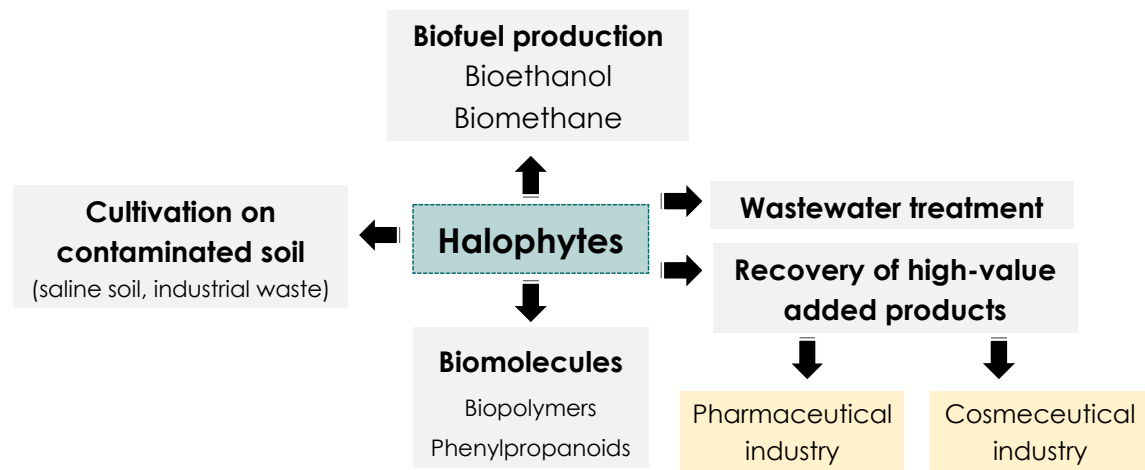
Figure 2: Workflow for possible utilization methods of halophytes

Figure 3: *B. indica* (Wight) A.J. Scott



Figure 4: *A. alopecuroides* (Delile) Fenzl ex Bunge

## 1.5. Aim of the study

Complex chemical compounds, such as alkaloids, terpenoids, flavonoids, saponins, tannins, etc. are suggested to have wide array of bioactivities owing to their structural diversity [76,77]. Among the promising sources of natural products is halophytes that can survive in extreme environmental conditions owing to their chemical content of complex molecules, in addition to their powerful antioxidant system [20,78,79]. All over the world, about 2500 species of halophytes are known and they can be utilized as edible, fodder, biofuel, medicine, chemicals, and ornamentals [15]. Recently, the scientific interest and the economic significance of halophytes have been highly demanding due to the medicinal and nutraceutical potential of its bioactive compounds [21].

The halophyte herbs, *B. indica* and *A. alopecuroides*, are deemed to be among the promising sources of natural compounds that need chemical and biological investigation. The knowledge about therapeutic potential of these halophytes is still ambiguous. Despite their possible content of various chemicals, these halophytes are being discarded as "waste" which generate serious environmental problems. Thus, utilization of these natural sources could be a sustainable resource for recovery of value-added products that can be employed in medicinal and industrial fields. The main purposes of this study was to investigate the chemical content and biological significance of *B. indica* and *A. alopecuroides* to emphasize the possible opportunities to utilize them in the treatment of non-communicable diseases (NCDs).

Non-communicable diseases (NCDs) are one of the challenges that greatly burden economy and health systems in many countries. Globally, NCDs are one of the leading causes of death, and around 41 million people killed by NCDs each year especially in low- and middle-income countries. Unfortunately, more than 15 million people die from NCDs between the ages of 30 and 70 years [80]. Cardiovascular diseases as heart attacks and stroke, cancers, dementia, AD, chronic respiratory diseases, obesity, and diabetes are types among NCDs. They account for 85% of deaths in Egypt, with cancer representing the second most common cause of mortality (14%). Egypt has released a plan for preventing and controlling NCDs, including cancer, which was initiated in 2018 [81]. The main goal of this plan is to achieve a reduction by 15% in the mortality from NCDs.

Consequently, there are many opportunities to utilize halophytes as a cheap natural source of candidate compounds for the treatment of NCDs and related complications.

To conclude, as halophytes deemed to contain complex scaffolds of compounds with multiple health properties [42,82], this study conducted to develop a utilization method for the recovery of high value-added molecules from halophytes that grow in arid and semi-arid regions of Egypt or Sahara Desert. Hence, these halophytes cannot be discarded as waste but instead can be regarded as a cheap source of highly valuable metabolites with potential health effects to be employed in drug discovery and cosmetic approaches. Therefore, the objectives of this study were; (i) to perform detailed chemical studies on *B. indica* and *A. alopecuroides*, followed by structural characterization of the metabolites; (ii) to investigate the potential of metabolites for the treatment of Alzheimer's disease (AD), cancer, and skin diseases as shown in Figure 5.
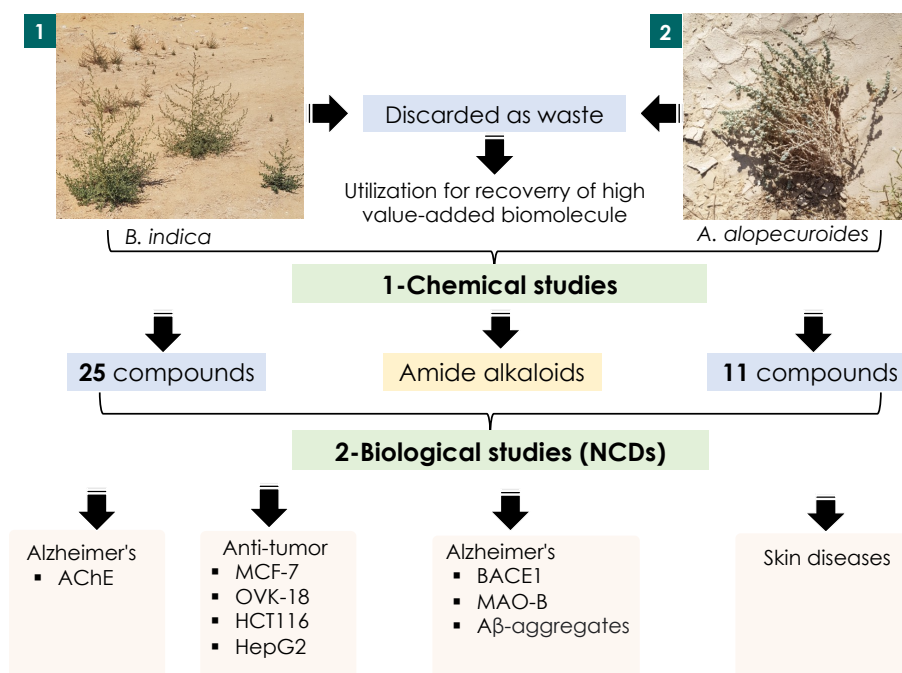


Figure 5: The main aspects for recovery of value-added compounds from halophytes in the study

# Chapter 2: Bassiamide A, a new alkaloid from the halophyte herb *Bassia indica*

## 2.1. Introduction

Halophytes are salt-tolerant plants able to grow in sandy areas, rocky coasts, and salt marches [79]. Bioactivities as anti-oxidant, anti-inflammatory, and anti-tumor are related with the ethnomedicinal activity of various halophyte species [83]. Nowadays, several studies concerned with the potential of salt-tolerant plants as promising sources of bioactive constituents [84]. Nutrients and bioactive compounds, such as polyphenols, terpenes, alkaloids, and other secondary metabolites have been discovered in several halophyte species [13]. Additionally, various species have been utilized for therapeutic purposes; for example: *Atriplex stocksii* has been reported for the treatment of fever, jaundice, and liver diseases; *Chenopodium album* has been used for constipation; the Mediterranean saltbush *Atriplex halimus* has been reported for the treatment of diabetes; *Bassia eriphora* has been reported for AD treatment; *Suaeda fruticosa* has been known for its antibacterial activity, etc. [16,33,82]. Moreover, halophytes have been recognized as potential health products (functional foods, nutraceuticals, bioactive products) in various economic fields such as pharmaceutical and cosmetic industries [85].

*Bassia* is a genus in Chenopodiaceae and represented with several species growing in Egypt including *Bassia indica* (Wight) A.J. Scott [10]. Plants within genus *Bassia* have been used for ornamental and therapeutic purposes [30,33,86,87]. Phytoecdysteroids, alkaloids, flavonoids, and saponins are among types of compounds have been discovered in genus *Bassia* [33,49,88–90]. Furthermore, species of genus *Bassia* have been discovered to display various biological activities, such as anti-fungal [26], analgesic, anti-inflammatory [91], anti-allergic [86], antipyretic, anti-tumor [30,61], antiviral [92], antioxidant [93], and anticholinesterase activity [50].

*Bassia indica* (Wight) A.J. Scott is an annual xero-halophyte herb or shrub endemic to Egypt. In the literature, *B. indica* has been reported to display bioactivities as cardiotonic, anticancer, and antioxidant [94]. Importantly, *B. indica* is widely distributed in the Egyptian ecosystem and considered a significant  economic source of chemical compounds. However, the chemical constituents and biological activities are still not fully reported. Nowadays, the healthcare consumers demanding more less use of synthetic chemicals and thus researchers are paying more attention toward the naturally occurring molecules

to fight various diseases. Hence, as a part of this study to isolate and identify new bioactive compounds from the halophytic plants of Egypt; the current study has resulted in isolation and identification of a new alkaloid, a rare occurring lignanamide, together with four known lignanamides and one lignan, from the aerial parts of *B. indica*. Furthermore, the study provides a future prospect toward the utilization of more species of Chenopodiaceae or Amaranthaceae plants.

## 2.2. Experimental

### 2.2.1. Plant material

The aerial parts of *B. indica* were collected from desert areas in Ihnasia ancient city, Beni-Suef, Egypt in August 2019. The plant was kindly identified by Prof. Ibrahim A. El-Garf, Professor of Botany, Faculty of Science, Cairo University, Egypt. A voucher specimen (BIC–2019) was deposited at the herbarium of Pharmacognosy and Medicinal Plants Department, Faculty of Pharmacy, Al-Azhar University, Cairo, Egypt.

### 2.2.2. Material for chromatographic studies

Columns for the isolation of compounds were obtained from GE Healthcare Biosciences, Uppsala, Sweden. Purification of compounds was performed using NP-silica gel (75–150 µm) and reversed-phase C18 (38-63 µm) obtained from Wako Company (Osaka, Japan). A Sephadex LH-20 was obtained from Sigma Aldrich (St. Louis, MO, USA) and a Diaion HP-20 was purchased from Mitsubishi Chemical Corporation (Tokyo, Japan). Moreover, medium-pressure liquid chromatography (MPLC) Pure C-850 Flash prep® (Buchi, Flawil, Switzerland) with UV and ELSD detection was used for purification of isolates using a C18 flash column (C-18, 20 µM) and preparative column Zorbax Extend-C18 PrepHT (21.2 × 150 mm, 5 µm, Agilent, Made in USA). The final purification of some compounds was performed on preparative RP-TLC glass plates 60 RP–18 $F_{254}$S (20 × 20 cm) (Merck, Darmstadt, Germany). TLC analysis was performed on precoated aluminum sheets of silica gel 60 $F_{254}$S (with fluorescent indicator 254 nm); layer thickness 0.2 mm; 20 × 20 cm pre-coated (Merck, Germany). Also, reversed-phase silica gel 60 RP-18 $F_{254}$S; 5 × 7.5 cm pre-coated aluminum sheets (Merck, Darmstadt, Germany) were used for investigation of fractions and isolated compounds. The solvent systems were applied for TLC investigation including *n*-Hexane–EtOAc 4:1; 1:1; 1:4, $CH_2Cl_2$–MeOH  4.5:0.5;

4:1; 1:1, CH$_2$Cl$_2$–MeOH-H$_2$O 4:1:0.2; 6.1:3.2:0.7, H$_2$O–MeOH, 7:3; 4:1; 1:1, H$_2$O–ACN, 7:3; 4:1; 1:1. Chromatograms were visualized under UV light at 254 and 365 nm and sprayed with 5% MeOH-H$_2$SO$_4$ and anisaldehyde–MeOH–H$_2$SO$_4$ reagents, followed by heating at 105 °C for 5 min.

### 2.2.3. Material for biological study

Galantamine hydrobromide was used in anti-acetylcholinesterase experiment as a positive control (Wako company, Osaka, Japan). Compounds were tested in various concentrations 0.1–250 µg/mL. Acetylcholinesterase enzyme from *Electrophorus electricus* (electriceel), 518 U/mg, was purchased from Sigma (St. Louis, MO, USA). Ellman's reagent, 5,5'-dithiobis [2-nitrobenzoic acid] (DTNB), was obtained from Wako company, Osaka, Japan. The buffer used in the anticholinesterase assay is buffer A and B. Buffer A is composed of Tris HCl (50 mM, molecular weight = 121.14) and the PH adjusted to 8, then the mixture mixed with 0.1 % BSA (100 mg Bovine serum albumin). Buffer B is composed of Tris HCL (50 mM, PH = 8), 0.1 M NaCl (molecular weight = 58.44), and 0.02 M MgCl$_2$.6H$_2$O (molecular weight = 203.03). Additionally, acetyl thiocholine iodide (20.48 mg in 5 ml Millipore H$_2$O) was used as substrate in the bioassay whereas 5.945 mg DTNB dissolved in 5 ml buffer B was used as Ellman's reagent.

### 2.2.4. Methods

### 2.2.4.1. HPLC analysis of the total methanol extract of *B. indica*

The aqueous methanol extract of *B. indica* was redissolved in MeOH to a final concentration of 5.0 mg/mL for HPLC analysis. Before injection for chromatographic separation, solution was filtered through Millipore 0.20 µM filters (Millex-LG, Japan). Agilent 1260–LC system (Agilent Technologies, Santa Clara, CA, USA) equipped with a vacuum degasser, autosampler, a binary pump and DAD detector (Agilent Technologies, Santa Clara, CA, USA) was used for the chromatographic separation, which was achieved by using a YMC-Triart C18 column (YMC Company, Kyoto, Japan; 150 × 4.6 mm, 5 µM), operated at 40 ºC with a flow rate of 0.4 mL/min. The mobile phases used were 0.1% formic acid in water (phase A) and 0.1% formic acid in acetonitrile (phase B). The analytes were eluted as follows: 0–1 min, 5% B; 1–40 min, 5–100% B; 40–50 min, 100% B; Finally, the B content was decreased to the initial conditions (5%) in 1 min and

the column re-equilibrated for 10 min. A volume of 10 μL of extract was injected. The detection was monitored with a DAD and ELSD detector. For data acquisition and monitoring the hardware, Agilent OpenLAB Chromatography Data System (CDS) EZChrom software (Agilent Technologies, Santa Clara, CA, USA) was used.

## 2.2.4.2. Phytochemical screening

In phytochemical screening, the prepared crude extract that contain primary and secondary metabolites was analyzed for the presence of phytoconstituents as carbohydrates, alkaloids, terpenes, saponins, and flavonoids [95]. In this study, the aqueous methanol extract of *B. indica* was phytochemically screened for its chemical constituents according to the standard methods available in the literature.

## 2.2.5. Chromatographic studies

Following phytochemical screening, a simple separation technique as thin-layer chromatography (TLC) is generally utilized to analyze the content and type of compounds present in the plant samples. In TLC, the extract and fractions are loaded on precoated silica gel plates which is then kept in a chromatographic chamber containing suitable developing solvents. This technique is composed of a mobile phase and a stationary phase, whereby compounds are separated based on their polarity. The standard techniques mentioned in chromatographic books (TLC, CC) were followed [96].

## 2.2.6. Extraction and isolation of compounds

The dried aerial parts of *B. indica* (1.3 Kg) were shade dried, finely pulverized, extracted with 80% methanol (7 L) three times at room temperature. The combined extracts were evaporated under reduced pressure to get a crude extract (138.5 g). The dried crude extract was then suspended in distilled water (500 mL) and successively partitioned with *n*-hexane (*n*-hex, 32 g), dichloromethane (DCM, 8 g), ethyl acetate (EtOAc, 4 g), *n*-butanol (Bu, 22 g) as shown in Figure 6.

The DCM fraction (7.5 g) was subjected to an open column chromatography using NP-silica gel (75–150 μm) eluted with *n*-hexane-EtOAc–MeOH (1:0:0–0:1:1 v/v) to afford 5 subfractions (D1–D5) as shown in Figure 7. Compound **1** was obtained after purification over a Sephadex LH-20 eluted with 100% MeOH. Subfraction D-3 (284.4 mg) was

purified using MPLC with RP-C18 column (20 µM, 4 g) eluted with $H_2O$–MeOH followed by purification over an open column packed with RP–18 silica gel eluted with $H_2O$–MeOH (6.5:3.5 v/v) to afford compounds **2** (6.7 mg) and **3** (10.5 mg).

The EtOAc fraction (3 g) was subjected to an open column chromatography packed with NP-silica gel (75–150 µm) eluted with *n*-hexane–EtOAc–MeOH (4:1:0–0:1:1 v/v) to afford 7 fractions followed by monitoring by TLC. The fractions that showed similar pattern were pooled together to afford 5 subfractions (Fr.E1 – Fr.E5) as shown in Figure 8. The fraction E4 was purified over a Sephadex LH-20 column eluted with 100% MeOH to obtain compound **4** (6.5 mg). Additionally, fraction E5 was subjected to further fractionation over MPLC with RP-C18 flash column (40 µM, 12 g) eluted gradually with $H_2O$–MeOH to give 5 subfractions (Fr.E5A – Fr.E5E). Compounds **5** (4.2 mg), **6** (6.5 mg), and **7** (2.5 mg) were obtained after purification of fraction E5C over silica gel CC eluted with $CH_2Cl_2$–MeOH (9.5:0.5) and ODS-18 ($H_2O$–MeOH).

The *n*-Butanol fraction (21 g) was chromatographed over a Diaion HP-20 using five mobile phases of $H_2O$–MeOH (1:0, 4:1, 1:1, 1:4, 0:1, each 10 L) to afford 5 fractions (Bu1 – Bu5) as shown in Figure 9. Fraction Bu3 was chromatographed over MPLC with RP-C18 flash column eluted with $H_2O$–MeOH (4:1 to 0:1) to give 3 fractions Bu3-1 – Bu3-3. Fraction Bu3-2 (1 g) was purified over MPLC with RP-C18 flash column (2 columns, each 12 gm) using $H_2O$–MeOH (4:1) as mobile phase to obtain 3 subfractions (Bu3-2A – Bu3-2C). Subfraction Bu3-2C was further purified over a preparative HPLC column (Zorbax Extend-C18 PrepHT, 21.2 × 150 mm, 5 µm) connected to MPLC and eluted with $H_2O$–MeOH (8:2–0:1) followed by final purification with RP–TLC with mobile phase of $H_2O$–MeOH (1:1) to furnish Compound **8** (4.5 mg).
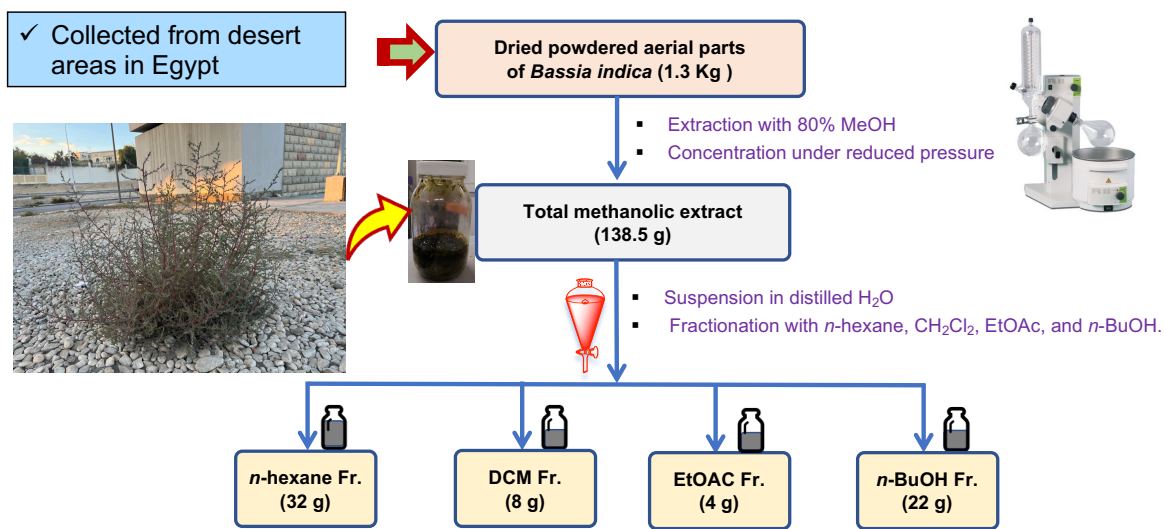
Figure 6: Extraction and fractionation of *B. indica*
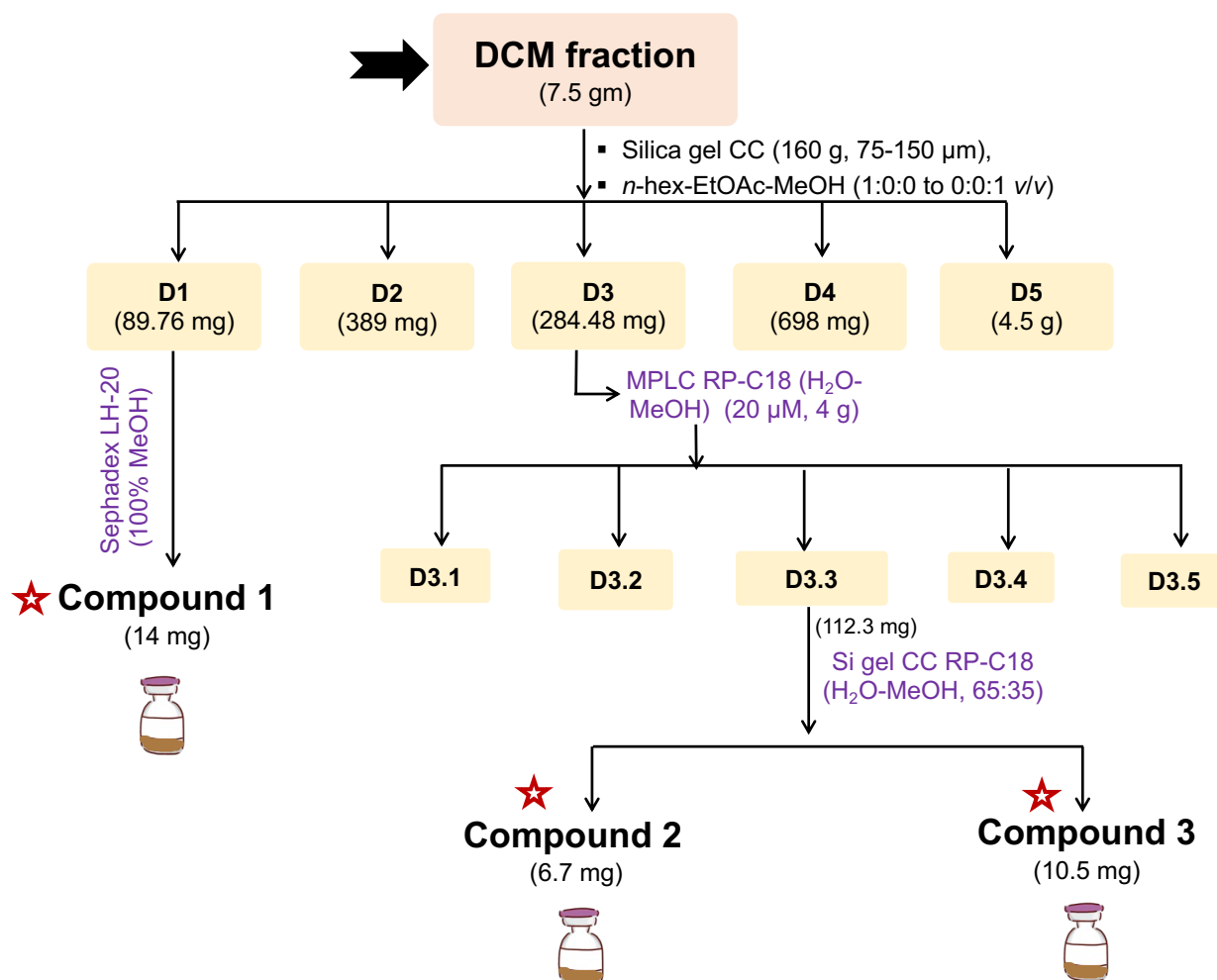
Figure 7: Isolation of compounds **1**–**3** from DCM extract of *B. indica*
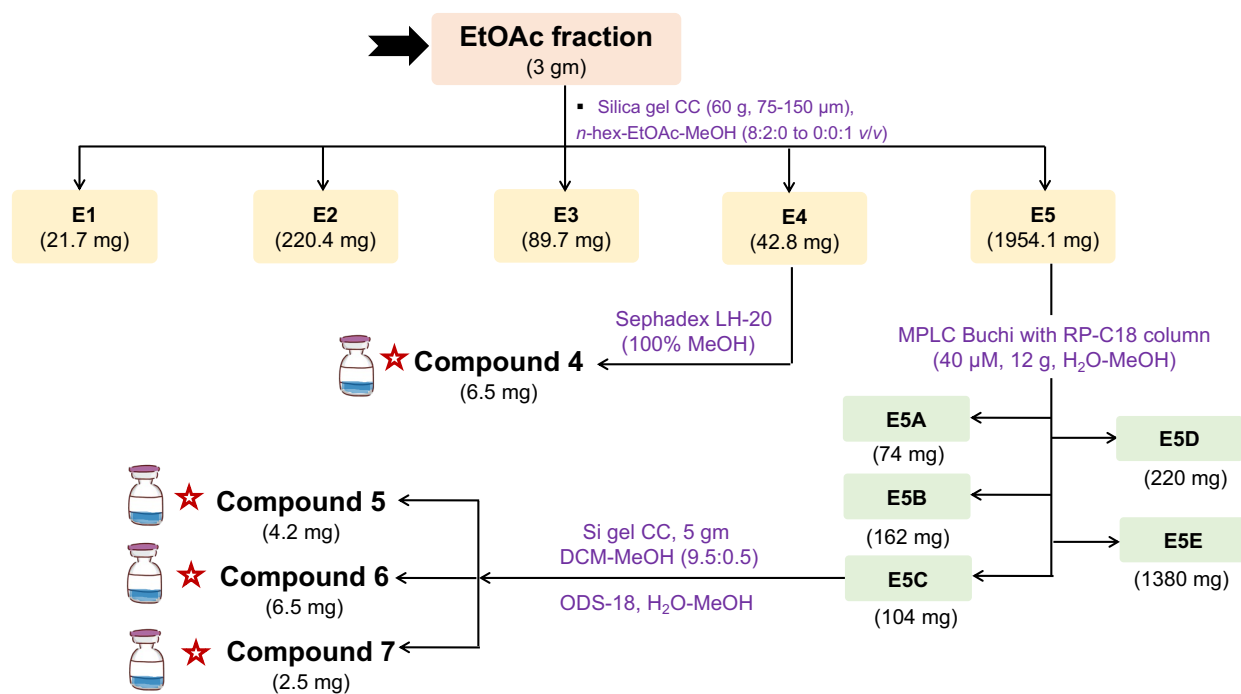
Figure 8: Isolation of compounds **4**–**7** from ethyl acetate extract of *B. indica*
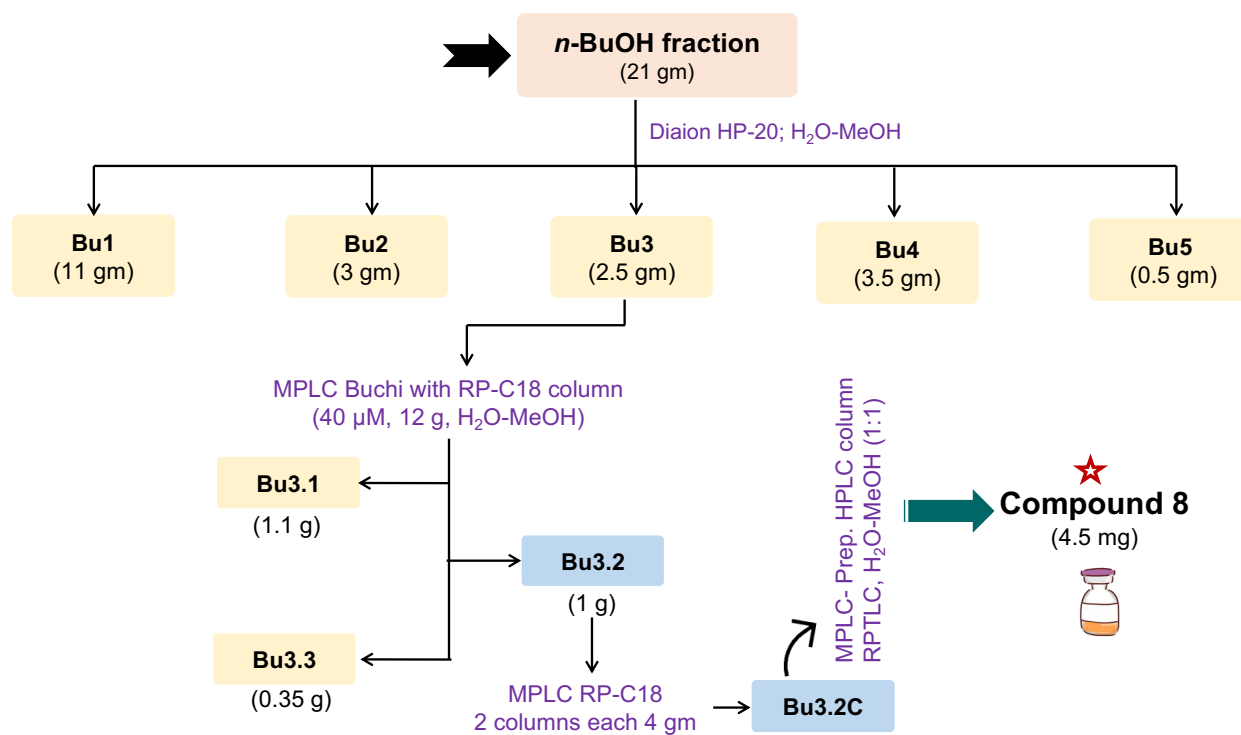
Figure 9: Isolation of compound **8** from *n*-butanol extract of *B. indica*

## 2.2.7. Procedure for identification of the isolated compounds

Optical rotations of isolates were recorded on a JASCO P-2200 digital polarimeter (JASCO International Co., Tokyo, Japan). Structures of isolates were identified by measuring the nuclear magnetic resonance spectroscopy (NMR). 1D ($^1$H, $^{13}$C) and 2D (HSQC, HMBC, COSY) NMR experiments were recorded on a DRX 600 spectrometer (Bruker Daltonics, Billerica, USA) using CD$_3$OD or DMSO-$d_6$ as solvent. Chemical shift was expressed in ppm while $J$ values were reported in Hz. Additionally, a quadrupole time-of-flight (qTOF) mass spectrometer (Agilent Technologies, USA) was operated to record HR-ESI-MS of the purified compounds.

## 2.2.8. Evaluation of acetylcholinesterase inhibitory activity

The inhibitory activity of isolates toward acetylcholinesterase enzyme was measured by the *in vitro* Ellman's assay [97]. In the assay, acetylcholinesterase enzyme can hydrolyze the substrate acetylthiocholine iodide to produce acetate and thiocholine. In a neutral and alkaline medium, thiocholine can reacts with DTNB to give a yellow colored complex, 2-nitro-5-thiobenzoate, which can be measured spectrophotometrically at 405 nm. To sum up, in a 96-well plate, 25 µL of 15 mM ACTI, 125 µL of 3 mM DTNB in buffer B (50 mM Tris HCl, PH = 8, 0.1 M NaCl, 0.02 M MgCl$_2$·6H$_2$O), 50 µL of buffer A (50 mM Tris-HCl, PH 8, 0.1% BSA) and 25 µL of tested sample (dissolved in 25% DMSO or methanol) were mixed, and the absorbance was  measured using a microplate reader at 405 nm every 16 s ten times. Then, 25 µL of AChE (0.25 U/mL in buffer A) was added and the absorbance was measured ten times every 16 s. A solution of 25% DMSO or methanol was used as a negative control. Absorbance was plotted against time and enzyme activity was calculated from the slope and expressed as a percentage compared to an assay using a buffer without any inhibitor. To avoid any increase in absorbance due to the color of the compounds or spontaneous hydrolysis of the substrate, the absorbance before addition of the enzyme was subtracted from the absorbance after adding the enzyme.

## 2.3. Results and discussion

The preliminary phytochemical screening of aqueous methanol extract of *B. indica* showed the presence of flavonoids, saponins, and nitrogenous compounds. The aqueous methanol extract of *B. indica* was sequentially partitioned using solvents of successive polarities (*n*-hexane, dichloromethane, ethyl acetate, and *n*-butanol). Different chromatographic procedures, including column chromatography (CC) packed with normal and reversed phase silica gel, Sephadex LH-20, Diaion HP-20, MPLC, and preparative TLC, were performed and led to isolation of eight compounds (**1**-**8**) as shown in Figure 10.

### 2.3.1. Determination of the isolated compounds

The chemical investigation of the aqueous methanol extract prepared from the dried aerial parts of *B. indica* has resulted in isolation and characterization of eight compounds (Figure 7). The structures of isolated compounds were elucidated based on different spectroscopic measurements including ^{1}H, ^{13}C, HSQC, HMBC, COSY NMR and HR-MS analysis. They were identified as *β*-sitosterol (**1**) [98], syringaresinol (**2**) [99], *N-trans*-feruloyl-3-methoxytyramine (**3**) [100], *N-trans*-feruloyltyramine (**4**) [101], *S*-(–)-*N-trans*-feruloylnormetanephrine (**5**) [102], *S*-(–)-*N-trans*-feruloyloctopamine (**6**) [103], *R*-(+)-*N-trans*-feruloyloctopamine (**7**)[104], and *N*-[(3-(3-methyl-1-oxo-butyl)amino)propyl]-3-(3,4-dihydroxyphenyl)prop-2-enamide (**8**), and named as bassiamide A.



3  $R_1$ = H,   $R_2$ = OCH$_3$
4  $R_1$ = H,   $R_2$ = H
5  $R_1$ = OH, $R_2$ = OCH$_3$
6  $R_1$ = OH, $R_2$ = H (7'*S*)
7  $R_1$ = OH, $R_2$ = H (7'*R*)
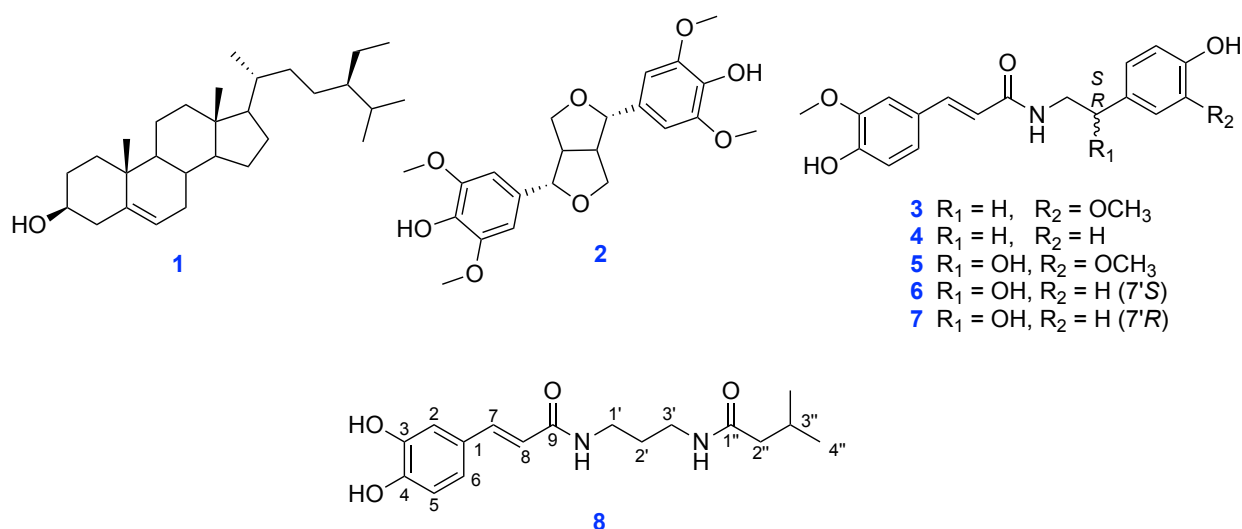
Figure 10: Chemical structures of isolated compounds **1**–**8** from *B. indica*

Compounds **6** and **7** were obtained from EtOAc fraction. Compound **7** is a rare occurring *R*-isomer amide alkaloid derivative and has been reported only isolated from root bark of *Lycium chinense* without determination of the configuration of C-7' position [104]. Hence, the configuration of C-7' in this study was determined for the first time. In this study, compound **7** was purified and completely separated from its *S*-isomer derivative (**6**), and other lignanamides through several purification steps. Moreover, the chemical structure of **7** was established through full NMR data and HRESIMS, as well as the published data for relative compounds in the literature [63,105]. The absolute configuration at C-7' was determined as *R*-isomer through measurement of optical rotation $[\alpha]_D^{25} + 24.3$ (*c* 0.02, MeOH). Accordingly, the isolated lignanamide (**7**) reported as a new finding of a rare occurring *R*-isomer *N-trans*-feruloyloctopamine.
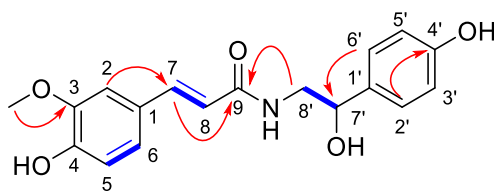


Figure 11: Key 2D correlation of compounds **6** and **7** from *B. indica*

HMBC ⟶　　COSY ▬▬

Compound **6**, $[\alpha]_D^{25} - 35.1$ (*c* 0.02, MeOH), was obtained as yellow amorphous powder. Optical rotation measurement of this compound indicated that **6** is *S*-isomer [63,105]. The molecular formula was determined to be $C_{18}H_{19}NO_5$ on the basis of the $[M - H]^-$ ion peak at *m/z* 328.1196 in the HRESIMS (calculated for $C_{18}H_{18}NO_5$, 328.1185). The $^1$H-NMR data of **6** (Table 4) indicated the existence of seven aromatic protons, two olefinic protons, one $CH_2$ protons, one methine proton, and one methoxy group. The presence of characteristic signals in the aromatic region indicated two benzene rings, one disubstituted and the other is trisubstituted. Signals resonated at $\delta_H$ 7.15 (d, *J* = 2.0 Hz), 6.80 (d, *J* = 8.2 Hz), and 7.04 (dd, *J* = 2.0, 8.2 Hz) were assigned for H-2, H-5, and H-6, respectively. On the other hand, set of aromatic signals appeared as a pair of *ortho*-coupled doublets at $\delta_H$ 7.24 (d, *J* = 8.3 Hz) and 6.78 (d, *J* = 8.3 Hz) were assigned for

(H-2', H-6') and (H-3', H-5'). A singlet signal at $\delta_H$ 3.89 was attributed to a methoxy group. The $\alpha, \beta$-unsaturated ketone with (E)-configuration confirmed by pair of downfielded doublets at $\delta_H$ 7.46 (d, $J$ = 15.6 Hz) and 6.47 (d, $J$ = 15.6 Hz). The downfielded signal at $\delta_H$ 4.73 (dd, $J$ = 4.9, 7.8 Hz) indicated a methine proton of C-7' which revealed that hydroxyl group was linked there.

The $^{13}$C-NMR data of **6** (Table 4) showed resonances for all 18 carbon atoms comprising six quaternary, two olefinic, one aliphatic $CH_2$, one aliphatic CH, seven aromatic CH, one $CH_3$. The downfield signals at $\delta_C$ 169.5 (C-9) indicated an amide C-atom. Signals resonated at $\delta_C$ 142.3 (C-7) and 118.6 (C-8) indicated a C=C bond in the compound. The two benzene rings were confirmed by signals at $\delta_C$ 128.2 (C-1), 111.5 (C-2), 149.3 (C-3), 149.9 (C-4), 116.5 (C-5), 123.3 (C-6), 134.7 (C-1'), 128.5 (C-2', C-6'), 116.1 (C-3', C-5'), 158.1 (C-4'), respectively. The N-connected aliphatic methylene was suggested by signals at $\delta_C$ 48.8, while signals at $\delta_C$ 73.4 revealed the presence of aliphatic methine group. In HMBC spectrum, cross-peaks between H-7 and C-9, H-2 and C-7, and H-5 and C-1 confirmed trisubstituted benzene ring and olefinic linkage. Moreover, the attachment of hydroxyethyl linkage to disubstituted benzene ring was proved by correlation of H-8'/C-1' and H-7'/H-6' as shown in Figure 11. Additionally, the cross interaction of H-8' with C-9 confirmed the attachment of dopamine derived part of compound with substituted cinnamic acid part which finally confirm the structure of **6**. In COSY experiment, the interaction of H-5/H-6, H-7/H-8, and H-7/'H-8' further confirm the structure of **6.** From the above-mentioned data, **6** was identified as (E)-S-(−)-N-[2-hydroxy-2-(4-hydroxy-phenyl)-ethyl]ferulamide, commonly known as N-trans-feruloyloctopamine.

The molecular formula of compound **7** was established to be to be $C_{18}H_{19}NO_5$ from the negative ion peak at $m/z$ 328.1195 [M − H]⁻ (calculated for $C_{18}H_{18}NO_5$, 328.1185). Additionally, the NMR data of **7** was very similar to **6**. Thus, **7** was identified as (E)-R-(+)-N-[2-hydroxy-2-(4-hydroxy-phenyl)-ethyl]ferulamide which is commonly known as N-trans-feruloyloctopamine. This is the first study concerning the isolation and characterization of R-(+)-N-trans-feruloyloctopamine.

Compound **8** was isolated as bright yellow amorphous powder. In HRESIMS analysis, the molecular formula of **8** was established by to be $C_{17}H_{24}N_2O_4$ according to the negative

ion peak in MS-spectrum at $m/z$ 319.1668 [M–H]$^-$ (calculated for $C_{17}H_{23}N_2O_4$, 319.1657). The $^1$H-NMR of **8** (Table 5) showed several characteristic signals. Two signals resonated at $\delta_H$ 7.21 (d, $J$ = 15.6 Hz) and $\delta_H$ 6.31 (d, $J$ = 15.6 Hz) were assigned for *trans*-coupled protons H-7 and H-8, while three peaks at $\delta_H$ 6.93 (d, $J$ = 1.9 Hz), $\delta_H$ 6.82 (dd, $J$ = 1.9, 8.1 Hz), and $\delta_H$ 6.74 (d, $J$ = 8.1 Hz) revealed the existence of trisubstituted aromatic protons. On the other hand, the *n*-propyl moiety is proved by signals at $\delta_H$ 3.14 (m), $\delta_H$ 3.04 (m), and $\delta_H$ 1.41 (m), whereas signals at $\delta_H$ 2.02 (d, $J$ = 6.0 Hz), $\delta_H$ 1.50 (m), and two doublet signals at $\delta_H$ 0.85 (d, $J$ = 6.7 Hz) and $\delta_H$ 0.84 (d, $J$ = 7.3 Hz) were assigned for 3-methylbutyl substitution moiety. The $^{13}$C-NMR spectrum and HSQC spectrum revealed 17 carbon signals which classified as 5 quaternary carbons ($\delta_C$ 145.5, 147.2, 126.4 for two oxygenated and one non-oxygenated quaternary carbons of aromatic moiety respectively, and $\delta_C$ 165.3 and 171.8 for two carbonyl groups), 6 methines (including two olefinic carbons at $\delta_C$ 138.9 and 118.6, while signals at $\delta_C$ 113.8, 115.7, 120.3 were assigned for aromatic methines, and $\delta_C$ 18.7 was assigned for aliphatic methine (-CH) of butyl moiety), 4 methylene carbons (three downfielded signals at $\delta_C$ 38.3, 38.1, and 37.4 and one upfielded methylene at $\delta_C$ 26.8 ppm), and two methyls ($\delta_C$ 13.6 and 13.9). Additionally, the HMBC spectrum showed correlations between $\delta_H$ 7.21 / $\delta_C$ 165.3, 113.8, and 120.3, together with a correlation of $\delta_H$ 6.82 / $\delta_C$ 147.2, confirming the presence of caffeic acid moiety. The *N*-connected methylenes of *n*-propyl moiety were confirmed by the HMBC correlations of $\delta_H$ 3.14, 3.04 with $\delta_C$ 165.3 and 171.8 respectively, whereas $^1$H-$^1$H COSY correlation of $\delta_H$ 1.41/ $\delta_H$ 3.14 and 3.04 was attributed for the additional methylene of *n*-propyl moiety as shown in Figure 12. In addition, the HMBC correlations of $\delta_H$ 2.02 and $\delta_H$ 1.50 with $\delta_C$ 171.8, together with $^1$H-$^1$H COSY correlations of $\delta_H$ 0.85 & 0.84 with methine at $\delta_H$ 1.50 confirmed the presence of 3-methylbutyl side chain. Finally, the structure of this alkaloid was confirmed by $^1$H-$^1$H COSY correlations of H-5/H-6, H-7/H-8, H-2'/H-1' and H-3', H-2"/H-3", and H-3"/H-4" and 3"-CH$_3$. Accordingly, the structure of **8** was determined as *N*-[(3-(3-methyl-1-oxo-butyl)amino)propyl]-3-(3,4-dihydroxyphenyl)prop-2-enamide, namely bassiamide A.
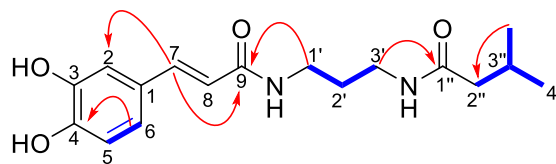
Figure 12: Key 2D correlations of compound **8** from *B. indica*

HMBC → COSY ▬

## 2.3.2. Determination of anti-acetylcholinesterase activity

Alzheimer's disease (AD) is an age-associated neurodegenerative disorder accompanied by memory loss, language difficulties, and cognitive disturbance in adults with age over 60. One of the key factors associated with pathology of AD is the depletion of a neurotransmitter acetylcholine (Ach) in brains. Ach is a neurotransmitter that is hydrolyzed through acetylcholinesterase (AChE). Recently, one of the most promising options for treatment of AD is to improve cholinergic neurotransmission and inhibit degradation of ACh in the CNS by using acetylcholinesterase inhibitory compounds [9].

In the present study, the acetylcholinesterase inhibitory activity of compounds (**1**-**8**) were tested. The obtained inhibitory values are shown in Table 6.

**Table 4**. $^1$H and $^{13}$C-NMR data for compounds **6** and **7** in CD$_3$OD (δ in ppm, *J* in Hz)

| Position | 6 $^1$H (*J* in Hz) | 6 $^{13}$C | 7 $^1$H (*J* in Hz) | 7 $^{13}$C |
|---|---|---|---|---|
| 1 | — | 128.2 | — | 128.1 |
| 2 | 7.15 d (2.0) | 111.5 | 7.09 d (1.9) | 111.5 |
| 3 | — | 149.3 | — | 149.4 |
| 4 | — | 149.9 | — | 150.0 |
| 5 | 6.80 d (8.2) | 116.5 | 6.77 d (8.2) | 116.1 |
| 6 | 7.04 dd (2.0, 8.2) | 123.3 | 6.99 dd (1.9, 8.2) | 123.3 |
| 7 | 7.46 d (15.6) | 142.3 | 7.41 d (15.7) | 142.1 |
| 8 | 6.47 (d, *J* = 15.6 Hz) | 118.6 | 6.37 d (15.7) | 118.7 |
| 9 | — | 169.5 | — | 169.2 |
| 1' | — | 134.7 | — | 134.4 |
| 2', 6' | 7.24 d (8.3) | 128.5 | 7.20 d (8.6) | 130.7 |
| 3', 5' | 6.78 d (8.3) | 116.1 | 6.69 d (8.6) | 116.3 |
| 4' | — | 158.1 | — | 157.0 |
| 7' | 4.73 dd (4.9, 7.8 Hz) | 73.4 | 4.69 dd (7.8, 5.1) | 73.5 |
| 8' | 3.54 dd (13.6, 4.9) | 48.8 | 3.49 dd (11.3, 5.0) | 47.5 |
| | 3,.45 dd (13.6, 4.9) | | 3.38 dd (9.2, 6.3) | |
| *O*-Me | 3.89 s | 56.4 | 3.86 s | 56.4 |

**Table 5**: $^1$H and $^{13}$C-NMR data for compounds **8** in DMSO-$d_6$ ($\delta$ in ppm, $J$ in Hz)

| Position | $^1$H ($J$ in Hz) | $^{13}$C |
|---|---|---|
| 1 | — | 126.4 |
| 2 | 6.93 d (1.9) | 113.8 |
| 3 | — | 145.5 |
| 4 | — | 147.2 |
| 5 | 6.74 d (8.1) | 115.7 |
| 6 | 6.82 dd (1.9, 8.1) | 120.3 |
| 7 | 7.21 d (15.6) | 138.9 |
| 8 | 6.31 d (15.6) | 118.6 |
| 9 | — | 165.3 |
| 1' | 3.14 m | 38.3 |
| 2' | 1.41 m | 26.8 |
| 3' | 3.04 m | 38.1 |
| 1" | — | 171.8 |
| 2" | 2.02 d (6.0) | 37.4 |
| 3" | 1.50 m | 18.7 |
| 4" | 0.85 d (6.7) | 13.9 |
| 3"-CH$_3$ | 0.84 d (7.3) | 13.6 |

**Table 6**: Anti-cholinesterase activity of isolated compounds **1**–**8**

| Compound | $IC_{50}$ (µg/mL) |
| --- | --- |
| 1 | 55.8 ± 3.8 |
| 2 | >250 (17%) |
| 3 | >250 (12%) |
| 4 | >250 (20%) |
| 5 | >250 (19.4%) |
| 6 | >250 |
| 7 | >250 (34%) |
| 8 | >250 |

### 2.3.3. Significance of lignanamides

Lignanamides are naturally occurring subgroup of lignan with an amide group. They are derived from oxidative coupling between phenylpropanoid units, and they are considered safe and able to provide potential health benefits [106] . Various pharmacological activities have been discovered for lignanamides, such as neuroprotection, anti-inflammatory, anti-hyperlipidemic [100], antioxidant [107], antimicrobial, antitubercular [108], anti-trypanosomal, antidiabetic activity [109], and reducing melanin hyperpigmentation in skin [63]. Phenolic amides, known as lignanamides, are chemically derived from the linkage of hydroxycinnamic acid and tyramine moiety through an amide bond. They are either simple monomers or oxidatively coupled to form dimers [107].

Nowadays, lignanamides have attracted the attention of chemists and natural product researchers to be either purified or chemically synthesized because of their interesting biological activities. Several studies showed that foods contain antioxidant constituents particularly phenolic amide derivatives are beneficial in decreasing the risk of dementia, improve cognitive functions and memory. Previous studies showed that lignanamides were isolated and identified from few members of Chenopodiaceae, for example, genus *Chenopodium* [110], genus *Atriplex* [52], genus *Nanophyton*, and genus *Salsola* [111].

Dimorphamides A–C and *N-trans*-feruloyltyramine are examples of lignamaides derivatives (dimers or monomers) previously reported from *Atriplex dimorphostagia* [112]. *N*-[2-(3,4-dihydroxyphenyl)-2-hydroxyethyl]-3-(4-methoxyphenyl) prop-2-enamide, *N*-[2-(3,4-dihydroxyphenyl)-2-hydroxyethyl]-3-(3,4-dimethoxyphenyl)prop-2-enamide, and *N*-[2-(3-hydroxy-4-methoxyphenyl)-2-hydroxyethyl]-3-(4-methoxyphenyl)-prop-2-enamide, have been isolated and identified from *Salsola foetida* and displayed tyrosinase inhibitory activity [63]. Moreover, *N*-(*E*)-*m*-hydroxycinnamoyl]tyramine, *N*-(*E*)-caffeoyltyramine, and *N*-(*E*)-feruloyltyramine have been reported from *Atriplex semibaccata* [52].

Even though the significance of lignanamides in food and pharmaceutical industry, they have not been reported in genus *Bassia*. Hence, in this study, lignanamides were targeted for their isolation and identification to enrich the chemical composition and provide a medicinal importance to the plant *B. indica*.

## 2.4. Conclusion

In summary, the chemical investigation of *B. indica* has resulted in purification and structure identification of 8 compounds including one new alkaloid, one lignan, and five lignanamides which subsequently enrich the chemical composition of this herb. The results of this study might provide new insights and prospects toward utilization of other halophytes of the family Chenopodiaceae owing to their content of lignanamides and nitrogenous compounds.

Additionally, the outcomes of this study provide an economic and medicinal importance of the plant *B. indica* since the plant can grow in saline, arid areas, and considered a cheap source of bioactive constituents. Interestingly, the isolated compounds in this study are reported for the first time in genus *Bassia*, from which two lignanamides, *S*-(–)-*N*-*trans*-feruloylnormetanephrine and *R*-(+)-*N*-*trans*-feruloyloctopamine, were first reported in family Chenopodiaceae. In addition, one new alkaloid named bassiamide A was isolated and identified here for the first time.

**Chapter 3: A novel acylated flavonol tetraglycoside and rare oleanane saponins with a unique acetal-linked dicarboxylic substituent from xero-halophyte *Bassia indica***

## 3.1. Introduction

Pharmaceutical agents have long been derived from medicinal plants. Accordingly, the long-term objectives of natural product researchers are to discover new pharmaceutical candidates based on plant-derived leads by using chemistry and biology approaches [113]. Up to date, there are many examples of plant-derived compounds that have been developed into effective drugs for treatment of various diseases, such as infectious diseases, Alzheimer, diabetes, and cancer, etc. [6].

Neurodegenerative diseases cause alterations in the CNS with psychological and physiological effects. AD is a neurological disorder affecting mainly elderly people and characterized with brain dysfunction and impaired memory[114]. The disease is accompanied by biochemical changes in the cholinergic system, including a significant decline in the neurotransmitter, acetylcholine (ACh). Acetylcholinesterase (AChE) is a hydrolyzing enzyme which cleaves ACh into choline and acetate. Consequently, targeting inhibition of AChE to elevate ACh levels in brain is a trend in drug discovery [9,115]. Currently, there is an urgent need to discover new efficient therapies for fighting AD and natural products are an emerging approach for AD therapy.

Halophytes are potential economic sources of nutrients, bioactive compounds, in addition to the ability to display substantial health benefits[13]. The halophyte family, Chenopodiaceae, comprised about 1400 species in 105 genera with several species growing in the Egyptian ecosystem [10]. According to previous studies, several chemicals related to diverse chemical classes have been discovered in Chenopodiaceae including alkaloids, saponins, flavonoid glycosides, ecdysteroids, sesquiterpenoids, lignanamides, phenolic acids, and coumarins [49,62,88,116–118], some of which showed significant bioactivities, such as antioxidant, anticholinesterase, anti-inflammatory, analgesic, antihyperlipidemic, antihypertensive, anti-tumor, hepatoprotective, antidiabetic, and tyrosinase inhibitory activity [50,52,53,63,70,91,119,120].

*B. indica* (Wight) A.J. Scott is a xero-halophyte herb, which is widely grown in Egypt. It is commonly discarded by rural people in Egypt leading to the waste of natural resources. Therefore, the utilization of such halophyte extracts with high nutritional and pharmaceutical values for their chemical and biological characterization represents a powerful tool in drug discovery with much less cost. As a continuation of our ongoing

efforts for the discovery of effective substances from halophytic plants, this study was designed aiming at isolation, identification, and characterization of compounds from *B. indica* growing in Egyptian desert lands in order to valorize such kind of plants and to shed more light toward utilization of halophytes as promising sources of novel bioactive constituents. Finally, the current study reports on the isolation and identification of **16** compounds including one new acylated flavonol tetraglycoside, a rarely occurring flavonol triglycoside, and two rare occurring *seco*-glycosidic oleanane saponins. The anticholinesterase activity of the isolated compounds was also determined.

## 3.2. Experimental

### 3.2.1. Plant material

See chapter 2

### 3.2.2. Material for chromatographic studies

Glass columns of variable dimensions were purchased from GE Healthcare Biosciences, Uppsala, Sweden. Biotage selekt equipped with RP-C18 flash columns (Biotage Selekt, Sfär C18 D Duo column, 30 µm, 30 and 60 g) obtained from Biotage Japan Ltd., Japan. Diaion HP-20 (Mitsubishi Chemical Corporation, Tokyo, Japan) was used for fractionation. The deionized water (18 MΩ cm) was obtained by using a Milli-Q purification system from Millipore (Bedford, MA, USA). Silica gel (normal phase; 75-150 µm) and RP-C18 (38-63 µm) were obtained from Wako Company (Osaka, Japan). Solvents used for extraction and chromatographic fractionation were purchased from Wako Pure Chemical Industries (Osaka, Japan). The final purification of isolates was successively achieved by MPLC (Pure C-850 Flash prep®, Buchi, Switzerland). HPLC preparative column (Zorbax Extend-C18 PrepHT, 21.2 × 150 mm, 5 µm, Agilent, USA) was also used for purification. Furthermore, compounds were purified on a preparative NP-TLC (Wako Pure Chemical Corporation, Osaka, Japan) and RP-TLC (Merck, Darmstadt, Germany). TLC investigation was carried out on plates precoated with silica gel $GF_{254}$ and RP18 $F_{254}$ (Merck, Darmstadt, Germany), then chromatograms were visualized under UV light at (254 and 365 nm) and sprayed with 10% MeOH-$H_2$SO4 and/or Liebermann–Burchard reagents, followed by heating for 5 min at 105°C. The NMR solvents, methanol-$d_4$ (CD$_3$OD), dimethyl sulfoxide (DMSO-$d_6$), deuterium oxide (D$_2$O),

and pyridine-$d_5$ (C$_5$D$_5$N), were purchased from Cambridge Isotope Laboratories (Andover, MA, USA).

### 3.2.3. Material for biological study

See Chapter 2

### 3.2.4. Extraction and isolation of phytoconstituents

The extraction of the aerial parts of *B. indica* were done as described in Chapter 2. The EtOAc fraction (3 g) was subjected to an open column chromatography packed with NP-silica gel and eluted with *n*-hexane-EtOAc-MeOH (4:1:0–0:1:1 v/v) to afford 7 fractions, followed by monitoring by TLC, then fractions with similar pattern were pooled together to get 5 subfractions (E1 – E5) as shown in Figure 13.

The fraction E-2 was purified over a Sephadex LH-20 and eluted with 100% MeOH to afford 3 subfractions (E2.1 – E2.3). Fraction E2.1 was subjected to purification over NP-TLC with CH$_2$Cl$_2$-MeOH (9:1) to obtain compounds **9** (6 mg), **10** (12 mg), **11** (8 mg), and **12** (10 mg). Subfraction E2.2 was subjected to a silica gel CC eluted with CH$_2$Cl$_2$–MeOH (9:1) to get **13** (19 mg) and **14** (8.5 mg). Compound **15** (3.3 mg) was obtained from fraction E2.3 after purification over a Sephadex LH–20 eluted with 100% MeOH. Additionally, fraction E5 was subjected to fractionation over MPLC with RP-C18 flash column (40 µM, 40 g) and eluted with H$_2$O–MeOH to give 5 subfractions (E5A – E5E). The fraction E5A was purified over a Sephadex LH-20 (100% MeOH) to obtain compound **16** (10 mg). Subfraction E5B was purified over a Sephadex LH-20 (100% MeOH) and NP-TLC (CH$_2$Cl$_2$–MeOH; 9:1) to obtain compound **17** (6.2 mg) and compound **18** (4.5 mg). Finally, the fraction E5E was purified over a Sephadex LH-20 eluted with 100% MeOH to obtain compound **19** (9 mg), and the rest of fraction was subjected to further purification over MPLC with RP-C18 and Sephadex LH-20 to afford compound **20** (7.5 mg).

The *n*-Butanol fraction (21 g) was chromatographed over a Diaion HP-20 using 5 mobile phases of H$_2$O–MeOH (1:0, 4:1, 1:1, 1:4, 0:1, each 10 L) to afford 5 fractions (Bu1 – Bu5) as seen in Figure 14. Fraction Bu3 was chromatographed over MPLC with RP-C18 flash column and eluted with H$_2$O–MeOH (4:1 to 0:1) to get 3 fractions Bu3-1 to Bu3-3. Fraction

Bu3–2 (1 g) was purified over MPLC with RP-C18 flash column (2 columns, each 4 gm) using $H_2O$–MeOH (4:1) as a mobile phase to obtain three subfractions (Bu3-2A – Bu3-2C). Subfraction Bu3-2B was further purified over MPLC with RP-C18 column (4 g) and eluted with $H_2O$–MeOH (4:1) to yield compound **21** and compound **22**.

The saponin containing fraction of *n*-BuOH extract was identified by a froth test where subfraction 4 (Bu4) was found to contain saponin compounds. Consequently, fraction Bu4 (3.5 g) was fractionated over Biotage system with RP-C18 column (30 μm, 30 gm) to obtain four fractions (Bu4-1 – Bu4-4). Subfraction Bu4-4 was purified over MPLC with RP-C18 flash column (2 columns, each 4 g) to obtain compound **23** (8 mg). Subfraction Bu4.4C was purified over an open column chromatography packed with RP-C18 eluted with $H_2O$–ACN (3.5:1.5) to obtain compounds **24** (12 mg).
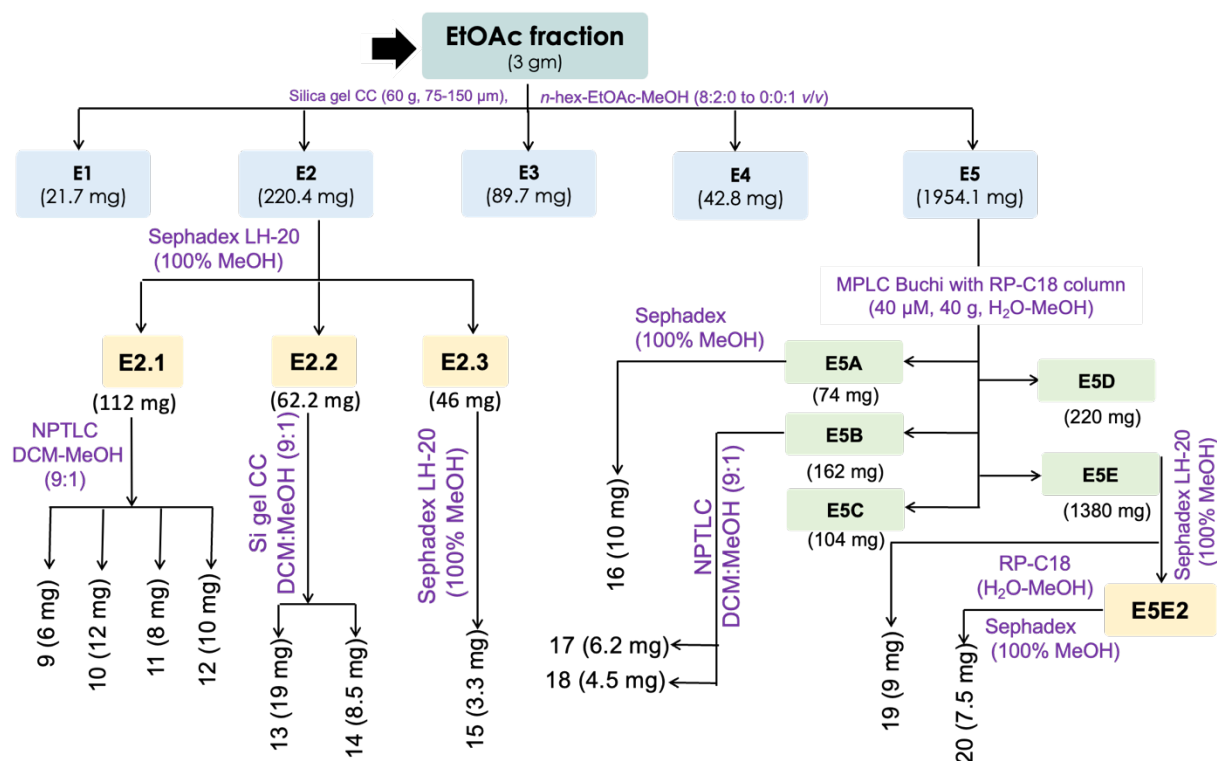


Figure 13: Isolation of compounds **9**–**20** from ethyl acetate extract of *B. indica*
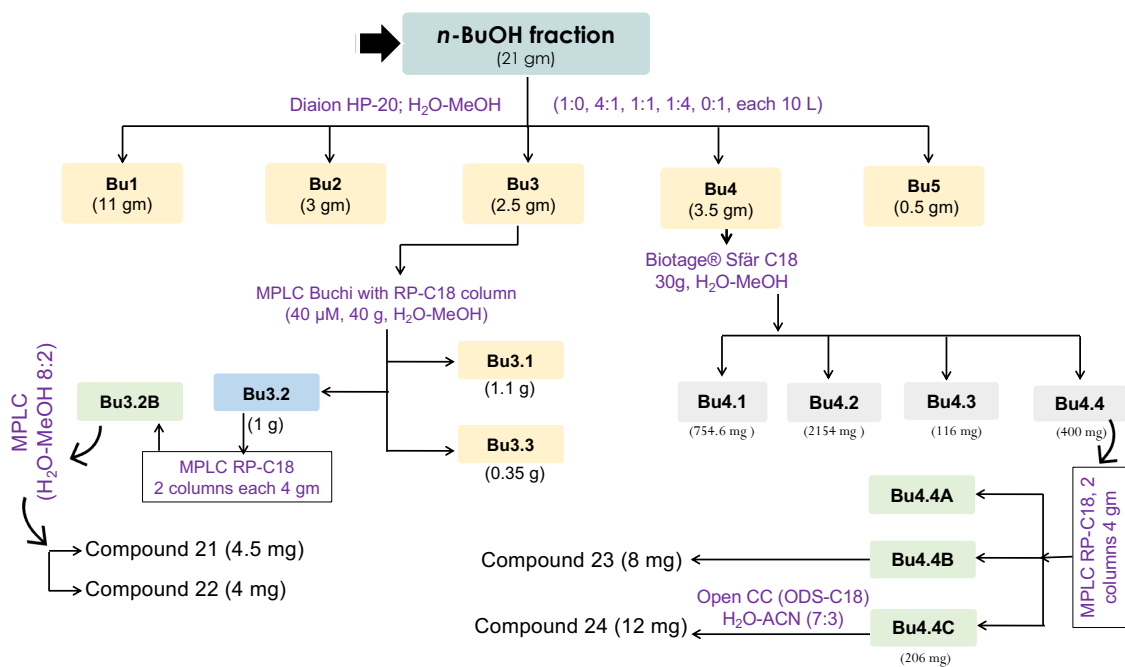
Figure 14: Isolation of compounds **21**–**24** from *n*-BuOH extract of *B. indica*

### 3.2.5. Procedure for identification of the isolated compounds

Optical activity of the isolates was measured on a JASCO P-2200 polarimeter. The chemical structure of pure isolates was identified by measuring the nuclear magnetic resonance spectroscopy (NMR) on a DRX 600 spectrometer (Bruker Daltonics, USA). Hence, 1D and 2D were recorded using $CD_3OD$, $C_5D_5N$, $D_2O$, and DMSO-$d_6$ as solvents. The chemical shift was expressed in ppm while $J$ values were reported in Hz. HRESIMS data for compounds were recorded on a quadrupole time-of-flight mass spectrometer (Agilent QTOF-LC-MS, Agilent Technologies, USA).

### 3.2.6. Evaluation of acetylcholinesterase inhibitory activity

The inhibitory activity of isolated compounds was evaluated against acetylcholinesterase enzyme *via* the *in vitro* Ellman's assay [97] as described in Chapter 2.

## 3.3. Results and discussion

The phytochemical investigation of the aq. MeOH extract prepared from the dried aerial parts of *B. indica* resulted in isolation of previously undescribed acylated flavonol tetraglycoside, along with a rare flavonol triglycoside and two rare triterpene *seco*-glycosidic oleanane saponins having a unique acetal-linked dicarboxylic acid substitution, in addition to 12 known compounds (Figure 15). The isolated compounds were categorized into phenolic acids, phenolic glycoside, dihydroxy coumarin, nucleic acids, flavonol aglycone, flavonol glycosides, and oleanane saponins. The structure of isolates was elucidated based on different spectroscopic techniques including ^{1}H, ^{13}C, APT, HSQC, HMBC, COSY NMR and HR-MS analysis.

### 3.3.1. Determination of isolated compounds

The chemical structure of isolated known compounds was determined based on various spectroscopic measurements, as well as comparison with published NMR data. They were identified as vanillic acid (**9**) [121], *o*-hydroxybenzoic acid (**10**) [122], *p*-hydroxybenzoic acid (**11**) [123], 6,7-dihydroxy coumarin (**12**) [124], methyl caffeate (**13**) [125], caffeic acid (**14**) [126], quercetin (**15**) [127], uracil (**16**) [128], thymidine (**17**) [112], tachioside (**18**) [129], isorhamnetin-3-*O*-*β*-D-glucoside (**19**), kaempferol-3-*O*-rutinoside (**20**) [130].

**9** $R_1$ = COOH, $R_2$ = H, $R_3$ = OCH$_3$, $R_4$ = OH
**10** $R_1$ = COOH, $R_2$ = OH, $R_3$ = H, $R_4$ = H
**11** $R_1$ = COOH, $R_2$ = H, $R_3$ = H, $R_4$ = OH
**18** $R_1$ = OH, $R_2$ = OCH$_3$, $R_3$ = H, $R_4$ = $\beta$-D-Glc

**12**

**13** R = OCH$_3$
**14** R = OH

**15** $R_1$ = OH, $R_2$ = OH
**19** $R_1$ = OCH$_3$, $R_2$ = $\beta$-D-Glc
**20** $R_1$ = H, $R_2$ = S1
**21** $R_1$ = H, $R_2$ = S2
**22** $R_1$ = OCH$_3$, $R_2$ = S3

**16**

**17**

**23** $R_1$ = $\beta$-D-Glc, $R_2$ = S2
**24** $R_1$ = $\beta$-D-Glc, $R_2$ = S3

**S1**

**S2**

**S3**

**S4**

**S5**
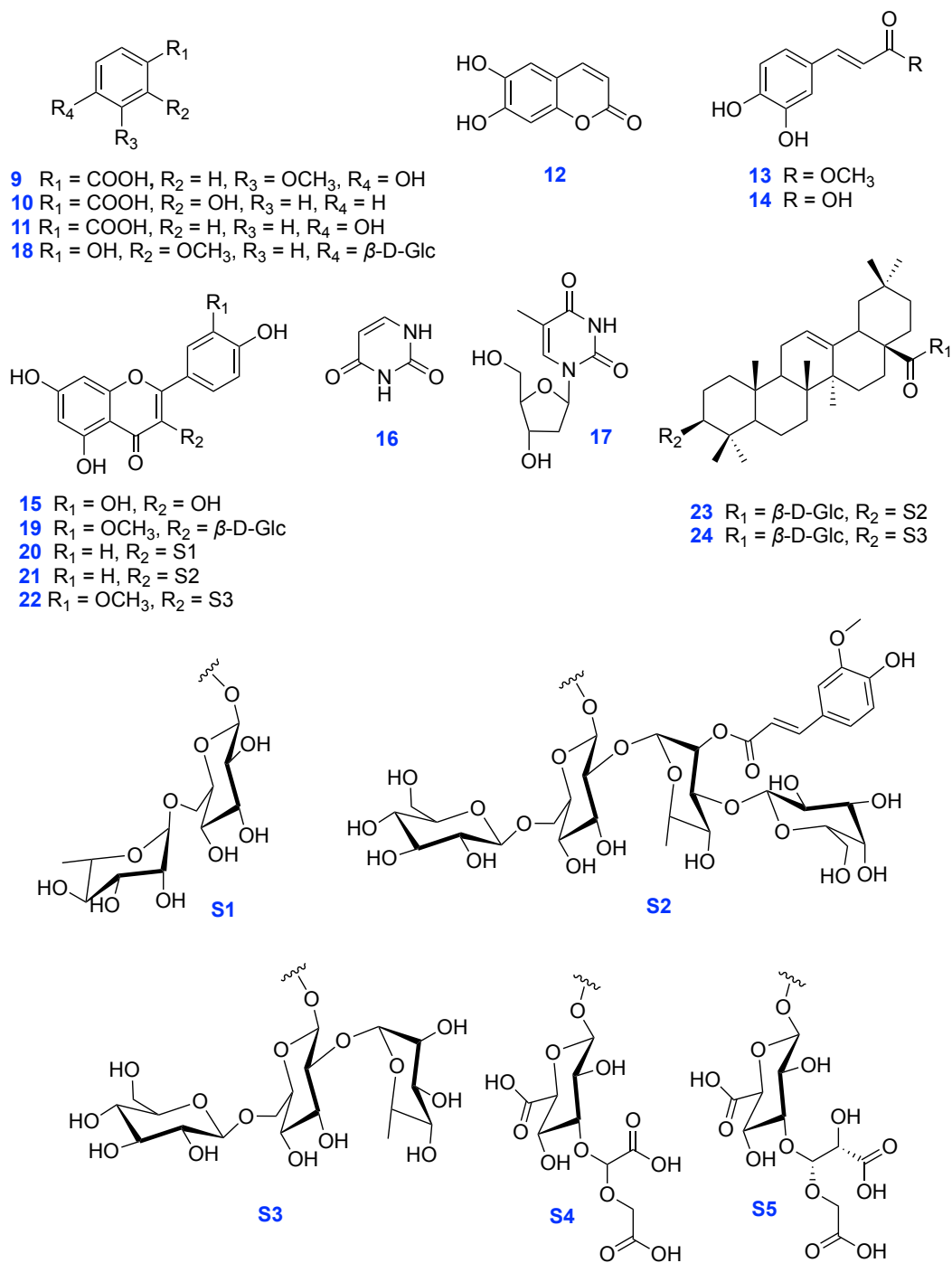
Figure 15: Chemical structures of isolated compounds **9**–**24** from *B. indica*

Compound **21** was isolated from *n*-BuOH fraction as yellow needles. Optical rotation of **21** was $[\alpha]_D^{25}$ – 30.1 (*c* 0.02, MeOH). The molecular formula was deduced to be $C_{49}H_{58}O_{28}$ from HRESIMS based upon the molecular ion peak at *m/z* 1093.3028 [M – H]⁻ (calculated for $C_{49}H_{57}O_{28}$, 1093.3036). The $^{1}H$, $^{13}C$, HSQC, HMBC, $^{1}H$-$^{1}H$ COSY experiments confirmed the presence of a flavonol moiety, four sugar moieties, in addition to a feruloyl moiety. The $^{1}H$ NMR data (Table 7) indicated several characteristic signals, one broad singlet aromatic proton at $\delta_H$ 7.14, six aromatic protons at $\delta_H$ 6.17 d (*J* = 1.6 Hz), 6.34 d (*J* = 1.6 Hz), 7.91 d (*J* = 8.7 Hz), 6.89 d (*J* = 8.7 Hz), 6.72 d (*J* = 8.3 Hz), 6.96 brd (J = 8.5 Hz), two doublet olefinic protons at $\delta_H$ 6.34 d (*J* = 15.6 Hz), 7.43 d (*J* = 15.6 Hz), one singlet aromatic methoxy proton at $\delta_H$ 3.78, and one doublet aliphatic methyl signal at $\delta_H$ 0.93 d (*J* = 6.2 Hz). The sugar moieties were identified by the presence of four anomeric signals resonated at $\delta_H$ 5.59 d (*J* = 7.6 Hz), 5.11 brs, 4.30 d (*J* = 7.6 Hz), 4.27 d (*J* = 7.6 Hz), in addition to signals at $\delta_H$ 3.05 – 4.84 for sugar protons. The $^{13}C$ NMR of **21** (Table 7) showed 49 carbon signals which were categorized into 2 methyls (one methoxy and one methyl of rhamnose), 3 methylenes, 29 methines, and 13 quaternary carbon signals, as confirmed with the aid of HSQC experiment. According to the HSQC data, the four anomeric protons were detected in $^{1}H$-NMR spectrum and found to be correlated with corresponding carbons 5.59 d / 97.9, 5.11 brs / 99.8, 4.30 d / 100.8, 4.27 d / 103.5. Furthermore, one doublet proton at $\delta_H$ 0.93, $\delta_C$ 18.1 indicated a rhamnose moiety. The $^{1}H$ and $^{13}C$ NMR spectral data, as well as comparison with previously published data exhibited a kaempferol glycoside [131,132]. The $^{13}C$ NMR also exhibited a methoxylated carbon signal at $\delta_C$ 56.1, alongside glycoside carbon signals at $\delta_C$ 61.2 – 84.5 ppm. The presence of a feruloyl moiety with *trans*-geometry was deduced basically from tow olefin doublets $\delta_H$ 6.34 and 7.43 which were correlated with carbons at $\delta_C$ 115.9 and 144.8, respectively. The HMBC correlation of anomeric proton at $\delta_H$ 5.59 and C-3 ($\delta_C$ 133.2) confirmed the glycosidic linkage at C-3 of the aglycone as shown in Figure 16. Other HMBC and HSQC correlations revealed that the *β*-D-glucopyranosyl sugar was the primary *O*-linked sugar at C-3. The HMBC cross-peaks of anomeric protons at $\delta_H$ 5.11 and 4.30 with C-2" ($\delta_C$ 80.1) and C-6" ($\delta_C$ 66.5), respectively, depicted that two sugars were linked to the primary sugar. The deshielded signal at $\delta_C$ 84.5 of C-3''' of rhamnose moiety suggested that another sugar monomer is linked there, which was then confirmed

by HMBC correlations of H-1'''' ($\delta_H$ 4.27) with C-3'''. Moreover, a feruloyl moiety was proved to be attached at H-2''' of rhamnose moiety as HMBC correlation was detected between downfielded triplet proton observed at $\delta_H$ 4.84 and carbonyl group of the feruloyl moiety at $\delta_C$ 166.2. Additionally, long range HMBC correlation between $\delta_H$ 6.34 (H-7''''') and carbonyl group (C-9''''') at $\delta_C$ 166.2 clearly confirmed the feruloyl moiety. The sugar moieties were determined through the total acid hydrolysis followed by examinations over TLC with authentic sugar samples that indicated the presence of glucose, rhamnose, and galactose. Hence, the absolute configuration of sugars has been determined as $\beta$- for glucose and galactose and $\alpha$- for rhamnose [133]. Accordingly, from the above-mentioned data, **21** was identified as kaempferol-3-*O*-$\beta$-D-glucopyranosyl-(1→6)-*O*-[$\beta$-D-galactopyranosyl-(1→3)-2-*O*-*trans*-feruloyl-$\alpha$-L-rhamnopyranosyl-(1→2)]-$\beta$-D-glucopyranoside.

Compound **22** was obtained as yellow amorphous powder and purified from *n*-BuOH fraction. It is a very rare flavonol triglycoside which has been previously reported only from *Allium Neapolitanum* [134]. Thus, **22** was isolated and elucidated through comparing our data with the published NMR data, as well as HRESIMS analysis. The molecular formula was determined to be $C_{34}H_{42}O_{21}$ based upon the molecular ion peak in negative ion mode at *m/z* 785.2136 [M − H]⁻, (calculated for $C_{34}H_{41}O_2$ 785.2140).

Consequently, **22** was identified as isorhamnetin-3-*O*-$\beta$-D-glucopyranosyl-(1→6)-*O*-[$\alpha$-L-rhamnopyranosyl-(1→2)]-$\beta$-D-glucopyranoside. The isolation and identification of this compound is a new finding in Chenopodiaceae or Amaranthaceae and reported to be a rare occurring in nature.

Compound **23** was obtained as white amorphous powder from *n*-BuOH fraction. The molecular formula of **23** was established by HRESIMS to be $C_{46}H_{70}O_{19}$ from the [M − H]⁻ ion at *m/z* 925.4428 (calculated for $C_{46}H_{69}O_{19}$, 925.4433). The $^1$H, $^{13}$C, and HSQC NMR spectra of **23** showed characteristic signals for oleanolic acid aglycone, seven tertiary methyl signals at $\delta_H$ 0.59 (H-25), 0.71 (H-30), 0.72 (H-26), 0.75 (H-27), 0.77 (H-24), 0.94 (H-29), 1.01 (H-23), olefinic proton at $\delta_H$ 5.14 (brs, H-12), in addition to two olefinic carbons at $\delta_C$ 122.1, $\delta_C$ 143.2, and carbonyl signal at $\delta_C$ 177.3, which are characteristic features for triterpene oleanane aglycone [135]. The $^{13}$C NMR spectrum (Table 8) exhibited

7 methyls, 12 methylene, 16 methine, 11 quaternary carbons. The HSQC correlations of $\delta_H$ 5.74 (d, $J$ = 8.1 Hz) and $\delta_H$ 4.67 (d, $J$ = 7.5 Hz) with $\delta_C$ 94.2 and $\delta_C$ 104.5 confirmed the presence of two sugar monomers. The HMBC cross-peaks of anomeric protons at $\delta_H$ 5.74 with $\delta_C$ 177.3 (C-28), $\delta_H$ 4.67 with $\delta_C$ 175.2 (C-6') and $\delta_C$ 89.6 (C-3) revealed that two sugars, *β*-D-glucose and *β*-D-glucuronic acid, were linked to C-28 and C-3, respectively. The deshielded signal at $\delta_C$ 84.4 of C-3' indicated that another side chain is linked there, which was then proved by HMBC correlations of $\delta_H$ 5.43 (H-2") with $\delta_C$ 84.4 (C-3') and $\delta_C$ 66.4 (C-3"). The suggested *seco*-glycosidic dicarboxylic substitution at C-3' was further confirmed by HMBC correlations of two protons at $\delta_H$ 4.56 (d, $J$ = 14.8 Hz), $\delta_H$ 4.45 (d, $J$ = 15.2) with $\delta_C$ 101.4 (C-2") and 177.1 (C-4") as seen in Figure 17. Finally, from the above-mentioned data, **23** was identified as 3-*O*-[2'-(2"-*O*-glycolyl)-glyoxylyl-*β*-D-glucuronopyranosyl]-28-*O*-*β*-D-glucopyranosyl-olean-12-en-3*β*-ol-28-oic acid. It was found in a good agreement with the isolated one in the literature [66]. The compound is a rare occurring *seco*-glycosidic oleanane saponin.

Compound **24** was obtained as white amorphous powder from *n*-BuOH fraction. The HRESIMS spectrum of **24** showed a [M – H]$^-$ ion at *m/z* 955.4538 (calcd. for $C_{47}H_{71}O_{20}$ 955.4539). Thus, the molecular formula established to be $C_{47}H_{72}O_{20}$. The $^1$H and APT NMR spectra of **24** showed seven methyl signals at $\delta_H$ 0.59 (H-25), 0.71 (H-30), 0.72 (H-26), 0.75 (H-27), 0.77 (H-24), 0.94 (H-29), 1.01 (H-23), one signal at $\delta_H$ 3.10 (dd, J = 3.5, 11.5 Hz, H-3), one olefinic proton at $\delta_H$ 5.14 (brs, H-12), two olefinic carbons at $\delta_C$ 122.6 and 143.6, and carbonyl signal at $\delta_C$ 177.8 indicating a triterpene oleanane aglycone [135]. The signals at $\delta_H$ 4.58 (d, $J$ = 2.5 Hz), $\delta_H$ 5.50 (d, $J$ = 2.5 Hz), $\delta_H$ 4.70 (d, $J$ = 15.5 Hz), and $\delta_H$ 4.40 (d, $J$ = 15.4) revealed the presence of oxo-propionic acid and glycolyl moieties. The APT NMR and HSQC data exhibited the presence of 47 carbon signals including seven methyls, twelve methylene, seventeen methine, eleven quaternary carbons. The HSQC correlations of $\delta_H$ 5.73 (d, $J$ = 8.2 Hz) and $\delta_H$ 4.68 (d, $J$ = 7.5 Hz) with $\delta_C$ 94.7 and $\delta_C$ 105.1 revealed the presence of two anomeric carbons for two sugar monomers, which is in a good agreement with the published data for very related saponin compounds in the literature [64,136]. The deshielded carbon signal at $\delta_C$ 83.5 of C-3' of glucuronic acid suggested that another side chain is linked there, where the HMBC correlations of $\delta_H$ 5.50 with $\delta_C$ 83.5 (C-3') confirmed the acetal-linked dicarboxylic acid

substitution at C-3'. Moreover, the *seco*-glycosidic acetal-linked substitution moiety was proved by other HMBC correlations of H-2" at $\delta_H$ 4.58 with $\delta_C$ 177.6 (C-1") and $\delta_C$ 104.9 (C-3"), in addition to the correlations of protons at $\delta_H$ 4.70, $\delta_H$ 4.40 (H-4"a and H-4"b) with $\delta_C$ 177.9 (C-5") and $\delta_C$ 104.9 (C-3") as shown in Figure 17. The two stereocenters of the 2" and 3" positions of *seco*-glycosidic substitution were assigned to be *R* and *S*, respectively, based on comparison of the detailed NMR data with the related dimethyl ester derivative previously published in the literature [136]. Based upon all the above-mentioned evidences, compound **24** was elucidated as (2'*R*,3'*S*)-3-*O*-[2'-hydroxy-3'-(2"-*O*-glycolyl)-oxo-propionic acid-*β*-D-glucuronopyranosyl]-28-*O*-*β*-D-glucopyranosyl-olean-12-en-3*β*-ol-28-oic acid.

### 3.3.2. Acetylcholinesterase inhibitory activity of the isolated metabolites from *B. indica*

Alzheimer's disease (AD) was first identified by Alois Alzheimer in 1907 and it is one of the most common dementia types in the world with a rapid growing number of cases [137]. Some of common symptoms of AD include psychomotor dysregulation, delusions, and hallucinations[138]. The principal function of acetylcholinesterase enzyme is the termination of nerve impulse transmission at cholinergic synapses by degradation of acetylcholine (ACh) [139]. The neurotransmitter acetylcholine in the brain is responsible for learning and memory functions; hence, the decreased levels of acetylcholine, loss of cholinergic function, and the abnormal cholinergic signaling are related to the pathophysiology of AD. Therefore, the inhibition of AChE to elevate the levels of acetylcholine and improve the cholinergic functions in brain serves as a strategy and one of the effective approaches for the treatment of AD, dementia, ataxia, and Parkinson's disease [97].

For the treatment of cognitive impairment and memory loss associated with AD, there are few available synthetic drugs such as tacrine, donepezil, and the natural based rivastigmine. However, gastrointestinal disturbances and bioavailability issues have been reported as side effects of currently available drugs. In addition, the current therapies are not satisfactory to stop the progression or development of AD. Consequently, the necessity for finding better AChE inhibitors from natural sources has gained attention. Variety of plants have been reported to exert AChE inhibitory activity and are effective

for the treatment of neurodegenerative disorders such as AD [140,141]. Based on Ellman's assay, several methods for testing of AChE inhibitory activity from natural sources have been reported. The plant *B. indica* has deemed as a very cheap source of novel bioactive compounds. Hence, from the economical point of view, it is very interesting to screen the bioactivity of this herb to provide basis for further research and development of this medicinal plant as a source of potential lead drugs for treatment of AD. Thus, the isolated compounds were evaluated for their capacity to inhibit AChE and some of them showed promising activity against AChE. Among the tested isolates, compounds **12, 15, 20, 24, 17,** and **23** exhibited marked inhibitory activity toward the acetylcholinesterase enzyme with $IC_{50}$ values 3.6, 18, 27.9, 29.6, 45.7, 63.1 µg.mL$^{-1}$, respectively, compared to the standard drug galantamine. Additionally, other compounds showed moderate inhibitory activity as shown in Table 9.

Flavonoids are a diverse group of polyphenolic compounds found in all parts of plants and they are important components of nearly all plant-based foods. It was previously reported that phenolic acids and flavonoids are capable to reduce the oxidative stress and consequently they are considered as potential leads for development of cholinesterase inhibitors that can be used for treatment of AD [142]. In addition, flavonoids and phenolic acid derivatives have been considered as health-promoting agents with *in vitro* and *in vivo* biological effects including anti-inflammatory, antioxidant, and nephroprotective properties [141,143]. Hence, the phenolic constituents can play an important role in the improvement of cognitive symptoms and protect against neurodegenerative disorders. Furthermore, phenolic acids have some benefits over the well-known inhibitors as they are commonly distributed in variety of foods and their daily intake with food has no adverse effects. As a result, the phenolic-derived phytoconstituents should be considered for the dietary prevention of AD [144].

From the structural activity relationship (SAR), it was concluded that the presence and position of hydroxyl (OH) group at ring A and ring B, and the unsaturated ring C is responsible for the maximal acetylcholinesterase inhibitory activity of most flavonoid compounds [141]. The literature showed that the maximum anticholinesterase activity of some flavonoids is due to the presence of OH group at position 5, 6 and 7 of ring A.

Therefore, the alteration of the position of OH group in ring A led to decreased or absence of the activity [141]. Flavonoids as quercetin (**15**) and related flavonoids in aglycone form showed significant inhibitory activity against AChE. Also, number of flavonoid glycosides have been reported for their efficacy against AChE [115,145]. In the current study, flavonoid glycosides (**19** and **20**) exhibited marked inhibitory activity, whereas the activity has been dramatically declined with the presence of more sugar moieties which are clearly shown in compounds **21** and **22**.

The activity of phenolic acids toward AChE was dependent mainly on the number and/or position of OH groups and propenoic acid side chain. For instance, the isolated compound **9** showed a relatively high activity in comparison with **10** and **11**. Also, compound **12** with catechol and cyclized pyrone moieties showed a significant inhibitory activity against AChE with $IC_{50}$ 3.6 μg/mL. In the literature, it was reported that the presence of propenoic (CH=CH-COOH) group (caffeic acid) has a significant effect on the activity toward AChE compared with $CH_2$-$CH_2$-COOH (hydrocaffeic acid) or COOH groups (protocatechuic acid) [144]. Besides, the methylated phenolic acids as methyl caffeate showed a marked decline in the inhibitory activity.
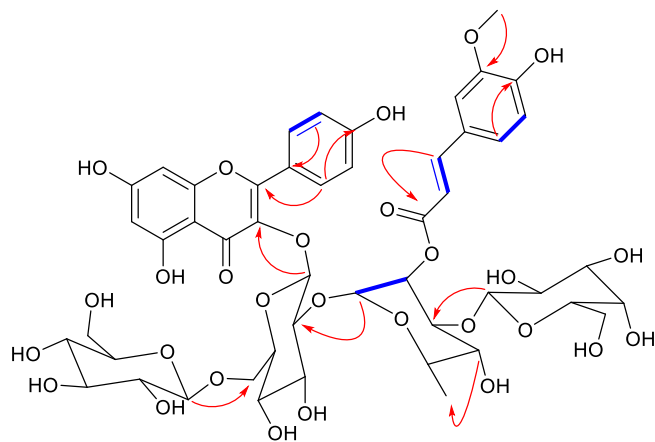
Figure 16: Key 2D correlations of compound **21** from *B. indica*

HMBC ⟶    COSY ▬▬



23

24
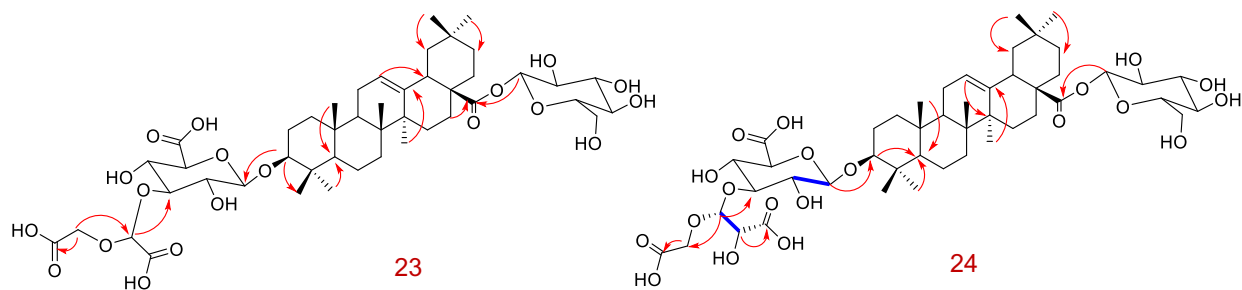
Figure 17: Key 2D correlations for **23** and **24** from *B. indica*

HMBC ⟶    COSY ▬▬

**Table 7**: $^1H$ and $^{13}C$-NMR data of compound **21** in DMSO-$d_6$ (δ in ppm, *J* in Hz)

| No. | δ_H | δ_C | No. | δ_H | δ_C | No. | δ_H | δ_C |
|---|---|---|---|---|---|---|---|---|
| | **Aglycone** | | | **α-L-Rhamnopyranoside** | | | **Feruloyl moiety** | |
| 1 | — | | 1''' | 5.11 brs | 99.8 | 1'''''' | — | 126.2 |
| 2 | — | 156.9 | 2''' | 4.84 t (8.6) | 72.3 | 2'''''' | 7.14 brs | 111.7 |
| 3 | — | 133.2 | 3''' | 3.68 m | 84.5 | 3'''''' | — | 148.3 |
| 4 | — | 177.8 | 4''' | 3.04 m | 72.3 | 4'''''' | — | 149.5 |
| 5 | — | 161.7 | 5''' | 3.17 m | 68.6 | 5'''''' | 6.72 d (8.3) | 115.7 |
| 6 | 6.17 d (1.6) | 99.1 | 6''' | 0.93 d (6.2) | 18.1 | 6'''''' | 6.96 brd | 122.9 |
| 7 | — | 164.4 | | **β-D-Glucopyranoside** | | 7'''''' | 6.34 d (15.6) | 115.9 |
| 8 | 6.34 d (1.6) | 94.1 | 1'''' | 4.30 d (7.6) | 100.9 | 8'''''' | 7.43 d (15.6) | 144.8 |
| 9 | — | 156.8 | 2'''' | 3.20* m | 70.8 | 9'''''' | — | 166.2 |
| 10 | — | 104.4 | 3'''' | 3.40 m | 68.9 | O-Me | 3.78 s | 56.1 |
| 1' | — | 121.5 | 4'''' | 3.51* m | 76.9 | | | |
| 2', 6' | 7.91 d (8.7) | 131.3 | 5'''' | 3.28 m | 75.9 | | | |
| 3', 5' | 6.89 d (8.7) | 115.7 | 6'''' | 3.51-3.70* m | 61.1 | | | |
| 4' | — | 160.2 | | **β-D-Galactopyranoside** | | | | |
| | **β-D-Glucopyranoside** | | 1''''' | 4.27 d (7.6) | 103.5 | | | |
| 1'' | 5.59 d (7.6) | 97.9 | 2''''' | 3.03-3.33* m | 70.7 | | | |
| 2'' | 3.51 m | 80.1 | 3''''' | 3.33-3.40* m | 77.4 | | | |
| 3'' | 3.67 m | 76.6 | 4''''' | 3.18 m | 68.7 | | | |
| 4'' | 3.74 m | 70.4 | 5''''' | 3.70* m | 76.8 | | | |
| 5'' | 3.01 m | 73.7 | 6''''' | 3.77 m | 61.5 | | | |
| | | | | 3.83 m | | | | |
| 6'' | 3.57 m | 66.5 | | | | | | |
| | 3.18 m | | | | | | | |

**Table 8**: $^1$H and $^{13}$C-NMR data of compounds **23** and **24** in $D_2O$-$C_5D_5N$ ($\delta$ in ppm, $J$ in Hz)

| No. | Compound 23 $\delta_H$ ($J$ in Hz) | $\delta_C$ | Compound 24 $\delta_H$ ($J$ in Hz) | $\delta_C$ |
|---|---|---|---|---|
| 1 | 0.85 m | 38.3 | 1.16 m | 39.2 |
| 2 | 1.64 m, 1.93 m | 25.2 | 1.73 m, 1.92 m | 25.7 |
| 3 | 3.11 dd (3.5, 11.6) | 89.6 | 3.10 dd (3.5, 11.6) | 90.0 |
| 4 | — | 37.7 | — | 38.7 |
| 5 | 0.46 brd | 54.9 | 0.45 d (11.7) | 55.3 |
| 6 | – | 17.5 | — | 17.9 |
| 7 | 1.15 m | 32.9 | 1.14 m | 36.3 |
| 8 | — | 41.1 | — | 41.6 |
| 9 | — | 48.6 | — | 47.4 |
| 10 | — | 35.8 | — | 38.1 |
| 11 | 1.55 m | 22.8 | 1.59 m | 23.2 |
| 12 | 5.14 brs | 122.1 | 5.14 brs | 122.6 |
| 13 | — | 143.2 | — | 143.6 |
| 14 | — | 45.4 | — | 45.8 |
| 15 | 1.25 m | 29.6 | 1.24 m | 29.0 |
| 16 | 1.82 m | 22.3 | 1.83 m | 22.8 |
| 17 | —— | 45.4 | – | 46.9 |
| 18 | 2.82 m | 40.6 | 2.83 m | 41.2 |
| 19 | 1.22 m | 46.4 | 1.22 m | 46.4 |
| 20 | – | 31.5 | – | 32.5 |
| 21 | 1.05 m | 32.0 | 1.05 m | 30.1 |
| 22 | 1.53 m | 32.2 | 1.53 m | 36.2 |
| 23 | 1.01 s | 27.2 | 1.01 s | 27.6 |
| 24 | 0.77 s | 15.9 | 0.77 s | 16.3 |
| 25 | 0.59 s | 14.5 | 0.59 s | 14.9 |
| 26 | 0.72 s | 16.4 | 0.72 s | 16.8 |
| 27 | 0.75 s | 25.1 | 0.75 s | 25.6 |
| 28 | — | 177.3 | — | 177.8 |
| 29 | 0.94 s | 32.2 | 0.94 s | 32.6 |
| 30 | 0.71 s | 22.7 | 0.71 s | 23.1 |

| | 3-*O-β*-D-Glucuronic acid | | 3- *O-β*-D-Glucuronic acid | |
|---|---|---|---|---|
| 1' | 4.67 d (7.5) | 104.5 | 4.68 d (7.5) | 105.1 |
| 2' | 3.84 m | 73.6 | 3.84 m | 74.1 |
| 3' | 3.97 m | 84.4 | 4.03 dd (9.5, 11.5) | 83.5 |
| 4' | 3.82 m | 72.1 | 3.82 m | 71.6 |
| 5' | 4.05 m | 76.9 | 4.04 m | 76.7 |
| 6' | — | 175.2 | — | 174.4 |
| **Substitution at C-3 of Glucuronic acid** | | | **Substitution at C-3 of Glucuronic acid** | |
| 1" | — | 174.4 | — | 177.6 |
| 2" | 5.43 s | 101.4 | 4.58 d (2.5) | 74.1 |
| 3" | 4.56 d (14.8) | 66.4 | 5.50 d (2.5) | 104.9 |
| | 4.45 d (15.2) | | | |
| 4" | — | 177.1 | 4.70 d (15.5) | 68.12 |
| | | | 4.40 d (15.4) | |
| 5" | — | – | — | 177.9 |
| | **28-*O-β*-D-Glucose** | | **28-*O-β*-D-Glucose** | |
| 1''' | 5.74 d (8.1) | 94.2 | 5.73 d (8.2) | 94.7 |
| 2''' | 3.80 m | 71.1 | 3.80 m | 71.2 |
| 3''' | 3.90 m | 69.4 | 3.90 m | 69.9 |
| 4''' | 3.78 m | 77.0 | 3.78 m | 77.3 |
| 5''' | 3.69 m | 77.0 | 3.69 m | 77.6 |
| 6''' | 4.07 m | 60.6 | 4.03 m | 61.1 |
| | 3.97 dd (6.6, 13.8) | | 3.95 m | |

**Table 9**: Anti-cholinesterase activity of isolated compounds **9**–**24**

| Compound | IC$_{50}$ (µg/mL) |
| :---: | :---: |
| **9** | 88.3 ± 1.10 |
| **10** | > 250 (48.5%) |
| **11** | 203.2 ± 4.5 |
| **12** | 3.6 ± 0.07 |
| **13** | NA* |
| **14** | 112.9 ± 3.08 |
| **15** | 18 ± 1.3 |
| **16** | NA* |
| **17** | 45.71 ± 0.57 |
| **18** | >250 (26%) |
| **19** | 93.2 ± 1.2 |
| **20** | 27.9 ± 0.8 |
| **21** | >250 (40.6%) |
| **22** | >250 (35%) |
| **23** | 63.11 ± 1.5 |
| **24** | 29.6 ± 1.7 |
| Galantamine | 12.5 ± 0.6 |

* No activity at tested concentration (250 µg/mL)

## 3.4. Conclusion

In summary, natural products have long been regarded as significant drug leads for treating various chronic diseases including AD. Considering the lack of efficacy and adverse effects associated with the available therapies for AD treatment, there is an urgent need for newer options for the treatment of AD.

The halophyte *B. indica* is a very cheap source of novel bioactive compounds. In the present study, the chemical investigation of *B. indica* has resulted in isolation and identification of 16 compounds including new acylated flavonol tetraglycoside, rare flavonol triglycoside, and two rarely occurring *seco*-glycosidic triterpene oleanane saponins, in addition to other flavonoids and phenolic acid derivatives. Interestingly, some isolated compounds showed promising therapeutic activity toward the acetylcholinesterase enzyme. Thus, the plant can be utilized as a potential source of lead drugs for medicinal purposes with economic values.

To the best of our knowledge, this is the first report concerning a detailed phytochemical and biological characterization of the halophyte herb *B. indica* and the outcomes from this study will inspire natural product researchers to valorize and study other halophytes of the family Chenopodiaceae.

# Chapter 4: Possible neuroprotective effects of amide alkaloids from *Bassia indica* and *Agathophora alopecuroides*

## 4.1. Introduction

AD is a neurodegenerative disease of the CNS that is considered to be among the health problems affecting millions of people, and for which there is no efficient therapy [146]. Current available drugs can improve the cognitive functions *via* elevating the levels of brain neurotransmitters; however, their efficiency is not steady for all patients, and they have limited duration of action [147]. Considering the complexity of AD and the limitation of a single treatment option, there is an urgent need for discovery of alternative treatment options [148]. It is worth mentioning that around 55 million people worldwide suffer from dementia with the development of nearly 10 million new cases every year, and the number supposed to reach 152 million by 2050 [149]. Accumulation of abnormal amyloid-β (Aβ), phosphorylated tau-protein, β-secretase, and monoamine oxidase enzymes are key factors that play significant role in pathogenesis of AD and neurotoxicity [146,150]. Thus, modulation and inhibition of these therapeutic targets are promising approaches to treat AD. Recently, plant-derived compounds are considered promising alternatives with significant therapeutic activity in treatment of neurodegenerative diseases, and consequently might play an important role in drug discovery [151].

Halophytes are plants with substantial economic potential and an important source of medication [152]. Globally, halophytes have been utilized in traditional medicine for their therapeutic and nutritional properties. Notably, the medicinal activity of halophytes are due to their production of various biosynthesized compounds as a response to salt stress-induced oxidative damage. Besides, the chemical composition of halophytes and their nutritional values make them a food source with functional properties [42,153]. Nevertheless, the chemical and biological investigation of various species still barely reported.

*B. indica* and *A. alopecuroides* are halophytic herbs with therapeutic purposes that are distributed in the Egyptian ecosystem. Previous chemical studies have revealed the presence of nitrogenous compounds, flavonoids, and saponins in Chenopodiaceae plants [63,116,154]. Although phenolics and other chemicals previously reported in halophytes displayed anti-acetylcholinesterase activity, the therapeutic potential of *B. indica* in treatment of AD has not been elucidated yet. Additionally, the herb *A. alopecuroides* is

rich in phenolic content which can provide a neuroprotective activity in fighting AD; however, its chemical and biological investigation still unexplored [22].

As a follow-up for the utilization of halophytes and evaluation of their therapeutic potential in management of neurodegenerative diseases, the current study was conducted aiming at isolation of nitrogenous compounds from *B. indica* and *A. alopecuroides* to describe their neuroprotection as shown in Figure 18. As a result, seven amide alkaloids were isolated from *B. indica* and *A. alopecuroides*. The isolated compounds were found to follow both Lipinski's and Veber's rules of drug likeness [155,156]. Consequently, the isolated compounds could be considered good scaffolds for the development of future anti-Alzheimer drugs.
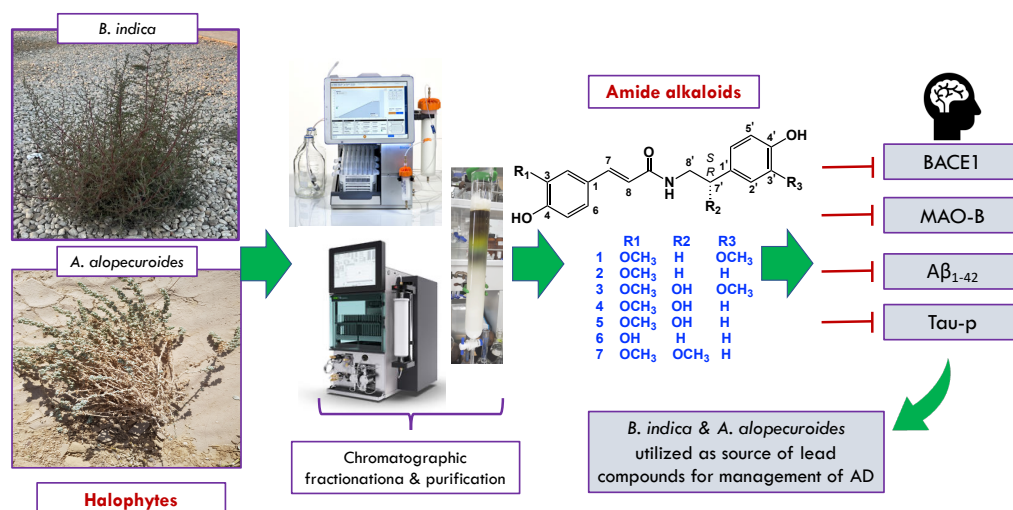


Figure 18: Outline of the present study

## 4.2. Experimental

### 4.2.1. Plant material

The aerial parts of *B. indica* were collected from desert areas in Egypt (Ihnasia ancient city) in August 2019. In addition, the aerial parts of *A. alopecuroides* were collected from desert areas southeast of Maadi, Egypt (Wadi Degla protectorate). The plants were kindly identified by Prof. Ibrahim A. El-Garf, Professor of Botany, Faculty of Science, Cairo University, Egypt. The voucher specimens, BIC-2019 and AG-2019, were deposited at the herbarium of Pharmacognosy and Medicinal Plants Department, Faculty of Pharmacy, Al-Azhar University, Egypt.

### 4.2.2. Material for chromatographic studies

The *n*-hexane, dichloromethane, ethyl acetate, methanol, and acetonitrile used as solvents for extraction and purification were purchased from Wako Pure Chemical Industries (Osaka, Japan). NP-silica gel (75-150 µm), RP-C18 (38-63 µm), and open column chromatography, were purchased from Wako Pure Chemical Industries (Osaka, Japan). A Diaion HP-20 was purchased from Mitsubishi Chemical Co. (Tokyo, Japan), and Biotage selekt (Uppsala, Sweden) equipped with NP-silica or RP-C18 flash columns chromatography (Sfär C18 D Duo column, 30 µm, 30 and 60 g) were used for further fractionation. Purification of compounds was achieved by MPLC Pure C-850 Flash prep® (Buchi, Flawil, Switzerland) with UV and ELSD detection. A preparative HPLC column (Inertsil ODS-3, 5 µm, 20×250 mm) obtained from GL Sciences Inc., Japan was also used for purification of compounds. A preparative RP-TLC (60 RP-18 $F_{254}$S, Merck, Darmstadt, Germany) was used for further purification. TLC silica gel 60 $F_{254}$ plates were purchased from Merck (Darmstadt, Germany), dimethyl sulfoxide (DMSO) and methanol-$d_4$ (CD₃OD) were purchased from Cambridge Isotope Laboratories (Andover, MA, USA). Other analytical grade chemicals used in the present study were supplied by Merck Co. (Japan).

### 4.2.3. Material for biological study

Human phospho-tau protein enzyme-linked immunosorbent assay kit used for screening phosphorylated tau (MBS013458) was obtained from MyBioSource Inc. (San Diego, CA, USA). BACE1 fluorescence human β-secretase (BACE1) inhibitor screening Kit (K720-

100), and fluorescence β-amyloid$_{1\text{-}42}$ ligand screening assay kit (K570-100), and inhibitor screening kit for monoamine oxidase-B (K797-100), were purchased from BioVision, USA.

### 4.2.4. Extraction and isolation of phytoconstituents

The powdered aerial parts of *B. indica* (1.3 Kg) and *A. alopecuroides* (0.9 kg) were extracted with 80% methanol. The collected extracts were evaporated under reduced pressure to get crude extracts of 138.5 g and 100 g, obtained from *B. indica* (as described in Chapter 2) and *A. alopecuroides* (Figure 19), respectively. The crude extract of *B. indica* was suspended in $H_2O$ and successively partitioned with *n*-hexane, $CH_2Cl_2$, EtOAc, and *n*-BuOH, while the crude extract of *A. alopecuroides* was subjected to fractionation over a Diaion HP-20 and eluted with $H_2O$-MeOH to obtain 28.5 g of MeOH fraction (Figure 19).
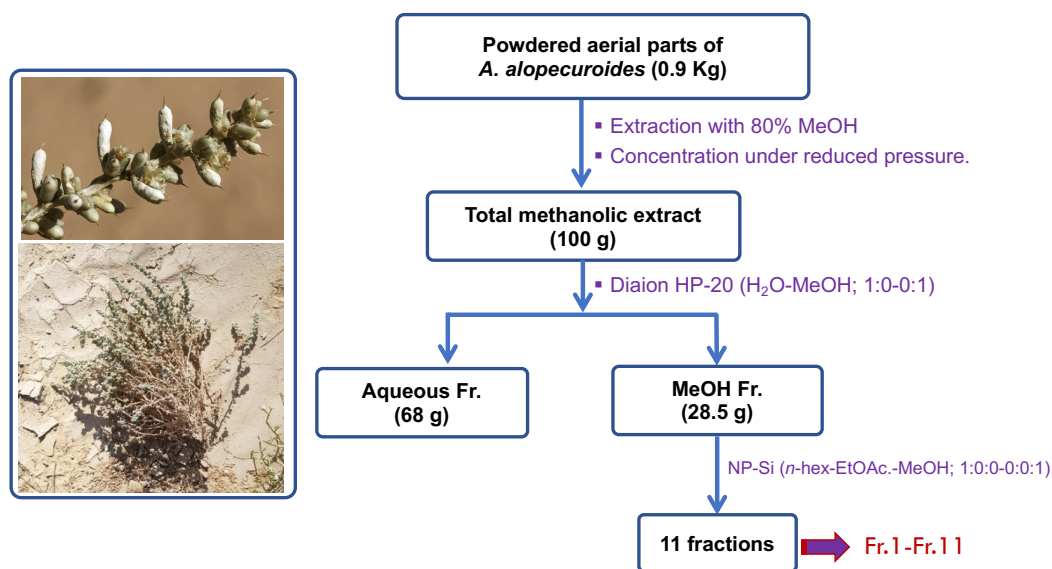


Figure 19: Extraction and fractionation of *A. alopecuroides*

For isolation of compounds from *B. indica*, following partitioning of dichloromethane fraction using NP-silica gel and eluted gradually with *n*-hex-EtOAc-MeOH, the fraction D3.2 (50.5 mg) was purified over RP-TLC eluted with an isocratic mobile phase of $H_2O$-MeOH (65:35) to obtain compound **1** (4.5 mg). Subfraction E3 of ethyl acetate fraction (89 mg) was purified over MPLC with RP-C18 (4 g) eluted with $H_2O$-MeOH (8:2 to 5:5) to afford compound **2** (7.0 mg). E5C and E5D subfractions (178 mg) were purified over HPLC preparative column (Inertsil ODS-3, 5 μm, 20 × 250 mm, 5 mL/min) and eluted with $H_2O$-MeOH-FA (65:35:0.1) to obtain **3** (0.9 mg), **4** (6.4 mg), and **5** (0.7 mg).

For purification of compounds from *A. alopecuroides*, the methanol fraction was chromatographed over Biotage Selekt with NP-silica gel and eluted with *n*-hex-EtOAc-MeOH; 1:0:0-0:0:1 to obtain 11 fractions. Fraction 6 (160 mg) was purified by MPLC with RP-C18 column (4 g) eluted with $H_2O$-ACN-0.1% FA to get compound **6** (20 mg). Moreover, fraction 7 (212 mg) was purified over RP-C18 (2 columns, each is 4 g) and eluted with $H_2O$-ACN in presence of 0.1% FA to obtain **7** (9.1 mg). Compounds **2** and **4** (3.0 and 8.0 mg, respectively), purified from the aq. methanol extract of *B. indica* in this study, were also purified from methanol fraction of *A. alopecuroides*.

### 4.2.5. Procedure for identification of the isolated compounds

The NMR spectra of isolates were recorded on Bruker DRX-600 spectrometer (Bruker Daltonics, Billerica MA, USA) with tetramethylsilane (TMS) as an internal standard. A Jasco P-2200 polarimeter (Jasco, Tokyo, Japan) was used for measuring the optical rotations of compounds. The chemical shifts were expressed as δ values. The HR-MS of compounds was determined using a quadrupole time-of-flight (qTOF) mass spectrometer (Agilent Technologies, USA). FT-IR measurements of samples were obtained using FTIR-620 spectrophotometer (JASCO International, Co. Ltd., Tokyo, Japan).

### 4.2.6. *In vitro* MAO-B enzyme inhibition assay

The inhibitory activity of MAO-B enzyme by isolated compounds was evaluated by a fluorometric method with inhibitor screening kit for monoamine oxidase-B, BioVision, USA (K797- 100). The assay was performed according to the manufacturer protocol. The test sample (10 μL/well) and recombinant enzyme solution (50 μL/well) were added to black flat-bottom 96-well microplate and incubated for 10 min at 37 °C. After incubation,

the reaction was initiated by adding working solution (40 μL/well) with 37 μL assay buffer and 1 μL developer solution, 1 μL substrate solution, and 1 μL OxiRed probe. The plate was incubated for a 30 min at 37 °C. In control group, 10 μL of 0.02% DMSO solution was used instead of test sample; hence, the assay mixture included enzyme, developer solution, substrate solution, and OxiRed probe without sample. Whereas sample assay included the same assay mixture but with isolates. Selegiline, a selective inhibitor of MAO-B, was used as the reference drug. Fluorescence reading was observed under excitation at 535 nm and emission at 587 nm for 10-40 min. The percentage inhibition was calculated using the following formula:

% Relative inhibition = $1 - \frac{X2-X1}{C2-C1}$

The assay was expressed in terms of relative fluorescence units (RFU), where X2: Fluorescence of test sample measured at T2 time; X1: Fluorescence of test sample measured at T1 time; C2: Fluorescence of a control measured at T2 time; and C1: Fluorescence of a control measured at T1 time.

### 4.2.7. *In vitro* anti-amyloidogenic assay (A$\beta_{1-42}$ fibril formation)

The crude MeOH extracts of *B. indica* and *A. alopecuroides*, and isolates were assayed to determine their ability to inhibit the A$\beta_{1-42}$ aggregation with β-amyloid$_{1-42}$ (A$\beta_{42}$) ligand screening assay kit (K570-100, Bio Vision, CA, USA). The isolated compounds were dissolved in DMSO to obtain a concentration range of 0.1 to 100 μg/mL. In a white flat-bottom 96-well microplate, 50 μL of each sample, 70 μL of a mixture of (68 μL of A$\beta_{1-42}$ assay buffer and 2 μL of A$\beta_{1-42}$ probe I) and 80 μL of diluted A$\beta_{1-42}$. The peptide control well included 50 μL of assay buffer, whereas for solvent control, tested samples replaced by 50 μL of DMSO. Following 3 h incubation at 37 °C, fluorescence measured at Ex/Em = 440/490 nm. The RFU of blank control was set as 100%, and percentage of Relative Inhibition was calculated from the following equation:

% Relative Inhibition = (RFU of PC × RFU of S)/ (RFU of S) x 100

Where: PC, is the Peptide Positive Control or Solvent Control; S, is Sample Screen. IC$_{50}$ was calculated by plotting the values of % inhibition versus their corresponding log concentration.

**4.2.8. *In vitro* BACE1 inhibition assay**

The BACE-1 inhibitory assay was done according to the manufacturer protocol using a BACE inhibitor screening assay kit, BioVision, USA (K720-100). Briefly, 2 µL of the diluted BACE1 enzyme was added into sample, enzyme control, and solvent control wells. Following incubation for 5 min at 25 °C, 50 µL of substrate solution (made by mixing BACE1 assay buffer 48 µL and BACE1 substrate 2 µL) was added into each well, then mixed with gentle shaking. The produced fluorescence was measured (Ex/Em: 245 nm/500 nm) in a microplate reader (FLX800$^{TM}$, Bio-Tek Instruments, Inc., Winooski, VT, USA). The inhibition calculated from the following equation:

% Relative inhibition = $\frac{\text{Slope of EC} - \text{Slope of S}}{\text{Slope of EC}} \times 100$

Where, Slope of EC is the slope of enzyme control, slope of S is the slope of sample screen.

**4.2.9. *In vitro* tau-protein inhibition assay**

The inhibition of phosphorylated tau-protein was performed according to the manufacturer protocol using a human phospho-tau protein enzyme-linked immunosorbent assay kit (MBS013458). This quantitative sandwich ELISA kit was known to have LOD of 1.0 pg.mL$^{-1}$ for phosphorylated tau. Briefly, in ELISA microwell strip plate (96-well), 50 µL of standard (S1-S7) added to standard wells and 50 µL of each sample (50 µg/mL) was added to every sample well, while nothing added to blank wells. 100 µL of HRP-conjugate reagent was added to all wells except for blank ones, then the plate covered with a closure plate membrane and incubate for 60 minutes at 37 °C. After washing all wells, 50 µL of chromogen solution A was added to every well, then 50 µL of chromogen solution B, and the plate was gently mixed and incubated for 15 minutes at 37 °C. Finally, the formation of a colored product was spectrophotometrically measured at 450 nm using ROBONIK P2000 Elisa Reader after terminating the reaction by the addition of the 50 µL stop solution.

**Statistical analysis**

All experimental results in the current study were obtained from three repeated biological experiments. The results were expressed as the means ± SD (n = 3).

### 4.2.10. *In silico* investigations

**Molecular docking**

The molecular docking experiments were performed using AutoDock Vina software [157]. All isolated compounds structures were docked into the MAO-B and BACE1 crystal structures (PDB codes: 6FWC and 4WY1, respectively). The binding site for each protein was determined according to the enzyme's co-crystallized ligand. The co-ordinates of the grid box were x = -1.12; y = -18.86; z = 33.74 for BACE1, and x= 51.37; y= 155.39; z= 27.85 for MAOB. The size of the grid box was set to be 10 Å. Exhaustiveness was set to be 24. Ten poses were generated for each docking experiment. Docking poses were analyzed and visualized using PyMOL software [157].

**Molecular dynamics simulation**

Desmond v. 2.2 software was used for performing MDS experiments [158–160]. This software applies the OPLS force field. Protein systems were built using the system builder option, where the protein structure was embedded in an orthorhombic box of TIP3P water together with 0.15 M Na$^+$ and Cl$^-$ ions in 20 Å solvent buffer. Afterward, the prepared systems were energy minimized and equilibrated for 10 ns. Desmond software automatically parameterizes inputted ligands during the system building step according to the OPLS force field. For simulations performed by NAMD [161], the parameters and topologies of the compounds were calculated either using the Charmm27 force field with the online software Ligand Reader and Modeler (http://www.charmm-gui.org/?doc=input/ligandrm) [162] or using the VMD plugin Force Field Toolkit (ffTK). Afterward, the generated parameters and topology files were loaded to VMD to readily read the protein–ligand complexes without errors and then conduct the simulation step.

**Binding free energy calculations**

Binding free energy calculations ($\Delta G$) were performed using the free energy perturbation (FEP) method. This method was described in detail in the recent article by Kim and co-workers [161]. Briefly, this method calculates the binding free energy $\Delta G_{binding}$ according to the following equation: $\Delta G_{binding} = \Delta G_{Complex} - \Delta G_{Ligand}$. The value of each $\Delta G$ is estimated from a separate simulation using NAMD software. Interestingly, all input files required for simulation by NAMD can be papered by using the online website CharmmGUI

(https://charmm gui.org/?doc=input/afes.abinding). Subsequently, we can use these files in NAMD to produce the required simulations using the FEP calculation function in NAMD. The equilibration was achieved in the NPT ensemble at 300 K and 1 atm (1.01325 bar) with Langevin piston pressure (for "Complex" and "Ligand") in the presence of the TIP3P water model. Then, 10 ns FEP simulations were performed for each compound, and the last 5 ns of the free energy values was measured for the final free energy values [158]. Finally, the generated trajectories were visualized and analyzed using VMD software. It is worth noting that Ngo and co-workers in their recent benchmarking study found that the FEP method of determination of $\Delta G$ was the most accurate method in terms of predicting enzyme inhibitors [162].

## 4.3. Results and discussion

### 4.3.1. Identification of the isolated compounds

A total of seven amide alkaloids (phenolic amides) were isolated from the dried aerial parts of *B. indica* and *A. alopecuroides* (Figure 20).



|   | $R_1$ | $R_2$ | $R_3$ |
|---|-------|-------|-------|
| 1 | $OCH_3$ | H | $OCH_3$ |
| 2 | $OCH_3$ | H | H |
| 3 | $OCH_3$ | OH | $OCH_3$ |
| 4 | $OCH_3$ | OH | H |
| 5 | $OCH_3$ | OH | H |
| 6 | OH | H | H |
| 7 | $OCH_3$ | $OCH_3$ | H |
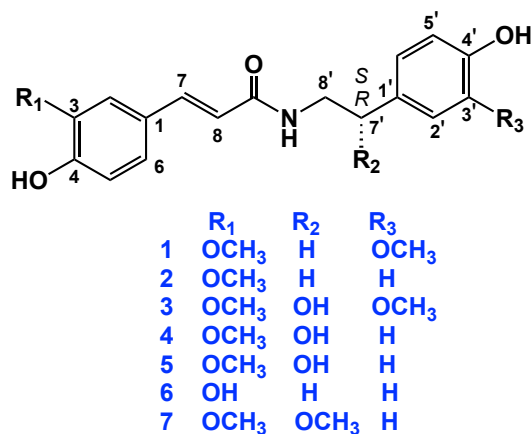
Figure 20: Amide alkaloids **1**–**7** isolated from *B. indica* (**1**–**5**) and *A. alopecuroides* (**2**, **4**, **6**, and **7**)

*N-trans*-feruloyl-3-methoxytyramine (**1**): yellow amorphous powder; $^1H$ and $^{13}C$ NMR data, see Table 10 and Table 11; HRESIMS *m/z* 342.1352 [M–H]$^-$ (calculated for $C_{19}H_{20}NO_5$, 342.1341).

*N-trans*-feruloyltyramine (**2**): yellow amorphous powder; $^1H$ and $^{13}C$ NMR data see Table 10 and Table 11; HRESIMS *m/z* 312.1244 [M–H]$^-$ (calculated for $C_{18}H_{18}NO_4$, 312.1236). IR (ZnSe): 3317, 1670, 1513, 1270.8 cm$^{-1}$.

*S*-(–)-*N-trans*-feruloylnormetanephrine (**3**): white amorphous powder; $[\alpha]_D^{25} - 35.0$ (c 0.01, MeOH); $^1H$ and $^{13}C$ NMR data see Table 10 and Table 11; HRESIMS *m/z* 358.1301 [M–H]$^-$ (calculated for $C_{19}H_{20}NO_6$, 358.1291).

*S*-(–)-*N-trans*-feruloyloctopamine (**4**): yellow amorphous powder; $[\alpha]_D^{25} - 35.1$ (c 0.02, MeOH); $^1H$ and $^{13}C$ NMR data see Table 10 and Table 11; HRESIMS *m/z* 328.1196 [M–H]$^-$ (calculated for $C_{18}H_{18}NO_5$, 328.1185). IR (ZnSe): 3360, 2965, 1660, 1593, 1278 cm$^{-1}$.

*R*-(+)-*N-trans*-feruloyloctopamine (**5**): yellow amorphous powder; $[\alpha]_D^{25} + 24.3$ (c 0.01, MeOH); $^1H$ and $^{13}C$ NMR data see Table 10 and Table 11; HRESIMS *m/z* 328.1195 [M–H]$^-$ (calculated for $C_{18}H_{18}NO_5$, 328.1185).

*N-trans*-caffeoyltyramine (**6**): white amorphous powder; $^1H$ and $^{13}C$ NMR data see Table 10 and Table 11; ESIMS *m/z* 298.1089 [M–H]$^-$ (calculated for $C_{17}H_{16}NO_4$, 298.1079). IR (ZnSe): 3398, 2970, 1650, 1590 cm$^{-1}$.

*S*-(–)-3-(4-hydroxy-3-methoxyphenyl)-*N*-[2-(4-hydroxyphenyl)-methoxyethyl]acrylamide (**7**): brownish yellow amorphous powder; $[\alpha]_D^{25} - 12.2$ (c 0.01, MeOH); $^1H$ and $^{13}C$ NMR data see Table 10 and Table 11; HRESIMS *m/z* 342.1356 [M-H]$^-$ (calculated for $C_{19}H_{20}NO_5$, 342.1341). IR (ZnSe): 3400, 2914, 1650, 1503, 1268 cm$^{-1}$.

The isolated compounds **1**, **2**, **4**, **6**, and **7** were subjected to *in silico* investigation to provide more scientific data regarding their binding mechanisms with some molecular targets implicated in AD.

To the best of our knowledge, compound **7** is first reported in Chenopodiaceae family, while compounds **2**, **4**, and **6** are first reported in genus *Agathophora*. Moreover,

compounds **2**, **4**, **6**, and **7** were first isolated from the plant *A. alopecuroides*. The isolated lignanamides in the present study were evaluated for their inhibition activity on BACE1, MAO-B, $A\beta_{1-42}$ aggregation, and hyperphosphorylated tau protein. The biosynthetic pathway of this class of molecules is shown in Figure 21.
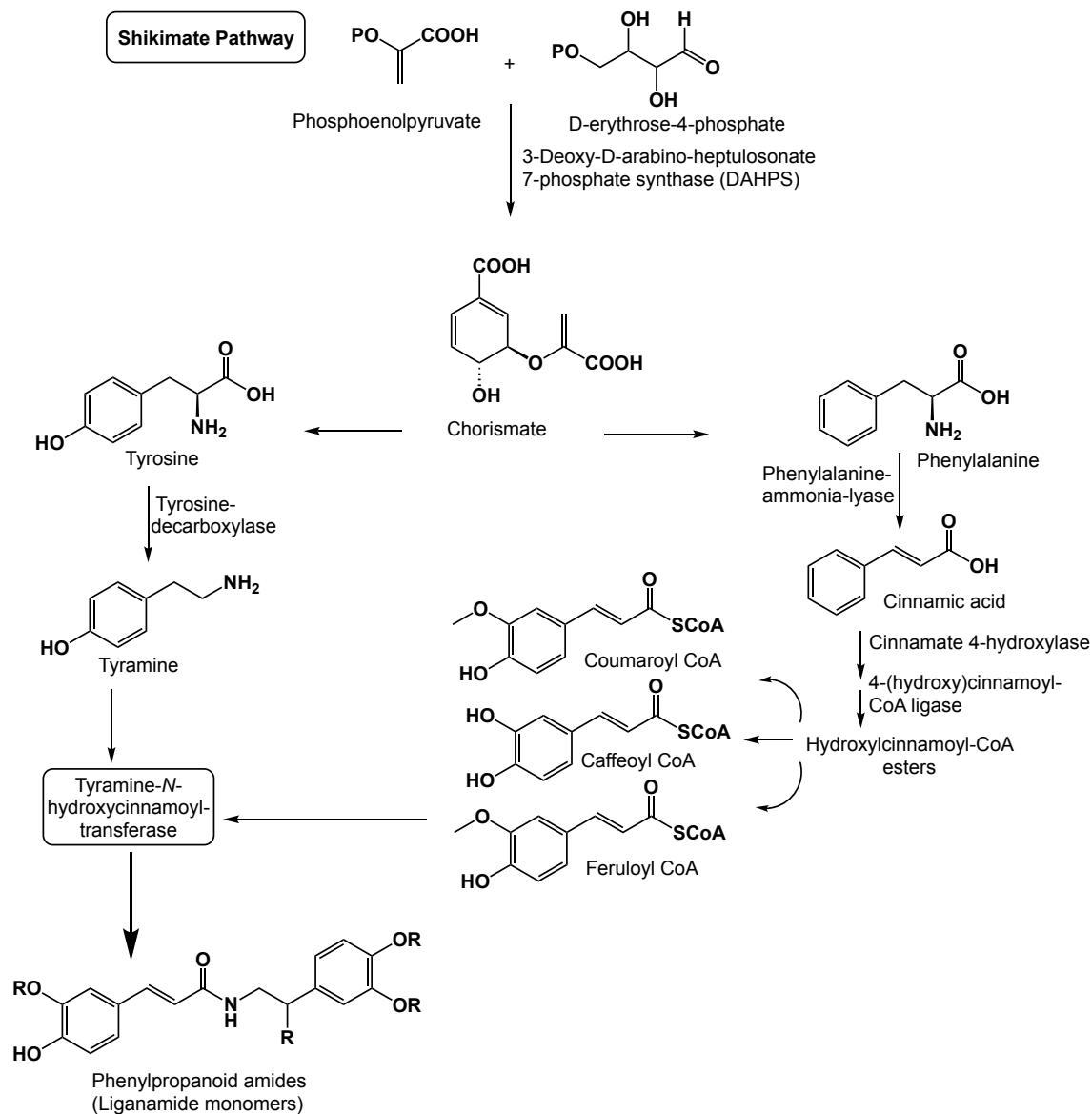


Figure 21: The biosynthetic pathway of phenylpropanoid amides

**Table 10**: ^{1}H-NMR spectral data of amide alkaloids **1**–**7**

| Position | 1 | 2 | 3 | 4 | 5 | 6 | 7 |
|---|---|---|---|---|---|---|---|
| 1 | — | — | — | — | — | — | — |
| 2 | 7.09, d (1.9) | 7.12, d (1.9) | 7.00, d (1.9) | 7.15 d (2.0) | 7.09, d (1.9) | 7.01, d (1.9) | 7.11, d (2.0) |
| 3 | — | — | — | — | — | — | — |
| 4 | — | — | — | — | — | — | — |
| 5 | 6.77, d (8.1) | 6.79, d (8.2) | 7.09, d (8.2) | 6.80, d (8.2) | 6.77, d (8.2) | 6.78, d (8.4) | 6.79, d (8.1) |
| 6 | 7.00, dd (1.9, 8.1) | 7.03, dd (8.2, 1.9) | 6.71, dd (8.2, 1.9) | 7.04, dd (2.0, 8.2) | 6.99, dd (1.9, 8.2) | 6.91, dd (8.4, 1.9) | 6.98, dd (2.0, 8.1) |
| 7 | 7.43, d (15.7) | 7.44, d (15.7) | 7.25, d (15.5) | 7.46, d (15.6) | 7.41, d (15.7) | 7.40, d (15.7) | 7.30, d (15.6) |
| 8 | 6.39, d (15.7) | 6.40, d (15.7) | 6.38, d (15.5) | 6.47, d (15.6) | 6.37, d (15.7) | 6.35, d (15.6) | 6.52, d (15.6) |
| 9 | — | — | — | — | — | — | — |
| 1' | — | — | — | — | — | — | — |
| 2' | 6.81, d, (2.0) | 7.07, d (8.6) | 6.88, d (1.8) | 7.24, d (8.3) | 7.20, d (8.6) | 7.07, d (8.3) | 7.11, d (8.3) |
| 3' | — | 6.73, d (8.6) | — | 6.78, d (8.3) | 6.69, d (8.6) | 6.74, d (8.3) | 6.60, d (8.3) |
| 4' | — | — | — | — | — | — | — |
| 5' | 6.72, d (8.0) | 6.73, d (8.6) | 6.71, d (8.2) | 6.78, d (8.3) | 6.69, d (8.6) | 6.74, d (8.3) | 6.60, d (8.3) |
| 6' | 6.66, dd (8.0, 2.0) | 7.07, d (8.6) | 6.90, dd (1.8. 8.2) | 7.24, d (8.3) | 7.20, d (8.6) | 7.07, d (8.3) | 7.11, d (8.3) |
| 7' | 2.76, t. (7.3) | 2.77, t (7.4) | 4.53, dd (7.3, 4.3) | 4.73, dd (4.88, 7.76) | 4.69, dd, (7.8, 5.1) | 2.76, t (7.4) | 4.16, m |
| 8' | 3.48, t (7.3) | 3.48, t (7.4) | 3.46, d (13.0, 7.0) 3.21, dd (13.1, 7.0) | 3.54, dd (13.6, 4.9) 3.45, dd (13.6, 4.9) | 3.49, dd (11.3, 5.0) 3.38, dd (9.2, 6.3) | 3.47, t (7.4) | 3.34, m 3.33, m |
| 3-OMe | 3.86, s | 3.89, s | 3.76, s | 3.89, s | 3.86, s | — | 3.80, s |
| 3'-OMe | 3.82, s | — | 3.72, s | — | — | — | — |
| 7'-OMe | — | — | — | — | — | — | 3.17, s |
| Solvent | CD$_3$OD | CD$_3$OD | DMSO-$d_6$ | CD$_3$OD | CD$_3$OD | CD$_3$OD | DMSO-$d_6$ |

**Table 11**: $^{13}$C-NMR spectral data of amide alkaloids **1–7**

| Position | 1 | 2 | 3 | 4 | 5 | 6 | 7 |
|---|---|---|---|---|---|---|---|
| 1 | 127.6 | 127.9 | 129.2 | 128.2 | 128.1 | 128.3 | 126.4 |
| 2 | 111.4 | 111.5 | 110.4 | 111.5 | 111.5 | 115.1 | 110.8 |
| 3 | 149.6 | 149.5 | 147.4 | 149.3 | 149.4 | 148.7 | 148.8 |
| 4 | 151.0 | 150.6 | 149.0 | 149.9 | 150.0 | 146.7 | 148.3 |
| 5 | 116.7 | 116.6 | 115.1 | 116.5 | 116.1 | 116.5 | 115.6 |
| 6 | 123.4 | 123.4 | 122.9 | 123.3 | 123.3 | 122.1 | 121.6 |
| 7 | 142.2 | 142.1 | 139.8 | 142.3 | 142.1 | 142.2 | 139.0 |
| 8 | 118.3 | 118.4 | 118.7 | 118.6 | 118.7 | 118.4 | 119.0 |
| 9 | 169.3 | 169.3 | 166.7 | 169.5 | 169.2 | 169.3 | 165.4 |
| 1' | 132.0 | 131.3 | 134.9 | 134.7 | 134.4 | 131.3 | 129.8 |
| 2' | 113.4 | 130.7 | 114.6 | 128.5 | 130.7 | 130.7 | 128.0 |
| 3' | 144.0 | 116.3 | 145.8 | 116.1 | 116.3 | 116.3 | 115.2 |
| 4' | 146.1 | 157.0 | 145.9 | 158.1 | 157.0 | 156.9 | 157.1 |
| 5' | 116.2 | 116.3 | 115.2 | 116.1 | 116.3 | 116.3 | 115.2 |
| 6' | 122.3 | 130.7 | 120.1 | 128.5 | 130.7 | 130.7 | 128.0 |
| 7' | 36.2 | 35.8 | 71.7 | 73.4 | 73.5 | 35.8 | 81.5 |
| 8' | 42.5 | 42.6 | 47.3 | 48.8 | 47.5 | 42.5 | 45.2 |
| 3-OMe | 56.3 | 56.4 | 55.7 | 56.4 | 56.4 | — | 55.8 |
| 3'-OMe | 56.3 | — | 55.5 | — | — | — | — |
| 7'-OMe | — | — | — | — | — | — | 55.5 |
| Solvent | CD$_3$OD | CD$_3$OD | DMSO-$d_6$ | CD$_3$OD | CD$_3$OD | CD$_3$OD | DMSO-$d_6$ |

### 4.3.2. Inhibitory effect on BACE1

β-site amyloid precursor protein cleaving enzyme-1 (BACE1) is a key protein that plays a crucial role in the abnormal production of Aβ, which is one of major factors in AD [163]. Consequently, the isolates were evaluated for their inhibition against BACE1. As seen in Table 12, the results showed that compounds **1** and **7** displayed promising inhibition activity against BACE1 with $IC_{50} < 6$ μg/mL. Moreover, compounds **2** and **6** displayed inhibition activity with $IC_{50}$ values of $11.6 \pm 0.39$ and $10.2 \pm 0.34$ μg/mL, respectively.

### 4.3.3. Inhibition activity on MAO-B

Monoamine oxidase-B (MAO-B) has been deemed a potential therapeutic target for neurodegenerative diseases. Overactivity of MAO-B is associated with aberrant levels of gamma amino butyric acid (GABA), neurotoxicity, neuroinflammation, and Aβ production [150]. Therefore, the discovery of bioactive compounds with the capacity to inhibit MAO-B could play a potential role in AD treatment. In this study, the crude MeOH extracts of *B. indica* and *A. alopecuroides* showed promising activity towards MAO-B with $IC_{50}$ values $8.7 \pm 0.29$ and $1.7 \pm 0.06$ μg/mL, respectively. Fortunately, the isolated lignanamides in this study displayed potential inhibition activity against MAO-B with $IC_{50}$ values ranging from 0.71 to 5.92 μg/mL. Interestingly, compounds **1**, **2**, **6** and **7** displayed the utmost potential MAO-B inhibition effects with $IC_{50}$ values of $0.71 \pm 0.02$, $2.24 \pm 0.08$, $2.62 \pm 0.09$, and $1.52 \pm 0.05$ μg/mL, respectively, comparable to selegiline ($IC_{50} = 0.55 \pm 0.02$).

### 4.3.4. Inhibition activity on Aβ$_{1-42}$ aggregation

One of the key factors in neurodegeneration is amyloid-β accumulation which results in aggregation of neurotic senile plaques [146]. Amyloid-β is neurotoxic and correlated with the severity of AD symptoms, cognitive impairments, and neuronal cell death [164]. Considering the fact that various therapeutic strategies have been concerned with inhibition of Aβ-aggregate formation, the isolated compounds were evaluated for their inhibition effect on Aβ-aggregation. The study results demonstrated that the MeOH extract of *A. alopecuroides* has a potential inhibition activity on neurotoxic Aβ-formation ($IC_{50} = 3.01 \pm 0.10$ μg/mL). Among the isolates, compounds **1**, **2**, and **7** exhibited extraordinary activity against Aβ-aggregation with $IC_{50}$ values of $0.3 \pm 0.01$, $1.2 \pm 0.04$,

and 2.62 $\pm$ 0.09 µg/mL, respectively, comparable to positive control (IC$_{50}$ = 1.93 $\pm$ 0.06 µg/mL) as shown in Table 12.

## 4.3.5. Inhibition activity on tau-protein

Tau is a microtubule-associated protein which plays an important role in cell integrity [165]. Tau-protein hyperphosphorylation lead to dissociation from microtubules and subsequently abnormal tau aggregation and formation of neurotoxic neurofibrillary tangles (NFTs) [166]. The inhibition of tau-aggregation is one of the possible approaches to blocking tau-mediated neurotoxicity. In the current study, the results of the *in vitro* evaluation of the crude extracts of *B. indica* and *A. alopecuroides* against tau-protein revealed that *A. alopecuroides* reduces the concentration of phosphorylated tau-protein to 2.27 $\pm$ 0.12 pg/mL comparable to control which was nearly 5-fold higher (10.8 $\pm$ 0.68 pg/mL). In addition, the assay results indicated that the isolated compounds showed variable activity against phosphorylated tau-protein. Notably, compounds **1**, **2**, and **7** were the most potent candidates with capacity to reduce the concentration of phosphorylated tau-protein with values 1.62 $\pm$ 0.13, 2.12 $\pm$ 0.11, 2.79 $\pm$ 0.23 pg.mL$^{-1}$, respectively, comparable to control group which was nearly 5- to 7-fold higher as shown in Table 12.

On the basis of above evidence, a methoxy group in the tyramine moiety of the isolated molecules such as in compounds **1** and **7** plays a crucial rule, not in terms of MAO-B enzyme inhibition activity but also for the inhibition activities on BACE1 enzyme and A$\beta_{1-42}$ aggregation.

**Table 12**: Inhibitory activities of compounds (IC$_{50}$) against the predicted protein targets. All values are expressed in µg/mL concentration ± SD of three independent experiments (level of tau-p expressed in pg/mL ± SD)

| Compound | BACE1 | MAO-B | Aβ$_{1-42}$ aggregation | Tau-p (pg/mL) |
|---|---|---|---|---|
| *B. indica* | 28.9 ± 0.97 | 8.7 ± 0.29 | 40.6 ± 1.36 | 6.62 ± 0.14 |
| *A. alopecuroides* | 15.4 ± 0.52 | 1.7 ± 0.06 | 3.01 ± 0.10 | 2.27 ± 0.12 |
| 1 | 5.39 ± 0.18 | 0.71 ± 0.02 | 0.3 ± 0.01 | 1.62 ± 0.13 |
| 2 | 11.6 ± 0.39 | 2.24 ± 0.08 | 1.2 ± 0.04 | 2.12 ± 0.11 |
| 4 | 36.1 ± 1.21 | 5.92 ± 0.2 | 13.1 ± 0.44 | 5.53 ± 0.14 |
| 6 | 10.2 ± 0.34 | 2.62 ± 0.09 | 6.05 ± 0.2 | 6.14 ± 0.19 |
| 7 | 5.64 ± 0.19 | 1.52 ± 0.05 | 2.62 ± 0.09 | 2.79 ± 0.23 |
| LY2811376 | 0.8 ± 0.03 | — | — | 2.09 ± 0.08 |
| Selegiline | — | 0.55 ± 0.02 | — | — |
| Tacrine | — | — | 1.93 ± 0.06 | — |
| Control | — | — | — | 10.8 ± 0.68 |

### 4.3.6. Molecular modeling and *in silico*-based analysis

To gain more insights into the possible mode of interactions between the active compounds and both MAO-B and BACE1, several modeling and *in silico*-based analysis were carried out. First, the structures of active compounds (**1**, **2**, **4**, **6**, and **7**) were docked into the active sites of both enzymes. Ten binding poses were generated for each compound and each enzyme. Usually, poses with lowest affinity scores are the true binding poses. To confirm this assumption, the structure of co-crystalized inhibitors were re-docked into the active site of each enzyme. The generated poses of the lowest binding affinity in kcal/mol were the closest ones to the original crystalized binding mode (RMSDs = 0.953 Å and 1.142 Å for MAOB and BACE1, respectively; Figure 22). Moreover, we calculated the absolute binding free energies ($\Delta G_{binding}$) of each generated binding pose for each compound, where the top-scoring binding poses generated from the docking step were also the best in terms of $\Delta G_{binding}$ (Table 13). This step was achieved with the aid of molecular dynamics simulation (MDS)-based free energy perturbation method [162].
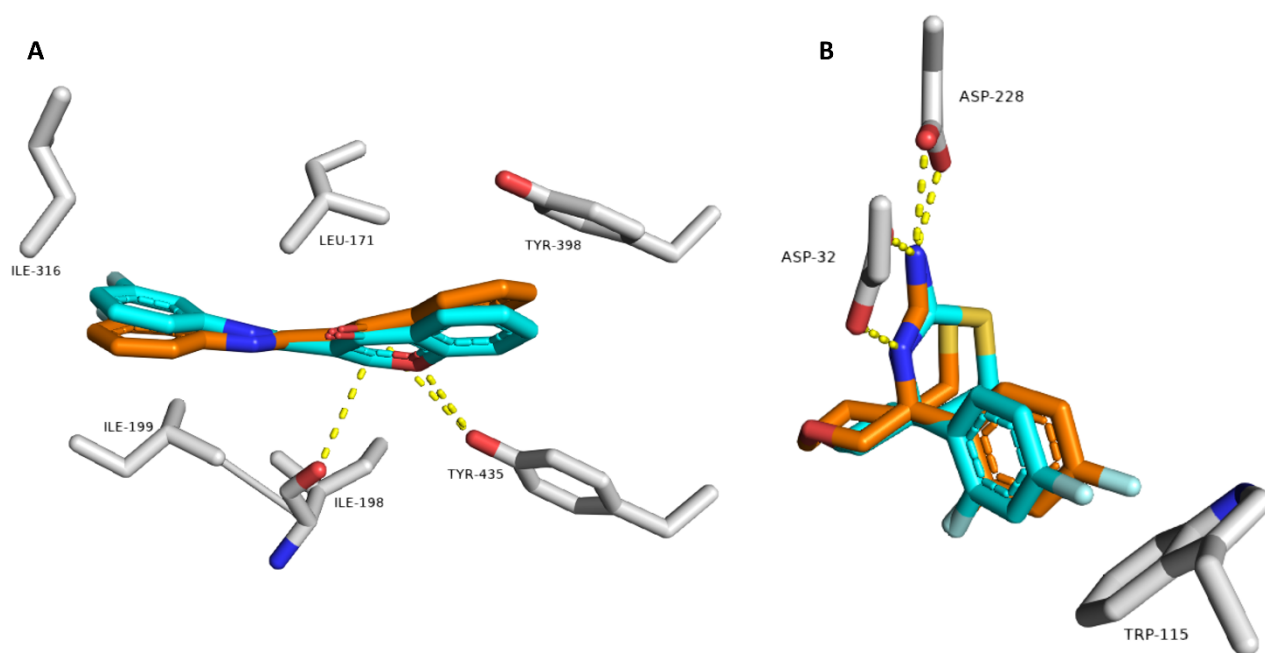
Figure 22: Binding modes of the co-crystalized inhibitors' structures inside the active sites of both MAOB and BACE1 (A and B, respectively). Cyan-colored structures represent the original binding modes inside the crystalized proteins (PDB codes: 6FWC and 4WY1, respectively). Orange-colored structures represent the re-docked binding modes with RMSDs of 0.953 Å and 1.142 Å, respectively from the original crystalized ones.

**Table 13**: Docking scores and the estimated absolute binding free energies (in kcal/mol) of the investigated structures (compounds **1**, **2**, **4**, **6**, and **7**) along with that of the reported co-crystalized inhibitors

| Structure | BACE1 (Vina score) | MAO-B (Vina score) | BACE1 ($\Delta G_{binding}$) | MAO-B ($\Delta G_{binding}$) |
|---|---|---|---|---|
| **1** | −9.6 | −10.3 | −8.9 | −8.9 |
| **2** | −9.2 | 10.2 | −9.5 | −9.2 |
| **4** | −5.1 | −9.8 | −5.5 | −9.4 |
| **6** | −8.9 | −10.2 | −7.9 | −9.9 |
| **7** | −9.0 | −9.9 | −8.1 | −9.8 |
| **MAOB inhibitor** | — | −9.8 | — | −9.5 |
| **BACE1 inhibitor** | −9.1 | — | −9.4 | — |

 Second, each generated binding pose, selected from the previous step, was subjected to 50 ns long MDS runs to get more insight into the dynamic binding stability and behavior of each structure inside the corresponding binding sites.

MAOB's active site is a tunnel-shaped binding site, and hence, each docked structure was perfectly fitted inside it. To study the key binding interactions of each structure during the MDS runs, the highly-populated poses for each structure were extracted from the MDS trajectories of each MDS experiment.

As seen in Figure 23 A-E, each structure showed very good alignment with the structure of co-crystalized inhibitor, and hence, they showed identical biding interactions. Each structure was able to achieve stable H-bonding with ILE-198 and TYR-435. Furthermore, they achieved multiple stable hydrophobic interactions with LEU-171, ILE-198, ILE-199, ILE-316, and TYR-398.

Their average RMSDs inside the binding site over the course of MDS were convergent ranging from 1.7 Å to 2.4 Å indicating stable binding interactions with the enzymes binding site. Accordingly, the calculated $\Delta G_{binding}$ values were convergent (ranged from −8.9 to −9.8 kcal/mol; Table 13), and in turn, their *in vitro* inhibitory activities were also convergent (Table 12).

These structure and biophysics-based information revealed the potential of the isolated amide alkaloids as very promising scaffold for the future development of new MAOB inhibitors.



Figure 23: A-E: Binding modes of the structures of compounds **1**, **2**, **4**, **6**, **7** inside MAOB's binding site (Brick-red coloured structures) in alignment with that of the co-crystalized inhibitor (Cyan-coloured structure). F: RMSDs of the structures of compounds **1**, **2**, **4**, **6**, **7** inside MAOB's binding site along with that of the co-crystalized inhibitor over 50 ns long MDS runs.

In regard to BACE1, structures under investigation (compounds **1**, **2**, **4**, **6**, and **7**) showed three different binding modes inside the enzyme's active site. As shown in Figure 24, the first binding mode for **1**, **2**, and **6** showed extended structure inside the binding site, where they interacted differently form the co-crystalized inhibitor. However, this binding mode was stable over the course of simulation (average RMSD = 1.6 Å to 1.9 Å; $\Delta G_{binding}$ ranged from –7.9 to –9.5 kcal/mol; Table 4) showing stable H-bonds with GLY-11, TRP-76, and THR-232 and two hydrophobic interaction with TYR-71 and TRP-115 similarly to the co-crystalized inhibitor. Accordingly, their calculated $IC_{50}$ values (Table 12) indicated good inhibitory activity against the enzyme activity *in vitro* (Figure 24 A,B,D).

The second binding mode was that of compound **4** (Figure 24C), where the hydroxyl group at C-7' forced the whole structure to take another orientation due to the steric clash with TRP-115. However, this orientation, which was the best among the generated docking poses in terms of docking score and $\Delta G_{binding}$, was relatively the least stable one in comparison with the other compounds. Its average RMSD over the course of MDS was 5.4 Å and its calculated $\Delta G_{binding}$ was –5.5 kcal/mol indicating relatively lower binding affinity than that of the remaining compounds. The third binding mode was that of compound **7**, where the compound's structure took an orientation made it perfectly aligned with the structure of the co-crystalized inhibitor (Figure 24E). Interestingly, the binding mode of **7** was almost identical to that of **4** at the beginning of MDS; however, it starts to change to the current one at 2 ns, where it was not able to be stabilized by H-bonding (i.e., with ASN-37, ILE-126, and ARG-128) similarly to compound **4** because of the additional methyl group of the C-7' hydroxyl group.

The current binding mode of compound **7** was stabilized with a network of H-bonds with GLY-230, THR-231, in addition to two hydrophobic interactions with TYR-71 and TRP-115. This binding mode achieved highest binding affinity toward BACE1's binding site ($\Delta G_{binding}$ = –8.1 kcal/mol), and hence, its inhibitory activity was the second potent ($IC_{50}$ = 5.64 $\pm$ 0.19 μg/mL) after compound **1** ($IC_{50}$ = 5.39 $\pm$ 0.18 μg/mL).

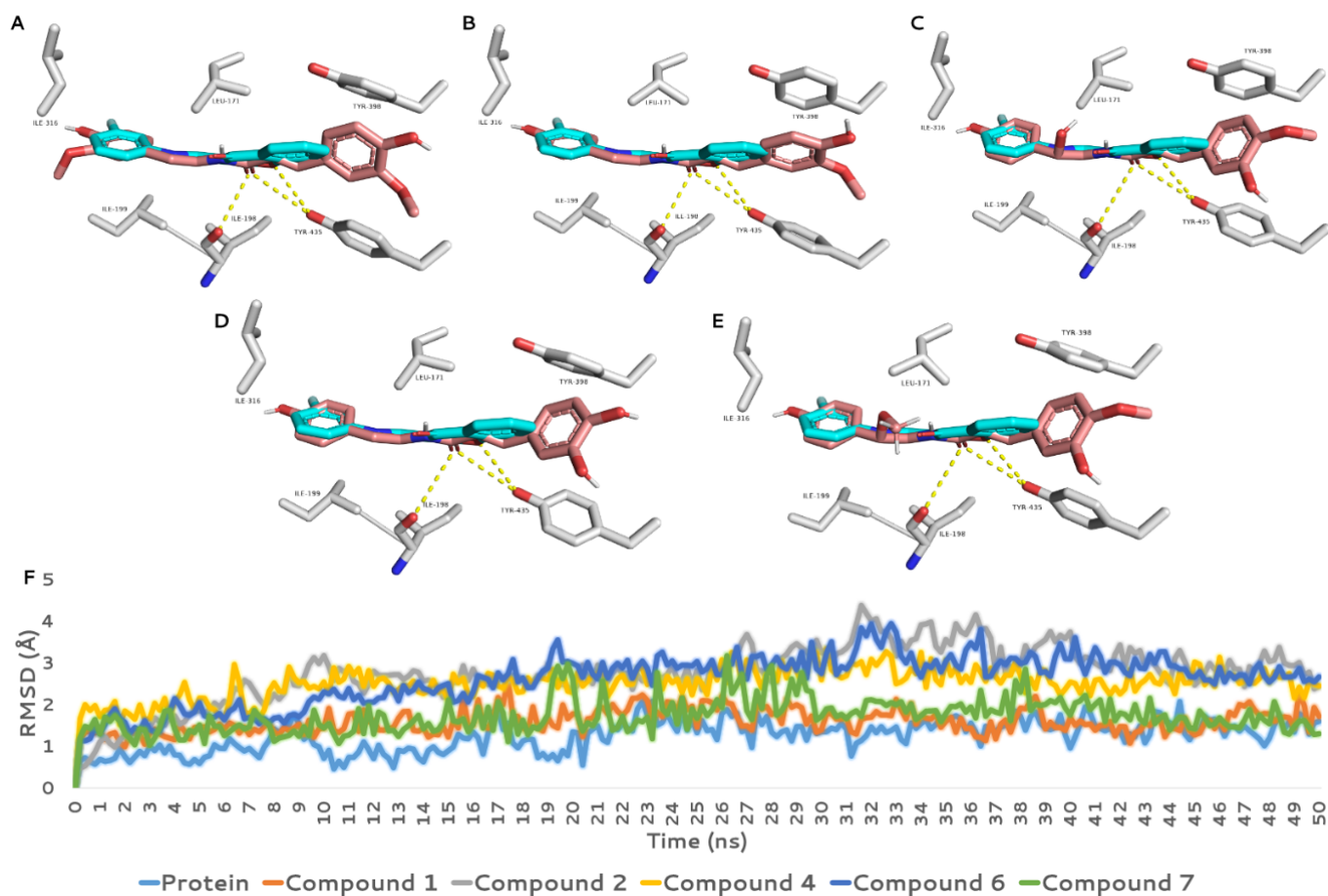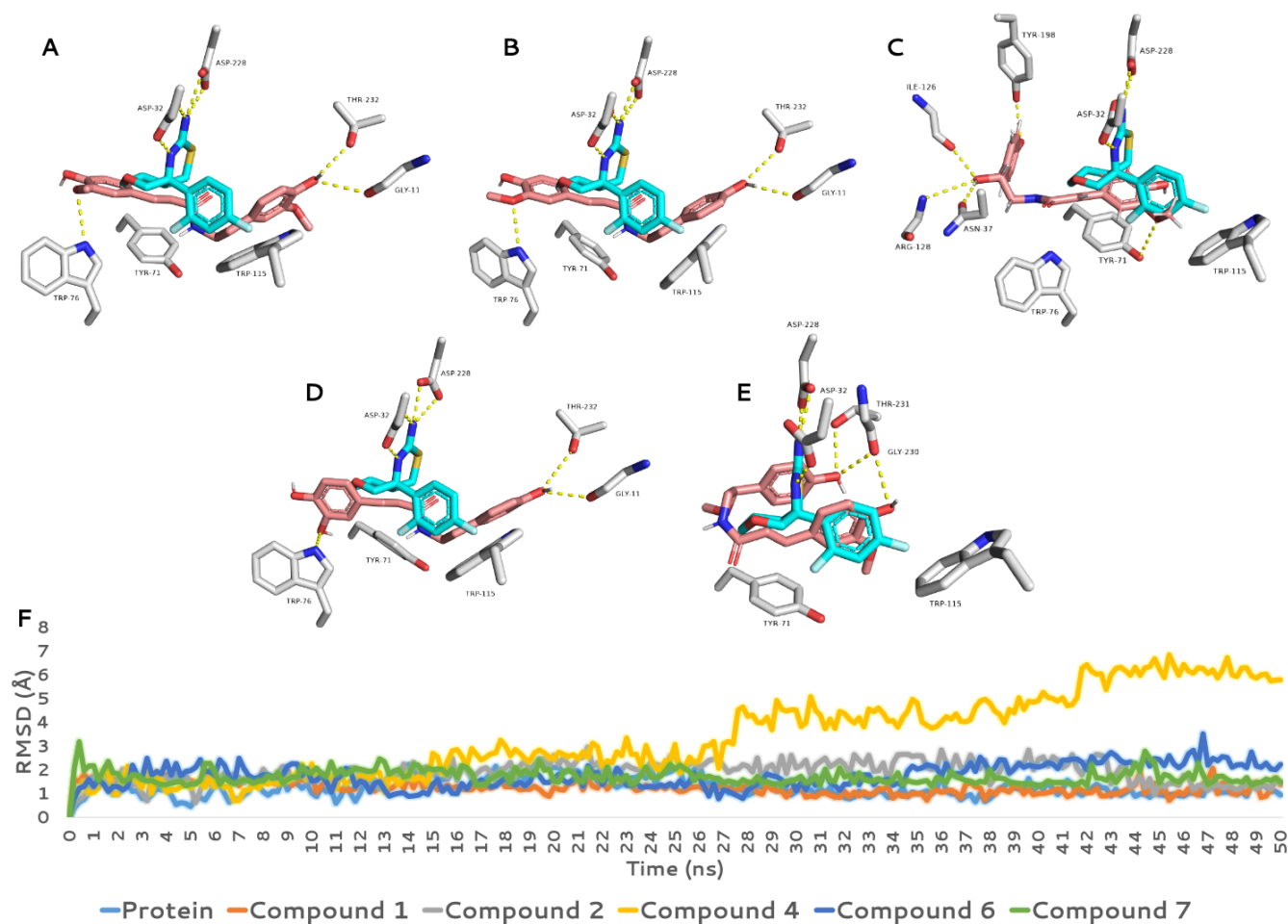Figure 24: A-E: Binding modes of the structures of compounds **1**, **2**, **4**, **6**, **7** inside BACE1's binding site (Brick-red coloured structures) in alignment with that of the co-crystalized inhibitor (Cyan-coloured structure). F: RMSDs of the structures of compounds **1**, **2**, **4**, **6**, **7** inside BACE1's binding site along with that of the co-crystalized inhibitor over 50 ns long MDS runs.

## 4.4. Conclusion

In summary, halophytes have been regarded as an economic potential source of bioactive constituents; however, the widely distributed *B. indica* and *A. alopecuroides* have not been completely utilized yet. Since more and more research focusing on the utilization of medicinal plants as promising sources of candidate compounds against AD, we focused on the isolation of amide alkaloids from the halophytic herbs, *B. indica* and *A. alopecuroides*.

AD is a well known for its multifactorial nature; consequently, it demands bioactive molecules with multimodal action that can act on more than one target to overcome the possible drug-drug interactions of the combined therapy. The present study describes the isolation and spectroscopic characterization of seven amide alkaloids from the aerial parts of *B. indica* and *A. alopecuroides* and highlights the potential utilization of crude extracts obtained from both plants and the isolated compounds in management of AD through multi-targeting of BACE1, MAO-B, $A\beta_{1-42}$ aggregation, and hyperphosphorylated tau protein. The isolated compounds showed extraordinary inhibition activity against all tested targets. Moreover, compounds **1**, **2**, and **7** demonstrated strong inhibition of BACE1, MAO-B, $A\beta_{1-42}$ aggregation, and hyperphosphorylated tau protein followed by compounds **4** and **6**.

Considering previous reports that have discussed the possibility of neuroprotection activity of *N-trans*-feruloyltyramine through stimulation of neurogenesis and neurotrophins [167], in addition to the role of *N-trans*-caffeoyltyramine and *N-trans*-coumaroyl tyramine in reduction of BACE1 gene expression [151], our study results suggested the contribution of amide alkaloids as effective lead compounds for the development of AD therapies. Furthermore, this study reveals the beneficial effects of *B. indica* and *A. alopecuroides* in the prevention as well as in the potential treatment of neurodegenerative diseases owing to their content of phenyl amides.

By reviewing the literature, there are no or limited studies about the valorization of halophytic herbs utilized in this study, in addition to the limited studies on the activity of lignanamides in management of AD and this can encourage scientists

to utilize more halophytic plants to target AD. In the future, further *in vivo* experiments will be needed to support the primary results obtained in our study.

Modeling and biophysics-based simulation studies showed an interesting structural information about the putative mode of interactions of these compounds inside the active sites of both MAOB and BACE1. Hence, such new information can be very helpful during the development of new inhibitor molecules using the scaffold of the amide alkaloids reported here.

# Chapter 5: Anti-cancer and anti-inflammatory activities of the halophyte herb *Bassia indica*

## 5.1. Introduction

Cancer is among the leading causes of death and a major public health problem worldwide [168]. According to the World Health Organization (WHO), cancer accounting for nearly 10 million deaths in 2020, or nearly one in six deaths. The most common causes of cancer deaths in 2020 were lung, colon and rectum, breast, and liver cancers [169]. The incidence of cancer and its mortality is rapidly growing worldwide that greatly burden health care systems and societies [170]. The current available drugs for cancer treatment is conventional chemotherapy; however, the development of drug resistance is one of the caused by chemotherapy [171]. For years, herbal remedies have used as a complementary therapy for different types of cancer; subsequently, natural compounds have been applied as alternative therapies in treatment of cancer [172]. It is worth noting that wide variety of plant-based anticancer therapies are in clinical use, and they exhibited significant efficacy [76]. On the other hand, inflammation plays an important role in cancer metastasis. Moreover, many studies have shown that the risk of cancer occurrence and development is associated with inflammation [173].

Cyclooxygenase-2 is a physiological enzyme with important roles in many biological functions especially in the mechanism of pain and inflammation, among other roles; consequently, considered a molecule of high interest to the pharmaceutical community as a target [173]. Based on previous studies, COX-2 is associated with several diseases, including cancer and tumor proliferation, asthma, and rheumatoid arthritis [174,175]. Additionally, COX-2 promotes angiogenesis and tissue invasion of tumors, and resistance to apoptosis [176]. Despite the efficacy of nonsteroidal anti-inflammatory drugs (NSAIDs) in management of inflammatory conditions, the adverse effects produced as gastrointestinal ulcers and cardiovascular events have limited their applications [177]. Accordingly, the search for newer therapies with the capacity to selectively inhibit COX-2 has been emerged as one of useful approaches in managing inflammatory conditions. As more and more studies have demonstrated that COX-2 might contribute to immunosuppression *via* multiple ways; hence, the inhibition of COX-2 is a great opportunity for cancer treatment in combination with immunotherapy [173].

*Bassia indica* (Wight) A. J. Scott is a halophytic herb distributed in the Egyptian ecosystem and other areas of the world [10]. In relation to ethnomedicine, the plant has been reported as an anti-tumor and anti-oxidant [94]. The biological investigation of anti-tumor properties of this plant has not been elucidated yet. Furthermore, the phytochemical and biological research on *B. indica* has been barely limited, and thus there is still a need to explore the biological properties of this plant. Therefore, the current study was conducted to provide a more detailed view of the anti-inflammatory and anti-tumor activities of the pant *B. indica*. In this study, twenty-five compounds obtained from *B. indica* were evaluated for their cytotoxicity and anti-inflammatory activities.

## 5.2. Experimental

### 5.2.1. Plant material

See Chapter 2

### 5.2.2. Material for chromatographic studies

See Chapters 2 and 3

### 5.2.3. Material for biological study

The inhibitory activity against COX-2 was evaluated by *in vitro* COX-2 enzyme inhibition assay using a fluorometric COX-2 inhibition kit (K547−100; BioVision, CA, USA). The human breast adenocarcinoma (MCF-7), ovarian endometrioid carcinoma (OVK-18), colorectal carcinoma (HCT116), and human liver carcinoma (HepG2), were purchased from Riken Bioresource Center of Japan (Ibaraki, Japan). Cells were cultured in Dulbecco's modified Eagle's medium (DMEM; Wako Pure Chemical Industries, Osaka, Japan), with a humid atmosphere of 5% $CO_2$ at 37 ºC. Hep-G2 (human liver cancer cell line) was cultured in Eagle's minimum essential media (EMEM; Wako Pure Chemical Industries, Osaka, Japan). The culture media were supplemented with 10% fetal bovine serum (FBS), 100 U/mL penicillin, and 100 U/mL streptomycin. 5-fluorouracil was used as a positive control.

### 5.2.4. Extraction and isolation of phytoconstituents

The aerial parts of *B. indica* (1.3 Kg) were dried, ground, and extracted with 80% methanol (7 L) four times. The dried crude extract (138.5 g) was suspended in $H_2O$ and partitioned with *n*-hexane, dichloromethane, ethyl acetate, and *n*-butanol. Part of the $CH_2Cl_2$ fraction (2 g) was subjected to fractionation over an open column with silica gel (75-150 µm) eluted with *n*-hexane–EtOAc–MeOH (1:0:0–0:1:1) to afford five subfractions (D1–D5). Compound **1** (7.1 mg) obtained after purification of fraction D1 over a Sephadex LH-20 (100% MeOH). Fraction D-3 (90 mg) was purified with MPLC (RP-C18, 20 µM, 4 g) eluted with $H_2O$–MeOH (8:2–5:5) yielding compounds **2** (3.1 mg), and **3** (6.2 mg). The EtOAc fraction (2 g) was subjected to fractionation over MPLC with a NP-flash column (40 g) eluted successively with *n*-hexane–EtOAc–MeOH (4:1:0–0:1:1 v/v) to obtain 5 fractions (E1–E5). Fraction E2 was chromatographed over a Sephadex LH-20 with 100% MeOH to obtain 3 fractions (E2-1 to E2-5). Fraction E-2-1 (46 mg) was purified over NP-TLC using $CH_2Cl_2$–MeOH (4.5:1) to obtain compounds **4** (6 mg), **5** (6.5 mg), **6** (7 mg), and **7** (5.5 mg). Fraction E-2.2 (30 mg) was subjected to purification over silica gel CC eluted $CH_2Cl_2$–MeOH (4.5:1) to afford compound **8** (5.2 mg), and compound **9** (4.5 mg). Compound **10** (2.9 mg) was obtained from fraction E-2.3 after purification over a Sephadex LH-20 eluted with 100% MeOH. Fraction E4 was purified over Sephadex LH-20 column eluted with 100% MeOH to obtain compound **11** (2.5 mg). Fraction E5 was subjected to purification over MPLC with RP-C18 flash column (40 µM, 12 g) eluted with $H_2O$–MeOH to obtain five subfractions E-5-A to E-5-E). Fraction E-5-A (24 mg) was purified over a Sephadex LH-20 to afford compounds **12** (4 mg), while **13** (4.2 mg) and **14** (3.5 mg) were obtained after purification over NP-TLC (DCM-MeOH; 9:1). Fraction E-5-C (89 mg) was purified over HPLC preparative column to obtain compounds **15** (3.2 mg), **16** (4.5 mg), and **17** (2.5 mg). Fraction E-5-E (250 mg) was purified over ODS-18 and Sephadex LH-20 to obtain compounds **18** (5.6 mg) and **19** (3.7). The *n*-Butanol fraction (12 g) was chromatographed over a Diaion HP-20 using five mobile phases of $H_2O$-MeOH (1:0, 4:1, 1:1, 1:4, 0:1, each 10 L) to yield 5 fractions (BU-1 to BU-5). Fraction BU-3 (1.1 g) was partitioned over MPLC with RP-C18 flash column using $H_2O$–MeOH (4:1 to 0:1) and preparative HPLC column to obtain compounds **20** (4 mg), **21** (2.3 mg), **22** (1.2 mg). Fraction BU-4 (1.5 g) was subjected to fractionation over Biotage with 30 g

RP-C18 column to obtain 3 fractions (BU-4-1 to BU-4-3). Fraction BU-4-3 was purified over ODS-18 eluted with $H_2O$–ACN–0.1% FA to obtain **23** (8.5 mg**)**, **24** (9.3 mg), **25** (11.5 mg).

### 5.2.5. *In vitro* COX-2 inhibition assay

The inhibitory potential of methanol extract and isolated compounds from *B. indica* was evaluated by *in vitro* COX-2 enzyme inhibition assay using a fluorometric COX-2 inhibition kit (K547−100; BioVision, CA, USA). The kit comprises COX-2 enzyme, COX assay buffer, COX probe (in DMSO), COX cofactor (in DMSO), arachidonic acid, NaOH, and selective inhibitor celecoxib. The COX-2 enzyme solution was prepared by adding $ddH_2O$ (110 µL) to the lyophilized powder in the kit.  Then, COX assay buffer (398 µL) and COX Cofactor (2 µL) were mixed to prepare the diluted COX cofactor. Dilute arachidonic acid/NaOH solution was prepared by adding 5 µL arachidonic acid and 5 µL of NaOH together, then diluted with 90 µL $ddH_2O$. Then, in a white, flat-bottomed, opaque 96-well plates, the reaction mixture consisted of COX assay buffer (76 µL), COX probe (1 µL), diluted COX cofactor (2 µL), and COX-2 enzyme solution (1 µL). The test samples were prepared in 10 µL of COX assay buffer as test inhibitors and then added to the above mixture. After that, the assay mixture was incubated at 25 °C for 5–10 min. A 10 µL of diluted arachidonic acid/NaOH solution were added to each well. Measure fluorescence (Ex/Em = 535/587 nm) kinetically at 25 °C for 5-min intervals by a microplate reader (BioTek Instruments, Winooski, USA). Blank, control, and all concentrations of inhibitors were analyzed in 4 replicates. Results were expressed as percentage COX-2 inhibition by equating the fluorescence intensity of the test solution with that of the control.

### 5.2.6. MTT assay

The cytotoxic activity of crude methanol extract and isolated compounds against MCF-7, OVK-18, HepG2, and HCT-116 cancer cell lines were determined by MTT colorimetric assay [178]. Briefly, cells were cultured in a 96-well plates at a density of $5 \times 10^4$ cells/well. After 24 h, the cells were treated with different concentrations of the isolated compounds (0.1–400 µg/mL, dissolved in DMSO), then incubated for 48 h. Following incubation, 100 µL fresh medium, and 20 µL MTT (5 mg/mL) were added to each well, then incubated again for 4 h. After that, the supernatant was removed and 100 µL of isopropanol HCl was added to each well and kept in dark for 4 h to dissolve the formed formazan crystals. The absorbance was measured at 570 nm using a microplate reader (Biotek, Winooski, USA). 5-fluorouracil was used as a positive control.

## 5.3. Results and discussion

The chemical investigation of 80% aq. methanol extract of *B. indica* yielded twenty-five compounds (Figure 25). The isolated compounds were determined based on their spectroscopic data, as well as a comparison with those published in the literature. The isolated compounds were categorized into steroid, lignan, amide alkaloids, coumarin, nucleic acid derivatives, phenolic glycoside, flavonoids, and triterpene oleanane saponins as seen in Figure 26.

The isolates were identified as β-sitosterol (**1**) [98], syringaresinol (**2**) [99], *N-trans*-feruloyl-3-methoxytyramine (**3**) [100], vanillic acid (**4**) [121], *o*-hydroxybenzoic acid (**5**) [122], *p*-hydroxybenzoic acid (**6**) [123], 6,7-dihydroxy coumarin (**7**) [124], methyl caffeate (**8**) [125], caffeic acid (**9**) [126], quercetin (**10**) [127], *N-trans*-feruloyltyramine (**11**) [101], uracil (**12**) [128], thymidine (**13**) [112], tachioside (**14**) [129], *S*-(–)-*N-trans*-feruloylnormetanephrine (**15**) [102], *S*-(–)-*N-trans*-feruloyloctopamine (**16**) [103], *R*-(+)-*N-trans*-feruloyloctopamine (**17**) [104], isorhamnetin-3-*O*-glucoside (**18**) [179], kaempferol-3-*O*-rutinoside (**19**) [130], kaempferol-3-*O*-β-D-glucopyranosyl-(1→6)-*O*-[β-D-galactopyranosyl-(1→3)-2-*O-trans*-feruloyl-α-L-rhamnopyranosyl-(1→2)]-β-D-glucopyranoside (**20**), isorhamnetin-3-*O*-β-D-glucopyranosyl-(1→6)-*O*-[α-L-rhamnopyranosyl-(1→2)]-β-D-glucopyranoside (**21**), *N*-[(3-(3-methyl-1-oxo-butyl)amino)propyl]-3-(3,4-dihydroxyphenyl)prop-2-enamide (**22**), 3-*O*-[2'-(2''-*O*-glycolyl)-glyoxylyl-β-D-glucuronopyranosyl]-28-*O*-β-D-glucopyranosyl-olean-

12-en-3β-ol-28-oic acid (**23**), (2'*R*,3'*S*)-3-*O*-[2'-hydroxy-3'-(2"-*O*-glycolyl)-oxo-propionic acid-*β*-D-glucuronopyranosyl]-28-*O*-*β*-D-glucopyranosyl-olean-12-en-3*β*-ol-28-oic acid (**24**), chikusetsusaponin V (**25**) [180,181].
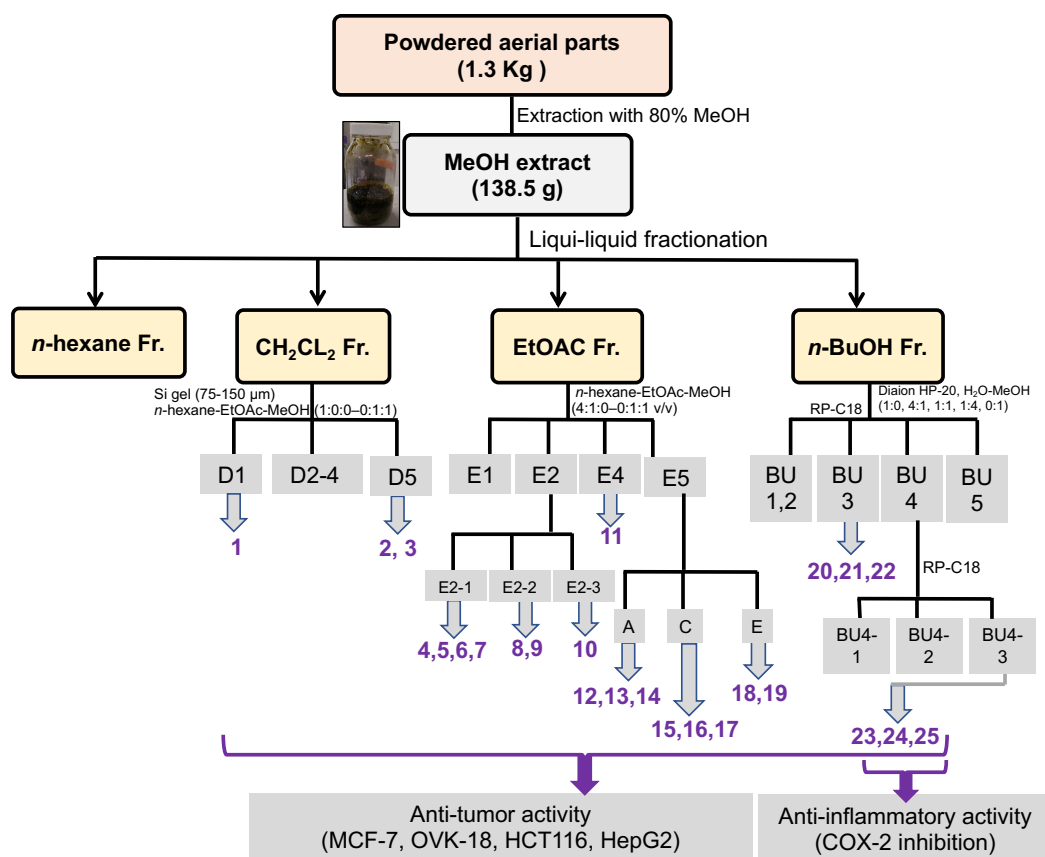


Figure 25: Schematic isolation of compounds **1**–**25** from *B. indica*

**3** R₁ = H, R₂ = OCH₃
**11** R₁ = H, R₂ = H
**15** R₁ = OH, R₂ = OCH₃
**16** R₁ = OH, R₂ = H (7'S)
**17** R₁ = OH, R₂ = H (7'R)

**4** R₁ = COOH, R₂ = H, R₃ = OCH₃, R₄ = OH
**5** R₁ = COOH, R₂ = OH, R₃ = H, R₄ = H
**6** R₁ = COOH, R₂ = H, R₃ = H, R₄ = OH
**14** R₁ = OH, R₂ = OCH₃, R₃ = H, R₄ = β-D-Glc

**8** R = OCH₃
**9** R = OH

**10** R₁ = OH, R₂ = H
**18** R₁ = OCH₃, R₂ = β-D-Glc
**19** R₁ = H, R₂ = S1
**20** R₁ = H, R₂ = S2
**21** R₁ = OCH₃, R₂ = S3

**23** R₁ = β-D-Glc, R₂ = S4
**24** R₁ = β-D-Glc, R₂ = S5
**25** R₁ = β-D-Glc, R₂ = S6

Figure 26: Structures of isolated compounds **1**–**25**

### 5.3.1. Anti-inflammatory activity of the isolated compounds

Inflammation has deemed a key factor in cancer development [182]. The formation of prostaglandins is governed by either cyclooxygenase-1 (COX-1) or cyclooxygenase-2 (COX-2) from arachidonic acid and led to the inflammatory process. A prostanoid lipid, prostaglandin E2 (PGE2), has been correlated with cancer cell survival, metastasis, angiogenesis, and immunosuppression [182]. The enzymes, COX-1 and COX-2 are critical for formation of PGE2, and they are up-regulated in colorectal, breast, stomach, lung, and pancreatic cancers [182]. Hence, the discovery of potent anti-inflammatory compounds from natural plant sources through inhibition of COX-2 is of great importance in pharmaceutical field. In the present study, the COX-2 enzyme inhibiting activity of crude extract of *B. indica*, as well as the isolated triterpenoid saponins, were evaluated as shown in Figure 27 . Based on previous data published in the literature, the saponin content in the *n*-butanol fraction of the halophytes extracts is a significant factor for the anti-inflammatory potential [183]. Therefore, the isolated saponins (**23**-**25**) from *B. indica* were investigated for their possible anti-inflammatory effect via inhibition of the COX-2 enzyme.

As seen in Figure 28, the methanol extract of *B. indica* exhibited promising anti-inflammatory activity through inhibition of COX-2 with an $IC_{50}$ = 7.97 ± 0.4 µg/mL. Importantly, compound **23** exhibited significant inhibitory activity on COX-2 enzyme with $IC_{50}$ value of 3.05 ± 0.15 µg/mL compared to that of reference drug celecoxib ($IC_{50}$ = 1.75 ± 0.09 µg/mL). Furthermore, compounds **24** and **25** showed moderate inhibition activity against COX-2 with $IC_{50}$ values of  24.89 ± 1.26, and 19.65 ± 0.99 µg/mL, respectively.

By reviewing literature, previous studies revealed the potential anti-inflammatory activity of halophyte plants owing to their chemical composition[184,185]. Previous studies demonstrated that saponin derivatives contribute to anti-inflammatory activity of plant crude extracts. Triterpene oleanane saponin isolated from the halophyte *Anabasis setifera* displayed a potential anti-inflammatory activity [183]. Also, phenolics and flavonoids are suggested to contribute to the anti-inflammatory activity [183,185,186]. The extract of the herb *Suaeda fruticosa* displayed the utmost anti-inflammatory activity by inhibiting nitric oxide (NO) release owing to its phenolic content [185]. Additionally, polyphenols mainly flavonoids can have anti-inflammatory mediated by the modulating action on the

expression of the iNOS gene and consequently inhibit the production of NO [187]. Thus, the anti-inflammatory potential of *B. indica* might be explained due to the presence of saponins and phenolic derivatives.
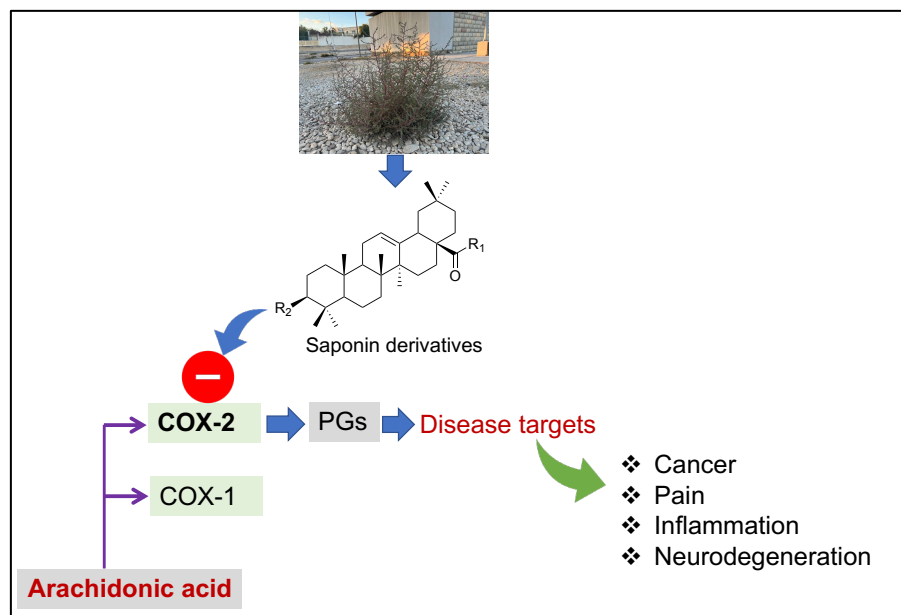


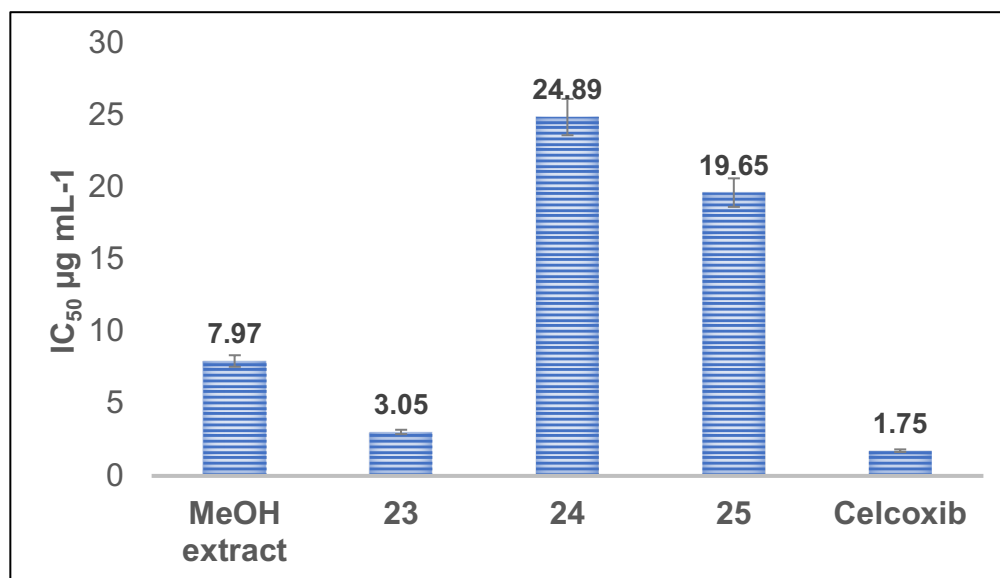Figure 27: Schematic graph for COX-2 inhibition mechanism by saponins



Figure 28: Anti-inflammatory activity of *B. indica* methanolic extract and the isolated compounds **23–25** against COX-2 ($IC_{50}$ μg/mL)

### 5.3.2. Anti-tumor activity of the isolated compounds

Cancer is a disease with great burden worldwide. Millions of people are diagnosed with cancer each year, and about 10 million deaths emerged in 2020 [169]. It is noteworthy that the history of the development of anti-cancer drugs has been shaped by natural products and approximately 25% of newly approved anti-cancer drugs between 1981 and 2019 were based on natural products [188]. Recently, significant advances have been made in cancer treatment; however, the incidence rates and mortality are still high. Therefore, approaches have been emerged to develop more effective and less toxic cancer treatment options [188,189].

In this study, compounds (**1−25**) were investigated for their cytotoxicity against four cancer cell lines [Human breast adenocarcinoma (MCF-7), human ovarian endometrioid carcinoma (OVK-18), colorectal carcinoma (HCT116), human liver carcinoma (HepG2), normal human dermal fibroblast (NHDF), and normal human colon epithelial cells (CCD841) cell lines] were determined by MTT colorimetric assay [178]. All the tested samples (**1-25**) did not show cytotoxicity to normal cell lines (NHDF) and CCD841, reflecting their selectivity to the human cancer cell lines, except for compound **9** as shown in Table 14.

With regard to OVK-18, the methanol extract, and compounds **11**, **2**, and **3** showed good cytotoxicity with $IC_{50}$ = 7.27 ± 1.08, 1.74 ± 1.56, 4.03 ± 0.21, and 4.00 ± 0.26 µg/mL, respectively, while compounds **14** and **17** displayed moderate activity with $IC_{50}$ = 21.50 ± 10.67 and 16.33 ± 1.95, respectively, when compared to the positive control as seen in Table 14. Regarding MCF-7, compound **13** displayed potent cytotoxicity with $IC_{50}$ < 0.1 µg/mL, while compounds **7** and **3** showed good activity with $IC_{50}$ = 1.47 ± 0.22 and 4.55 ± 0.38 µg/mL, respectively. Importantly, compound **1** showed significant activity against human colorectal carcinoma and liver adenocarcinoma with $IC_{50}$ values less than 0.1 µg/mL. Additionally, compounds **2**, **4**, **5**, and **6** displayed potent cytotoxicity against HepG2 cell line with $IC_{50}$ less than 0.1 µg/mL, while compound **9** showed moderate activity with $IC_{50}$ = 2.88 ± 0.81 µg/mL. Moreover, compounds **2**, **3**, and **9** showed moderate activity against HCT116 cell line with $IC_{50}$ = 26.95 ± 4.38, 18.16 ± 2.20, and 19.80 ± 8.05 µg/mL, respectively.

Among the isolated triterpene saponins, compound **25** displayed potent cytotoxicity against HCT116 with $IC_{50}$ less than 0.1 µg/mL, while **23** showed moderate activity with an $IC_{50}$ = 44.31 ± 5.79 µg/mL. It is worth mentioning that among the tested lignanamides (**3**, **11**, **15**, **16**, and **17**), compound **11** displayed the highest potential activity against OVK-18 with $IC_{50}$ = 1.74 ± 1.56 µg/mL, while **3** showed activity against MCF-7 and OVK-18 with $IC_{50}$ = 4.00 ± 0.26 and 4.55 ± 0.38 µg/mL, respectively. Also, the rare occurring *R*-isomer amide derivative (**17**) showed moderate activity against OVK-18 with $IC_{50}$ = 16.33 ± 1.95 µg/mL. Consequently, the absence of hydroxyl group at position C-7' is essential for the activity except when the configuration of C-7' is *R*-isomer. Furthermore, the presence of the methyl group in compound **9** markedly enhances the activity when compared to compound **8**.

By reviewing the literature, it is to be noted that the anti-tumor activity of *β*-sitosterol related to induction of apoptosis and inhibiting proliferation by activation of caspase-3 and induction of Bax/Bcl-2 ratio [190]. The furofuran lignan (syringaresinol) showed cytotoxicity against Hep-2 (larynx epidermoid carcinoma), HeLa (human cervix carcinoma), and C6 (rat glioma) cell lines with $IC_{50}$ ranging from 0.23-0.63 µg/mL [191]. The amide alkaloid, *N-trans*-feruloyltyramine, showed cytotoxic activity against human lung (A549 and K562) cancer cell lines with $IC_{50}$ = 37.20 and 41.52 µmol $L^{-1}$, respectively. Also, aesculetin (6,7-dihydroxy coumarin) induces apoptosis in HeLa cells through a ROS-mediated mitochondrial dysfunction pathway [192]. Moreover, methyl caffeate induces apoptosis through activation of the mitochondrial pathway and induction of DNA damage [193]. Therefore, the cytotoxic activity of *B. indica* might be attributed to its content of diverse metabolites with significant anti-tumor activities.

**Table 14**: Cytotoxic activities of compounds **1–25** against MCF-7, OVK-18, HCT-116, HepG2, NHDF and CCD841.

| Compound | IC$_{50}$ (µg.mL$^{-1}$) | | | | | |
|---|---|---|---|---|---|---|
| | MCF-7 | OVK-18 | HCT-116 | Hep-G2 | NHDF | CCD841 |
| **MeOH extract** | > 200 | 7.27 ± 1.08 | > 200 | > 200 | > 400 | > 400 |
| **1** | 49.78 ± 4.88 | > 400 | < 0.1 | < 0.1 | > 400 | > 400 |
| **2** | 22.95 ± 6.22 | 4.03 ± 0.21 | 26.95 ± 4.38 | < 0.1 | > 400 | > 400 |
| **3** | 4.55 ± 0.38 | 4.00 ± 0.26 | 18.16 ± 2.20 | > 400 | > 400 | > 400 |
| **4** | >400 | > 400 | > 400 | < 0.1 | > 400 | > 400 |
| **5** | >400 | > 400 | > 400 | < 0.1 | > 400 | > 400 |
| **6** | >400 | > 400 | < 200 | < 0.1 | > 400 | > 400 |
| **7** | 1.47 ± 0.22 | 82.42 ± 1.18 | > 400 | ND | > 400 | > 400 |
| **8** | >400 | > 400 | > 400 | > 400 | > 400 | > 400 |
| **9** | >400 | > 400 | 19.80 ± 8.05 | 2.88 ± 0.81 | 143.92 ± 4.90 | > 400 |
| **10** | >400 | > 400 | ND | > 400 | > 400 | > 400 |
| **11** | 224.59 ± 12.11 | 1.74 ± 1.56 | ND | ND | > 200 | > 400 |
| **12** | 55.92 ± 23.79 | > 400 | >400 | > 400 | > 400 | > 400 |
| **13** | < 0.1 | > 400 | ND | > 400 | > 400 | > 400 |
| **14** | 129.14 ± 5.91 | 21.50 ± 10.67 | > 400 | ND | > 400 | > 400 |
| **15** | > 400 | > 400 | > 400 | > 400 | > 400 | > 400 |
| **16** | > 400 | > 400 | > 400 | > 400 | > 400 | > 400 |
| **17** | > 400 | 16.33 ± 1.95 | > 400 | 151.60 ± 5.54 | > 400 | > 400 |
| **18** | > 400 | > 400 | > 400 | > 400 | > 400 | > 400 |
| **19** | > 400 | > 400 | > 400 | > 400 | > 400 | > 400 |
| **20** | > 400 | 141.79 ± 16.33 | > 400 | 284.22 ± 6.60 | > 400 | > 400 |

| | | | | | | |
|---|---|---|---|---|---|---|
| **21** | > 400 | >200 | > 400 | 159.87 ± 19.08 | > 400 | > 400 |
| **22** | > 200 | >200 | > 200 | >200 | > 200 | > 200 |
| **23** | 136.64 ± 3.51 | 44.31 ± 5.79 | > 400 | 178.45 ± 9.01 | > 400 | > 200 |
| **24** | > 400 | > 400 | > 400 | > 400 | > 400 | > 400 |
| **25** | > 400 | > 400 | < 0.1 | > 400 | > 400 | > 400 |
| **5-FU** | 12.2 ± 1.56 | 10.2 ± 2.28 | 5.8 ± 0.22 | >100 | >100 | >100 |

ND = not determined, n = 3 ± SE

## 5.4. Conclusion

The halophyte herb *B. indica* has been reported as anti-tumor in traditional medicine. Therefore, aiming at finding providing more scientific basis for this traditional usage, we have further evaluated this species for anticancer and anti-inflammatory activity.

To our knowledge, the current study marks the first anti-inflammatory and anti-tumor of the constituents from *B. indica*. Besides, the study highlights the potential utilization of halophytes as a source of pharmaceutical candidates through the determination of the key active metabolites from *B. indica* which are responsible for the anti-tumor and anti-inflammatory activities.

Importantly, the oleanane saponin derivatives showed considerable anti-inflammatory activity. Moreover, other isolated phytochemicals showed varying anti-tumor activity against MCF-7, OVK-18, HCT-116, and Hep-G2.

The findings of this study might explain the beneficial health properties of *B. indica* and its phytochemicals in management of inflammation and cancer; however, further studies are needed in the future to validate the exact mechanisms as an anti-inflammatory and anti-tumor. Moreover, further *in vivo* experiments are needed to support the primary results obtained in this study.

**Chapter 6: Undescribed glucosylceramide, flavonol triglycoside, and oleanane saponin from the halophyte *Agathophora alopecuroides*: Promising candidates for stimulating ceramide synthesis**

## 6.1. Introduction

Halophytes are salt-tolerant plants distributed in saline and desert areas [78]. They are among the promising sources of bioactive phytochemicals for nutritional and therapeutic purposes [13,20,152]. The Mediterranean basin is a rich source of wild and edible halophytes that can grow in coastal and salty areas. In relation to ethnomedicine, halophytes have been used as food and folk remedies for centuries. Consequently, they have been suggested as potential sources for food industry and medicinal products with functional and health properties [13,82,117,194,195]. Further utilization of halophytes in chemical and biological studies is very promising owing to their economic potential as significant sources of nutraceuticals and very cheap sources of candidate compounds with structural diversity that display broad spectrum of bioactivities [183,196,197]. Flavonoids, alkaloids, terpenoids, nitrogenous compounds, and saponins are among the types of bioactive chemicals distributed in halophytes [63,64,69,117,198].

Among the halophytes is *Agathophora alopecuroides* (Delile) Fenzl ex Bunge, native to Egypt and North Africa [10,199]. The use of *A. alopecuroides* for therapeutic purposes has been reported by Bedouins of the Sinai Peninsula of Egypt and in Algerian traditional medicine [22,200]. In the literature, there is no reported data from detailed chemical or biological investigations of *A. alopecuroides*.

The human skin is self-renewing organ which protect the body against infection, environmental, chemical, and biological hazards. The human skin is composed of epidermis, dermis and hypodermis, and acts as a barrier to maintain moisture [201,202]. Skin aging and other skin diseases, such as xerosis, atopic dermatitis, and psoriasis are associated with reduced levels of ceramides, which contribute to the epidermal barrier function as the main lipids of the skin's *stratum corneum* (SC) [203,204]. Ceramides account for 40-60% of total lipids in the skin and play an important role in the skin epidermis barrier function, epidermal differentiation, and water-holding capacity [205]. Ceramides are produced *via* two pathways, a de novo pathway and a salvage pathway. In a de novo pathway, synthesis of skin ceramides occurs in the basal layers of epidermis in the endoplasmic reticulum. The pathway begins with the condensation of L-serine and palmitoyl CoA by serine palmitoyl transferase producing 3-ketosphinganine which is then reduced to sphinganine by 3-ketosphinganine reductase. Following that, sphinganine is

acylated *via* sphinganine-*N*-acyl transferase generating a dihydroceramide, which is then reduced to ceramide by dihydroceramide desaturase [204,206]. According to previous reports, ceramide synthase-3 (CerS3) is highly expressed in keratinocytes and its expression is increased in differentiated keratinocytes [204]. CerS3 plays an important role in the production of ceramides in epidermis and subsequently contribute to restoration of the disrupted barrier function. Plant-derived constituents are perceived to be safer than synthetic chemicals and are preferable to them for therapeutic and cosmetic applications [207,208]. Recently, more research has been done in order to discover the beneficial effects of plant-derived compounds on human skin to overcome the reduced levels of skin ceramides in diseased and aged skin [209–211]. Among natural products, saponins and flavonoids have been recognized for their beneficial properties on human skin [201,212].

In continuation of our efforts for the utilization of halophytic plants as sources of candidate compounds with beneficial biological activities, the present study was conducted to gain a more detailed view of the protective and beneficial health effects of *A. alopecuroides* on the skin. The present study reports on the isolation and structural determination of three novel compounds (**6**, **8** and **10**), alongside eight known ones (**1**-**4**, **5**, **7**, **9** and **11**) from the methanol extract of *A. alopecuroides*. In addition, as ceramide synthase-3 (CerS3) plays a crucial role in epidermal hydration and restoration of the skin barrier function, the influence of *A. alopecuroides* extract and its isolated compounds on the mRNA expression levels of ceramide synthase (CerS3) in human keratinocyte cells (HaCaT) was evaluated.

## 6.2. Experimental

### 6.2.1. Plant material

The aerial parts of *A. alopecuroides* were collected from desert areas in Wadi-degla protectorate, Maadi, Egypt in August 2019. The plant sample was kindly identified by Prof. Ibrahim A. El-Garf, Department of Botany, Faculty of Science, Cairo University, Egypt. A voucher specimen (AG-2019) has been deposited at the herbarium of Pharmacognosy and Medicinal plants Department, Faculty of Pharmacy, Al-Azhar University, Cairo, Egypt.

## 6.2.2. Material for chromatographic studies

For fractionation and purification over column chromatography (CC), NP-silica gel (75-150 μm; Merck, Darmstadt, Germany), RP-C18 silica gel (38-63 μm; Wako Pure Chemical Corporation, Osaka, Japan), Sephadex LH-20 (Merck, Japan) and Diaion (Mitsubishi Chemical, Japan) were used. Final purification of compounds was achieved using high-performance flash chromatography (Biotage selekt; Biotage Japan Co., Ltd., a subsidiary of Biotage, Uppsala, Sweden) equipped with RP-C18 flash column chromatography (Sfär C18 D Duo column, 30 μm; 30 and 60 g; made in UK) and MPLC (Pure C-850 Flash prep®, Buchi, Switzerland) with UV-ELSD detection connected to normal- (Flash pure silica 20 μm; 4 and 12 g) or reversed-flash columns (Flash pure C18, 40 μm, 4, 12 and 40 g) and preparative HPLC column (Inertsil ODS-3, 5 μm, 20 × 250 mm, obtained from GL Sciences Inc., Japan). Precoated silica gel (Merck 60 $F_{254}$) plates were used for TLC investigation. The spots on TLC were detected by spraying with 5% $H_2SO_4$ solution and then heating at 110 °C.

## 6.2.3. Material for biological study

### a) Cell Culture (HaCaT cells)

Human keratinocytes cells (HaCaT) were cultured in Dulbecco's Modified Eagle's medium (DMEM) high glucose, obtained from Wako, Osaka, Japan, supplied with 10% heat-inactivated fetal bovine serum (FBS) (GE Healthcare HyClone, USA) and 1% penicillin-streptomycin (Wako, Osaka, Japan). The cells were incubated in a humidified atmosphere with 5% $CO_2$ at 37 °C.

### b) MTT Assay for cell viability

To evaluate the viability of cells, HaCaT cells were seeded into a 96-well plate at a density of $1×10^5$ cells/well and incubated overnight at 37 °C in humidified atmosphere with 5% $CO_2$. The cells were then treated with various concentrations of the isolated compounds for 24 h. Then, fresh media and 3-(4,5-Dimethyl-2-thiazolyl)-2,5-diphenyltetrazolium bromide (MTT) solution, obtained from Tokyo Chemical Industry, Tokyo, Japan, were added to each well and incubated for 4 h. After incubation, supernatant was discarded, and 100 μL of 40 mM HCl-isopropanol added to each well to dissolve the formed

formazan crystals. The absorbance was measured at 570 nm using a microplate reader. Control cells treated with solvent DMSO without samples.

## c) Real-Time PCR analysis

To evaluate the expression of ceramide synthase gene-3, HaCaT cells ($1 \times 10^5$ cells/well) were collected at 24 h after treatment either with the extract or isolated compounds **1–11** (10–400 µg/mL) in 24-well plates. According to the manufacturer's protocol, the total RNA was extracted from cells using a PureLink RNA Mini kit (Invitrogen, CA, USA). The cDNA was synthesized from the extracted total RNA using ReverTra Ace® qPCR RT Master Mix with gDNA Remover (Toyobo Co., Osaka, Japan). RT-quantitative PCR was performed using the THUNDERBIRD SYBR qPCR Mix (Toyobo Co., Japan) for CerS3. PCR was performed with primers as follows: 5′-ACATTCCACAAGGCAACCATTG-3′ and 5′-CTCTTGATTCCGCCGACTCC-3′ for CerS3. The PCR was performed by using an Agilent AriaMX Real-Time PCR system (Agilent Technologies, USA). The samples were tested in triplicate and the mRNA expression level of glyceraldehyde-3-phosphate dehydrogenase (GAPDH) was used to correct that of the enzyme.

## 6.2.4. Extraction and isolation of phytoconstituents

The air-dried powdered aerial parts of *A. alopecuroides* (0.9 kg) was extracted four times with 80% aq. MeOH (5 L) at room temperature (25 °C). A crude extract (ca. 100 g) was obtained, then suspended in $H_2O$ and partitioned over a Diaion HP-20 eluted with $H_2O$-MeOH (1:0-0:1) to get two fractions, $H_2O$ fraction (68 g) and methanol fraction (28.5 g). The MeOH fraction (27.5 g) was chromatographed on a Biotage selekt connected with flash column of NP-silica gel eluted with a gradient of *n*-hex-$CH_2Cl_2$-MeOH-$H_2O$ (1:0:0:0-0:0:1:0.5) to obtain 11 fractions (Fr. 1 – Fr. 11). Fraction Fr. 3 (531.5 mg) was purified using MPLC with NP-flash column (12 g) eluted with a gradient of *n*-hexane-EtOAc to obtain compound **1** (30 mg). Part of fraction Fr. 6 (1 g) was purified on a Biotage selekt with NP-flash column eluted with *n*-hex-EtOAc -MeOH; 1:0:0-0:0:1 to afford compound **2** (16 mg). The fraction Fr.7 was chromatographed on a Biotage selekt (60 g; RP-C18) eluting with $H_2O$-MeOH (1:0-0:1) to obtain 10 subfractions (Fr. 7.1 – Fr. 7.10). Subfraction Fr. 7.6 (1.1 g) was purified on MPLC (RP-C18; 40 g) eluting with $H_2O$-ACN-0.1% formic

acid (4.5:0.5:0.1-1:1:0.1) to obtain compound **3** (9 mg). Subfraction Fr. 7.7 (988 mg) was purified on MPLC (RP-C18; 40 g) and eluted with a gradient of $H_2O$-MeOH-0.1% formic acid (4:1:0.1-1:1:0.1) to afford compounds **4** and **5** (8.2 and 12.0 mg, respectively). Compound **6** (10.1 mg) was obtained after purification of subfraction Fr. 7.8 (956 mg) on MPLC (NP-flash column; 2 columns each 12 g) eluted with a mobile phase of $CH_2Cl_2$-MeOH-$H_2O$ (1:0:0, 9.5:1.5:0.1, 9:1:0.2, 8:2:0.2). Fraction Fr. 8 (3.5 g) was subjected to fractionation on a Biotage selekt (60 g; RP-C18) eluted with $H_2O$-MeOH (9:1–0:1) to obtain 5 subfractions (Fr. 8.1 – Fr.8.5). Subfraction 8.2 (obtained from 30% MeOH/$H_2O$, 700 mg) was purified on open column chromatography packed with RP-C18 silica gel eluted with an isocratic mobile phase of $H_2O$-MeOH (4:1) to furnish compounds **8** and **9** (4 and 9 mg, respectively). Subfraction 8.3 (obtained from 50% MeOH/$H_2O$, 510 mg) was purified on a Sephadex LH-20 with 100% MeOH to afford compound **7** (15 mg). Subfraction 8.4 (223 mg) was purified on open column packed with RP-C18 silica gel eluted with $H_2O$-ACN-0.1%formic acid (3.5:1.5:0.1) to furnish compounds **10** (12 mg) and **11** (14 mg).

### 6.2.5. Procedure for identification of isolated compounds

FAB-MS and HR-FAB-MS data were determined on a JEOL JMS-700 mass spectrometer (Jeol, Tokyo, Japan). HRESIMS data for compounds were recorded on a quadrupole time-of-flight mass spectrometer (Agilent QTOF-LC-MS, Agilent Technologies, USA). Optical rotations were determined using a JASCO P-2000 polarimeter (JASCO, Tokyo, Japan). 1D and 2D NMR spectra were determined on a DRX 600 spectrometer (Bruker Daltonics, USA). Agilent 1260 infinity II LC (Agilent Technologies, SantaClara, CA, USA) and Asahipak $NH_2P$-50 4E (4.6 × 250 mm) were used for determination of sugars in the isolated compounds.

## 6.3. Results and discussion

### 6.3.1. Identification of the isolated compounds

The 80% aqueous MeOH extract of the aerial parts of *A. alopecuroides* was partitioned by a Diaion HP-20 and eluted with $H_2O$-MeOH, then purified by an open column packed with RP-C18 silica gel and repeated medium-pressure liquid chromatography (MPLC) on

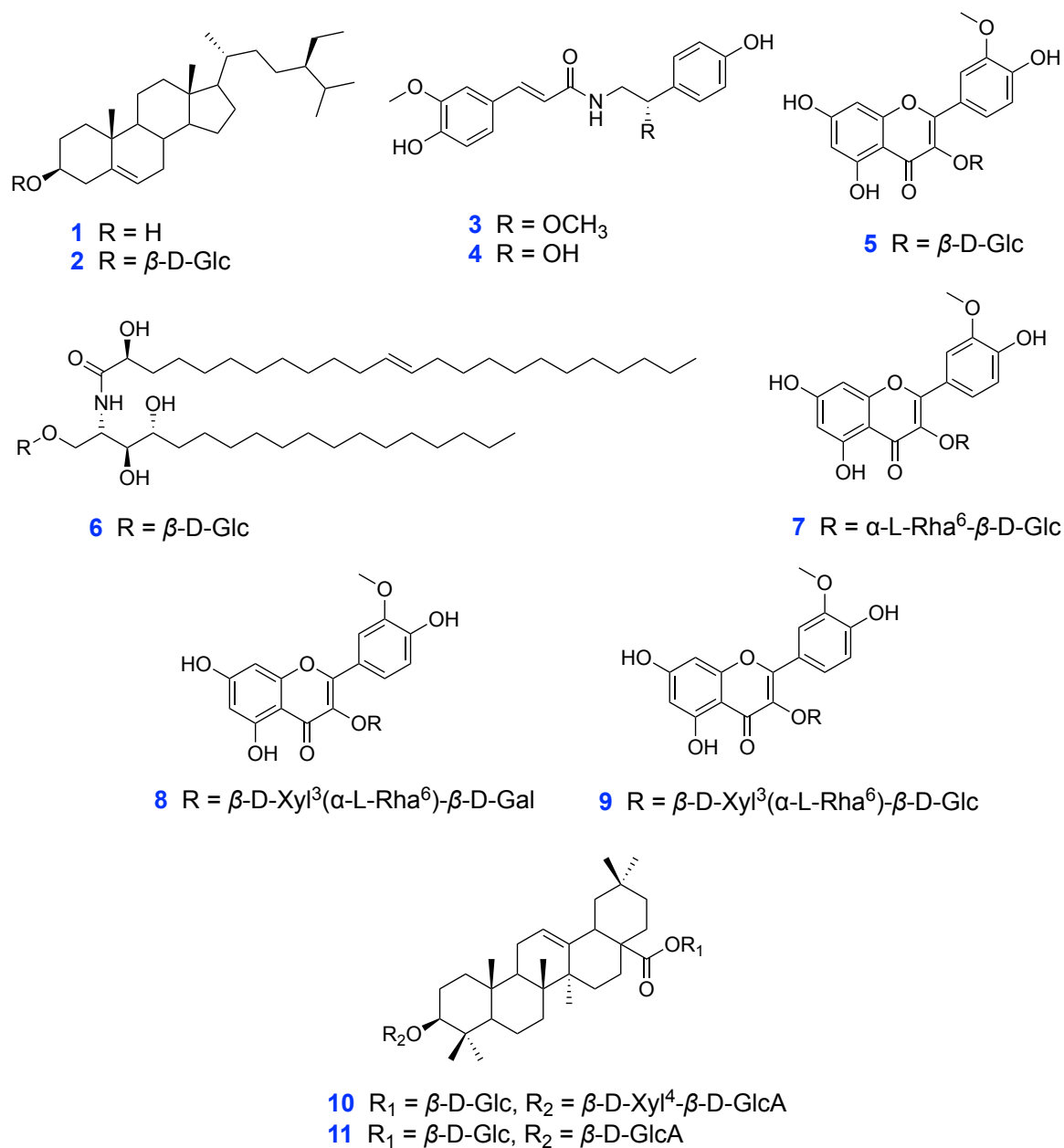normal- and reversed-phase RP-C18 silica gel yielding elven compounds (**1–11**) as shown in Figure 29.



**1** R = H
**2** R = *β*-D-Glc

**3** R = OCH$_3$
**4** R = OH

**5** R = *β*-D-Glc

**6** R = *β*-D-Glc

**7** R = α-L-Rha$^6$-*β*-D-Glc

**8** R = *β*-D-Xyl$^3$(α-L-Rha$^6$)-*β*-D-Gal

**9** R = *β*-D-Xyl$^3$(α-L-Rha$^6$)-*β*-D-Glc

**10** R$_1$ = *β*-D-Glc, R$_2$ = *β*-D-Xyl$^4$-*β*-D-GlcA
**11** R$_1$ = *β*-D-Glc, R$_2$ = *β*-D-GlcA

Figure 29: Chemical structures of isolated compounds **1–11** from *A. alopecuroides*

Compounds **6**, **8** and **10** were isolated and identified for the first time, together with 8 known compounds. Their structures were established by a detailed analysis of their spectral data including ^{1}H, APT, HSQC, HMBC and COSY NMR experiments and HR-ESI-MS.

The known isolated compounds were elucidated by comparison of their spectral data with those in the literature and were identified as *β*-sitosterol (**1**), *β*-sitosterol-3-*O*-*β*-D-glucoside (**2**), *S*-(−)-3-(4-hydroxy-3-methoxyphenyl)-*N*-[2-(4-hydroxyphenyl)-methoxy-ethyl]acrylamide (**3**), *S*-(−)-*N*-*trans*-feruloyloctopamine (**4**), isorhamnetin-3-*O*-*β*-D-glucoside (**5**), isorhamnetin-3-*O*-rutinoside (**7**), isorhamnetin-3-*O*-[*β*-D-xylopyranosyl-(1→3)-*α*-L-rhamnopyranosyl-(1→6)]-*β*-D-glucopyranoside (**9**), and chikusetsusaponin IVa (**11**) [52,101,213–218].

The current study is the first time any of these isolated compounds has been reported in relation to *A. alopecuroides*. Despite the distribution of reported flavonoids from the family Chenopodiaceae, here we report a flavonoid trisaccharide (**8**) for the first time, in addition to reporting **9** for only the second time.

Compound (**6**) was purified as a white amorphous powder, with positive Molish test suggesting its glycosidic nature $[\alpha]_D^{25} + 6.8$ (c 0.02, $C_5H_5N$). The structure elucidation of **6** was performed based on 1D, 2D and HR-FAB-MS. The molecular formula of **6**, $C_{48}H_{93}NO_{10}$, was deduced from HR-FAB-MS analysis which showed a characteristic molecular ion peak at *m/z* 844.6877 [M+H]$^+$, calcd for $C_{48}H_{94}NO_{10}$ (844.6878).

The ^{1}H-NMR of compound **6** (Table 15) exhibited a broad signal for the aliphatic long-chain $CH_2$ protons in the range of $\delta_H$ 1.24−1.38, in addition to a triplet signal at $\delta_H$ 0.89 (t, J = 6.9 Hz, 6H) attributed to two terminal methyl groups, indicating the presence of two long aliphatic chains [219,220].

In the APT NMR spectrum, the downfielded carbon signal at $\delta_C$ 70.9, alongside two non-equivalent proton signals at $\delta_H$ 4.72 (dd, *J* = 10.7, 6.7 Hz, 1H) and $\delta_H$ 4.54 (dd, *J* = 10.7, 4.7 Hz, 1H), suggested the existence of an oxymethylene group at C-1, which is attached to a sugar moiety. The sugar moiety was confirmed by an anomeric proton signal at $\delta_H$ 4.97 (d, J = 7.8 Hz, 1H) which was correlated with an anomeric carbon signal at $\delta_C$ 106.0 in HSQC, suggesting a hexose moiety in the structure [221,222]. The hexose moiety (β-D-

glucose) was additionally confirmed by complete acid hydrolysis and comparison with an authentic standard. Moreover, the carbon resonances at $\delta_H$ 76.4, 72.8, 72.9 assigned to C-3, C-4, and C-2', respectively, revealed the presence of three oxygenated methine groups which were further detected in the $^1$H-NMR spectrum at $\delta_H$ 4.31 (dd, J = 7.1, 4.7 Hz, 1H), 4.23 (dd, J = 6.9, 3.0 Hz, 1H), and 4.60 (dd, J = 7.9, 3.8 Hz, 1H). In addition, the N-attached carbon was confirmed by a carbon signal at $\delta_C$ 52.2 and a proton signal at $\delta_H$ 5.29 (m, 1H), while the signal at $\delta_C$ 176.1 attributed to a carbonyl group, suggesting the presence of an amide group, which was further confirmed by a doublet signal at $\delta_H$ 8.57 (d, J = 9.1 Hz, 1H) [223]. This also was confirmed by correlations in the HSQC spectrum revealing the glucosylceramide structure [222,224]. On the other hand, the olefin double bond between C-12' and C-13' was deduced from signals at $\delta_H$ 5.51 (dt) and 5.56 (dt), as well as carbon signals at $\delta_C$ 131.1 (C-12') and 131.3 (C-13'). In addition, the *trans*-geometry (*E*) of the double bond at C-12' was determined based on the downfielded chemical shifts of C-11' at $\delta_C$ 33.4 and C-14' at 33.8 and supported by the literature [222,225]. In the HMBC spectrum, the characteristic correlations of an amide proton at $\delta_H$ 8.57 (d, J = 9.1 Hz, 1H), H-2 at $\delta_H$ 5.29 (m), and H-2' at $\delta_H$ 4.60 (dd) with a carbonyl group at $\delta_C$ 176.1 confirmed the presence of a ceramide structure. Furthermore, HMBC correlations of H-1 at $\delta_H$ 4.72 and 4.54 / $\delta_C$ 106.0 (C-1''), N-H at $\delta_H$ 8.57 / $\delta_C$ 52.2 (C-2), and H-2 at $\delta_H$ 5.29 / $\delta_C$ 176.3 (C-1'), $\delta_C$ 76.4 (C-3) and $\delta_C$ 72.9 (C-4), also confirmed the glucosylceramide structure [226,227] as shown in Figure 30.
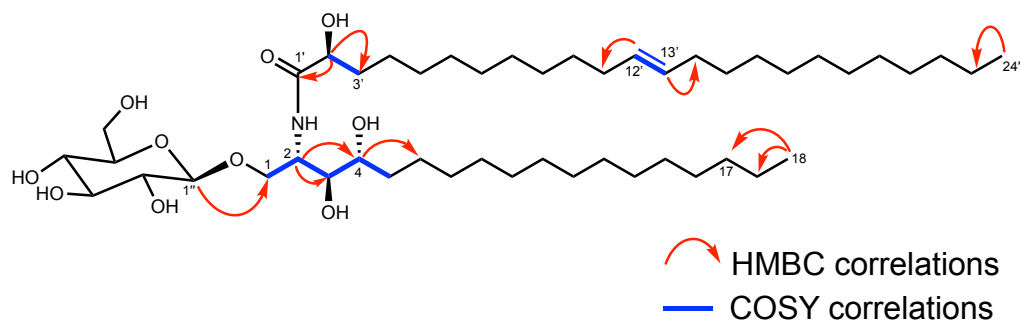


Figure 30: Key 2D correlations of compound **6** from *A. alopecuroides*

The relative stereochemistry of the long-chain base was determined by the ROESY spectrum as being similar to D-erythrose interactions between H-2 to H-1 and H-4, as in the naturally occurring sphingosine derivative, as well as compared with reported relatives in the literature [223,228,229]. The absolute stereochemistry was determined by ROESY which showed two groups of correlations (H-1", H-2', H-3) and (H-2, H-4) and the absence of correlation from H-2 to H-3, in addition to the chemical shifts of C-2, C-3 and C-4 which were in good agreement with the reported derivatives in the literature [221,228]. Additionally, the stereochemistry at different stereocenters of carbons C-2, C-3, C-4, and C-2' of **6** was deduced to be 2*S*, 3*S*, 4*R* and 2'*R*, respectively, based on a detailed comparison of the NMR data with various natural and synthetic derivatives with different stereocenters available in the literature [228,230,231]. This analysis finally confirmed the designed stereocenters in compound **6**. Based on the above-mentioned spectroscopic and spectrometric data, the structure of compound **6** was deduced to be (2'*R*,12'*E*)-*N*-[(2*S*,3*S*,4*R*)-1-(*β*-D-glucopyranosyloxy)-3,4-dihydroxy-octadec-2-yl]-2-hydroxytetracos-12-enamide and was named agathophamide A.

**Table 15**: $^1$H and APT-NMR data of compound **6** from *A. alopecuroides* in $C_5D_5N$ (δ in ppm, *J* in Hz)

| No. | δH | δC | No. | δH | δC |
|---|---|---|---|---|---|
| NH | 8.57 d (9.1) | | | **β-D-Glucose** | |
| 1 | 4.72 dd (10.7, 6.7), 4.54 dd (10.7, 4.7) | 70.9 | 1″ | 4.97 d (7.8) | 106.0 |
| 2 | 5.29 m | 52.2 | 2″ | 4.02 m | 75.6 |
| 3 | 4.31 dd (7.1, 4.7) | 76.4 | 3″ | 4.21 m | 71.9 |
| 4 | 4.23 dd (6.9, 3.0) | 72.8 | 4″ | 4.21 m | 79.0 |
| 5 | 1.93 m | 34.3 | 5″ | 3.88 m | 78.9 |
| 6 | 1.80 m | 26.3 | 6″ | 4.50 dd (11.8, 2.5) 4.35 dd (11.8, 5.3) | 63.1 |
| 7-16 | 1.24-1.38 | 30.3-30.6 | | | |
| 17 | 1.24-1.30 | 23.4 | | | |
| 18 | 0.89 t (6.9) | 14.7 | | | |
| 1′ | | 176.1 | | | |
| 2′ | 4.60 dd (7.9, 3.8) | 72.9 | | | |
| 3′ | 2.01 m | 36.0 | | | |
| 4′ | 1.85-1.75 m | 27.1 | | | |
| 5′ | 1.90 | 32.6 | | | |
| 6′ | 1.24-1.30 | 32.6 | | | |
| 7′ | 1.24-1.38 | 30.3 | | | |
| 8′ | 1.24-1.38 | 30.3 | | | |
| 9′ | 1.24-1.38 | 30.0 | | | |
| 10′ | 1.24-1.38 | 30.1 | | | |
| 11′ | 2.3 m | 33.4 | | | |
| 12′ | 5.51 dt (15.2, 6.1) | 131.1 | | | |
| 13′ | 5.56 dt (15.3, 6.1) | 131.3 | | | |
| 14′ | 2.21 m | 33.8 | | | |
| 15′-23′ | 1.24-1.38 | 30.3-30.6 | | | |
| 24′ | 0.89 t (6.9) | 14.7 | | | |

Compound (**8)** was isolated as yellow crystals, $[\alpha]_D^{25} - 15.2$ (c 0.02, MeOH). The molecular formula of **8** was determined to be $C_{33}H_{40}O_{20}$ based on the molecular ion peak at *m/z* 755.2046 [M–H]⁻ in HRESIMS, (calculated for $C_{33}H_{39}O_{20}$, 755.2035). The $^1H$, APT, HSQC, and HMBC NMR spectra revealed the existence of a flavonol moiety and three sugar moieties. The $^1H$-NMR spectrum displayed five aromatic protons at $\delta_H$ 6.40 (d, *J* = 2.0), 6.17 (d, *J* = 2.0), 8.00 (d, *J* = 2.1 Hz), 6.90 (d, *J* = 8.4 Hz), and 7.50 (dd, *J* = 8.4, 2.1 Hz) and one singlet methoxyl proton at $\delta_H$ 3.85, in addition to sugar protons in the area at $\delta_H$ 3.01–3.86 as shown in Table 16. Additionally, three anomeric protons were determined at $\delta_H$ 5.42 (d, *J* = 7.7 Hz), 4.40 (brs), and 4.25 (d, *J* = 7.5 Hz).

The APT NMR (Table 16) of **8** exhibited 33 carbon resonances that were categorized into 2 methyls (one methoxy and one methyl of rhamnose), 2 methylenes, 19 methines, and 10 quaternary carbon signals, as confirmed by HSQC experiment. Based on HSQC data, three anomeric protons were detected in the $^1H$-NMR spectrum and correlated with corresponding carbons 5.42 d / 102.0, 4.40 brs / 100.2, and 4.25 d / 105.4. Furthermore, one doublet proton at $\delta_H$ 1.21 (d, *J* = 6.2 H) and $\delta_C$ 18.0 indicated a rhamnose moiety. The upfield shift of C-3 and C-3' at $\delta_C$ 133.1 and 147.0, respectively, in APT-NMR and the previously published data for relative compounds indicated a kaempferol glycoside skeleton [232]. The APT NMR also exhibited a methoxylated carbon signal at $\delta_C$ 55.9, together with triglycoside carbon signals at $\delta_C$ 65.3-81.0 ppm. The HMBC correlations of the anomeric proton at $\delta_H$ 5.42 and C-3 ($\delta_C$ 133.1) revealed a glycosidic linkage at C-3 of the aglycone as shown in Figure 31. In addition, the correlation of a methoxy group at $\delta_H$ 3.85 and C-3′ at $\delta_C$ 147.0 indicated a methoxylated substitution at C-3'. Other HMBC cross-peaks of anomeric protons at $\delta_H$ 4.40 brs and $\delta_C$ 65.6 indicated that the rhamnose moiety was attached to C-6 of the primary sugar [52]. Also, the deshielded signal for C-3‴ of at $\delta_C$ 81.1 implied the interglycosidic linkage of rhamnose.

On the other hand, the existence of a xylopyranosyl moiety was confirmed by HMBC correlation of anomeric proton H-1‴′ $\delta_H$ 4.25 (d, *J* = 7.5 Hz) / $\delta_C$ 65.3 ($CH_2$), whereas the correlation of H-1‴′ with $\delta_C$ 81.1 confirmed the linkage of a xylose moiety to the C-3‴ of rhamnose. The sugar moieties were determined through the total acid hydrolysis followed by examinations over TLC ($CHCl_3$–MeOH–$H_2O$ 7:3:0.3; 8:5:1) and a HPLC-evaporative light-scattering detector (ELSD) system on Asahipak NH₂P-50 4E (4.6 × 250 mm) using

mobile phase H$_2$O-ACN (25:75) as compared with authentic samples that indicated the presence of galactose, rhamnose, and xylose. The coupling constants for the anomeric protons depicted a β-configuration for galactose and xylose, and an α-configuration for rhamnose [232]. Accordingly, from the above-mentioned data, **8** was identified as isorhamnetin-3-*O*-[*β*-D-xylopyranosyl-(1→3)-*α*-L-rhamnopyranosyl-(1→6)]-*β*-D-galacto-pyranoside (**8**), namely agathophoroside A.
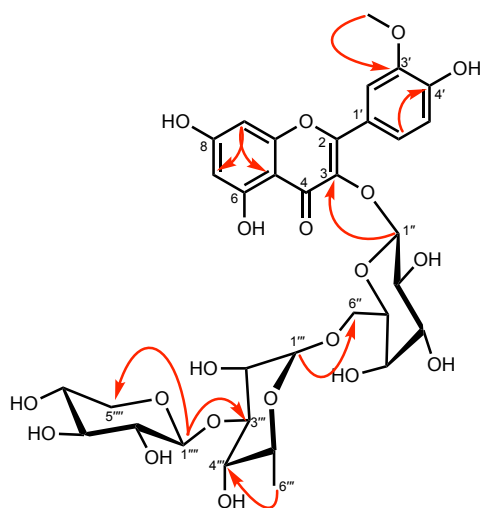


Figure 31: Key HMBC correlations of compound **8** from *A. alopecuroides*

**Table 16**:^{1}H and APT-NMR data of compound **8** from *A. alopecuroides* in DMSO-$d_6$ (δ in ppm, *J* in Hz)

| No. | δ$_H$ | δ$_C$ | No. | δ$_H$ | δ$_C$ |
|---|---|---|---|---|---|
| 1 | — | | | **α-L-Rhamnose** | |
| 2 | — | 156.2 | 1′′′ | 4.40 brs | 100.2 |
| 3 | — | 133.1 | 2′′′ | 3.86 dd (10.1, 7.9) | 73.0 |
| 4 | — | 177.2 | 3′′′ | 3.38 m | 81.1 |
| 5 | — | 156.5 | 4′′′ | 3.61 m | 69.8 |
| 6 | 6.40 d (2.0) | 93.9 | 5′′′ | 3.30 m | 73.8 |
| 7 | — | 165.2 | 6′′′ | 1.21 d (6.2) | 18.0 |
| 8 | 6.17 d (2.0) | 99.0 | | **β-D-Xylose** | |
| 9 | — | 161.1 | 1′′′′ | 4.25 d (7.5) | 105.4 |
| 10 | — | 103.6 | 2′′′′ | 3.43 m | 73.5 |
| 1′ | — | 121.6 | 3′′′′ | 3.09 m | 76.1 |
| 2′ | 8.00 d (2.1) | 113.5 | 4′′′′ | 3.50 m | 71.1 |
| 3′ | — | 147.0 | 5′′′′ | 3.01 m | 65.3 |
| 4′ | — | 149.5 | | | |
| 5′ | 6.90 d (8.4) | 115.2 | | | |
| 6′ | 7.50 dd (8.4, 2.1) | 122.0 | | | |
| 3′-OMe | 3.85 s | 55.9 | | | |
| **β-D-Galactose** | | | | | |
| 1″ | 5.42 d (7.7) | 102.0 | | | |
| 2″ | 3.59 m | 70.8 | | | |
| 3″ | 3.62 m | 73.0 | | | |
| 4″ | 3.62 m | 67.9 | | | |
| 5″ | 3.02 m | 73.8 | | | |
| 6″ | 3.37 m <br> 3.61 m | 65.6 | | | |

Compound (**10)** was obtained as a white amorphous powder, $[\alpha]_D^{25} - 32.0$ (c 0.02, $C_5H_5N$). The molecular formula was deduced to be $C_{47}H_{74}O_{18}$ on the basis of the high-resolution electrospray ionization mass spectrometry (HR-ESI-MS) [M–H]⁻ ion peak at *m/z* 925.4827 and was confirmed by the APT NMR data (Table 17).

The ¹H-NMR spectrum for compound **10** revealed seven tertiary methyl signals at $\delta_H$ 0.84 (Me-25), 0.91 (Me-30), 0.93 (Me-29), 1.00 (Me-23), 1.10 (Me-26), 1.30 (Me-27), and 1.31 (Me- 24), an olefinic proton at $\delta_H$ 5.43 (m) and three anomeric protons at $\delta_H$ 5.01 (d, *J* = 7.8 Hz), 5.36 (d, *J* = 7.5 Hz), and 6.34 (d, *J* = 8.2 Hz). The acid hydrolysis of compound **10** with 5% HCl afforded D-glucose, D-glucuronic acid, and D-xylose, which were analyzed by TLC and high-performance liquid chromatography (HPLC) using authentic sugars as references [233]. The APT spectral data displayed 47 carbon signals, categorized into olefinic carbons at $\delta_C$ 123.4 and 144.6, seven methyls, twelve methylene, fifteen methines, eight quaternary carbons, and three anomeric carbons.
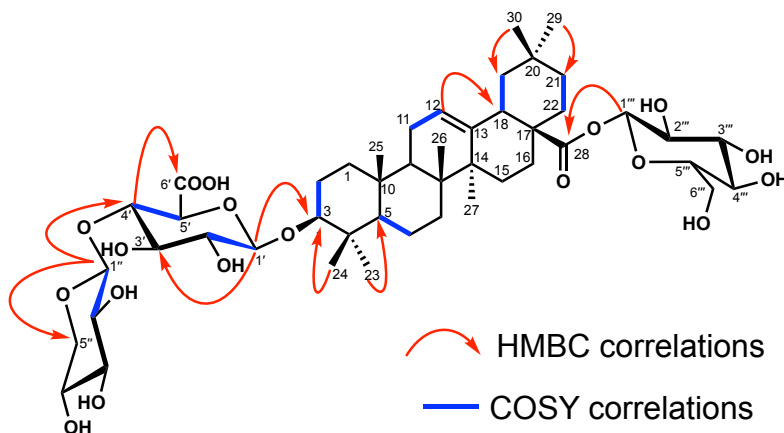


Figure 32:Key 2D correlations of compound **10** from *A. alopecuroides*

The HSQC correlations of $\delta_H$ 5.01 (d, *J* = 7.8 Hz), 5.36 (d, *J* = 7.5 Hz) and 6.34 (d, *J* = 8.2 Hz) with $\delta_C$ 107.2, 106.6, 96.3, respectively, confirmed the presence of three sugar moieties in the molecule. Furthermore, the HMBC cross-peaks of anomeric protons at $\delta_H$ 6.34 (d, *J* = 8.2 Hz) / $\delta_C$ 177.0 (C-28) and $\delta_H$ 5.01 (d, *J* = 7.8 Hz) with $\delta_C$ 89.7 (C-3) proved that two sugars, β-D-glucose and β-D-glucuronic acid, were linked to C-28 and C-3, respectively. Additionally, the deshielded signal at $\delta_C$ 86.8 of C-4' indicated that another side chain was linked there, which is then proved by the HMBC correlation of $\delta_H$ 5.36 (H-

1") with $\delta_C$ 86.8 (C-4') as seen in Figure 32. Furthermore, the HMBC correlation of 4.37 m (H-4') with 173.4 (C-6') confirmed that the xylose moiety was attached to C-4'. Finally, from the above-mentioned data, **10** was identified as 3-*O*-[4'-(*β*-D-xylopyranosyl)-*β*-D-glucuronopyranosyl]-28-*O*-*β*-D-glucopyranosyl-olean-12-en-3*β*-ol-28-oic acid, namely solysaponin A (**10**).

**Table 17**: ^{1}H and APT-NMR spectroscopic data of compound **10** from *A. alopecuroides* in $C_5D_5N$ (δ in ppm, *J* in Hz)

| No. | δ$_H$ | δ$_C$ | No. | δ$_H$ | δ$_C$ |
|---|---|---|---|---|---|
| 1 | 1.36 m | 39.1 | | **3-*O*-β-D-Glucuronic acid** | |
| | 0.86 m | | | | |
| 2 | 1.85 o* | 27.0 | 1′ | 5.01 d (7.8) | 107.2 |
| 3 | 3.38 dd (11.6, 3.8) | 89.7 | 2′ | 4.16 m | 71.4 |
| 4 | — | 39.1 | 3′ | 4.49 m | 72.0 |
| 5 | 0.79 d (11.8) | 56.2 | 4′ | 4.37 m | 86.8 |
| 6 | 1.49 m | 19.0 | 5′ | 4.62 brd (9.3) | 77.7 |
| | 1.27 o* | | | | |
| 7 | 1.75 o* | 37.4 | 6′ | — | 173.4 |
| 8 | — | 40.4 | | **β-D-Xylose** | |
| 9 | 1.58 m | 48.5 | 1″ | 5.36 d (7.5) | 106.6 |
| 10 | — | 34.5 | 2″ | 4.07 m | 75.1 |
| 11 | 1.89 m | 23.9 | 3″ | 4.18 m | 78.5 |
| 12 | 5.43 m | 123.4 | 4″ | 4.52 m | 72.0 |
| 13 | — | 144.6 | 5″ | 4.37 m | 67.9 |
| | | | | 3.73 m | |
| 14 | — | 42.5 | | **28-*O*-β-D-Glucose** | |
| 15 | 1.21 d (13.6) | 28.8 | 1‴ | 6.34 d (8.2) | 96.3 |
| | 1.32 o* | | | | |
| 16 | 1.85 m | 24.2 | 2‴ | 4.22 t (8.5) | 79.4 |
| 17 | — | 47.5 | 3‴ | 4.30 t (8.9) | 79.8 |
| 18 | 3.21 m | 42.2 | 4‴ | 4.37 t (9.1) | 71.6 |
| 19 | 1.26 m | 46.7 | 5‴ | 4.16 dd (14.1, 7.8) | 74.6 |
| | 1.79 m | | | | |
| 20 | — | 34.5 | 6‴ | 4.47 m | 62.7 |
| | | | | 4.43 m | |
| 21 | 1.37 m | 31.3 | | | |
| 22 | 2.12 m | 28.2 | | | |
| 23 | 1.00 s | 17.4 | | | |
| 24 | 1.31 s | 28.6 | | | |
| 25 | 0.84 s | 16.0 | | | |
| 26 | 1.10 s | 18.0 | | | |
| 27 | 1.30 s | 26.6 | | | |
| 28 | — | 177.0 | | | |
| 29 | 0.93 s | 33.6 | | | |
| 30 | 0.91 s | 24.1 | | | |

*Overlapped signal

To the best of our knowledge, compounds **6**, **8** and **10** were isolated and identified for the first time. Meanwhile, compound **9**, which is a flavonol triglycoside was reported in this study for the second time. This is the first report to perform a detailed investigation of the compounds constituting the plant *A. alopecuroides*.

## 6.3.2. Effect of *A. alopecuroides* extract and isolated compounds on viability of HaCaT cells

The effect of methanol extract of *A. alopecuroides* and isolated compounds on the viability of normal HaCaT cells was assessed by MTT assay. The cytotoxicity of isolated compounds from methanol extract on HaCaT cells was measured by MTT after treatment for 24 h. The assay results indicated that the normal HaCaT cells have satisfactory viability when treated either with the methanol extract of *A. alopecuroides* or with its various isolated compounds as shown in Figure 33.
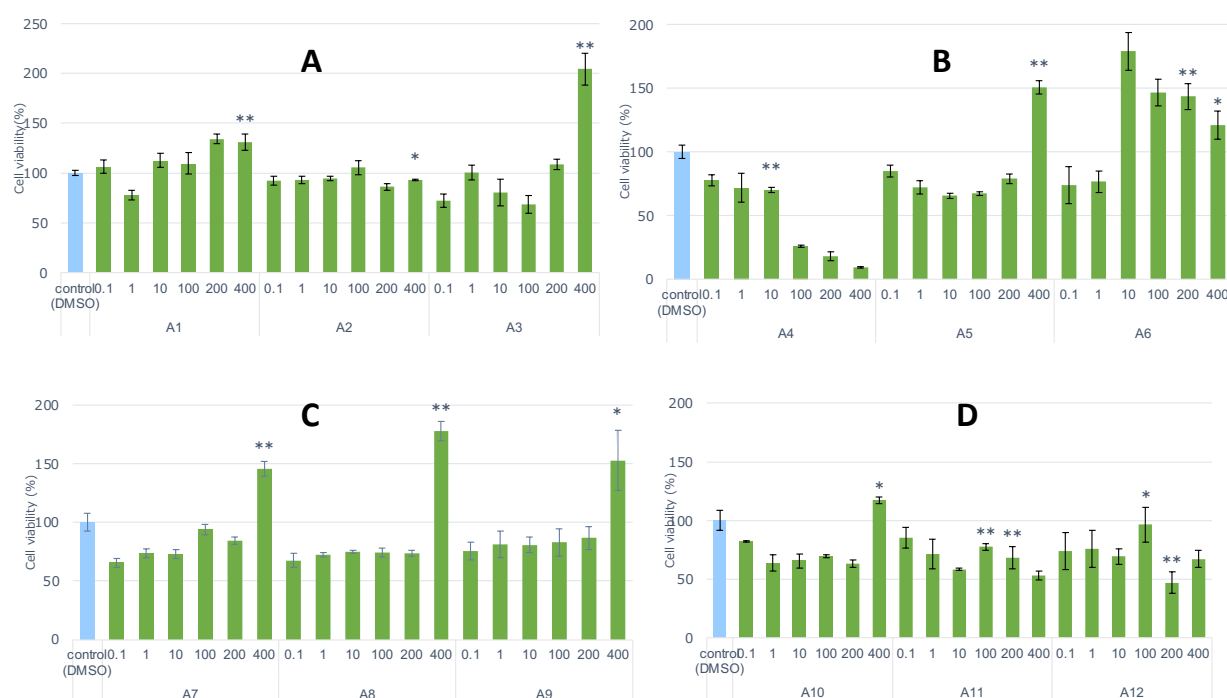


Figure 33: Effect of extract and isolated compounds on viability of HaCaT cells. A: Compounds **1**–**3**; B: Compounds **4**–**6**; C: Compounds **7**–**9**; D: Compounds **10**–**11** and methanol extract (A**12**). Cell viability was measured by MTT assay. HaCaT cells ($1×10^5$ cell/well) were seeded to a 96-well plate and incubated overnight. The cell viability was performed after treatment with isolated compounds for 24 h. Values are expressed as the mean ± SD of three wells; *$p<0.05$, **$p<0.01$.

### 6.3.3. Effect of *A. alopecuroides* extract and isolated compounds on ceramide synthesis

The influence of methanol extract of *A. alopecuroides* and the isolated compounds on mRNA expression levels of the ceramide synthesis-associated enzyme in HaCaT keratinocytes was evaluated. The study results (Figure 34) displayed that when HaCaT keratinocytes were cultured in the presence of methanol extract (100 µg/mL) for 24 h, the mRNA expression levels of ceramide synthase-3 (CerS3) were significantly increased. Additionally, the mRNA expression levels of CerS3 were significantly increased by compounds **1**, **2**, **5**, **8** and **10** at 400 µg/mL. Moreover, compound **4** (10 µg/mL) increased the mRNA expression of CerS3, an enzyme involved in ceramide synthesis. The results also showed that the *A. alopecuroides* extract and compound **4** have the potential to promote the expression of CerS3 genes by nearly 1.2-fold compared to that in control cells. Additionally, RT-PCR analysis demonstrated that compounds **2** and **5** significantly up-regulated the mRNA expression levels of CerS3 by nearly 4.3- and 4.4-fold, respectively. Meanwhile, compound **10** significantly up-regulated the mRNA expression levels of CerS3 by more than 3.2-fold while compounds **1** and **8** upregulated it by 1.9- and 1.3-fold, respectively.
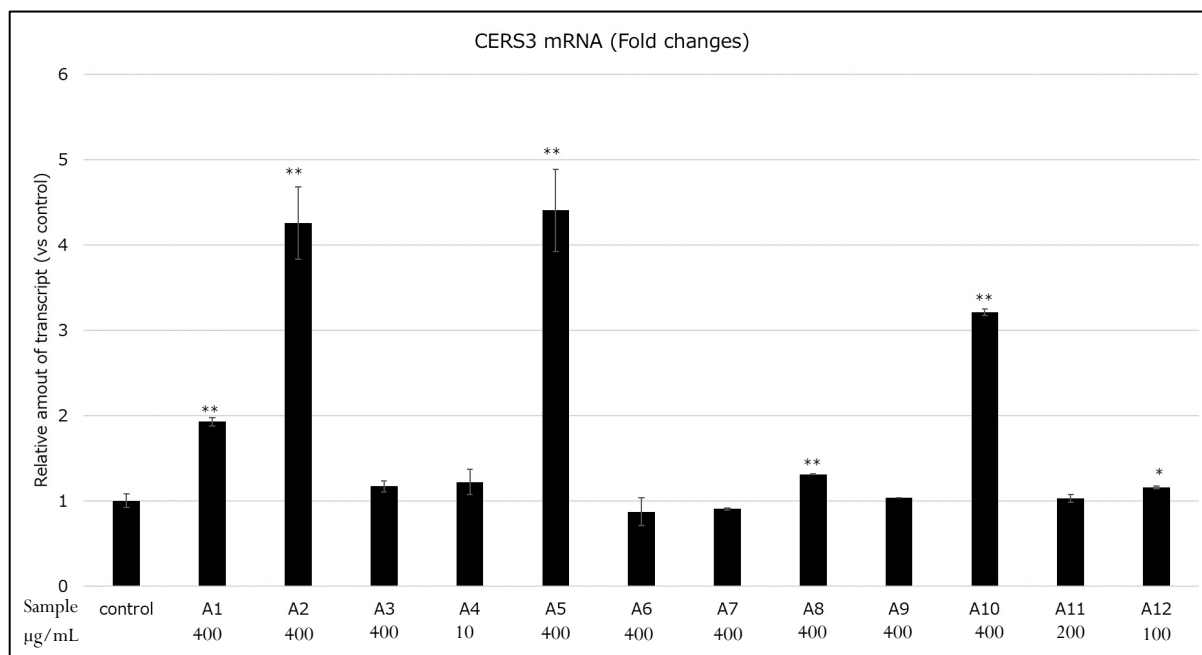
Figure 34: Effect of isolated compounds (A**1**–A**11**) and the extract of *A. alopecuroides* (A**12**) on mRNA expression levels of CerS3 involved in ceramide synthesis in HaCaT cells. HaCaT cells were cultured in the presence or absence of tested samples at 10-400 µg/mL for 24 h. RT-PCR analysis was performed as described in Material and methods part. Data are expressed as means ± SD of at least three independent experiments; *$p<0.05$, **$p<0.01$.

In the current study, glucosylceramide (**6**) did not show up-regulation of mRNA expression levels of CerS3 in this study. However, previous studies reported that the conversion of glucosylceramides to ceramides is required for healthy and competent skin barrier function [234]. Thus, the exogenous application of such phyto-derived glucosylceramides might play a crucial role in increasing stratum corneum ceramides through the enzymatic hydrolysis of glucosylceramides by β-glucocerebrosidase as shown in Figure 35.

Notably, there was no toxicity on tested HaCaT keratinocytes after treatment with methanol extract and isolated compounds. Thus, the halophyte herb *A. alopecuroides* is suggested to enhance the synthesis of ceramides that play a significant role in the restoration of human skin barrier function and consequently could be utilized for the treatment of atopic dry skin, aged skin, and other skin diseases such as xerosis and psoriasis.
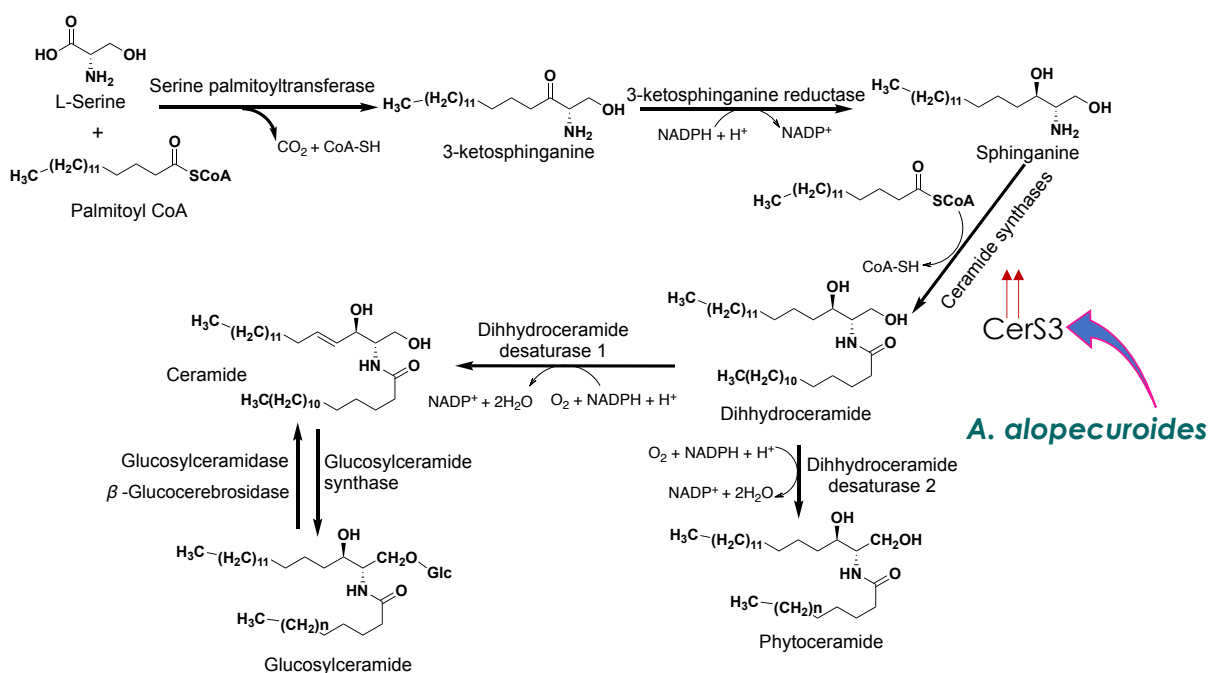


Figure 35: The mechanism of stratum corneum ceramide increase effect of A. alopecuroides

## 6.4. Conclusion

In conclusion, halophytes are very significant in industrial and medicinal use owing to their survival in severe environmental conditions, especially high levels of salinity, and thus produce a wide diversity of chemical compounds. The xero-halophyte herb *A. alopecuroides* is a halophyte species upon which very little chemical or biological analysis has been performed. Hence, the phytochemical investigation of this plant afforded three previously undescribed glucosylceramide (**6**), flavonol triglycoside (**8**), and triterpene oleanane saponin (**10**), alongside eight known compounds (steroids, lignanamides, and flavonoids) that enrich the chemical composition of this plant.

Several skin diseases are characterized by diminished levels of ceramides in the stratum corneum, in addition to disruption of skin barrier function. Hence, we evaluated the effect of methanol extract of *A. alopecuroides* and isolates on mRNA expression levels of ceramide synthase-3 in human keratinocytes (HaCaT cells). Our results demonstrated that *A. alopecuroides* has the potential to stimulate epidermal ceramide synthesis via enhancing the mRNA expression levels of CerS3. Thus, *A. alopecuroides* is a promising source of bioactive compounds with the capacity to recover aged dry skin including xerosis, atopic dermatitis and psoriasis, in addition to its ability to restore the disrupted skin barrier function.

**Chapter 7: Conclusion and prospective**

Halophytes are plants adapted to high salinity environments. They are widely distributed in coastal salt marshes, desert, and semi-arid regions of the world. Consequently, halophytes possess a complex secondary metabolites that help in adaptation mechanisms toward salt stress conditions. Yet, many points remain ambiguous related to the secondary metabolites contained in halophytes. There is an urgent demand for the development of utilization methods for halophytes that develop in Sahara Desert for the recovery of high value-added biomolecules that can be employed in drug discovery and cosmeceutical areas.

In this study, we have focused on *Bassia indica* and *Agathophora alopecuroides*, which are halophytes native to semi-arid regions of Egypt, for the isolation and identification of their constituents. Then, we evaluated the potential application of these isolated compounds for the treatment of Alzheimer's disease (AD), cancer, and skin diseases.

To begin with, the methanol extracts of *B. indica* and *A. alopecuroides* were prepared. Then, classic and modern chromatographic techniques were applied to obtain 36 compounds and several among them had promising therapeutic activity. Their structures were identified using extensive NMR and HR-MS analysis.

Among the isolated chemicals, seven novel compounds were encountered and characterized for the first time and they were identified as *R*-(+)-*N*-*trans*-feruloyl octopamine, *N*-[(3-(3-methyl-1-oxo-butyl)amino) propyl]-3-(3,4-dihydroxyphenyl)prop-2-enamide (Bassiamide A), kaempferol-3-*O*-*β*-D-glucopyranosyl-(1→6)-*O*-[*β*-D-galactopyranosyl-(1→3)-2-*O*-*trans*-feruloyl-*α*-L-rhamnopyranosyl-(1→2)]-*β*-D-glucopyranoside, (2'*R*,3'*S*)-3-*O*-[2'-hydroxy-3'-(2"-*O*-glycolyl)-oxo-propionic acid-*β*-D-glucuronopyranosyl]-28-*O*-*β*-D-glucopyranosyl-olean-12-en-3*β*-ol-28-oic acid, (2'*R*,12'*E*)-*N*-[(2*S*,3*S*,4*R*)-1-(*β*-D-glucopyranosyloxy)-3,4-dihydroxy-octadec-2-yl]-2-hydroxytetracos-12-enamide (Agathophamide A), isorhamnetin-3-*O*-[*β*-D-xylopyranosyl-(1→3)-*α*-L-rhamnopyranosyl-(1→6)]-*β*-D-galactopyranoside (Agathophoroside A), and 3-*O*-[4'-(*β*-D-xylopyranosyl)-*β*-D-glucuronopyranosyl]-28-*O*-*β*-D-glucopyranosyl-olean-12-en-3*β*-ol-28-oic acid (Solysaponin A).

In addition, we evaluated the biological activities of the isolated compounds that can be applied to drug discovery, functional food, and cosmeceutical areas. Therefore, we investigated the inhibition activity of isolated compounds against acetylcholinesterase, β-secretase, monoamine oxidase (MAO-B) enzymes, and amyloid β (Aβ) aggregation, which are known targets of Alzheimer's disease (AD) therapies.

6,7-Dihydroxycoumarin showed a promising anti-acetylcholinesterase activity. *N-trans*-feruloyl-3-methoxytyramine, *N-trans*-feruloyltyramine, *N-trans*-caffeoyltyramine and 3-(4-hydroxy-3-methoxyphenyl)-*N*-[2-(4-hydroxyphenyl)methoxyethyl]acrylamide showed multi-target inhibition activity against β-secretase, MAO-B, and anti-aggregation of Aβ peptides.

Moreover, the anti-tumor (cytotoxicity against different cancer cell lines) and anti-inflammatory (against COX-2) properties of the isolated compounds from *B. indica* were assessed. As a result, a series of isolated triterpene oleanane-type saponins have been shown to exhibit promising anti-inflammatory activity. *N-trans*-feruloyltyramine exerted significant cytotoxicity against OVK-18 with $IC_{50}$ = 1.74 µg/mL, while 6,7-dihydroxycoumarin showed a potent inhibition against MCF-7 with $IC_{50}$ = 1.47 µg/mL. Two compounds exhibited remarkable cytotoxicity against HCT116 with $IC_{50}$ < 0.1 µg/mL and six compounds exerted significant activity against HepG2.

Furthermore, we focused on ceramide synthase-3 (CerS3), which is related to epidermal hydration and skin barrier function, as a functional target related to skin diseases therapeutics and cosmetic applications. Thus, the influence of *A. alopecuroides* extract and its isolated compounds on the mRNA expression levels of CerS3 in human epidermal keratinocytes (HaCaT) were evaluated. As a result, we found that isorhamnetin-3-*O*-glucoside, β-sitosterol-3-*O*-glucoside, β-sitosterol and solysaponin A promote CerS3 gene expression.

In summary, this study describes the isolation and characterization of high value-added compounds contained in halophytes *B. indica* and *A. alopecuroides*. In this study, we evaluated the potential applications of the isolated compounds to drug discovery and cosmetic areas. A total of 36 compounds have been successfully isolated, including 7 novel ones. Our study results clarified the promising functionality of these compounds

that they can be employed as therapeutic agents for AD, anti-inflammatory, anticancer agents, and cosmetics. The results of this research are important findings that will lead to proposals for high-value-added utilization of the salt-tolerant plants *B. indica* and *A. alopecuroides*, which are biomass resources. Also, the chemical and biological properties reported here will be an important first step toward future drug discovery in the pharmaceutical and cosmetic fields.

# Appendices
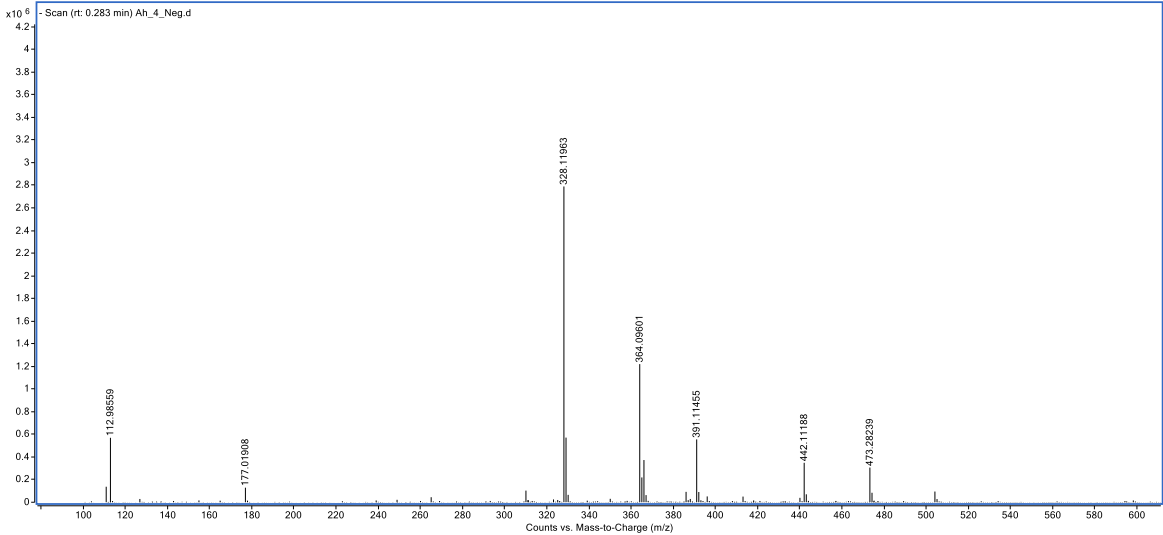


Figure S1: HR-MS of *S*-(−)-*N*-*trans*-feruloyloctopamine
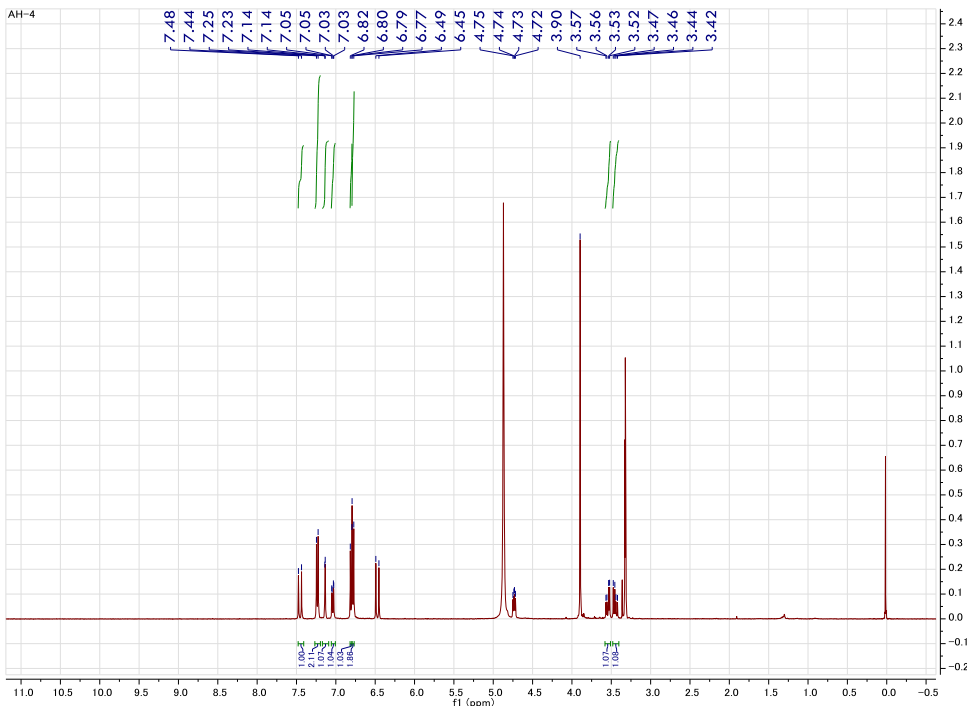


Figure S2: ¹H-NMR spectrum of *S*-(−)-*N*-*trans*-feruloyloctopamine (in CD₃OD, 400 MHz)
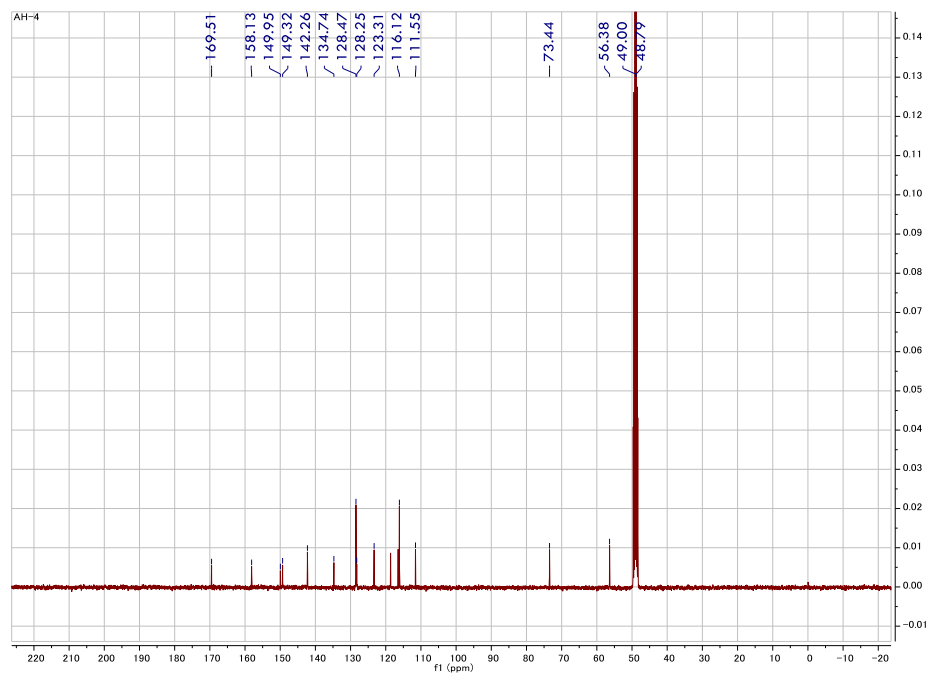
Figure S3: $^{13}$C-NMR spectrum of *S*-(−)-*N-trans*-feruloyloctopamine (in CD$_3$OD, 100 MHz)
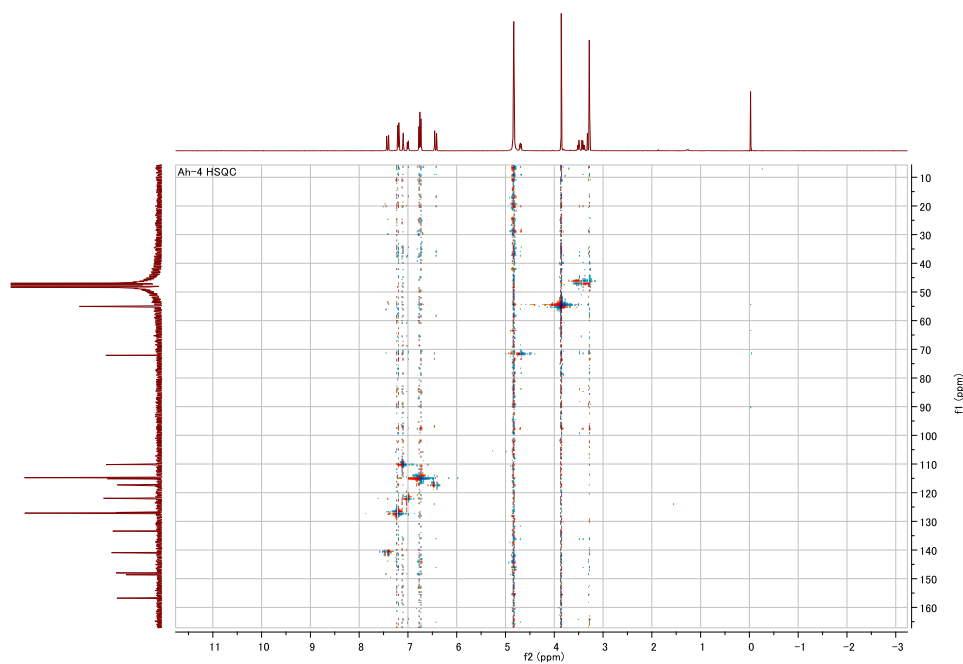


Figure S4: HSQC spectrum of *S*-(−)-*N-trans*-feruloyloctopamine
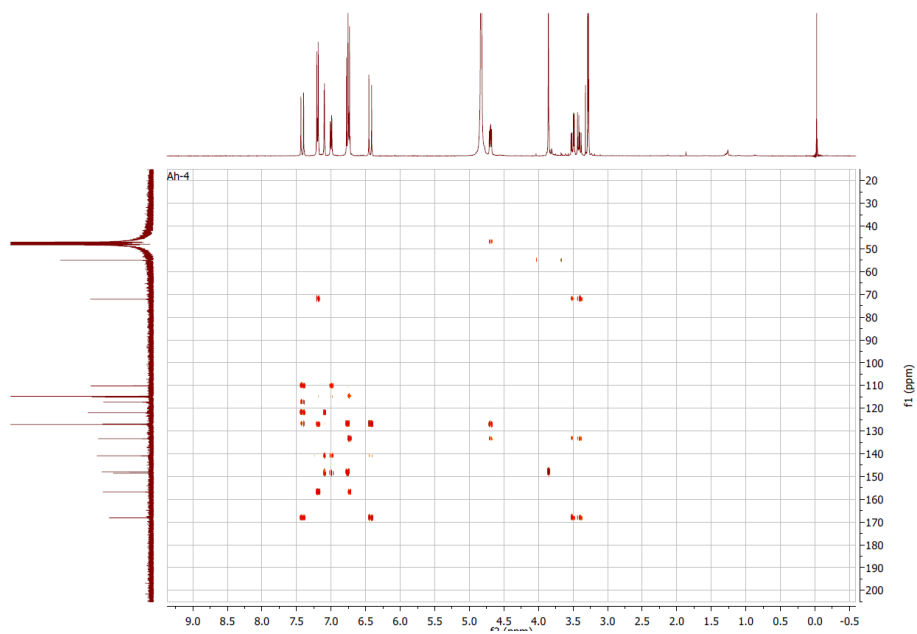
Figure S5: HMBC spectrum of *S*-(−)-*N*-trans-feruloyloctopamine
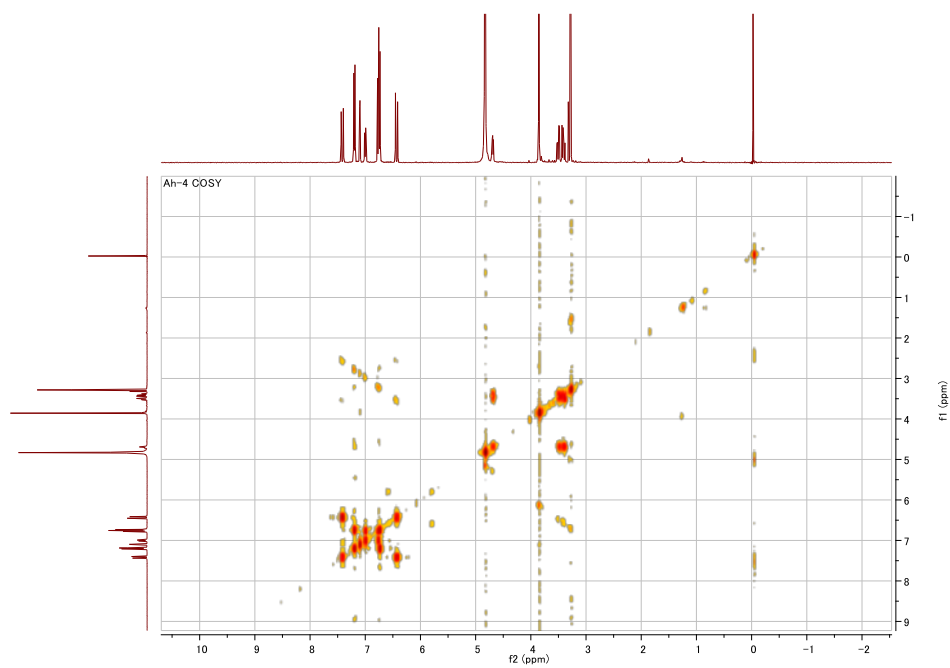


Figure S6:$^1$H-$^1$H COSY spectrum of *S*-(−)-*N*-trans-feruloyloctopamine
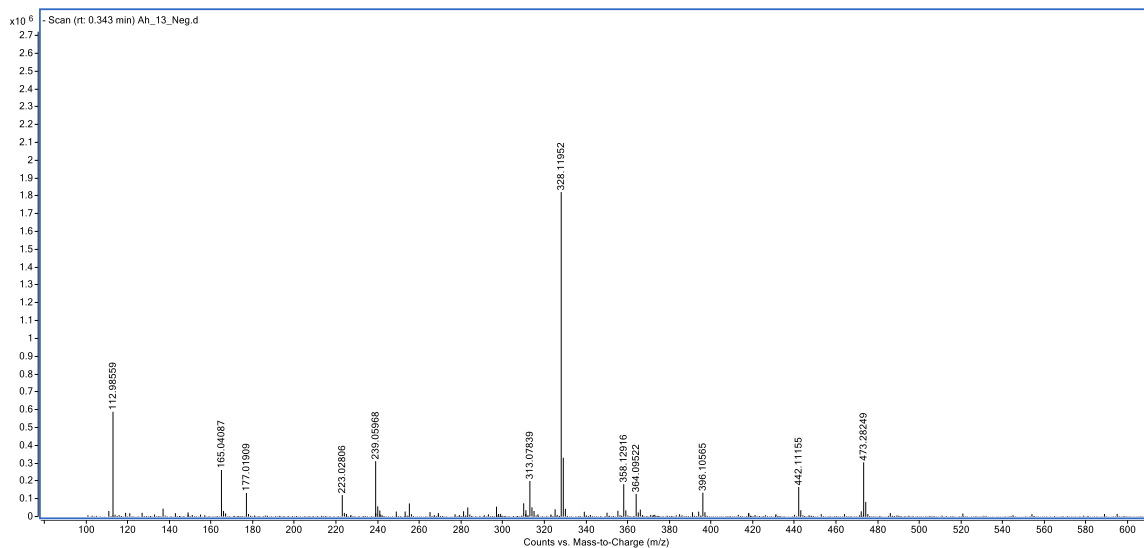
Figure S7: HR-MS of *R*-(+)-*N-trans*-feruloyloctopamine
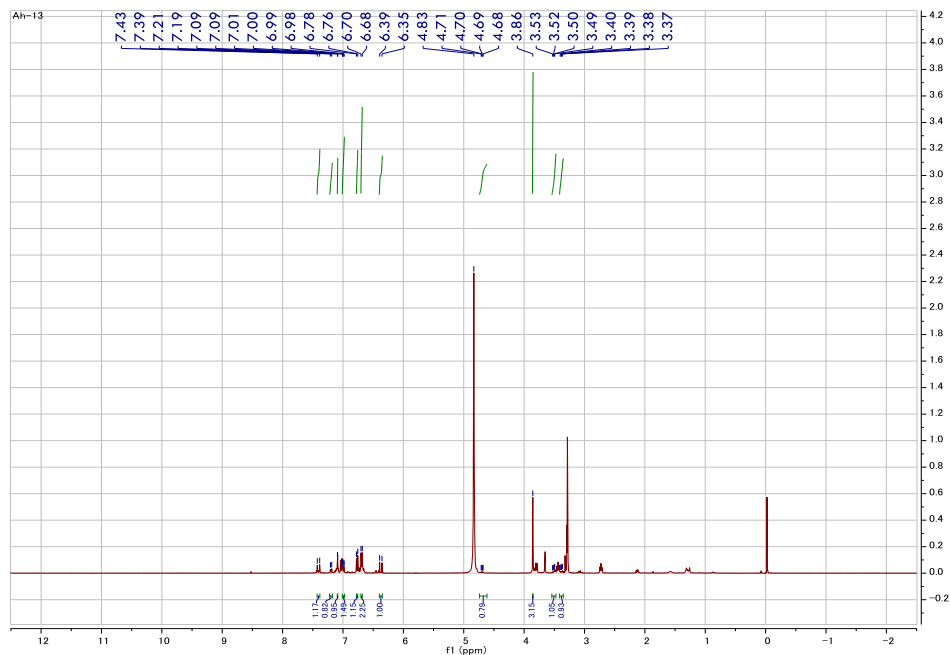


Figure S8: $^1$H-NMR of *R*-(+)-*N-trans*-feruloyloctopamine (in CD$_3$OD, 400 MHz)
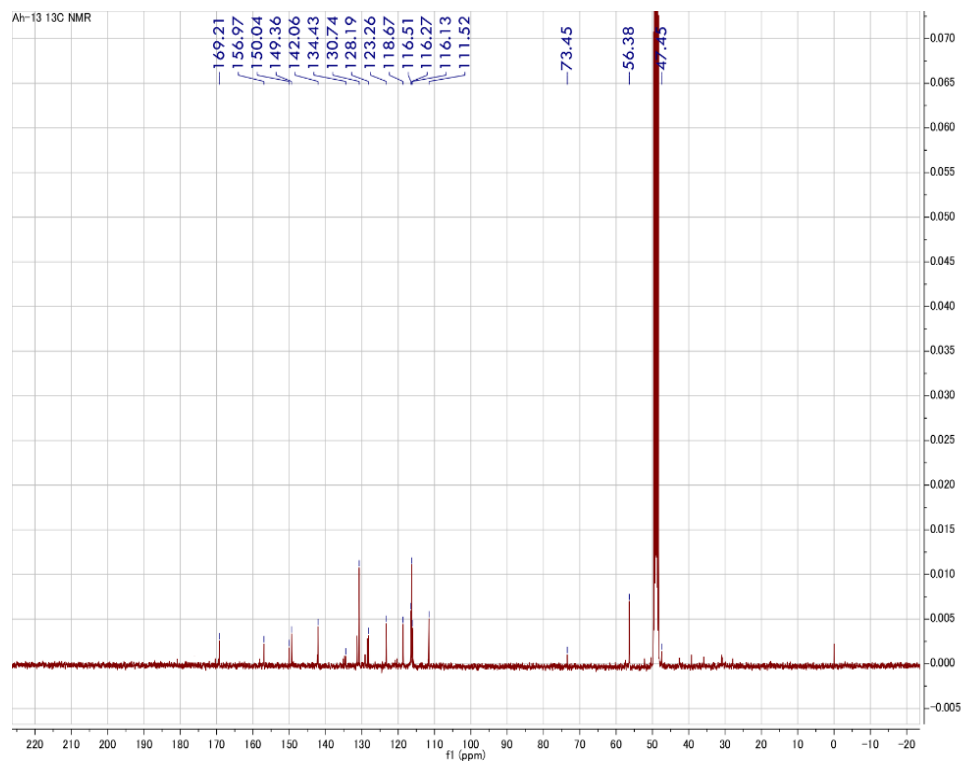
Figure S9: $^{13}$C-NMR spectrum of *R*-(+)-*N*-*trans*-feruloyloctopamine (in CD$_3$OD, 400 MHz)
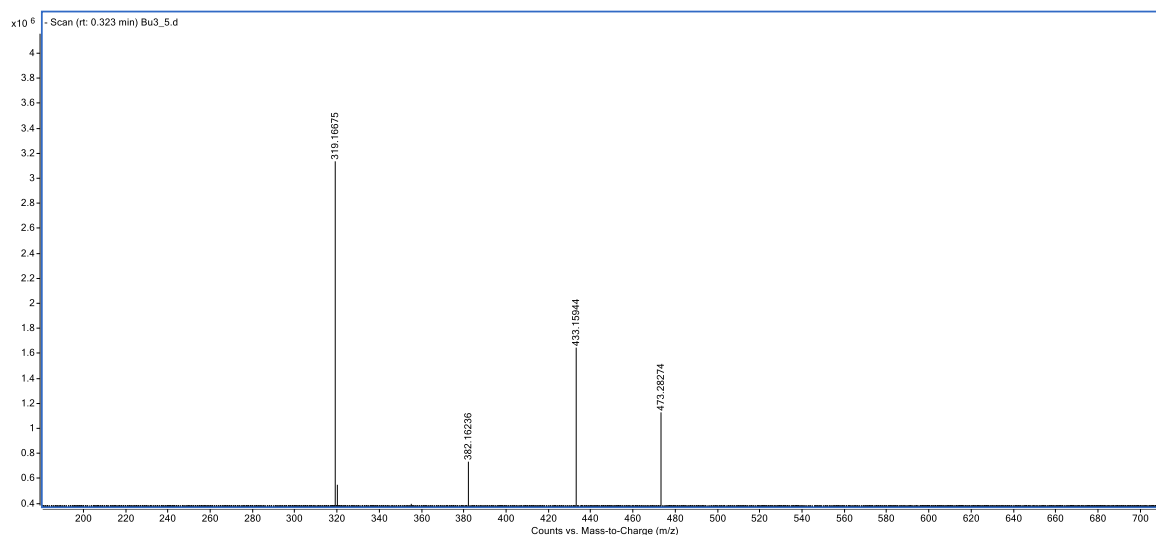
Figure S10: HR-MS of Bassiamide A
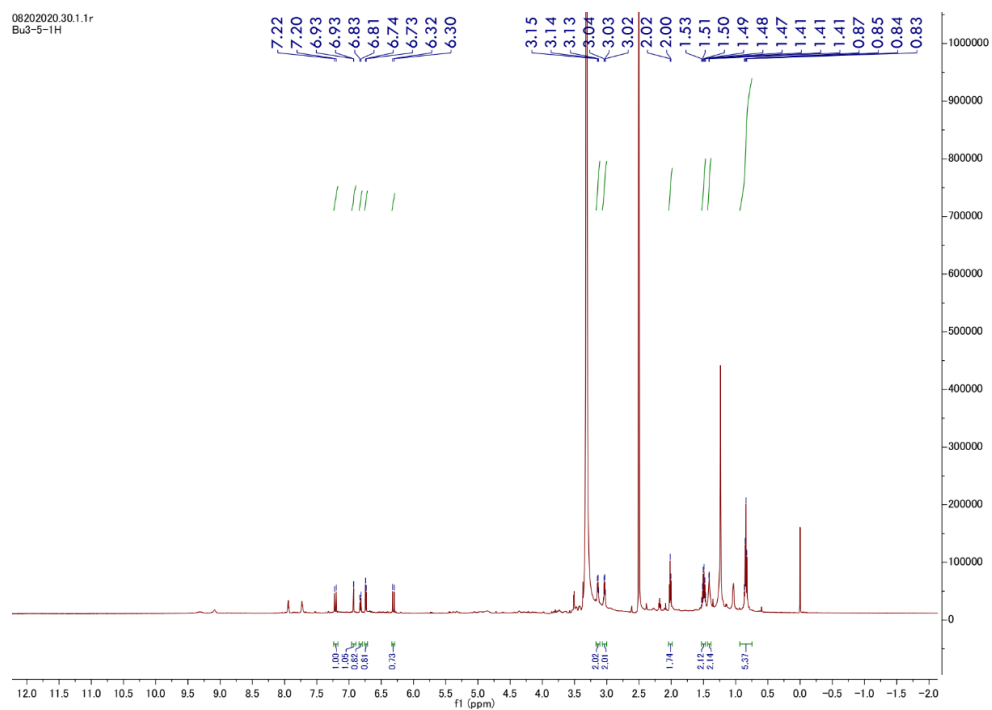


Figure S11: $^1$H-NMR spectrum of Bassiamide A (in DMSO-$d_6$, 600 MHz)
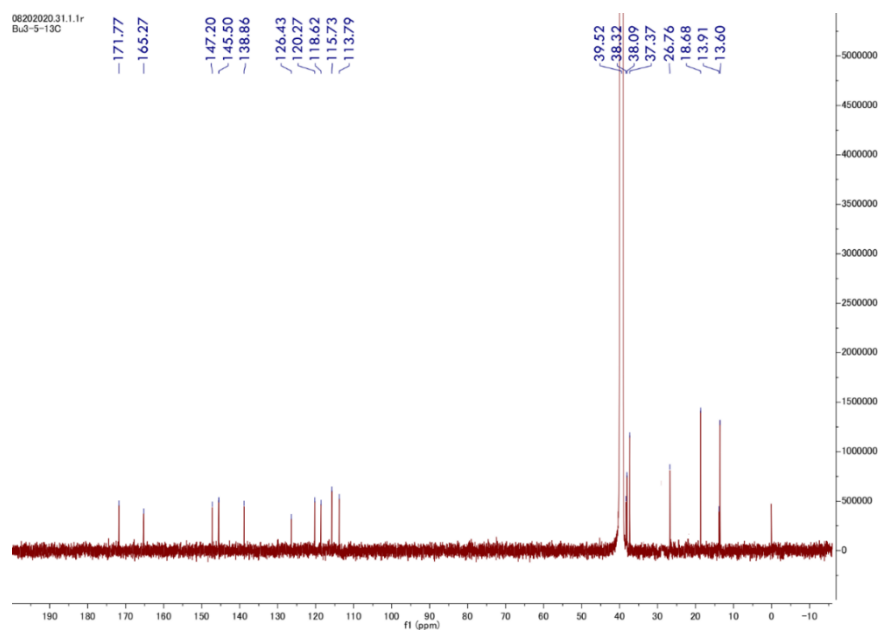
Figure S12: $^{13}$C-NMR spectrum of Bassiamide A (in DMSO-$d_6$, 600 MHz)
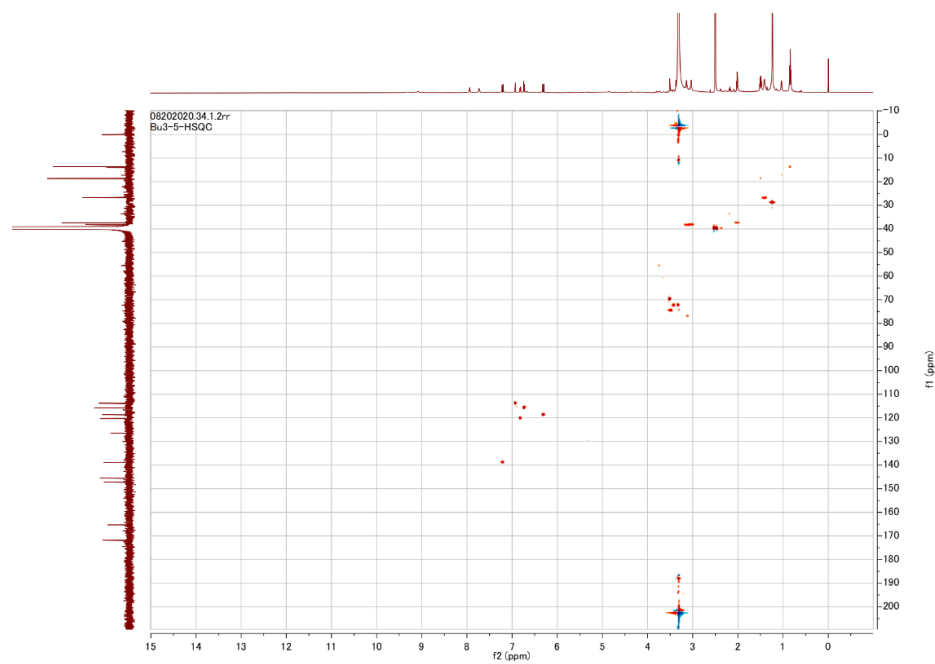


Figure S13: HSQC spectrum of Bassiamide A
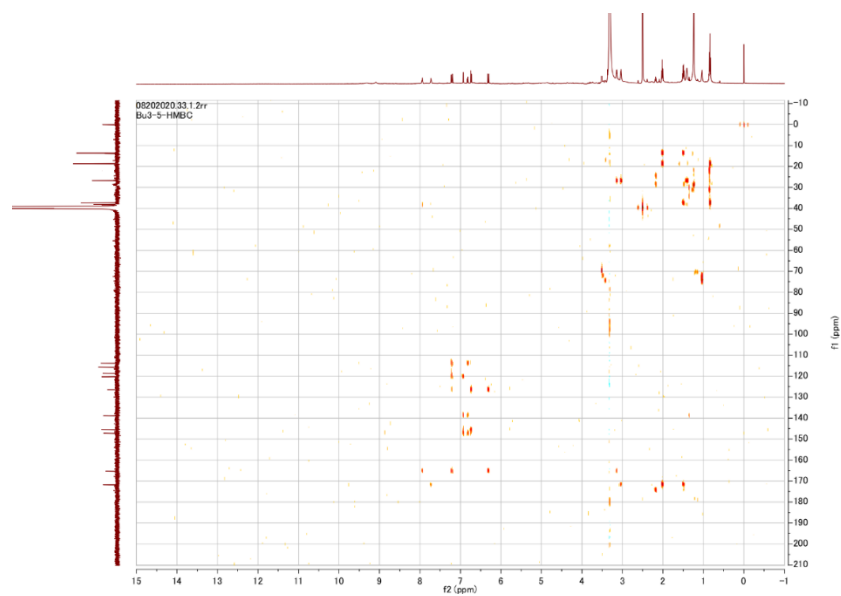
Figure S14: HMBC spectrum of Bassiamide A
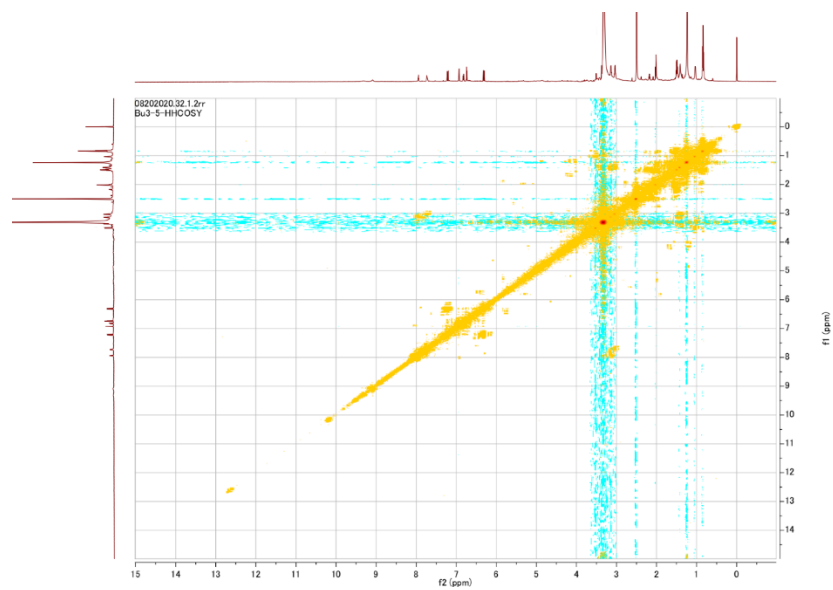


Figure S15: $^1$H-$^1$H COSY spectrum of Bassiamide A
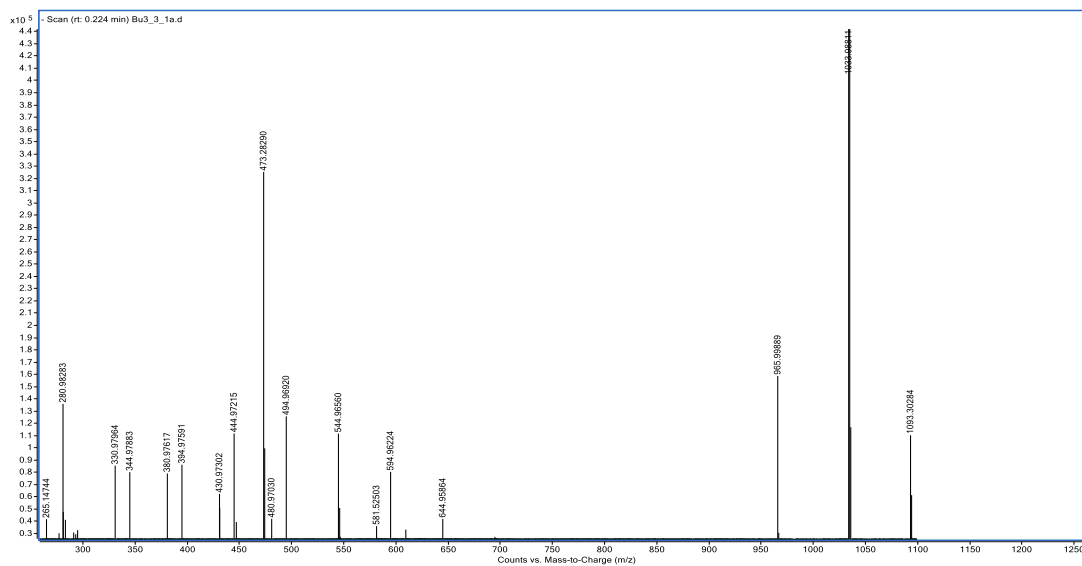
Figure S16: HR-MS of Kaempferol-3-*O*-*β*-D-Glc-(1→6)-*O*-[*β*-D-Gal-(1→3)-2-*O*-*trans*-feruloyl-*α*-L-Rha-(1→2)]-*β*-D-Glc
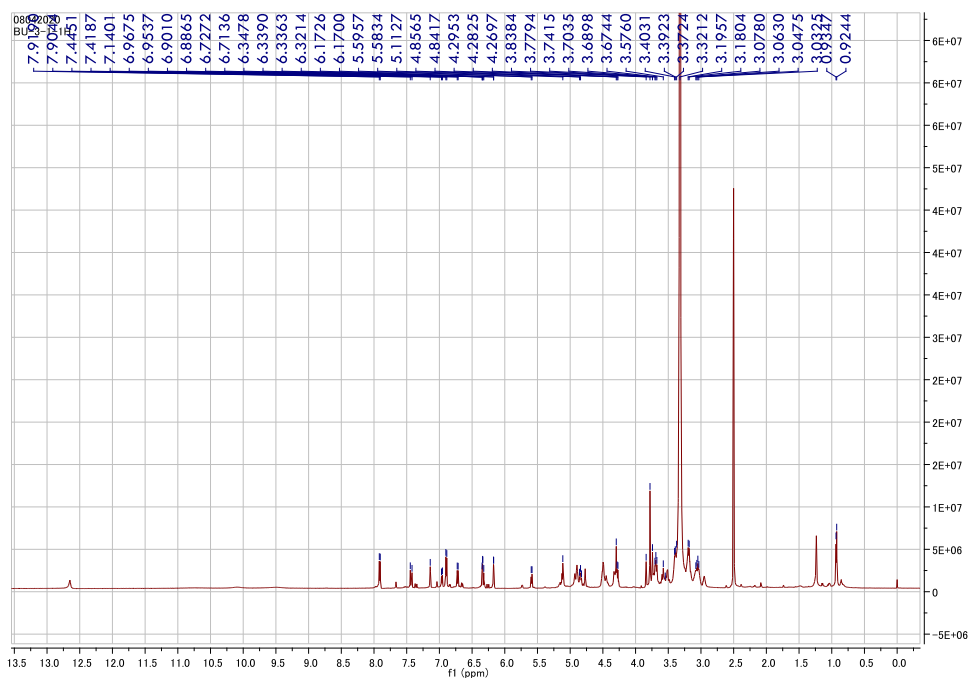


Figure S17: ¹H-NMR spectrum of Kaempferol-3-*O*-*β*-D-Glc-(1→6)-*O*-[*β*-D-Gal-(1→3)-2-*O*-*trans*-feruloyl-*α*-L-Rha-(1→2)]-*β*-D-Glc (in DMSO-*d₆*, 600 MHz)
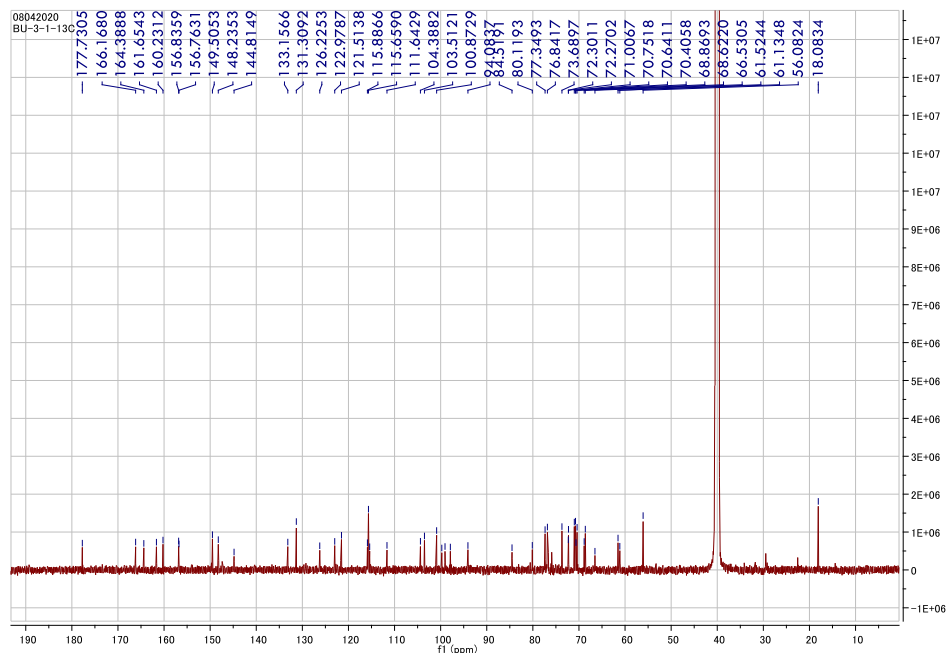
Figure S18: $^{13}$C-NMR spectrum of Kaempferol-3-*O*-*β*-D-Glc-(1→6)-*O*-[*β*-D-Gal-(1→3)-2-*O*-*trans*-feruloyl-*α*-L-Rha-(1→2)]-*β*-D-Glc (in DMSO-*d₆*, 150 MHz)
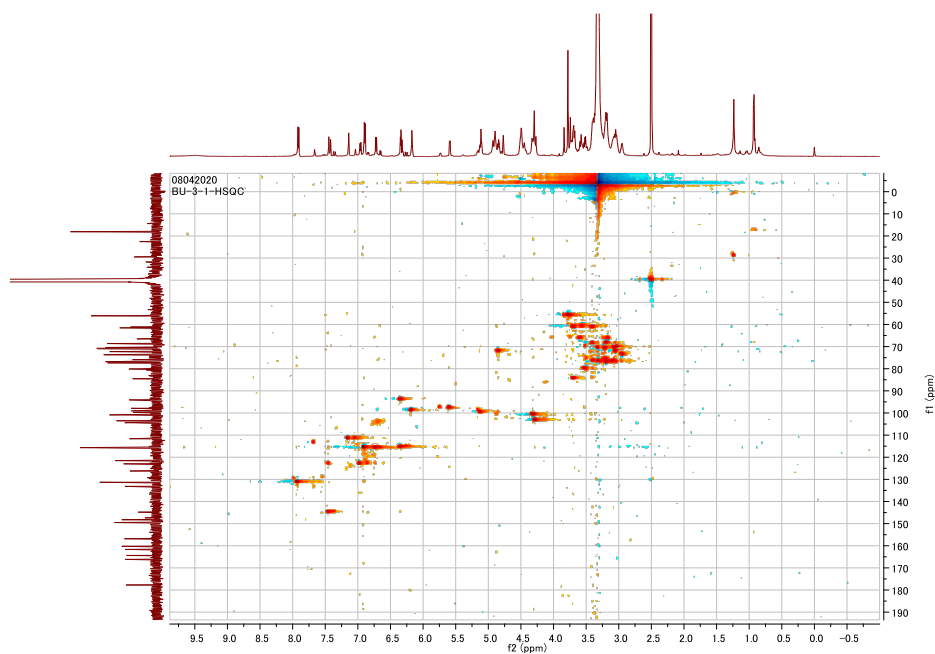


Figure S19: HSQC-NMR spectrum of Kaempferol-3-*O*-*β*-D-Glc-(1→6)-*O*-[*β*-D-Gal-(1→3)-2-*O*-*trans*-feruloyl-*α*-L-Rha-(1→2)]-*β*-D-Glc

164
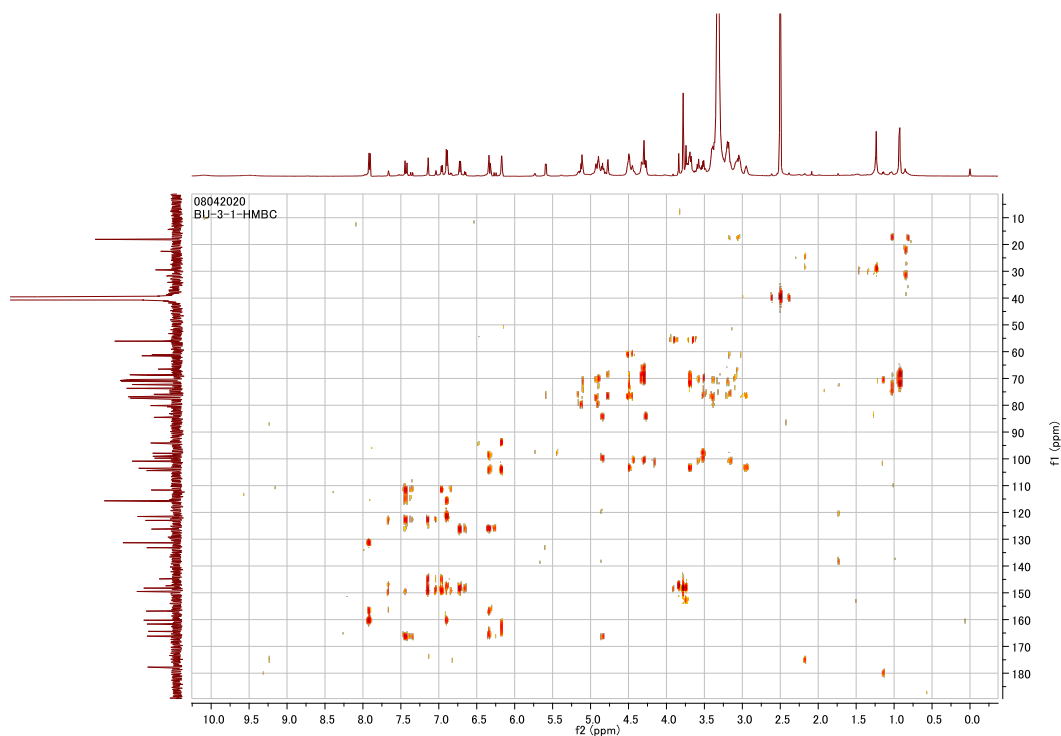
Figure S20: HMBC-NMR spectrum of Kaempferol-3-*O*-*β*-D-Glc-(1→6)-*O*-[*β*-D-Gal-(1→3)-2-*O*-*trans*-feruloyl-*α*-L-Rha-(1→2)]-*β*-D-Glc
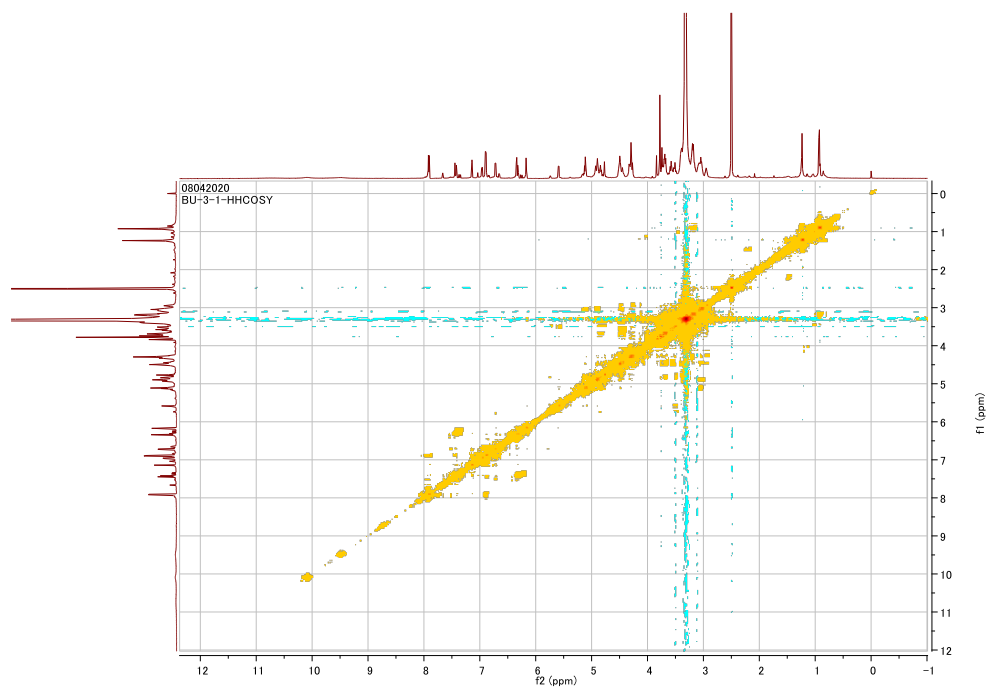


Figure S21: ¹H-¹H COSY NMR spectrum of Kaempferol-3-*O*-*β*-D-Glc-(1→6)-*O*-[*β*-D-Gal-(1→3)-2-*O*-*trans*-feruloyl-*α*-L-Rha-(1→2)]-*β*-D-Glc

Figure S22: HR-MS spectrum of 3-*O*-[2'-(2"-*O*-glycolyl)-glyoxylyl-*β*-D-GlcA]-28-*O*-*β*-D-Glc-olean-12-en-3*β*-ol-28-oic acid



Figure S23: $^1$H-NMR spectrum of 3-*O*-[2'-(2"-*O*-glycolyl)-glyoxylyl-*β*-D-GlcA]-28-*O*-*β*-D-Glc-olean-12-en-3*β*-ol-28-oic acid (in D$_2$O-Pyridine-*d$_5$*, 600 MHz)
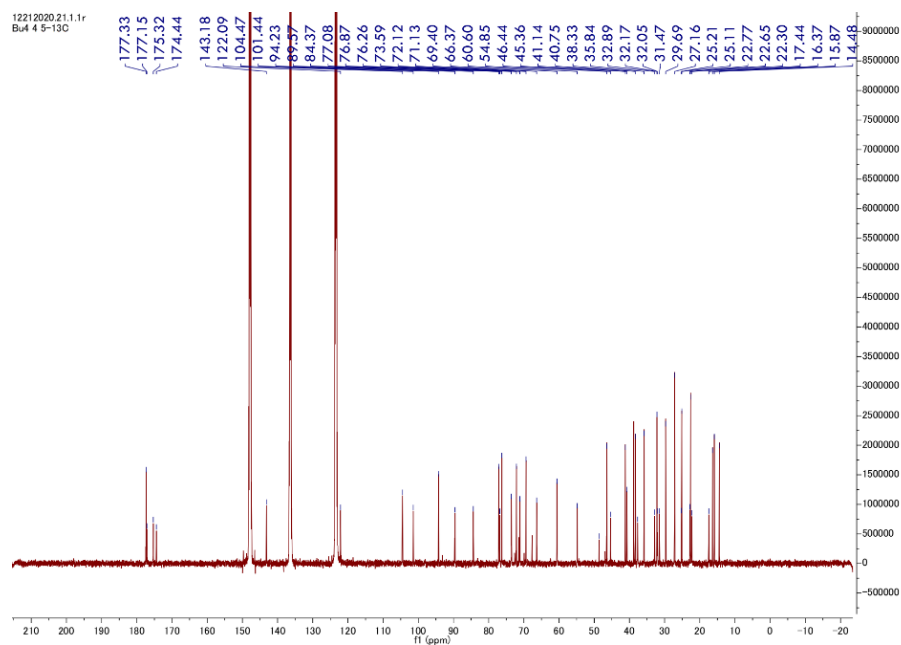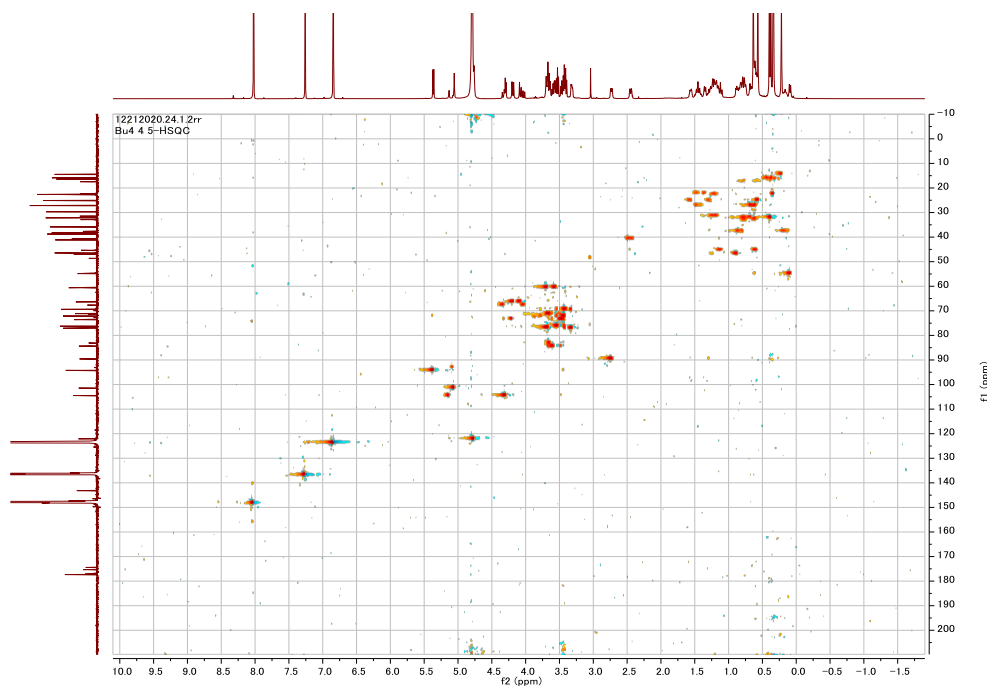
Figure S24: $^{13}$C-NMR spectrum of 3-*O*-[2'-(2''-*O*-glycolyl)-glyoxylyl-*β*-D-GlcA]-28-*O*-*β*-D-Glc-olean-12-en-3*β*-ol-28-oic acid (in D$_2$O-Pyridine-$d_5$, 150 MHz)



Figure S25: HSQC spectrum of 3-*O*-[2'-(2''-*O*-glycolyl)-glyoxylyl-*β*-D-GlcA]-28-*O*-*β*-D-Glc-olean-12-en-3*β*-ol-28-oic acid
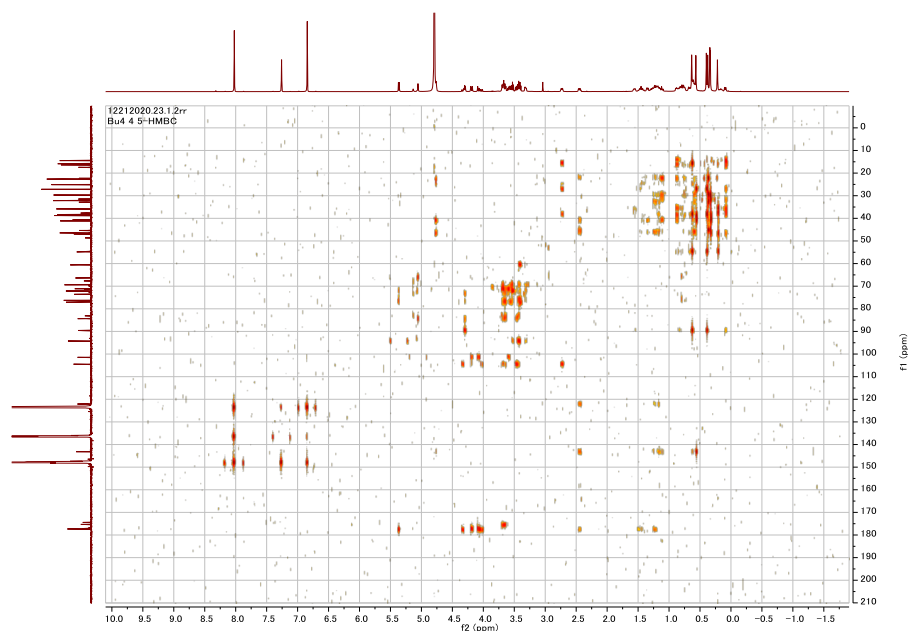
Figure S26: HMBC spectrum of 3-*O*-[2'-(2"-*O*-glycolyl)-glyoxylyl-*β*-D-GlcA]-28-*O*-*β*-D-Glc-olean-12-en-3*β*-ol-28-oic acid
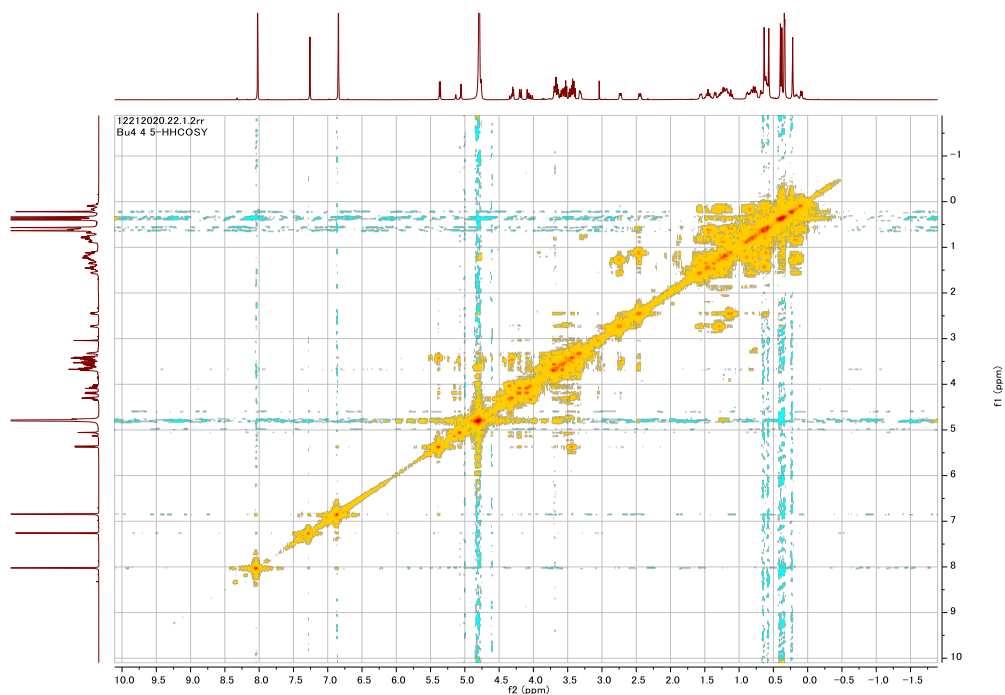


Figure S27: ^{1}H-^{1}H COSY spectrum of 3-*O*-[2'-(2"-*O*-glycolyl)-glyoxylyl-*β*-D-GlcA]-28-*O*-*β*-D-Glc-olean-12-en-3*β*-ol-28-oic acid
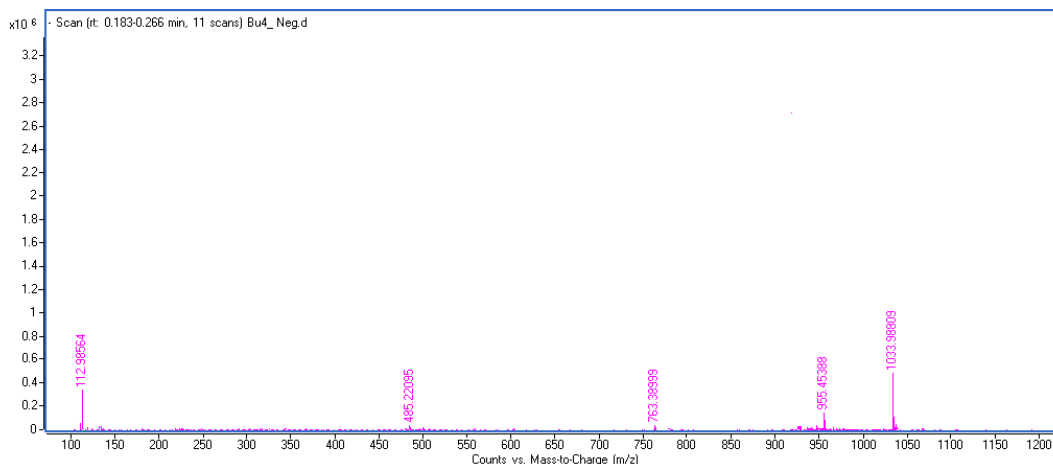
Figure S28: HR-MS spectrum of (2'*R*,3'*S*)-3-*O*-[2'-hydroxy-3'-(2"-*O*-glycolyl)-oxo-propionic acid-*β*-D-GlcA]-28-*O*-*β*-D-Glc-olean-12-en-3*β*-ol-28-oic acid
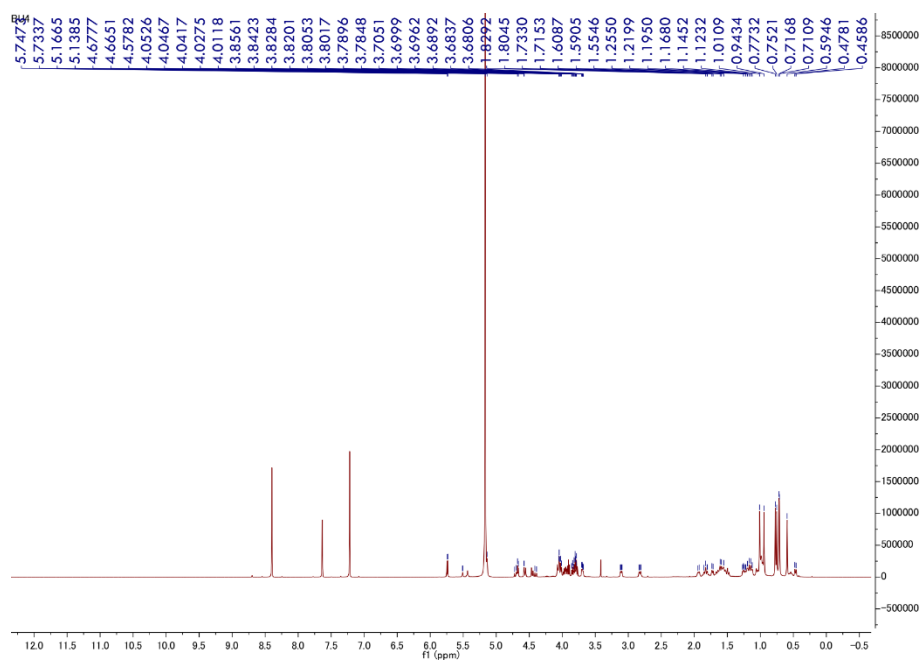


Figure S29: ^{1}H-NMR spectrum of (2'*R*,3'*S*)-3-*O*-[2'-hydroxy-3'-(2"-*O*-glycolyl)-oxo-propionic acid-*β*-D-GlcA]-28-*O*-*β*-D-Glc-olean-12-en-3*β*-ol-28-oic acid (in $D_2O$-Pyridine-$d_5$, 600 MHz)
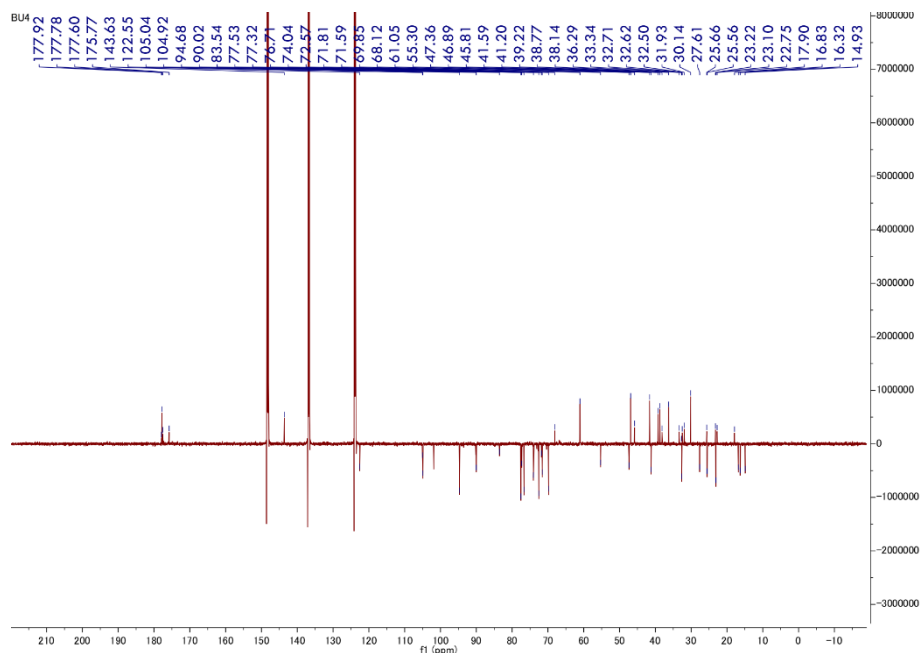
Figure S30: APT-NMR spectrum of (2'R,3'S)-3-O-[2'-hydroxy-3'-(2"-O-glycolyl)-oxo-propionic acid-β-D-GlcA]-28-O-β-D-Glc-olean-12-en-3β-ol-28-oic acid (in $D_2O$-Pyridine-$d_5$, 150 MHz)



Figure S31: HSQC spectrum of (2'R,3'S)-3-O-[2'-hydroxy-3'-(2"-O-glycolyl)-oxo-propionic acid-β-D-GlcA]-28-O-β-D-Glc-olean-12-en-3β-ol-28-oic acid
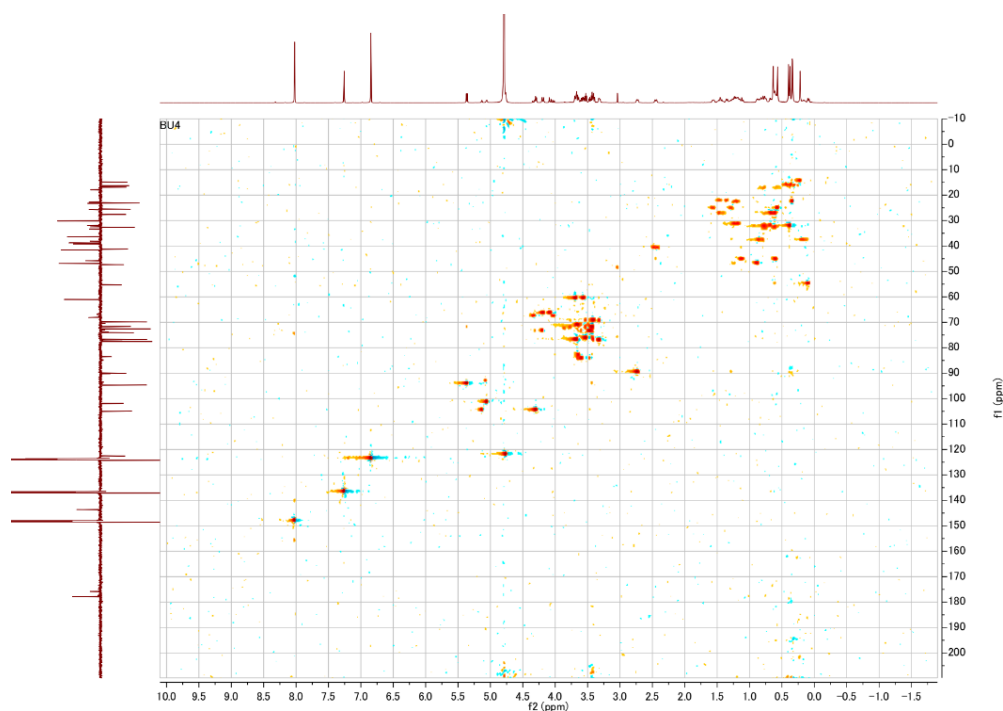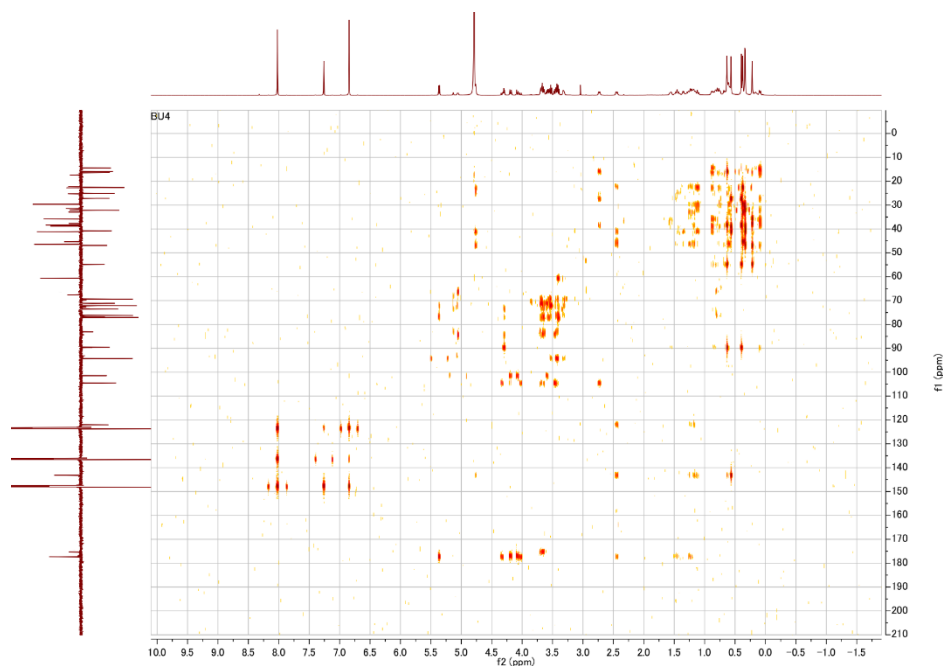
Figure S32: HMBC spectrum of (2'*R*,3'*S*)-3-*O*-[2'-hydroxy-3'-(2''-*O*-glycolyl)-oxo-propionic acid-*β*-D-GlcA]-28-*O*-*β*-D-Glc-olean-12-en-3*β*-ol-28-oic acid
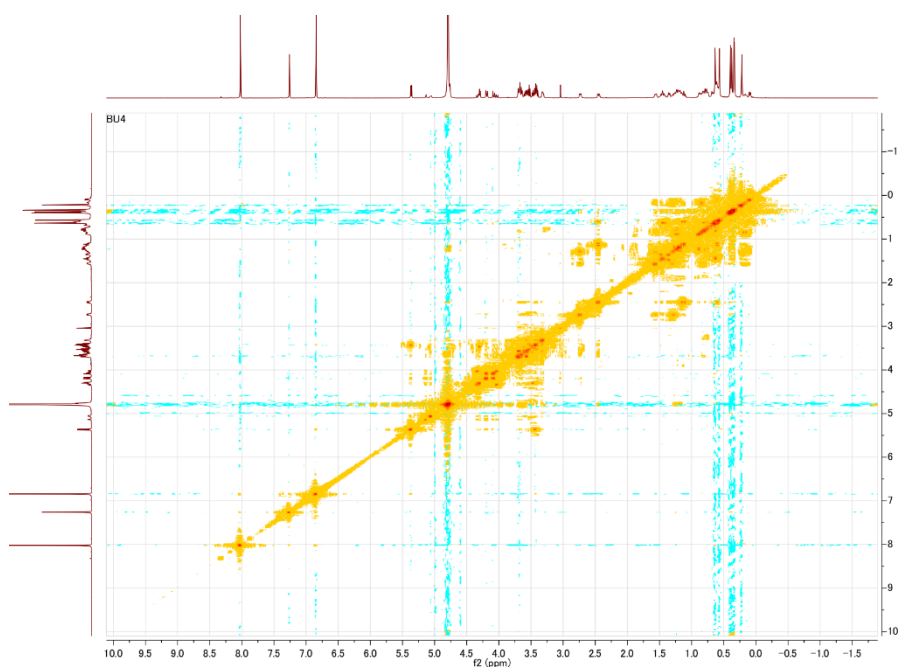


Figure S33: ^{1}H-^{1}H COSY spectrum of (2'*R*,3'*S*)-3-*O*-[2'-hydroxy-3'-(2''-*O*-glycolyl)-oxo-propionic acid-*β*-D-GlcA]-28-*O*-*β*-D-Glc-olean-12-en-3*β*-ol-28-oic acid
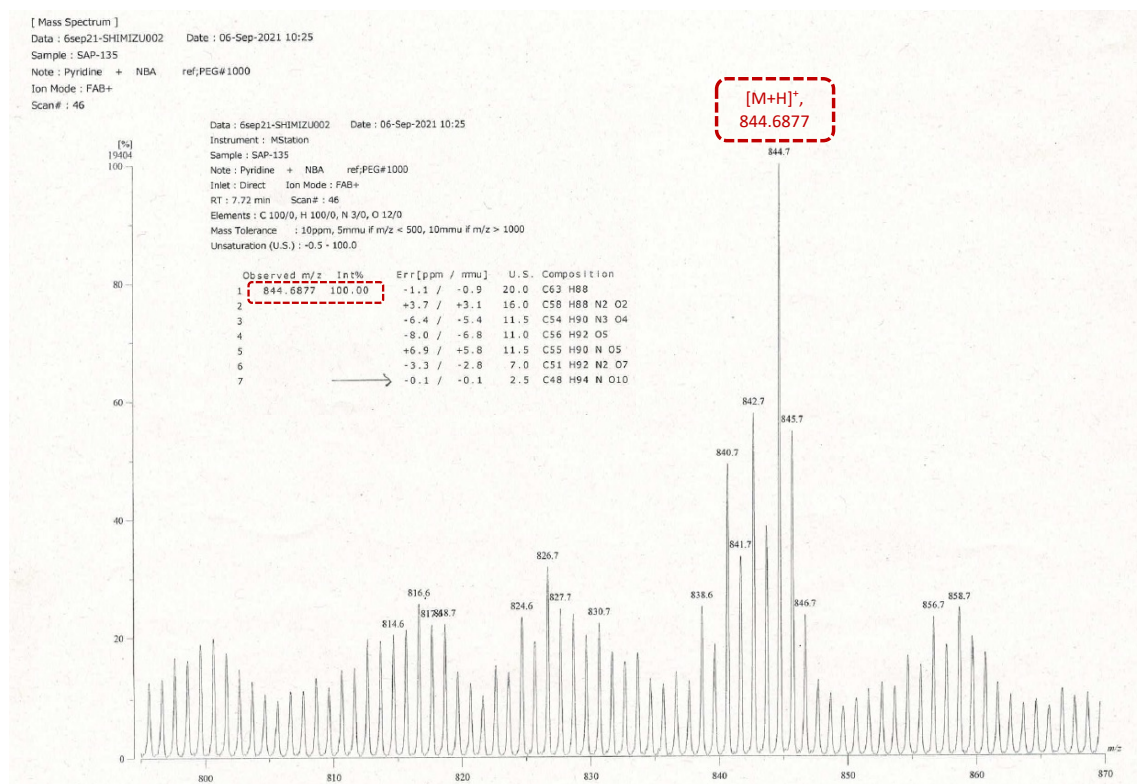
Figure S34: HR-FAB-MS of Agathophamide A
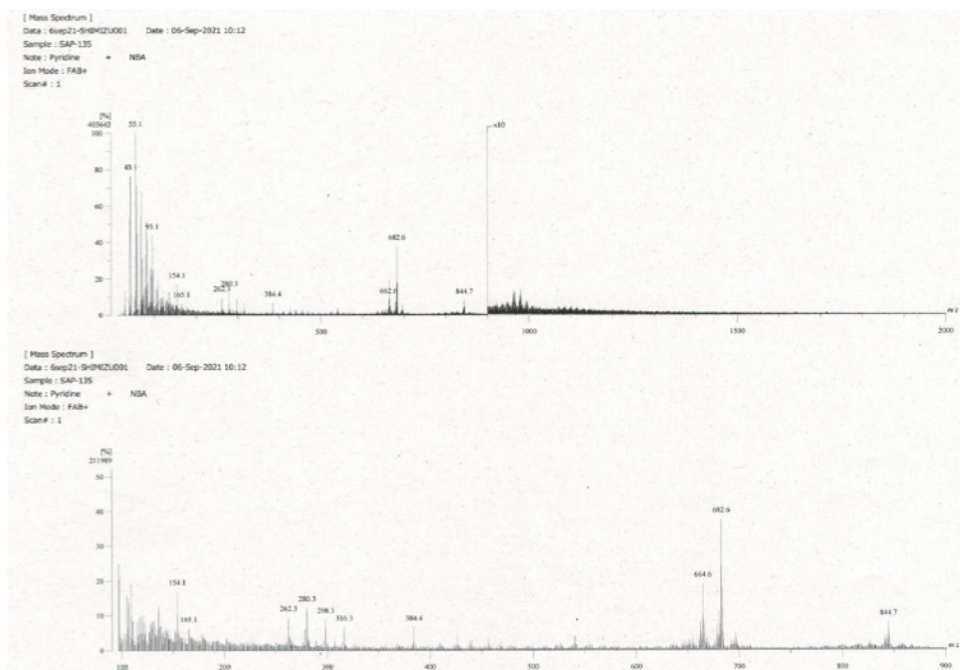


Figure S35: FAB-MS-MS fragmentation of Agathophamide A
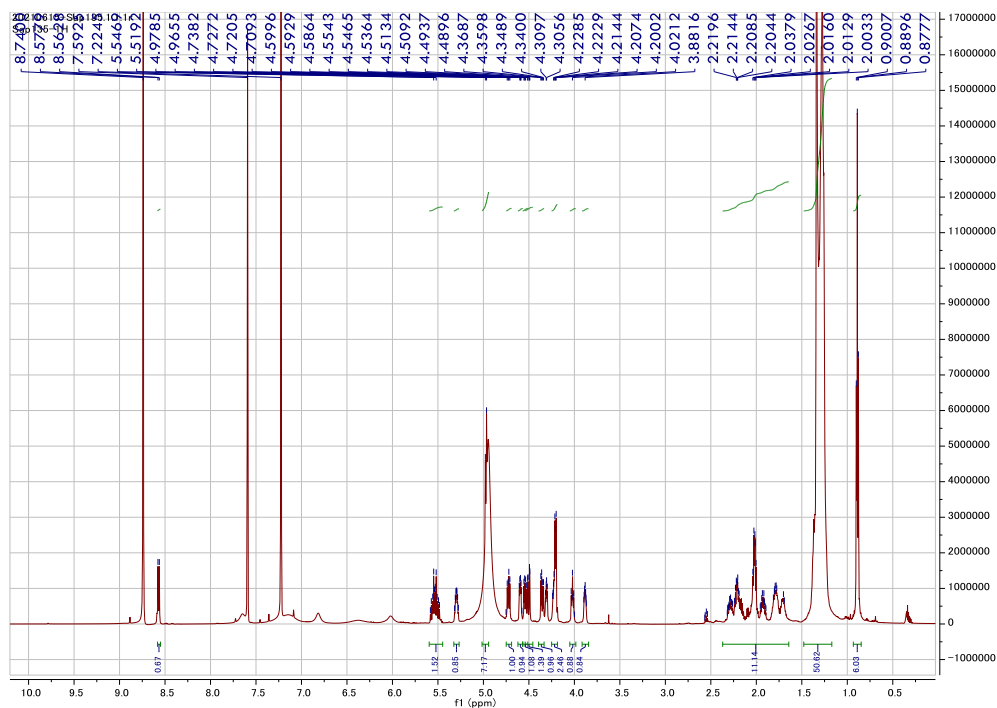
Figure S36: $^1$H-NMR spectrum of Agathophamide A (600 MHz, $C_5D_5N$)
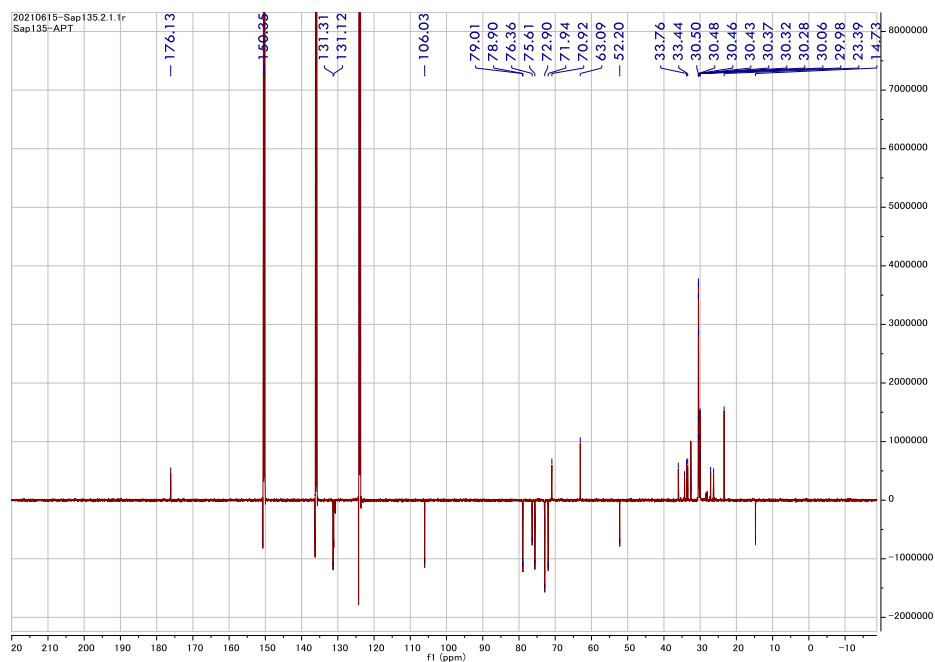


Figure S37: APT-NMR spectrum of Agathophamide A (150MHz, $C_5D_5N$)
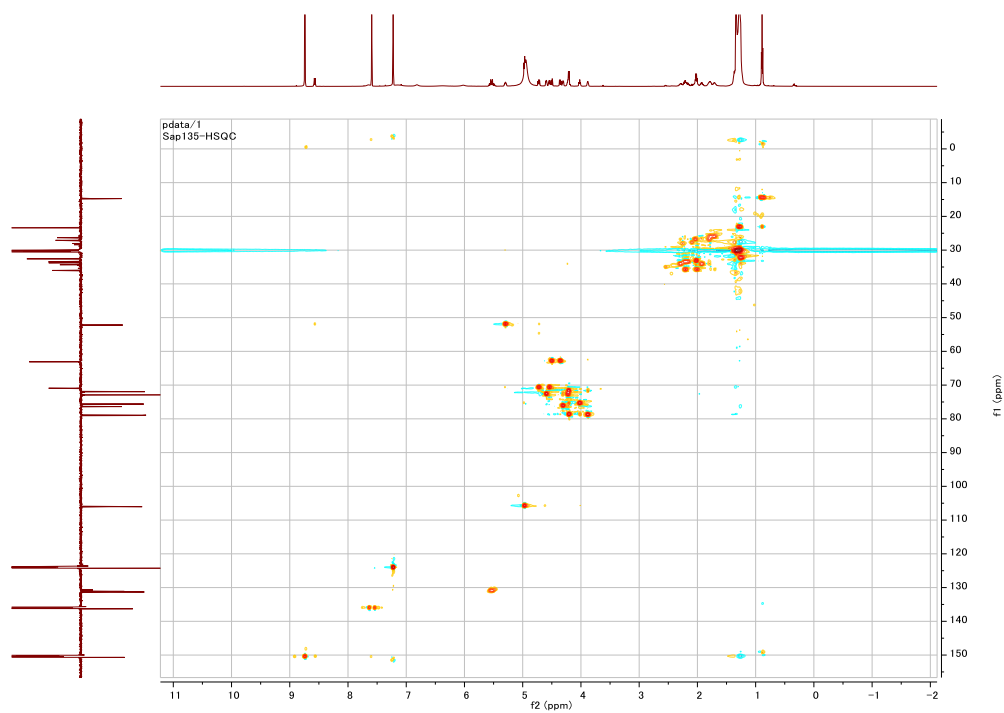
Figure S38: HSQC spectrum of Agathophamide A (in $C_5D_5N$)
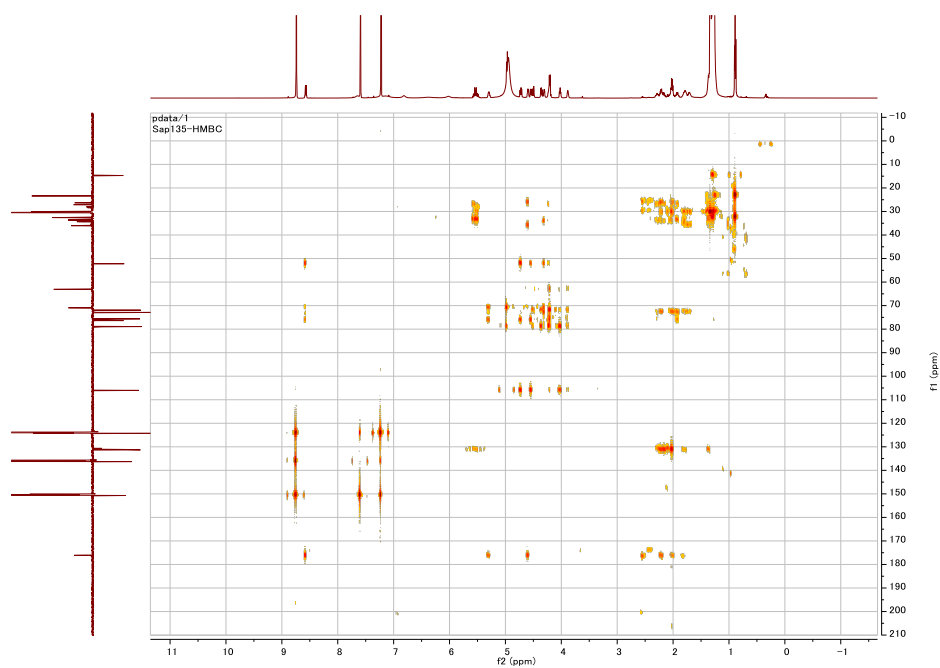


Figure S39: HMBC spectrum of Agathophamide A (in $C_5D_5N$)
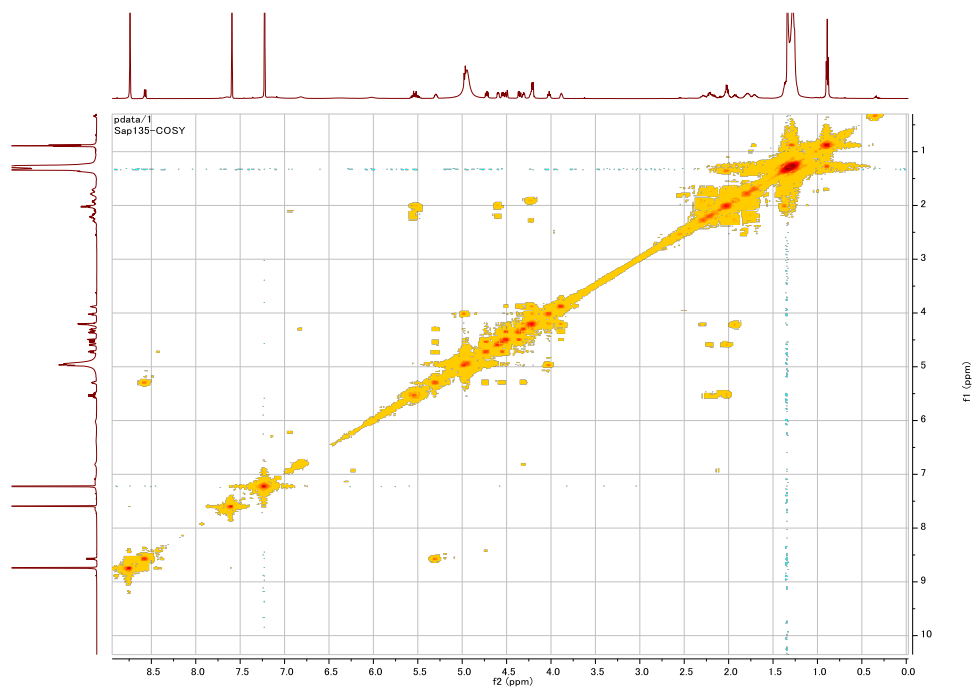
Figure S40: $^1H$-$^1H$ COSY spectrum of Agathophamide A (in $C_5D_5N$)
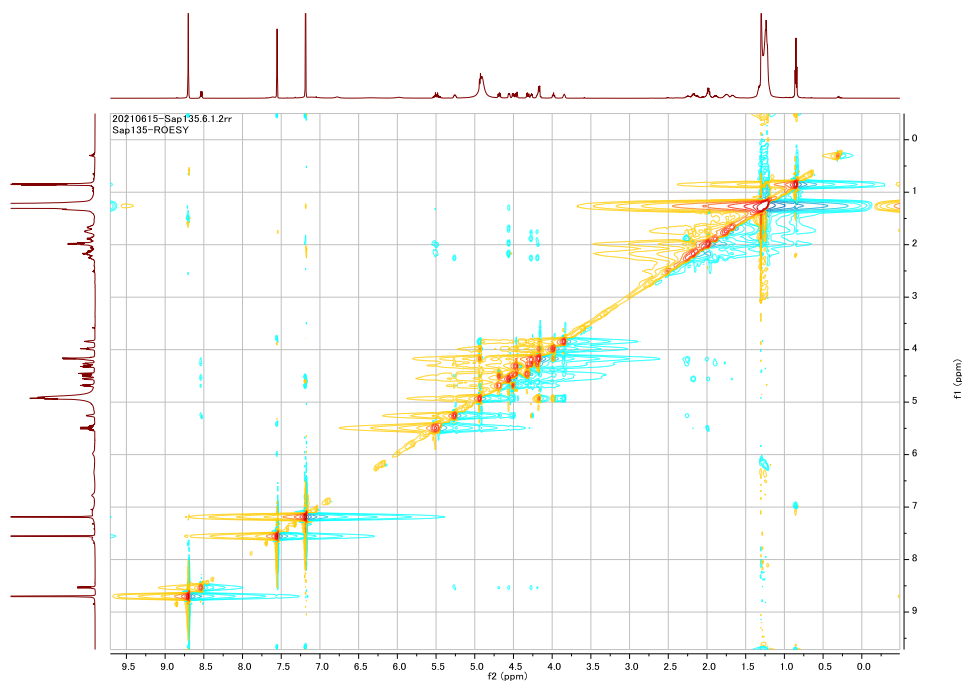


Figure S41: ROESY spectrum of Agathophamide A
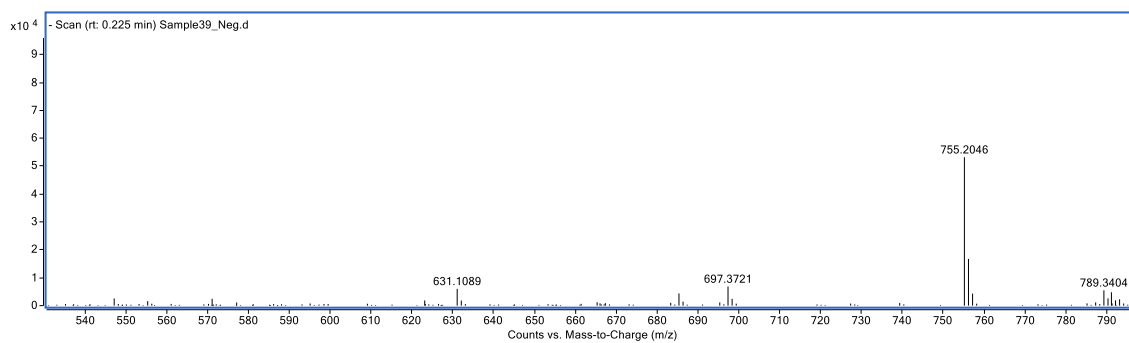
Figure S42: HR-MS of Agathophoroside A
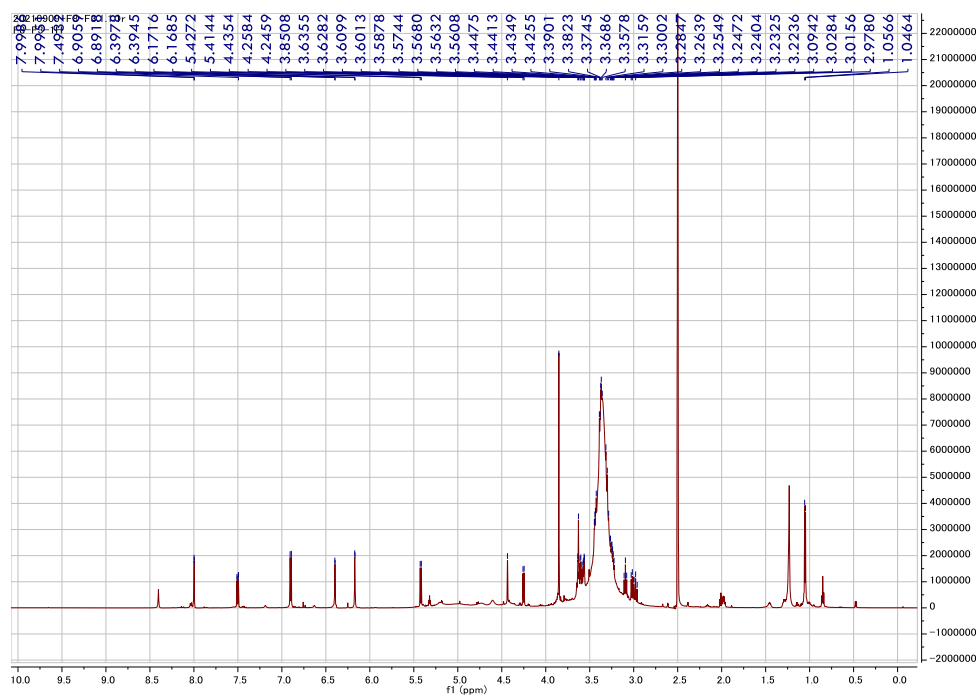


Figure S43: $^1$H-NMR spectrum of Agathophoroside A (600 MHz, DMSO-$d_6$)
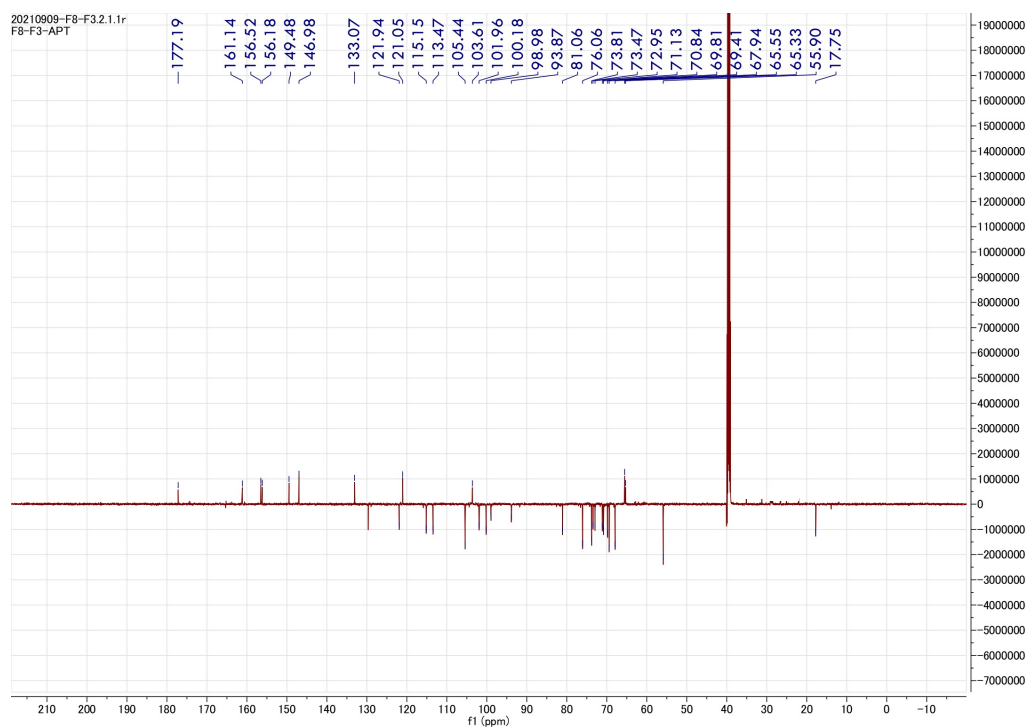
Figure S44: APT-NMR spectrum of Agathophoroside A (150 MHz, DMSO-$d_6$)
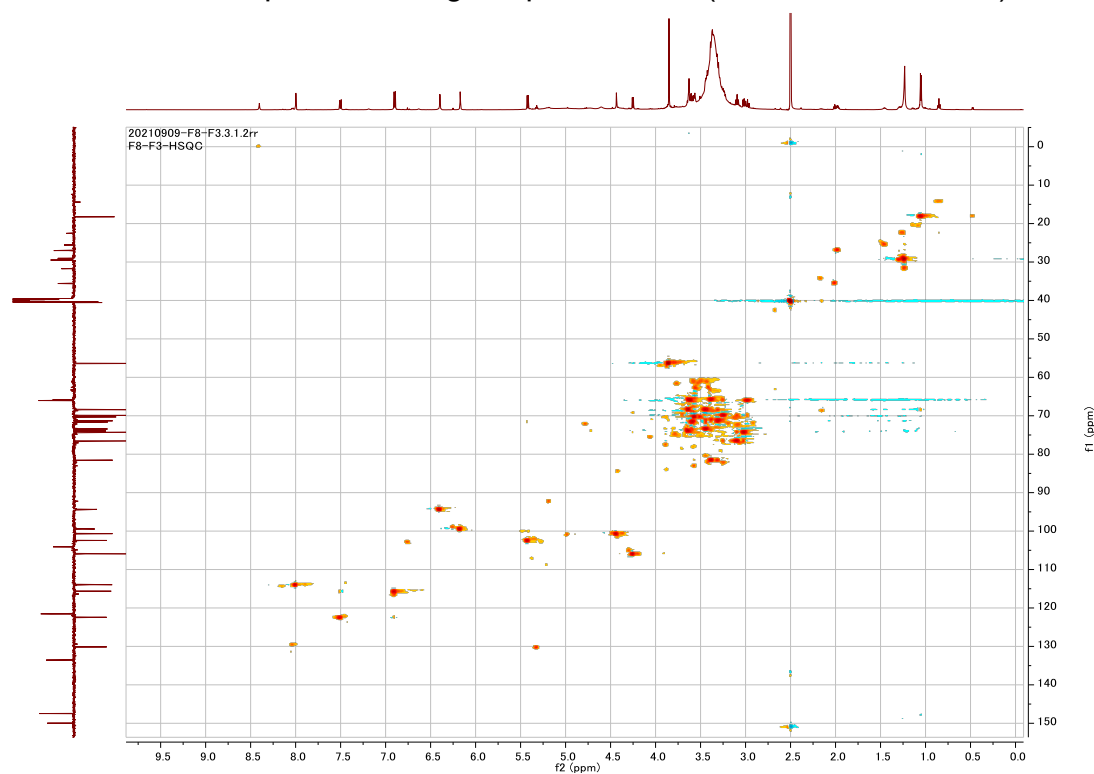


Figure S45: HSQC spectrum of Agathophoroside A (in DMSO-$d_6$)
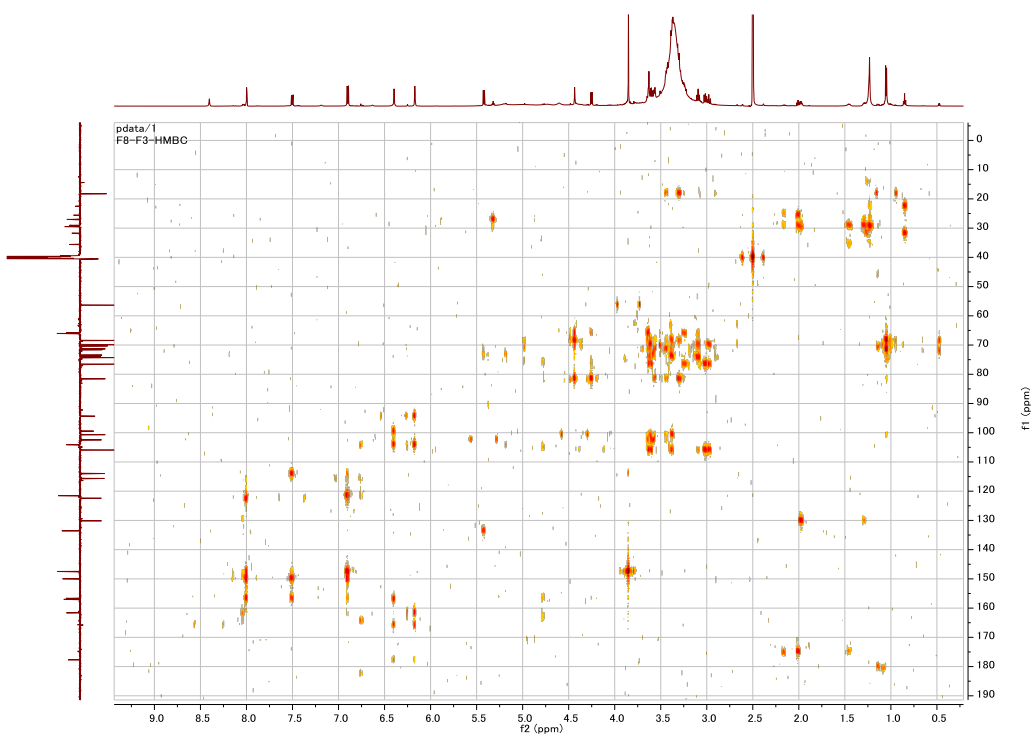
Figure S46: HMBC spectrum of Agathophoroside A (in DMSO-$d_6$)
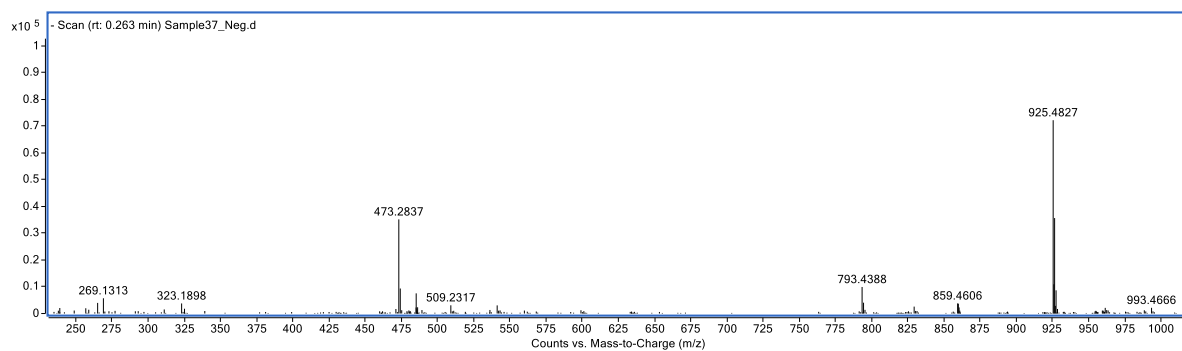


Figure S47: HR-MS of Solysaponin A
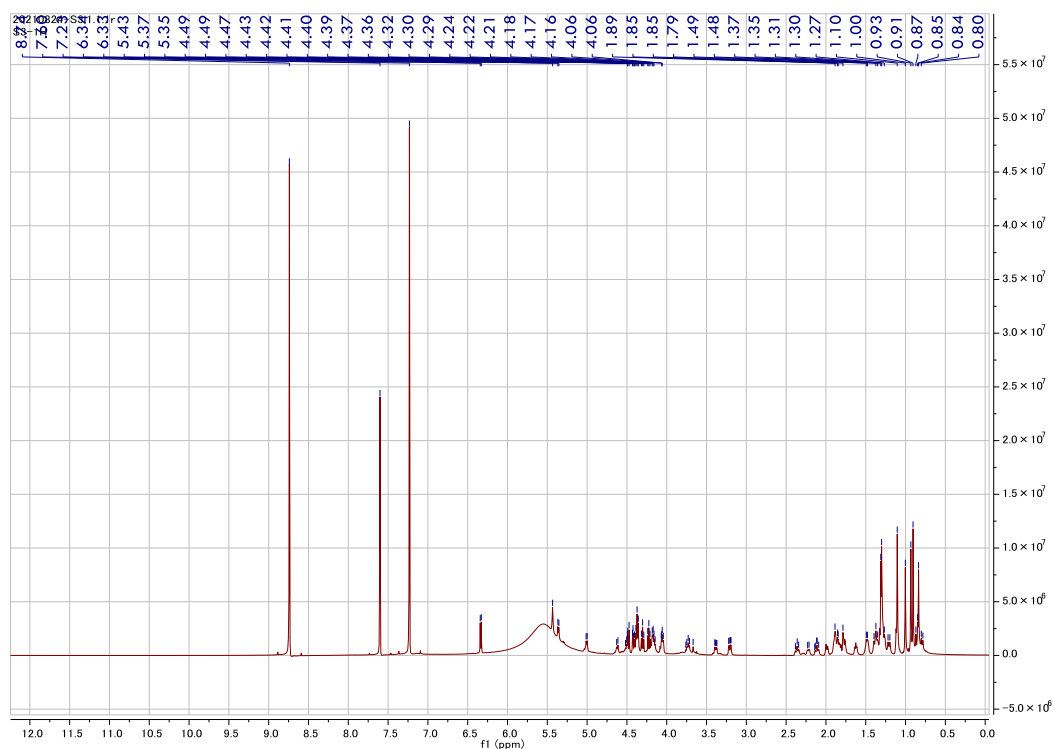
Figure S48: $^1$H-NMR spectrum of Solysaponin A (600 MHz, C$_5$D$_5$N)
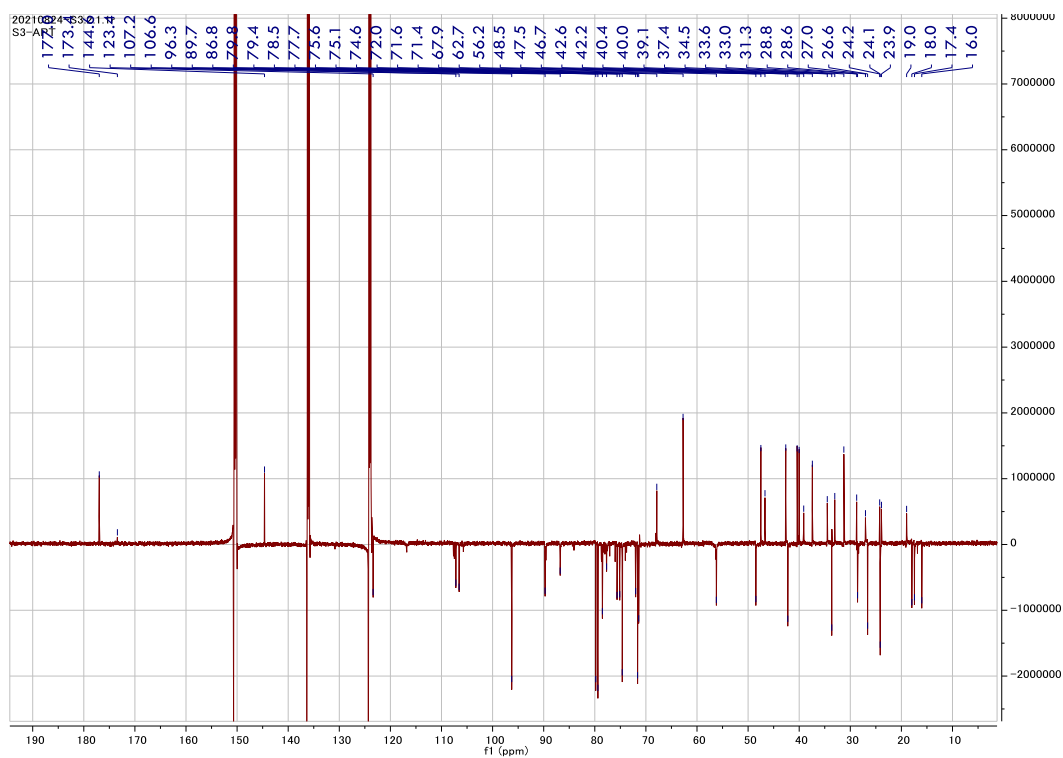


Figure S49: APT-NMR spectrum of Solysaponin A (in C$_5$D$_5$N)

179
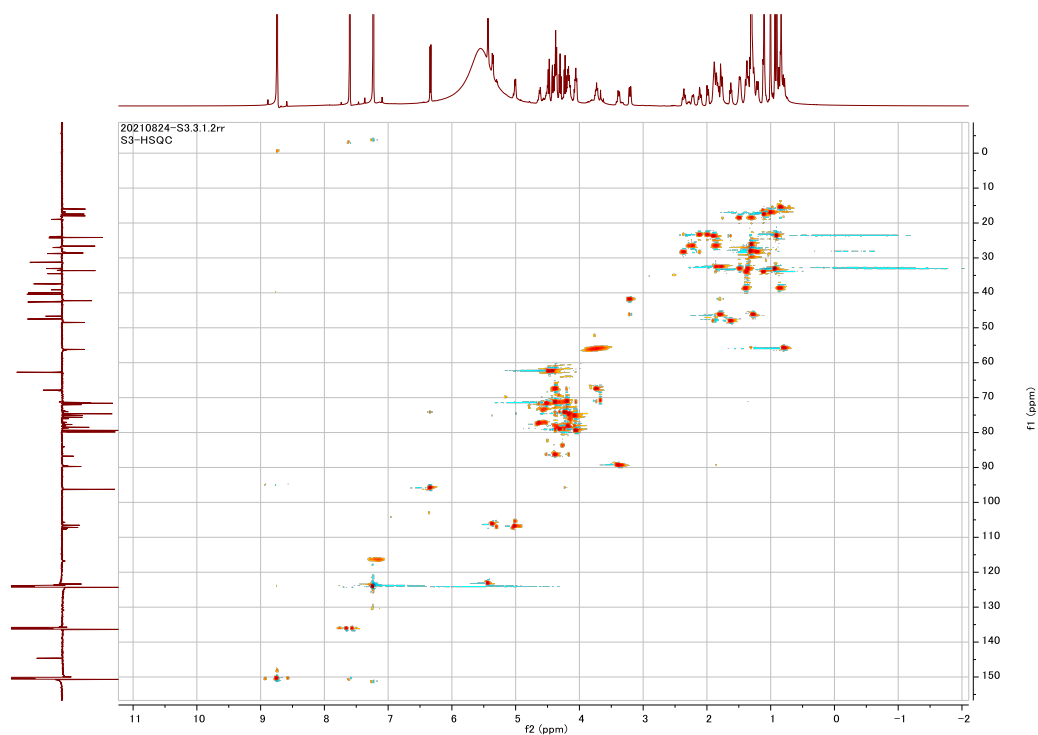
Figure S50: HSQC spectrum of Solysaponin A (in C$_5$D$_5$N)
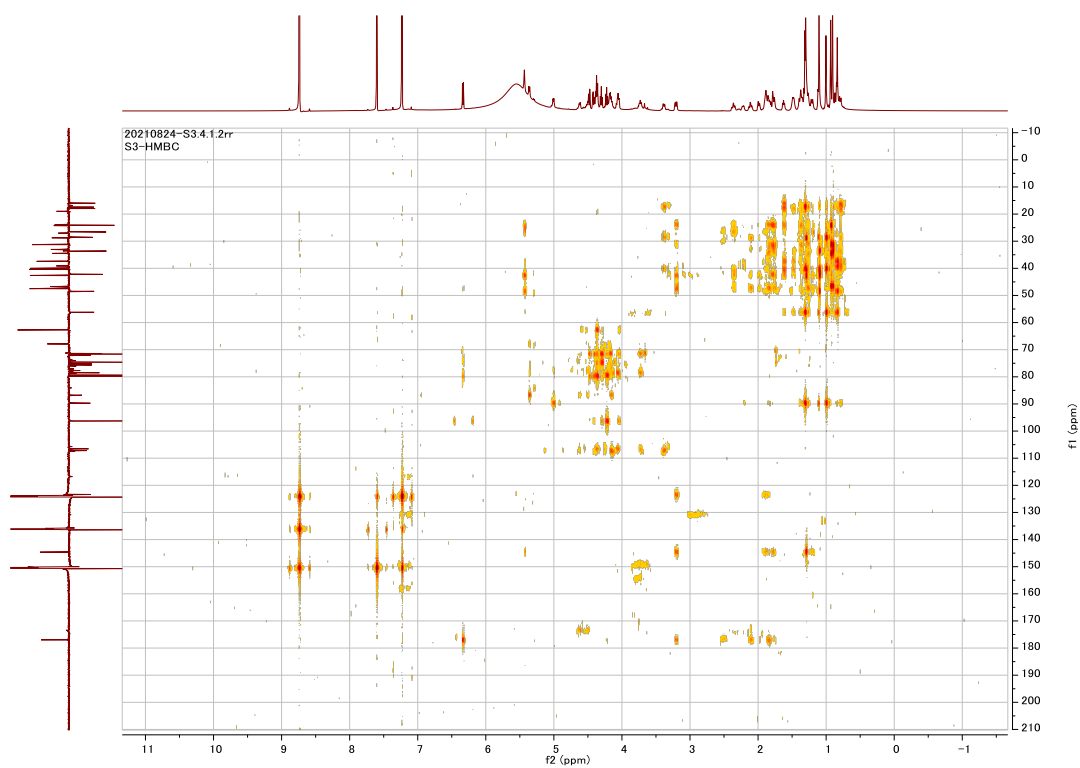
Figure S51: HMBC spectrum of Solysaponin A (in C$_5$D$_5$N)
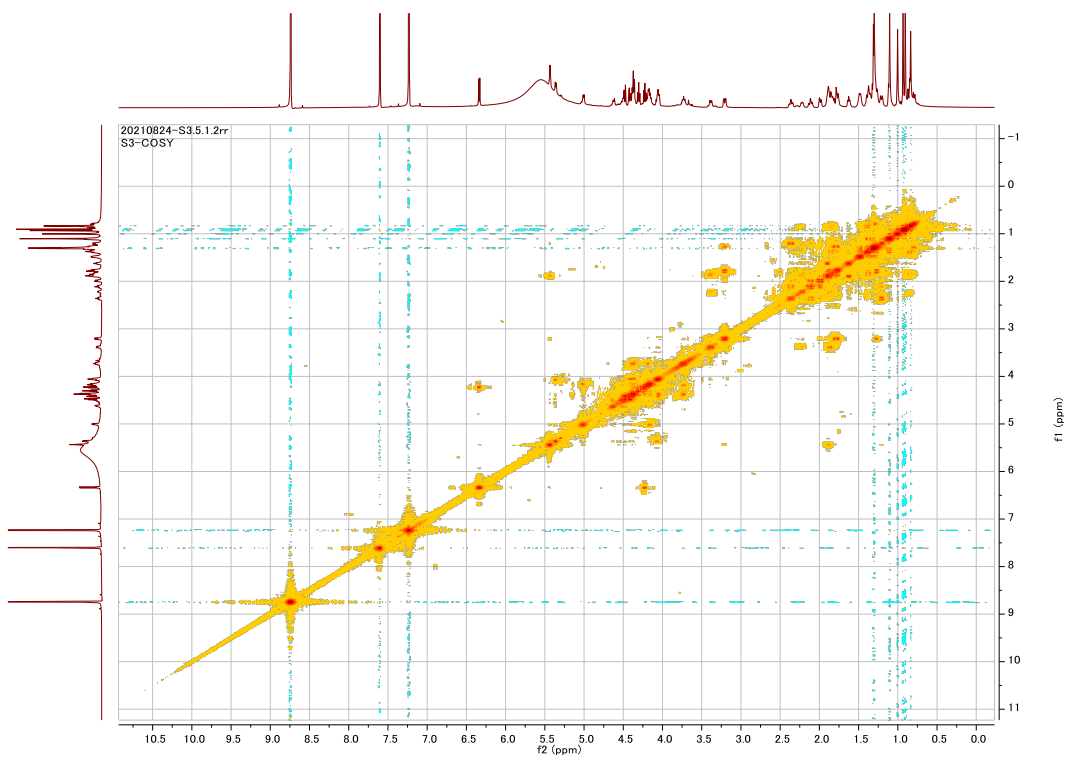
Figure S52: $^1$H-$^1$H COSY spectrum of Solysaponin A (in $C_5D_5N$)
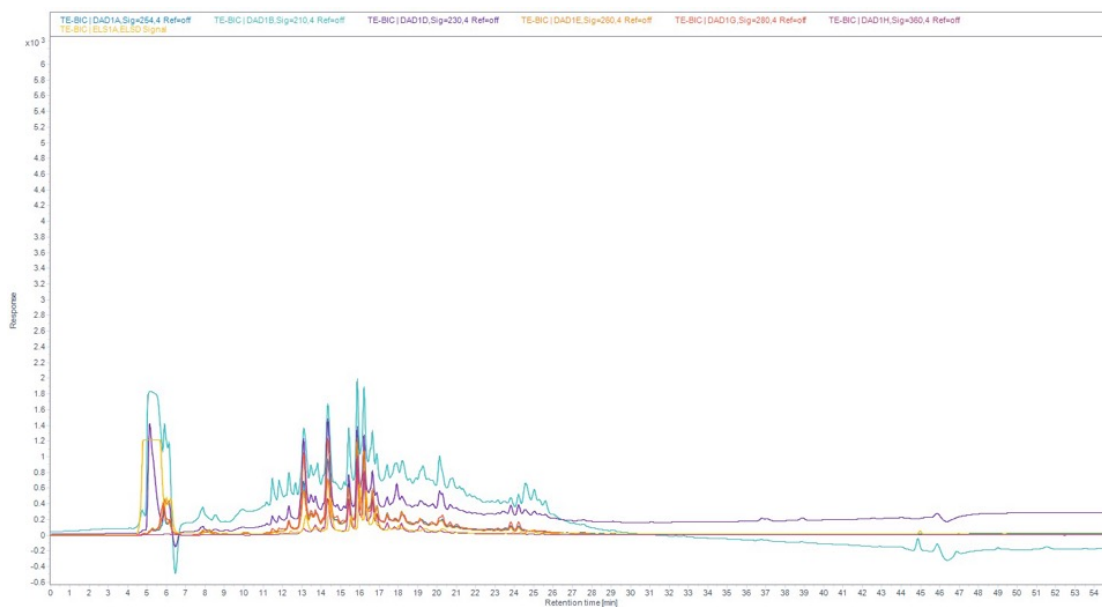


Figure S53: HPLC chromatogram of MeOH extract of *B. indica* (210-360 nm)

## References

1    T. Rodrigues, D. Reker, P. Schneider and G. Schneider, *Nature Chemistry*, 2016, **8**, 531–541.

2    J. Khazir, B. A. Mir, S. A. Mir and D. Cowan, *Journal of Asian Natural Products Research*, 2013, 15, 764–788.

3    D. J. Newman and G. M. Cragg, *Journal of Natural Products*, 2012, **75**, 311–335.

4    H. Yao, J. Liu, S. Xu, Z. Zhu and J. Xu, *Expert Opinion on Drug Discovery*, 2017, **12**, 121–140.

5    G. M. Cragg and D. J. Newman, *Biochimica et Biophysica Acta - General Subjects*, 2013, **1830**, 3670–3695.

6    N. E. Thomford, A. Senthebane, A. Rowe, D. Munro, P. Seele, A. Maroyi and K. Dzobo, *International Journal of Molecular Sciences*, 2018, **19**, 1578.

7    W. Liu, Q. Li, J. Hu, H. Wang, F. Xu and Q. Bian, *Bioorganic and Medicinal Chemistry*, 2019, **27**, 115150.

8    D. A. Dias, S. Urban and U. Roessner, *Metabolites*, 2012, **2**, 303–336.

9    P. Williams, A. Sorribas and M. J. R. Howes, *Natural Product Reports*, 2011, 28, 48–77.

10   V. Täckholm, *Students' Flora of Egypt*, 1974.

11   N. S. Abdel-Azim, K. A. Shams, A. A. A. Shahat, M. M. El Missiry, S. I. Ismail and F. M. Hammouda, *Research Journal of Medicinal Plant*, 2011, **5**, 136–144.

12   M. S. Al-Omar, H. A. Mohammed, S. A. A. Mohammed, E. Abd-Elmoniem, Y. I. Kandil, H. M. Eldeeb, S. Chigurupati, G. M. Sulaiman, H. K. Al-Khurayyif, B. S. Almansour, P. M. Suryavamshi and R. A. Khan, *Molecules*, 2020, **25**, 5457.

13   S. A. Petropoulos, A. Karkanis, N. Martins and I. C. Ferreira, *Trends in Food Science and Technology*, 2018, **74**, 69–84.

14   C. Vizetto-Duarte, F. Figueiredo, M. J. Rodrigues, C. Polo, E. Rešek and L. Custódio, *Sustainability*, 2019, **11**, 2197.

15   A. Roohi, B. Nazish, M. Maleeha, Nabgha-e-Amen and S. Waseem, *Journal of Medicinal Plants Research*, 2011, **5**, 7108-7118.

16    I. Chikhi, H. Allali, M. el Amine Dib, H. Medjdoub and B. Tabti, *Asian Pacific Journal of Tropical Disease*, 2014, **4**, 181–184.

17    R. Mohammed, S. S. El-Hawary and A. M. Abo-Youssef, *Journal of Natural Products*, 2012, **5**, 193–206.

18    P. Morales, I. C. F. R. Ferreira, A. M. Carvalho, M. C. Sánchez-Mata, M. Cámara, V. Fernández-Ruiz, M. Pardo-de-Santayana and J. Tardío, *LWT-Food Science and Technology*, 2014, **55**, 389–396.

19    R. Ozgur, B. Uzilday, A. H. Sekmen and I. Turkan, *Functional Plant Biology*, 2013, 40, 832–847.

20    M. Qasim, Z. Abideen, M. Y. Adnan, S. Gulzar, B. Gul, M. Rasheed and M. A. Khan, *South African Journal of Botany*, 2017, **110**, 240–250.

21    R. Ksouri, W. M. Ksouri, I. Jallali, A. Debez, C. Magné, I. Hiroko and C. Abdelly, *Critical Reviews in Biotechnology*, 2012, **32**, 289–326.

22    N. Hamza, B. Berke, A. Umar, C. Cheze, H. Gin and N. Moore, *Journal of Ethnopharmacology*, 2019, **238**, 111841.

23    P. Ninfali and D. Angelino, *Fitoterapia*, 2013, **89**, 188–199.

24    M. H. Rhee, H.-J. Park and J. Y. Cho, *Journal of Medicinal Plants Research*, 2009, **3**, 548–555.

25    R. A. El-shiekh, D. A. Al-Mahdy, S. M. Mouneir, M. S. Hifnawy and E. A. Abdel-Sattar, *Journal of Ethnopharmacol*, 2019, **238**,111893.

26    S. Javed, A. Javaid and M. Z. Qureshi, *International Journal of Bioogy and Biotechnology*, 2018, **15**, 661–666.

27    L. Barreira, E. Resek, M. J. Rodrigues, M. I. Rocha, H. Pereira, N. Bandarra, M. M. da Silva, J. Varela and L. Custódio, *Journal of Food Composition and Analysis*, 2017, **59**, 35–42.

28    S. P. A. de Oliveira, H. M. A. do Nascimento, K. B. Sampaio and E. L. de Souza, *Critical Reviews in Food Science and Nutrition*, 2021, **61**, 2022–2033.

29    Z. Mzoughi, H. Chahdoura, Y. Chakroun, M. Cámara, V. Fernández-Ruiz, P. Morales, H. Mosbah, G. Flamini, M. Snoussi and H. Majdoub, *Food Research International*, 2019, **119**, 612–621.

30   H. Y. Han, H. Kim, Y. H. Son, G. Lee, S. H. Jeong and M. H. Ryu, *Pharmacognosy Magazine*, 2014, **10**, S661–S667.

31   S. Oueslati, R. Ksouri, H. Falleh, A. Pichette, C. Abdelly and J. Legault, *Food Chemistry*, 2012, **132**, 943–947.

32   M. Moein, M. M. Zarshenas, S. Khademian and A. D. Razavi, *Trends in Pharmaceutical Sciences*, 2015, **1**, 39–43.

33   A. Musa, N. S. Al-Muaikel and M. S. Abdel-Bakky, *Der Pharma Chemica*, 2016, **8**, 169–178.

34   A. Poonia and A. Upadhayay, *Journal of Food Science and Technology*, 2015, **52**, 3977–3985.

35   S. Arora and P. Itankar, *Journal of Traditional and Complementary Medicine*, 2018, **8**, 476–482

36   T. Zhao, H. Pan, Y. Feng, H. Li and Y. Zhao, *Experimental and Therapeutic Medicine*, 2016, **12**, 3301–3307.

37   A. A. Matloub, M. A. Hamed and S. S. M. El Souda, *International Journal of Pharmacy and Pharmaceutical Sciences*, 2014, **6**, 187–196.

38   Y. M. Choi, S. Kang and J. Hong, *Korean Journal of Food Science and Technology*, 2016, **48**, 378–383.

39   Y. C. Ko, H. S. Choi, J.-H. Kim, S.-L. Kim, B.-S. Yun, D.-S. Lee, L. Tesoriere and A. Attanzio, *Molecules*, 2020, **25**, 4950–4964.

40   H. S. Kim, J. H. Kim, J. O. Lee, J. W. Moon, M. J. Kang, W. S. Byun, J. A. Han, S. J. Kim and S. H. Park, *Natural Product Communications*, 2020, **15**, 1–7.

41   M. S. Al-Said, N. A. Siddiqui, M. A. Mukhair, M. K. Parvez, P. Alam, M. Ali and A. Haque, *Saudi Pharmaceutical Journal*, 2017, **25**, 1005–1010.

42   S. S. Arya, S. Devi, K. Ram, S. Kumar, N. Kumar, A. Mann, A. Kumar and G. Chand, in *Ecophysiology, Abiotic Stress Responses and Utilization of Halophytes*, ed. M. Hasanuzzaman, K. Nahar, M. Öztürk, Springer, Singapore, 2019, 271–287.

43   A. Bahuguna, S. Bharadwaj, V. Bajpai, S. Shukla, D. Wook Won, I. Park, M. Na, S. Sonwal, Y. S. Huh, Y. K. Han, J. Simal-Gandara, J. Xiao and M. Kim, *Phytomedicine*, 2021, **90**, 153638.

44    H. Saleem, U. Khurshid, M. Sarfraz, M. I. Tousif, A. Alamri, S. Anwar, A. Alamri, I. Ahmad, H. H. Abdallah, F. M. Mahomoodally and N. Ahemad, *Food and Chemical Toxicology*, 2021, **154**, 112348.

45    A. Musa, M. M. Al-Sanea, N. H. Alotaibi, T. S. Alnusaire, S. R. Ahmed and E. M. Mostafa, *Indian Journal of Pharmaceutical Education and Research*, 2021, **55**, 483–490.

46    M. Imran, M. Khalid, M. Naeem Qaiser, M. Iqbal, B. Ali, S. Hussain Sumrra, I. Hussain, M. Ibrahim and D. Ghazi Khan, *International Journal of Agricultural and Applied Sciences*, 2017, **9**, 79–83.

47    A. Ben Nejma, M. Znati, A. Nguir, A. Daich, M. Othman, A. M. Lawson and H. Ben Jannet, *Journal of Pharmacy and Pharmacology*, 2017, **69**, 1064–1074.

48    N. Boughalleb, L. Trabelsi and F. Harzallah-Skhiri, *Natural Product Research*, 2009, **23**, 988–997.

49    S. Kumpun, A. Maria, S. Crouzet, N. Evrard-Todeschi, J. P. Girault and R. Lafont, *Food Chemistry*, 2011, **125**, 1226–1234.

50    I. E. Orhan, N. Kucukboyaci, I. Calis, J. P. Cerón-Carrasco, H. den-Haan, J. Peña-García and H. Pérez-Sánchez, *Phytochemistry Letters*, 2017, **20**, 373–378.

51    C. Jiratchayamaethasakul, Y. Ding, O. Hwang, S.-T. Im, Y. Jang, S. W. Myung, J. M. Lee, H. S. Kim, S. C. Ko and S. H. Lee, *Fisheries and Aquatic Sciences*, 2020, **23**, 1–9.

52    A. I. Elshamy, T. A. Mohamed, M. Suenaga, M. Noji, A. Umeyama, T. Efferth and M. E. F. Hegazy, *Phytochemistry Letters*, 2019, **34**, 74–78.

53    R. B. An, D. H. Sohn, G. S. Jeong and Y. C. Kim, *Archives of Pharmacal Research*, 2008, **31**, 594–597.

54    M. Agarwal, V. K. Srivastava, K. K. Saxena and A. Kumar, *Fitoterapia*, 2006, **77**, 91–93.

55    M. Bueno and M. P. Cordovilla, *Frontiers in Plant Science*, 2019, **10**, 439.

56    G. C. Nikalje, A. K. Srivastava, G. K. Pandey and P. Suprasanna, *Land Degradation and Development*, 2018, **29**, 1081–1095.

57    S. J. Lee, E. M. Jeong, A. Y. Ki, K. S. Oh, J. Kwon, J. H. Jeong and N. J. Chung, *Journal of Plant Physiology*, 2016, **206**, 133–142.

58  P. Dewick, Medicinal natural products: a biosynthetic approach, 2002.

59  I. Cesarino, A. Eudes, B. Urbanowicz and M. Xie, *Frontiers in Plant Science*, 2022, **13**, 463.

60  C. Y. Lin and A. Eudes, *Biotechnology for Biofuels*, 2020, **13**, 1–25

61  Q. Wang, D. Zhou, M. Wang, Y. Zhao, Y. Chen, M. Yin and X. Feng, *Chemistry of Natural Compounds*, 2014, **50**, 531–533.

62  N. Chhikara, K. Kushwaha, P. Sharma, Y. Gat and A. Panghal, *Food Chemistry*, 2019, **272**, 192–200.

63  K. M. Khan, G. M. Maharvi, A. Abbaskhan, S. Hayat, M. T. H. Khan, T. Makhmoor, M. I. Choudhary, F. Shaheen and Atta-ur-Rahman, *Helvetica Chimica Acta*, 2003, **86**, 457–464.

64  K. M. Mohamed, H. H. Hasanean, K. Ohtani and K. Yamasaki, *Bulletin of Pharmaceutical Sciences. Assiut*, 1998, **21**, 27–36.

65  Q. Yuan, D. Zhang, C. Liu, C. Zhang and D. Yuan, *Inflammation*, 2018, **41**, 2149–2159.

66  M. Yoshikawa, T. Murakami, M. Kadoya, H. Matsuda, O. Muraoka, J. Yamahara and N. Murakami, Chemical and Pharmaceutical Bulletin, 1996, **44**, 1212–1217.

67  T. Murakami, H. Matsuda, M. Inadzukil, K. Hirano and M. Yoshikawa, *Chemical and Pharmaceutical Bulletin*, 1999, **47**, 1717–1724.

68  W. Bylka, *Acta Physiologiae Plantarum* , 2004, **26**, 393–398.

69  R. Tundis, F. Menichini, F. Conforti, M. R. Loizzo, M. Bonesi, G. Statti and F. Menichini, *Journal of Enzyme Inhibition and Medicinal Chemistry*, 2009, **24**, 818–824.

70  Q. Z. Wang, P. Qiu, F. Liu, B. Wang, F. Q. Guan, X. Feng and S. Xu, *Journal of Asian Natural Products Research*, 2018, **20**, 1081–1087.

71  L. Nahar and S. D. Sarker, *Revista Brasileira de Farmacognosia* , 2005, **15**, 279–282.

72  M. DellaGreca, C. Di Marino, A. Zarrelli and B. D'Abrosca, *Journal of Natural Products*, 2004, **67**, 1492–1495.

73  Y. Zhou, M. Jin, C. Jin, C. Ye, J. Wang, R. Wang, C. Wei, W. Zhou and G. Li, *Phytochemistry Letters*, 2019, **30**, 186–189.

74    B. Duarte and I. Caçador, Sustainability, 2021, **13**, 1005–1018.

75    J. Bose, A. Rodrigo-Moreno and S. Shabala, Journal of Experimental Botany, 2014, **65**, 1241–1257.

76    F. Majolo, L. K. de Oliveira Becker Delwing, D. J. Marmitt, I. C. Bustamante-Filho and M. I. Goettert, *Phytochemistry Letters*, 2019, **31**, 196–207.

77    A. G. Atanasov, B. Waltenberger, E. M. Pferschy-Wenzig, T. Linder, C. Wawrosch, P. Uhrin, V. Temml, L. Wang, S. Schwaiger, E. H. Heiss, J. M. Rollinger, D. Schuster, J. M. Breuss, V. Bochkov, M. D. Mihovilovic, B. Kopp, R. Bauer, V. M. Dirsch and H. Stuppner, *Biotechnology Advances*, 2015, **33**, 1582–1614.

78    I. A. Saleh, K. Usman and M. H. Abu-Dieyeh, Halophytes as important sources of antioxidants and anticholinesterase compounds, Springer International Publishing, 2020.

79    R. Ksouri, W. M. Ksouri, I. Jallali, A. Debez, C. Magné, I. Hiroko and C. Abdelly, *Critical Reviews in Biotechnology*, 2012, **32**, 289–326.

80    WHO, https://www.who.int/news-room/fact-sheets/detail/noncommunicable-diseases, (accessed December 11, 2021).

81    WHO, https://extranet.who.int/nutrition/gina/en/node/40351, (accessed 2018).

82    S. A. Petropoulos, A. Karkanis, N. Martins and I. C. Ferreira, *Food and Chemical Toxicology*, 2018, **114**, 155–169.

83    V. Castañeda-Loaiza, C. Placines, M. J. Rodrigues, C. G. Pereira, G. Zengin, N. R. Neng, J. M. F. Nogueira and L. Custódio, *Natural Product Research*, 2020, **35**, 4753–4756.

84    F. Trampetti, C. Pereira, M. J. Rodrigues, O. Celaj, B. D'abrosca, G. Zengin, A. Mollica, A. Stefanucci and L. Custódio, *Journal of Pharmaceutical and Biomedical Analysis*, 2019, **165**, 119–128.

85    A. Buhmann and J. Papenbrock, *Functional Plant Biology*, 2013, **40**, 952–967.

86    Y. Y. Choi, M. H. Kim, J. Y. Lee, J. Hong, S. H. Kim and W. M. Yang, *Journal of Ethnopharmacology*, 2014, **154**, 380–385.

87    S. Jo, J. Ryu, H. Y. Han, G. Lee, M. H. Ryu and H. Kim, *Molecular Medicine Reports*, 2016, **13**, 1695–1700.

88    Y. Wen, Y. Chen, Z. Cui, J. Li and Z. Wang, *Planta Medica*, 1995, **61**, 450–452.

89     L. Dinan, *Journal of Chromatography A*, 1994, **658**, 69–76.

90     N. H. El-Sayed, A. S. Awaad, M. S. Hifnawy and T. J. Mabry, *Phytochemistry*, 1999, **51**, 591–593.

91     H. S. Yusufoglu, *Asian Pacific Journal of Tropical Disease*, 2015, **5**, 559–563

92     A. E. Al-Snafi, *Indo American Journal of Pharmaceutical Sciences*, 2018, **5**, 2213–2221.

93     H. E. Khalil, Y. M. Aljeshi , F. A. Saleh and T. S. Mohamed, *Journal of Chemical and Pharmaceutical Research,* 2017*,* **9***,* 210-215.

94     R. S. Youssef, *Journal of Medicinal Plants Research*, 2013, **7**, 2501–2513.

95     A. Harborne, *Phytochemical methods*, springer science & business media, 1998.

96     P. Houghton and A. Raman, *Laboratory handbook for the fractionation of natural extracts*, Springer Science & Business Media, 2012.

97     G. L. Ellman, K. D. Courtney, V. Andres and R. M. Featherstone, *Biochemical Pharmacology*, 1961, **7**, 88–95.

98     A. Othman, W. M. Afifi, M. Abd-Elraouf and L. D. Ismail, *Al-Azhar Journal of Pharmaceutical Sciences,* 2017, **56**, 10–19.

99     Y. Ma, Y. Bao, W. Zhang, X. Ying and D. Stien, *Natural Product Research*, 2020, **34**, 2276–2282.

100    F. Chen, X. jun Huang, Q. ping Liang, Y. peng Huang, T. Lan and G. xiong Zhou, *Natural Product Research*, 2019, **33**, 3378–3382.

101    R. R. King and L. A. Calhoun, *Phytochemistry*, 2005, **66**, 2468–2473.

102    B. Y. Yang, X. Yin, Y. Liu, H. L. Ye, M. L. Zhang, W. Guan and H. X. Kuang, *Phytochemistry Letters*, 2019, **30**, 160–164.

103    M. H. Oueslati, H. Ben Jannet, Z. Mighri, J. Chriaa and P. M. Abreu, *Journal of Natural Products*, 2006, **69**, 1366–1369.

104    D. G. Lee, Y. Park, M. R. Kim, H. J. Jung, Y. B. Seu, K. S. Hahm and E. R. Woo, *Biotechnology Letters*, 2004, **26**, 1125–1130.

105    H. Huang, Q. Chao, R. X. Tarll, H. Sun, D. Wang and S. Zhao, *Planta Medica*, 1999, **65**, 92–93.

106    W. Leonard, P. Zhang, D. Ying and Z. Fang, *Critical Reviews in Food Science and Nutrition*, 2020, **62**, 1608–1625.

107    X. Yan, J. Tang, C. dos Santos Passos, A. Nurisso, C. A. Simoes-Pires, M. Ji, H. Lou and P. Fan, *Journal of Agricultural and Food Chemistry*, 2015, **63**, 10611–10619.

108    N. Gaikwad, S. Nanduri and Y. V. Madhavi, *European Journal of Medicinal Chemistry*, 2019, **181**, 111561.

109    N. bo Qin, C. cui Jia, J. Xu, D. hong Li, F. xing Xu, J. Bai, Z. lin Li and H. ming Hua, *Fitoterapia*, 2017, **119**, 83–89.

110    F. Cutillo, B. D'Abrosca, M. DellaGreca, C. Di Marino, A. Golino, L. Previtera and A. Zarrelli, *Phytochemistry*, 2003, **64**, 1381–1387.

111    J. Han, L. Li, L. Han, X. Huang and T. Yuan, *Biochemical Systematics and Ecology*, 2015, **61**, 399–401.

112    A. Karim, I. Fatima, S. Hussain and A. Malik, *Helvetica Chimica Acta*, 2011, **94**, 528–533.

113    D. G. I. Kingston, *Journal of Natural Products*, 2010, **74**, 496–511.

114    Alzheimer's Association, *Alzheimer's & Dementia*, 2019, **15**, 321–387.

115    A. Mira, S. Yamashita, Y. Katakura and K. Shimizu, *Molecules*, 2015, **20**, 4813–4832.

116    R. R. Abd El-Latif, R. M. A. Mansour, M. Sharaf and A. Farag, *Journal of Asian Natural Products Research*, 2014, **16**, 434–439.

117    P. T. Nedialkov, Z. Kokanova-Nedialkova, P. T. Nedialkov and S. D. Nikolov, Pharmacognosy Reviews, 2009, **3**, 280.

118    A. F. Miftakhova, G. S. Burasheva, Z. A. Abilov, V. U. Ahmad and M. Zahid, Fitoterapia, 2001, **72**, 319–321.

119    Y. Zhou, M. Jin, C. Jin, C. Ye, J. Wang, J. Sun, C. X. Wei, W. Zhou and G. Li, *Natural Product Research*, 2020, **34**, 225–232.

120    R. Salah El Dine, H. M. Abdallah, Z. A. Kandil, A. A. Zaki, S. I. Khan and I. A. Khan, *Planta Medica*, 2019, **85**, 274–281.

121    A. H. Abou Zeid, M. S. Hifnawy and R. S. Mohammed, *Medicinal and Aromatic Plant Science and Biotechnology*, 2009, **3**, 42–49.

122    A. Bhattacherjee, T. Ghosh, R. Sil and A. Datta, *Natural Product Research*, 2014, **28**, 2199–2202.

123  N. Boutaoui, L. Zaiter, F. Benayache, S. Benayache, F. Cacciagrano, S. Cesa, D. Secci, S. Carradori, A. Giusti, C. Campestre, L. Menghini and M. Locatelli, *Molecules*, 2018, **23**, 1962.

124   P. T. Thuong, T. M. Hung, T. M. Ngoc, D. T. Ha, B. S. Min, S. J. Kwack, T. S. Kang, J. S. Choi and K. H. Bae, *Phytotherapy Research*, 2010, **24**, 101–106.

125  K. Takahashi, Y. Yoshioka, E. Kato, S. Katsuki, O. Iida, K. Hosokawa and J. Kawabata, *Bioscience, Biotechnology, and Biochemistry*, 2010, **74**, 741–745.

126  S. Shabbir, S. Khan, M. H. Kazmi, I. Fatima, A. Malik, F. Inamullah and R. B. Tareen, *Journal of Asian Natural Products Research*, 2021, **23**, 1037–1042.

127  I. A. Hussein, R. Srivedavyasasri, A. A. El-Hela, A. E. I. Mohammad and S. A. Ross, *Biochemical Systematics and Ecology*, 2020, **92**, 104113.

128  L. Xiaoling, X. Shihai, Y. Kai, G. Shuhao and Z. Xiangchao, *Zhong Yao Cai (Journal of Chinese Medicinal Materials)*, 2004, **27**, 254–256.

129  W. F. Jin, Z. H. Luo, Y. P. Sun, J. S. Liu, Y. Yu, G. Wang and G. K. Wang, *Natural Product Research*, 2020, **34**, 3145–3148.

130  T. Kanchanapoom, P. Sahakitpichan, N. Chimnoi, C. Petchthong, W. Thamniyom, P. Nangkoed and S. Ruchirawat, *Phytochemistry Letters*, 2021, **41**, 83–87.

131  Y. M. Amen, A. M. Marzouk, M. G. Zaghloul and M. S. Afifi, *Natural Product Research*, 2015, **29**, 511–517.

132  P. K. Agrawal, *Carbon-13 NMR of Flavonoids*, Elsevier, Amsterdam,1989.

133  J. G. Kim, J. W. Lee, T. P. L. Le, J. S. Han, Y. B. Cho, H. Kwon, D. Lee, M. K. Lee and B. Y. Hwang, *Journal of Natural Products*, 2021, **84**, 562–569.

134  A. Carotenuto, E. Fattorusso, V. Lanzotti, S. Magno, V. de Feo and C. Cicala, *Phytochemistry*, 1997, **44**, 949–957.

135  A. E. Mostafa, A. A. El-Hela, A. E. I. Mohammad, S. J. Cutler and S. A. Ross, *Phytochemistry Letters*, 2016, **17**, 213–218.

136  J. X. Li, T. Hareyama, Y. Tezuka, Y. Zhang, T. Miyahara and S. Kadota, *Planta Medica*, 2005, **71**, 673–679.

137  P. Fan, L. Terrier, A. E. Hay, A. Marston and K. Hostettmann, *Fitoterapia*, 2010, **81**, 124–131.

138   P. T. Francis, A. M. Palmer, M. Snape and G. K. Wilcock, *Journal of Neurology Neurosurgery and Psychiatry*, 1999, **66**, 137–147.

139   V. Schulz, *Phytomedicine*, 2003, **10**, 74–79.

140   N. H. Gay, K. Phopin, W. Suwanjang, N. Songtawee, W. Ruankham, P. Wongchitrat, S. Prachayasittikul and V. Prachayasittikul, *Neurochemical Research*, 2018, **43**, 619–636.

141   H. Khan, Marya, S. Amin, M. A. Kamal and S. Patel, *Biomedicine and Pharmacotherapy*, 2018, **101**, 860–870.

142   M. S. Refaey, R. A. Abdelhamid, H. Elimam, Y. A. M. M. Elshaier, A. A. Ali and M. A. A. Orabi, *Bioorganic Chemistry*, 2021, **108**, 104643.

143   V. P. Reddy, P. Aryal, S. Robinson, R. Rafiu, M. Obrenovich and G. Perry, *Microorganisms*, 2020, **8**, 199.

144   D. Szwajgier, *Zeitschrift für Naturforschung C*, 2013, **68**, 125–132.

145   M. Öztürk, U. Kolak, G. Topu, S. Öksüz and M. I. Choudhary, *Food Chemistry*, 2011, **126**, 31–38.

146   Y. C. Kuo and R. Rajesh, *Expert Review of Neurotherapeutics*, 2019, 19, 623–652.

147   M. Tolar, S. Abushakra and M. Sabbagh, *Alzheimer's and Dementia*, 2020, **16**, 1553–1560.

148   L. Blaikie, G. Kay and P. Kong Thoo Lin, *Medchemcomm*, 2019, **10**, 2052–2072.

149   WHO, https://www.who.int/news-room/fact-sheets/detail/dementia, (accessed September 2021).

150   J. H. Park, Y. H. Ju, J. W. Choi, H. J. Song, B. K. Jang, J. Woo, H. Chun, H. J. Kim, S. J. Shin, O. Yarishkin, S. Jo, M. Park, S. K. Yeon, S. Kim, J. Kim, M. H. Nam, A. M. Londhe, J. Kim, S. J. Cho, S. Cho, C. Lee, S. Y. Hwang, S. W. Kim, S. J. Oh, J. Cho, A. N. Pae, C. Justin Lee and K. D. Park, *Science advances*, 2019, **5**, eaav0316.

151   J. Rea Martinez, G. Selo, M. Á. Fernandez-Arche, B. Bermudez and M. D. García-Gimenez, *Journal of Natural Products*, 2021, **84**, 2447–2453.

152   S. S. Arya, S. Devi, K. Ram, S. Kumar, N. Kumar, A. Mann, A. Kumar and G. Chand, *Ecophysiology, Abiotic Stress Responses and Utilization of Halophytes*, 2019, 271–287.

153   V. Castañeda-Loaiza, M. Oliveira, T. Santos, L. Schüler, A. R. Lima, F. Gama, M. Salazar, N. R. Neng, J. M. F. Nogueira, J. Varela and L. Barreira, *Food Chemistry*, 2020, **333**, 127536.

154   T. Kuljanabhagavad, P. Thongphasuk, W. Chamulitrat and M. Wink, Phytochemistry, 2008, 69, 1919–1926

155   C. A. Lipinski, M. Discovery, F. Lombardo, C. A. Lipinski, B. W. Dominy and P. J. Feeney, *Advanced drug delivery reviews*, 1997, **23**, 3–25.

156   D. F. Veber, S. R. Johnson, H.-Y. Cheng, B. R. Smith, K. W. Ward and K. D. Kopple, *Journal of Medicinal Chemistry*, 2002, **45**, 2615–2623.

157   D. Seeliger and B. L. de Groot, *Journal of Computer-Aided Molecular Design*, 2010, **24**, 417–422.

158   J. C. Phillips, R. Braun, W. Wang, J. Gumbart, E. Tajkhorshid, E. Villa, C. Chipot, R. D. Skeel, L. Kalé and K. Schulten, *Journal of Computational Chemistry*, 2005, **26**, 1781–1802.

159   S. Release, *Maestro-Desmond Interoperability Tools, Schrödinger, New york, NY*, USA, 2020.

160   K. J. Bowers, D. E. Chow, H. Xu, R. O. Dror, M. P. Eastwood, B. A. Gregersen, J. L. Klepeis, I. Kolossvary, M. A. Moraes, F. D. Sacerdoti, J. K. Salmon, Y. Shan and D. E. Shaw, 2007, 43–43.

161   S. Kim, H. Oshima, H. Zhang, N. R. Kern, S. Re, J. Lee, B. Roux, Y. Sugita, W. Jiang and W. Im, *Journal of Chemical Theory and Computation*, 2020, **16**, 7207–7218.

162   S. T. Ngo, N. M. Tam, M. Q. Pham and T. H. Nguyen, *Journal of Chemical Information and Modeling*, 2021, **61**, 2302–2312.

163   C. Qi, Q. Zhou, W. Gao, M. Liu, C. Chen, X. N. Li, Y. Lai, Y. Zhou, D. Li, Z. Hu, H. Zhu and Y. Zhang, *Phytochemistry*, 2019, **165**, 112041.

164   M. H. Melchor, F. G. Susana, G. S. Francisco, H. I. Beltran, R. F. Norma, J. A. Lerma-Romero, P. Y. Lopez-Camacho and B. I. Gustavo, *RSC Advances*, 2018, **8**, 39667–39677.

165   S. Chinnathambi, Aggregation species of Amyloid-β and Tau oligomers in Alzheimer's Disease: Role in therapeutics and diagnostics., 2022, vol. 12.

166   K. Wojtunik-Kulesza, T. Oniszczuk, J. Mołdoch, I. Kowalska, J. Szponar and A. Oniszczuk, *International Journal of Molecular Sciences,* 2022*, ***23***,* 1212.

167   Z. Khan, S. M. Hong, J. W. Lee, E. Y. Moon, J. Huh, K. A. Chang and S. Y. Kim, *Journal of Functional Foods*, 2021, **80**, 104432.

168   J. Ferlay, M. Colombet, I. Soerjomataram, D. M. Parkin, M. Piñeros, A. Znaor and F. Bray, *International Journal of Cancer*, 2021, **149**, 778–789.

169   WHO, 2022. https://www.who.int/news-room/fact-sheets/detail/cancer, (accessed June 20, 2022).

170   H. Sung, J. Ferlay, R. L. Siegel, M. Laversanne, I. Soerjomataram, A. Jemal, F. Bray, *CA: a cancer journal for clinicians*, 2021, **71**, 209–249.

171   K. Shah and R. M. Rawal, *Current Drug Metabolism*, 2020, **20**, 1114–1131.

172   A. Rauf, M. Imran, I. A. Khan, M. ur-Rehman, S. A. Gilani, Z. Mehmood and M. S. Mubarak, *Phytotherapy Research*, 2018, **32**, 2109–2130.

173   D. Pu, L. Yin, L. Huang, C. Qin, Y. Zhou, Q. Wu, Y. Li, Q. Zhou and L. Li, *Frontiers in Oncology*, 2021, **11**, 248.

174   H. Moon, A. C. White and A. D. Borowsky, *Experimental & Molecular Medicine*, 2020, **52**, 538–547.

175   C. R. Bell, V. S. Pelly, A. Moeini, S. C. Chiang, E. Flanagan, C. P. Bromley, C. Clark, C. H. Earnshaw, M. A. Koufaki, E. Bonavita and S. Zelenay, *Nature Communications,* 2022, **13**, 1–17.

176   B. Liu, L. Qu and S. Yan, *Cancer Cell International*, 2015, **15**, 1–6.

177   V. Sharma, P. Bhatia, O. Alam, M. J. Naim, F. Nawaz, A. A. Sheikh and M. Jha, *Bioorganic chemistry*, 2019, **89**, 103007.

178   M. C. Alley, D. A. Scudiero, A. Monks, M. L. Hursey, M. J. Czerwinski, D. L. Fine, B. J. Abbott, J. G. Mayo, R. H. Shoemaker and M. R. Boyd, *Cancer Research*, 1988, **48**, 589–596.

179   H. M. Abdallah and A. Esmat, *Journal of Ethnopharmacology*, 2017, **205**, 51–56.

180   L. K. Han, Y. N. Zheng, M. Yoshikawa, H. Okuda and Y. Kimura, *BMC Complementary and Alternative Medicine*, 2005, **5**, 1–10.

181   A. Marouf, S. Desbene, T. C. Khanh, H. Wagner, M. Correia, B. Chauffert and M. A. Lacaille-Dubois, *Pharmaceutical Biology* , 2001, **39**, 263–267.

182   S. Zelenay, A. G. van der Veen, J. P. Böttcher, K. J. Snelgrove, N. Rogers, S. E. Acton, P. Chakravarty, M. R. Girotti, R. Marais, S. A. Quezada, E. Sahai and C. Reis E Sousa, *Cell*, 2015, **162**, 1257–1270.

183   A. M. Abdou, H. M. Abdallah, M. A. Mohamed, G. A. Fawzy and A. B. Abdel-Naim, *Archives of Pharmacal Research*, 2013, **36**, 715–722.

184   J. M. Lee, M. J. Yim, G. Choi, M. S. Lee, Y. G. Park and D. S. Lee, *Natural Product Sciences*, 2018, **24**, 40–46.

185   S. Oueslati, R. Ksouri, H. Falleh, A. Pichette, C. Abdelly and J. Legault, *Food Chemistry*, 2012, **132**, 943–947.

186   F. Medini, S. Bourgou, K. G. Lalancette, M. Snoussi, K. Mkadmini, I. Coté, C. Abdelly, J. Legault and R. Ksouri, *South African Journal of Botany*, 2015, **99**, 158–164.

187   W. Mazouz, N. E. H. Haouli, L. Gali, T. Vezza, C. Bensouici, S. Mebrek, T. Hamel, J. Galvez and S. Djeddi, *South African Journal of Botany*, 2020, **135**, 101–108.

188   M. Huang, J. J. Lu and J. Ding, *Natural Products and Bioprospecting,* 2021, **11**, 5–13.

189   M. T. Kabir, M. H. Rahman, R. Akter, T. Behl, D. Kaushik, V. Mittal, P. Pandey, M. F. Akhtar, A. Saleem, G. M. Albadrani, M. Kamel, S. A. M. Khalifa, H. R. El-Seedi and M. M. Abdel-Daim, *Biomolecules, 2021*, **11**, 392.

190   C. Park, D. O. Moon, C. H. Rhu, B. T. Choi, W. H. Lee, G. Y. Kim and Y. H. Choi, *Biological and Pharmaceutical Bulletin*, 2007, **30**, 1317–1323.

191   H. L. Teles, J. P. Hemerly, P. M. Pauletti, J. R. C. Pandolfi, A. R. Araújo, S. R. Valentini, M. C. M. Young, V. D. S. Bolzani and D. H. S. Silva, *Natural Product Research*, 2005, **19**, 319–323.

192   J. Yang, Y. L. Xiao, X. R. He, G. F. Qiu and X. M. Hu, *Journal of Asian Natural Products Research* , 2010, **12**, 185–193.

193   C. Balachandran, N. Emi, Y. Arun, Y. Yamamoto, B. Ahilan, B. Sangeetha, V. Duraipandiyan, Y. Inaguma, A. Okamoto, S. Ignacimuthu, N. A. Al-Dhabi and P. T. Perumal, *Chemico-Biological Interactions*, 2015, **242**, 81–90.

194   T. Lombardi, A. Bertacchi, L. Pistelli, A. Pardossi, S. Pecchia, A. Toffanin and C. Sanmartin, *Horticulturae* , 2022, **8**, 195.

195    A. Gadano, A. Gurni and M. A. Carballo, *Pharmaceutical Biology*, 2007, 45, 217–222.

196    M. Hasanuzzaman, S. Shabala and M. Fujita, *Halophytes and Climate Change: Adaptive mechanisms and potential uses*, 2019.

197    N. Kambouche, B. Merah, A. Derdour, S. Bellahouel, J. Bouayed, A. Dicko, C. Younos and R. Soulimani, *African Journal of Biotechnology*, 2009, **8**, 5589–5594.

198    P. Ninfali, E. Antonini, A. Frati and E. S. Scarpa, *Phytotherapy Research*, 2017, **31**, 871–884.

199    L. Boulos, Kew Bulletin, 1992, **47**, 283–287.

200    M. W. A. Halmy, in *Knowing our lands and resources. Indigenous and local knowledge of biodiversity and ecosystem services in Africa*, ed. M. Roué, N.Césard, Adou Yao, Y. C. A. Oteng-Yeboah, *UNESCO*, Paris, 2017, Ch. **8**, 107–145.

201    S. B. Paudel, J. Park, N. H. Kim, H. Choi, E. K. Seo, H. A. Woo and J. W. Nam, *Fitoterapia*, 2019, **139**, 104374.

202    C. H. Park, S. Y. Min, H. W. Yu, K. Kim, S. Kim, H. J. Lee, J. H. Kim and Y. J. Park, *International Journal of Molecular Sciences*, 2020, **21**, 4620.

203    F. F. Sahle, T. Gebre-Mariam, B. Dobner, J. Wohlrab and R. H. H. Neubert, *Skin Pharmacology and Physiology*, 2015, **28**, 42–55.

204    Y. Mizutani, S. Mitsutake, K. Tsuji, A. Kihara and Y. Igarashi, *Biochimie*, 2009, **91**, 784–790.

205    E. Kahraman, M. Kaykın, H. Ş. Bektay and S. Güngör, *Cosmetics*, 2019, **6**, 52.

206    L. Coderch, O. López, A. de La Maza and J. L. Parra, *American Journal of Clinical Dermatology*, 2003, **4**, 107–129.

207    Y. Pang, S. Wu, Y. He, Q. Nian, J. Lei, Y. Yao, J. Guo and J. Zeng, *Frontiers in Pharmacology*, 2021, **12**, 1909.

208    S. Mathur and C. Hoskins, *Biomedical Reports*, 2017, **6**, 612–614.

209    E. N. Tessema, T. Gebre-Mariam, R. H. H. Neubert and J. Wohlrab, *Skin Pharmacology Physiology*, 2017, **30**, 115–138.

210    M. Nowak-Perlak, K. Szpadel, I. Jabłońska, M. Pizon and M. Woźniak, *Molecules*, 2022, **27**, 591.

211  S. Wu, Y. Pang, Y. He, X. Zhang, L. Peng, J. Guo and J. Zeng, *Biomedicine and Pharmacotherapy*, 2021, **140**, 111741.

212  S. Takeda, K. Miyasaka, S. Shrestha, Y. Manse, T. Morikawa and H. Shimoda, *Molecules*, 2021, **26**, 5860.

213  G. Flamini, E. Antognoli and I. Morelli, *Phytochemistry*, 2001, **57**, 559–564.

214  M. Al-Oqail, W. H. B. Hassan, M. S. Ahmad and A. J. Al-Rehaily, *Saudi Pharmaceutical Journal*, 2012, **20**, 371–379.

215  C. Lee, J. Kim, H. Lee, S. Lee and Y. Kho, *Journal of Natural Products*, 2001, **64**, 659–660.

216  H. A. Hassanean and E. K. Desoky, *Phytochemistry*, 1992, **31**, 3293–3294.

217  S. Sen, N. Sahu and S. Mahato, *Phytochemistry*, 1992, **31**, 2919–2921.

218  J. Yin, C. S. Seo, I. H. Hwang, M. W. Lee and K. H. Song, *Nutrients*, 2018, **10**, 1221.

219  B. Ali, M. Ibrahim, I. Hussain, N. Hussain, M. Imran, H. Nawaz, S. Jan, M. Khalid, T. Ghous and M. S. H. Akash, *Revista Brasileira de Farmacognosia*, 2014, **24**, 277–281.

220  G. Mohamed, S. Ibrahim and S. Ross, *Phytochemistry Letters*, 2013, **6**, 340–344.

221  F. Tantangmo, B. N. Lenta, S. Ngouela, L. M. Kamdem, B. Weniger, E. Tsamo, A. Lobstein and C. Vonthron-Séné cheau, *Halvetica chemica acta*, 2010, **93**, 2210–2217.

222  J. H. Jung, C. O. Lee, Y. C. Kim and S. S. Kang, *Journal of Natural Products*, 1996, **59**, 319–322.

223  Y. Kawano, R. Higuchi, R. Isobe and T. Komori, *Liebigs Ann Chem*, 1988, **8**, 19–24.

224  R. F. A. Abdelhameed, E. E. Eltamany, D. M. Hal, A. K. Ibrahim, A. M. AboulMagd, T. Al-Warhi, K. A. Youssif, A. M. A. El-kader, H. A. Hassanean, S. Fayez, G. Bringmann, S. A. Ahmed and U. R. Abdelmohsen, *Marine Drugs*, 2020, **18**, 405.

225  A. I. M. Khedr, S. R. M. Ibrahim, G. A. Mohamed, S. A. Ross and K. Yamada, *Phytochemistry Letters*, 2018, **23**, 100–105.

226  T. Malyarenko, A. Kicha and V. Stonik, *Marine Drugs*, 2021, **19**, 330.

227　S. Sharma, S. K. Chattopadhyay, M. Singh, D. U. Bawankule and S. Kumar, *Phytochemistry*, 2014, **100**, 132–140.

228　W. Jin, K. L. Rinehart and E. A. Jares-Erijman, *Journal of Organic Chemistry*, 1994, **59**, 27–66.

229　P. Muralidhar, N. Krishna, M. M. Kumar, C. B. Rao and D. V. Rao, *Chemical and Pharmaceutical Bulletin*, 2003, **51**, 1193–1195.

230　H. K. Assaf, A. M. Nafady, A. E. Allam, A. N. E. Hamed, M. S. Kamel and K. Shimizu, *Natural Product Research*, 2017, **32**, 2452–2456.

231　T. Natori, M. Morita, K. Akimoto and Y. Koezuka, *Tetrahedron*, 1994, **50**, 2771–2784.

232　F. G. G. Ürményi, G. do N. Saraiva, L. M. Casanova, A. dos S. Matos, L. M. de Magalhães Camargo, M. T. V. Romanos and S. S. Costa, *Chemistry and Biodiversity*, 2016, **13**, 1707–1714.

233　N. L. Nguyen, T. H. Vo, Y. C. Lin, C. C. Liaw, M. K. Lu, J. J. Cheng, M. C. Chen and Y. H. Kuo, *Journal of Natural Products*, 2021, **84**, 259–267.

234　 S. Hamanaka, M. Hara, H. Nishio, F. Otsuka, A. Suzuki and Y. Uchida, *Journal of Investigative Dermatology*, 2002, **119**, 416–423.